Technische Universität München
Lehrstuhl für Ernährungsmedizin

Effect of maternal obesity with and without gestational diabetes on placental gene expression and early childhood obesity

Kirsten Uebel

Vollständiger Abdruck der von der Fakultät Wissenschaftszentrum Weihenstephan für Ernährung, Landnutzung und Umwelt der Technischen Universität München zur Erlangung des akademischen Grades eines

Doktors der Naturwissenschaften

genehmigten Dissertation.

Vorsitzender: Univ.-Prof. Dr. D. Haller

Prüfer der Dissertation:

1. Univ.-Prof. Dr. J. J. Hauner
2. Univ.-Prof. Dr. M. Klingenspor

Die Dissertation wurde am 05.09.2014 bei der Technischen Universität München eingereicht und durch die Fakultät Wissenschaftszentrum Weihenstephan für Ernährung, Landnutzung und Umwelt am 09.12.2014 angenommen.

Table of content

Summary

Maternal obesity and gestational diabetes mellitus (GDM) may independently influence offspring adipose tissue development and metabolic disease susceptibility. However, the molecular and physiological similarities and differences between these prenatal conditions and their role in fetal programming are poorly understood. The placenta is suggested to play a substantial role in the adaptation to the given maternal environment. Therefore, adipose tissue growth during early infancy and changes in placental morphology, transport of nutrients as well as hormone and cytokine production became the focus of research.

The *GesA* (**Ges**tational diabetes mellitus, maternal **a**diposity and early childhood obesity) study was conducted as a pilot study to analyze the effect of maternal adiposity and GDM on childhood obesity. Pregnant women were recruited and enrolled in three groups according to their pre-pregnancy BMI and glucose tolerance status: normoglycemic lean women (Body mass index (BMI): 18.5-25 kg/m^2; n = 15), obese women without GDM (BMI > 30 kg/m^2; n =13), and obese women with GDM (BMI > 30 kg/m^2; n = 16). Maternal and umbilical cord blood samples as well as term placental tissues were collected. Offspring anthropometry and body composition were repeatedly investigated from birth until year-1 *post partum.* The aim of the present thesis was 1) to analyze selected maternal and fetal plasma biomarkers as well as placental global gene expression and corresponding signaling pathways, 2) to characterize offspring body composition and growth between the groups and 3) to investigate the relationship of plasma biomarkers as well as placental target genes and proteins to offspring adipose tissue development. Maternal and cord blood samples were analyzed for lipid profiles, insulin, adipokines (leptin and adiponectin), interleukin (IL) 6 and C-reactive protein (CRP) levels. Infant fat mass was investigated by skinfold thickness measurements (SFT) and abdominal ultrasonography for further discrimination between subcutaneous (SCA) and preperitoneal adipose tissue (PPA). Transcriptomic analyses from villous placental biopsies were performed by DNA microarrays and target genes were validated by the reverse transcription quantitative polymerase chain reaction (RT-qPCR) method, while signaling pathways were further validated by Western Blotting.

It was shown that obese women with and without GDM had significantly increased levels of insulin, C-peptide, leptin and IL6, while the ratios of high molecular weight (HMW) to total adiponectin at 3rd trimester were significantly lower compared to the lean group. Cord plasma insulin levels and HOMA-indices were significantly increased in the GDM group, whereas levels of leptin, total and HMW adiponectin did not differ between the groups. Neonates of the obese GDM group showed significantly increased SCA and PPA at week-1 as well as significantly higher SFT and fat mass until week-6 compared to the lean group. At month-4 and year-1, no significant differences in adipose tissue growth were found between the

groups. Multiple linear regression analyses revealed that maternal fasted C-peptide and HMW adiponectin as well as cord insulin levels were predictive for newborn PPA that showed a significant relationship with PPA development at year-1. The placental microarray analysis revealed that most of the genes were differentially expressed between samples of obese women with and without GDM. The '*Genomatix'*-based pathway analysis found that genes implicated in *Fibroblast growth factor (FGF) signaling, Angiogenesis* and *Lipid metabolism,* were differentially regulated between placentas of lean and obese women without GDM. In addition, differentially regulated genes assigned to *Proliferation, Low-density lipoprotein receptor related protein/ wingless-int (Wnt) type/ β-catenin, Transforming growth factor β (TGF-β)* and *Vascular endothelial growth factor (VEGF) pathways,* were over-represented in placentas of obese GDM women compared to both normoglycemic groups. Surprisingly, in contrast to other studies reporting increased expression of inflammatory pathways as typical feature of pregnancies with pregravid obesity and GDM, no evidence for significant changes in placental genes and pathways of inflammatory processes was found. RT-qPCR validation of Wnt signaling-associated genes demonstrated that *Wingless-type MMTV integration site family, member 7A (WNT7A), dickkopf homolog 3 (DKK3), cadherin 11 (CDH11)* and *parathyroid hormone 1 receptor (PTH1R)* were differentially expressed in the placentas of the obese GDM group. In the Western blot analysis, the phosphorylated *v-akt murine thymoma viral oncogene homolog (pAKT)* and *glycogen synthase kinase 3β (pGSK3β)* as well as the *nuclear β-catenin* protein levels were significantly increased in placentas of obese diabetic women. Analyzing the relationship of placental expression data to infant adipose tissue distribution by multiple linear regressions, the pAKT-total AKT ratio and WNT7A gene expression emerged as positive determinants of infant PPA at week-1.

Altogether, the thesis showed that maternal pregravid obesity combined with GDM led to significantly increased offspring fat mass until week-6, which strongly suggests a pivotal role of GDM in these adverse offspring outcomes. However, the observed short adverse impact of intrauterine hyperglycemia seems to vanish within the first year of life. Importantly, the identification of maternal plasma biomarkers C-peptide and HMW adiponectin, and changing levels of placental pAKT-total AKT ratio and WNT7A in the insulin and Wnt signaling may present novel potential predictors for distinct PPA growth that was recently considered as cardiovascular risk factor in later life. Regarding the effect of fetal hyperinsulinemia on placental gene expression in the obese GDM group, it can be speculated whether elevated insulin levels as well as modulated placental insulin and Wnt/β-catenin signaling might result in changes of trophoblast differentiation as well as disturbances in villous maturity and angiogenesis. It will be of future interest to find out whether fetal hyperinsulinemia has similar effects on these pathways operating in adipose tissue development and growth.

Zusammenfassung

Mütterliche Adipositas und Schwangerschaftsdiabetes (Gestationsdiabetes, GDM) beeinflussen möglicherweise unabhängig voneinander die kindliche Fettgewebsentwicklung und die Prädisposition für Übergewicht und Stoffwechselerkrankungen im späteren Leben der Kinder. Die molekularen und physiologischen Gemeinsamkeiten bzw. Unterschiede der beiden pränatalen Konditionen und ihre Auswirkungen sind bisher nur unzureichend geklärt. Hierbei wird der Plazenta eine wichtige Rolle in der Adaptation an die mütterlichen Umgebungsbedingungen zugeschrieben. Deshalb rückten das Wachstum des Fettgewebes in der frühen Kindheit und die plazentalen Veränderungen bezüglich der Morphologie, Nährstoffversorgung sowie der Hormon- und Zytokinproduktion in den Fokus der Forschung.

Die *GesA*- (***Ges****tational diabetes mellitus, maternal* ***a****diposity and early childhood obesity*) Studie wurde als Pilot-Studie durchgeführt, um die Auswirkung von maternaler Adipositas und GDM auf die Fettgewebsentwicklung in der Kindheit zu analysieren. Dafür wurden schwangere Frauen rekrutiert und in drei Gruppen hinsichtlich ihres BMI vor der Schwangerschaft und ihrers Glucosetoleranz-Status eingeteilt: schlanke schwangere Frauen ohne GDM (Body mass index (BMI): 18.5-25 kg/m^2, n = 15), adipöse Schwangere ohne GDM (BMI > 30 kg/m^2, n = 13) und adipöse Schwangere mit GDM (BMI > 30 kg/m^2, n = 16). Blutproben der Schwangeren sowie entsprechende Nabelschnurblut- und Plazentaproben wurden gesammelt und die Messung der kindlichen Anthropometrie und Körperzusammensetzung von der Geburt bis zum 1. Lebensjahr wiederholt durchgeführt. Die Ziele der vorliegenden Arbeit waren (1) die Analyse ausgewählter mütterlicher bzw. fötaler Plasma-Biomarker sowie die Untersuchung der globalen Genexpression und differenziell regulierter Signalwege in den entsprechenden Plazenten, (2) die Charakterisierung der kindlichen Anthropometrie und Fettverteilung zwischen den Gruppen und (3) die Auswertung der Biomarker und plazentalen Zielgene bzw. Zielproteine in Zusammenhang mit der Fettgewebsentwicklung der Kinder.

Die mütterlichen und Nabelschnur-Blutproben wurden zur Analyse von Lipidprofilen, Insulin, Adipokinen (Leptin und Adiponektin), Interleukin (IL) 6 und C-reaktivem Protein (CRP) herangezogen. Zur Abschätzung der kindlichen Fettmasse wurden definierte Hautfaltendicken (SFT) gemessen und ergänzend dazu die Diskriminierung von subkutanem (SCA) und präperitonealem (PPA) Fettgewebe mittels abdomineller Ultraschalluntersuchung vorgenommen. Die Transkriptomanalyse von villösen Plazenta-Biopsien wurde mittels DNA-Microarrays durchgeführt und die Zielgene mit Hilfe der quantitativen Reverse-Transkriptase Polymerase-Kettenreaktion (RT-qPCR)-Methode validiert. Weiterhin wurden plazentale Signalwege auf Proteinebene durch Western Blot-Methoden überprüft.

In der vorliegenden Arbeit wurden bei adipösen Frauen mit und ohne GDM signifikant erhöhte Insulin-, C-Peptid-, Leptin- und IL6-Spiegel gemessen, während der Quotient aus *High Molecular Weight* (HMW)- und Gesamt-Adiponektin im 3. Trimester niedriger als bei den schlanken Frauen war. Sowohl die Insulin-Spiegel als auch die HOMA-Indizes waren im Nabelschnurblut in der Gruppe der adipösen diabetischen Mütter signifikant erhöht, hingegen fanden sich keine Unterschiede in den Leptin-, HMW- und Gesamt-Adiponektin-Werten zwischen den Gruppen. Die Neugeborenen der adipösen Mütter mit GDM zeigten signifikant erhöhte SCA- und PPA-Werte in der 1. Woche nach der Geburt sowie signifikant erhöhte SFT-Werte und Fettmassen bis zur 6. Lebenswoche. Bei den Untersuchungen nach 4 Monaten und dem 1. Lebensjahr hingegen wurden keine Unterschiede mehr zwischen den Gruppen bezüglich ihrer Fettgewebsentwicklung gefunden. Lineare Regressionsanalysen ergaben, dass die mütterlichen C-Peptid- und HMW-Adiponektin-Spiegel sowie die Insulin-Werte im Nabelschnurplasma jeweils in signifikant positiver Beziehung zum PPA des Neugeborenen standen, welches wiederum prädiktiv für die PPA-Entwicklung der einjährigen Kinder war. Die Microarray-Analyse in den Plazenten stellte heraus, dass die meisten differentiell exprimierten Gene in den beiden Gruppen der adipösen Frauen mit GDM und ohne GDM detektiert wurden. Aus der auf ‚*Genomatix*'-basierten Signalweg-Analyse ging hervor, dass Gene, die in den Signalwegen *Fibroblast growth factor (FGF)*, *Angiogenese* und *Lipidstoffwechsel* involviert sind, signifikant unterschiedlich in den Plazenten von schlanken und adipösen Schwangeren ohne GDM reguliert waren. Zudem waren die in den Plazenten von diabetischen Müttern differentiell regulierten Gene in den Signalwegen *Proliferation, Low-density lipoprotein receptor related protein/ wingless-int (Wnt) type/ β-catenin,Transforming Growth Factor β (TGF-β)* und *Vascular Endothelial Growth Factor (VEGF)* signifikant überrepräsentiert. Im Gegensatz zu anderen Studien, die eine erhöhte plazentale Expression von inflammatorischen Signalwegen als typisches Merkmal von Übergewicht und GDM in der Schwangerschaft beschrieben, war in den jeweiligen Gruppenvergleichen dieser Studie überraschenderweise keiner dieser Signalwege unterschiedlich reguliert. Die Messung von Wnt-assoziierten Genen mittels RT-qPCR-Verfahren bestätigte, dass die Expressionen von *Wingless-type MMTV integration site family, member 7A (WNT7A), Dickkopf homolog 3 (DKK3), Cadherin 11 (CDH11)* und *Parathyroid hormone 1 receptor (PTH1R)* in den Plazenten adipöser diabetischer Frauen differentiell reguliert waren. Darüber hinaus waren bei der Western Blot-Analyse die Levels des phosphorylierten *V-akt Murine Thymoma Viral Oncogene Homolog 1 (pAKT)* und der *Glycogensynthase-Kinase 3β (pGSK3β)* sowie des *nukleären β-Catenin* in den Plazenten von adipösen Diabetikerinnen signifikant erhöht. Bei der linearen Regressionsanalyse zur Bestimmung plazentaler Einflusswerte auf das kindliche Wachstum des Fettgewebes fand

sich ein signifikant positiver Zusammenhang zwischen dem *pAKT-AKT*-Quotienten bzw. der *WNT7A*-Genexpression und dem kindlichen *PPA*-Wachstum in der 1. Woche nach der Geburt.

Insgesamt zeigt die vorliegende Arbeit, dass vor der Schwangerschaft bestehendes Übergewicht in Kombination mit GDM bis zur 6. Lebenswoche nach der Geburt zu einer erhöhten kindlichen Fettmasse führte, was die zentrale Rolle des GDM als negative Folge für das Kind unterstreicht. Dennoch schien der kurzzeitige ungünstige Einfluss der intrauterinen Hyperglykämie auf das neonatale Wachstum und Fettgewebe innerhalb des 1. Lebensjahres verschwunden zu sein. Ein wesentlicher Aspekt der vorliegenden Arbeit war die Identifizierung von mütterlichen Biomarkern (C-Peptid und HMW-Adiponektin) und Parametern des plazentalen Insulin- und Wnt-Signalweges (*pAKT-AKT*-Quotient*, WNT7A*) als neue potentielle Prädiktoren für das Wachstum des *PPA*, das seit einiger Zeit als kardiovaskulärer Risikofaktor bewertet wird. In Bezug auf die gemessene fötale Hyperinsulinämie im Nabelschnurblut von diabetischen Müttern lässt sich vermuten, dass diese an der Modulation der Insulin- und Wnt/β-catenin-Signalwege in der Plazenta beteiligt ist. Beide Signalwege könnten möglicherweise mit veränderter Differenzierung der Trophoblasten sowie Störungen der villöser Reife und Angiogenese in Verbindung gebracht werden. Es wird von zukünftigem Interesse sein herauszufinden, ob die fötale Hyperinsulinämie ähnliche Auswirkungen auf diese beiden Signalwege im Wachstum und der Entwicklung des Fettgewebes hat.

1 Introduction

1.1 Obesity epidemic

Obesity is a growing public health problem in industrialized countries [1]. In 2009-2010, the prevalence of obesity (Body mass index (BMI) > 30 kg/m^2) in the United States (US) was 35.5 % among adult men and 35.8 % among adult women [2]. With regard to Germany, 43.8 % of men are overweight and even 23.3 % are obese, whereas 29.1 % of women had a BMI > 25 kg/m^2 and 23.9 % had a BMI > 30 kg/m^2 [3]. Particularly worrying is the continuous increase in obesity prevalence (0.5 % / year), showing that more than 20.5 % of US women at reproductive age were obese in 2009 [4]. The German obstetrical population is also strongly affected by the obesity epidemic indicating that 20.3 % of women aged between 20 and 29 years are overweight and 8.7 % are obese. In women aged between 30 and 39, the corresponding prevalence with 21.0 % and 14.3 %, respectively, is even higher [5]. Coincidentally, the prevalence of obesity (BMI ≥ 95th percentile of the BMI-for-age growth charts) in US children and adolescents was 16.9 % in 2011-2012 [6]. This dimension has not yet been achieved in Germany, but among children and adolescents participating in the KiGGS survey, 8.7 % were overweight and 6.3 % were even obese compared to a national reference [7]. The prevalence for obesity might be influenced by many pre- and perinatal factors. There is now growing evidence that maternal and paternal BMI are independent predictors for offspring weight development in early childhood [8]. Moreover, children of mothers with intrauterine hyperglycemia have a higher rate of being overweight at birth that is positively associated with BMI during infancy and adolescence [9,10].

1.2 Different types of diabetes mellitus

Diabetes is a chronic metabolic disease that occurs when the pancreas does not produce enough insulin, or when the insulin-sensitive tissues do not adequately respond to the secreted insulin [11]. Hyperglycemia is the common pathophysiological consequence of untreated diabetes that leads to serious damages especially of the eyes, kidneys, nerves, heart, and blood vessels [11]. The classification of type 1 and type 2 diabetes is based on the ethnology and the progress of β-cell dysfunction [12]. In the pathogenesis of type 1 diabetes mellitus, β-cell loss is irreversibly initiated by autoreactive cluster of differentiation (CD) 4$^+$-T cells. The main regulation of β-cell fate is mediated by cytokine signaling pathways. Accordingly, interleukin (IL) 1β and interferon (IFN)-γ induce the two transcriptional factors, nuclear factor (NF) κB and signal-transducer/activator of transcription protein (STAT) 1, that

initiate the β-cell destruction [12]. However, multiple environmental and genetic factors might be involved. For example, recent data suggest an association between the DR-DQ loci within the human leukocyte antigen (HLA) class II antigen region and the susceptibility for type 1 diabetes. Normally, a lifelong insulin replacement is required to control glucose metabolism. In contrast, type 2 diabetes mellitus is a multi-factorial disease including genetic predisposition and environmental factors like obesity, diet and physical inactivity [13]. The progressive apoptosis of β-cells is mainly promoted by glucotoxicity and lipotoxicity. The impaired peripheral insulin sensitivity and hyperinsulinemia are main characteristics of type 2 diabetes, while the attenuated β-cell action is predominant in later stages of this disease. A specific form is represented by gestational diabetes mellitus (GDM) that is defined as firstly occurred hyperglycemia during pregnancy including the manifestation of type 1 or type 2 diabetes [14].

1.3 Maternal intermediate metabolism in normal and GDM pregnancies

Normal pregnancy is characterized by various changes in lipid and carbohydrate metabolism which provide a constant nutrient supply to the fetus during high metabolic demands of the 2^{nd} and 3^{rd} trimester. The maternal intermediate metabolism in the second and third trimester is summarized in **Figure 1** emphasizing the differences between normal pregnancies and pregnancies complicated by GDM**.** In early pregnancy, glucose tolerance is improved with normal or slightly increased peripheral insulin sensitivity and hepatic glucose production [15]. With advancing gestation, a progressive increase in basal and postprandial insulin concentrations is measured in normal pregnancies. Placental hormones like human placental lactogen (hPL) and human placental growth hormone (hPGH) have been related to longitudinal decrease in insulin sensitivity in normal pregnancies resulting in physiological insulin resistance [15].

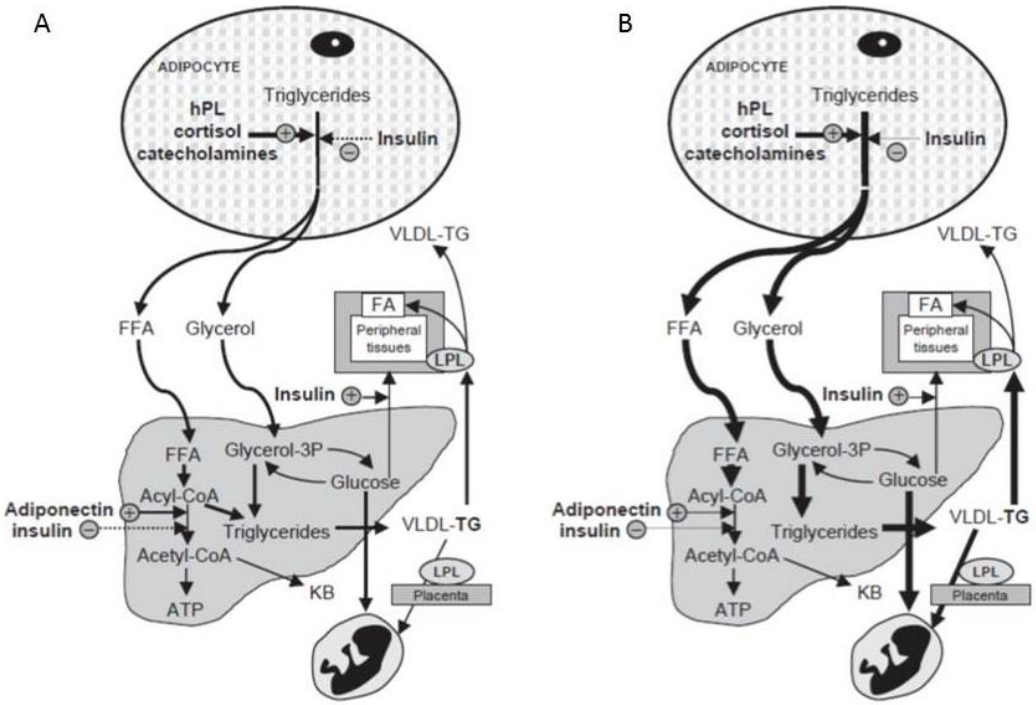

Figure 1: Intermediary metabolism in (A) normal pregnancy and (B) pregnancy with GDM. The thickness of the lines relates the degree of stimulation (solid lines) or inhibition (dash lines) of either the metabolic pathway or the hormonal effects. TG: triglycerides; KB: ketone bodies; FFA: free fatty acids; FA: fatty acids; hPL: human placental lactogen; LPL: lipoprotein lipase (modified from Bonet et al. [16]).

Thus, studies previously reported that pregnancy *per se* is associated with a strong reduction of insulin-stimulated glucose uptake in skeletal muscle that is further impaired by GDM **(Figure 2).** Underlying defective tyrosine phosphorylation of the insulin receptor (INSR) and insulin receptor substrate-1 (IRS1) in skeletal muscle and adipocytes among diabetic women was noted [17]. Moreover, higher levels of circulating cytokines, like tumor necrosis factor α (TNF-α), impair the INSR-IRS1-Phosphoinositol-3-kinase (PI3K) signaling by IRS1 serine/threonine phosphorylation in skeletal muscles favoring its degradation [18]. With proceeding pregnancy, adiponectin levels decline and contribute additionally to increased IRS1 serine phosphorylation via the AMP-activated protein kinase (AMPK)- mammalian target of rapamycin (mTOR)-Ribosomal protein S6 kinase 1, 70kDa (p70S6K1) signaling pathway exacerbating the insulin resistance (pathological insulin resistance) [17]. Furthermore, the elevated levels of the PI3K regulatory subunit (p85) act by blocking the association of PI3K (regulatory p85 - catalytic p110) with IRS1 and attenuate subsequently the PI3K activation during pregnancy. Together, the loss of PI3K activation through increased PI3Kp85 levels and IRS1 serine phosphorylation levels lead to reduced v-akt murine thymoma viral oncogene homolog 1 (AKT) phosphorylation and further decreased the translocation of the glucose transporter (GLUT4) to the plasma membrane and insulin-stimulated glucose uptake into the skeletal muscle cells [17]. Typically, women with GDM

already have preexisting insulin resistance that is impaired during pregnancy. A relative lack of insulin secretion to compensate this pathological insulin resistance causes maternal hyperglycemia (GDM). During the 1st and 2nd trimesters, increased estrogen, progesterone and insulin levels promote the accumulation of maternal fat depots and inhibit lipolysis [15]. The mobilization of fat stores and hyperlipidemia commonly occurs in mid and late pregnancy favoring the use of lipids as a maternal energy source while glucose and amino acids are provided for the fetus [15]. Thereby, placental hormones like hPL and catecholamines increase lipolysis, contributing to peripheral insulin resistance [16]. In pregnancies with pregravid obesity and GDM, variable findings related to dyslipidemia have been reported [19]. For triglycerides (TG), the majority of studies found higher levels in obese and/or GDM women due to pathological insulin resistance compared to lean subjects throughout pregnancy [20–22]. Although glucose is an important factor in fetal overgrowth, it is suggested that other nutritional components like lipids may be additionally involved in offspring growth and regulation of fat mass [23]. Thus, a correlation between maternal TG and neonatal body weight/ fat mass has been found in pregnancies with well controlled glucose levels and GDM, suggesting that differences in lipid metabolism rather than hyperglycemia play a role in adverse pregnancy outcomes [24,25]. Conflicting results have been found for cholesterol levels [19], but novel studies accumulate reporting that total cholesterol and low-density lipoprotein (LDL) cholesterol levels were decreased in obese compared to lean women at 2nd and 3rd trimester [21,26,27].

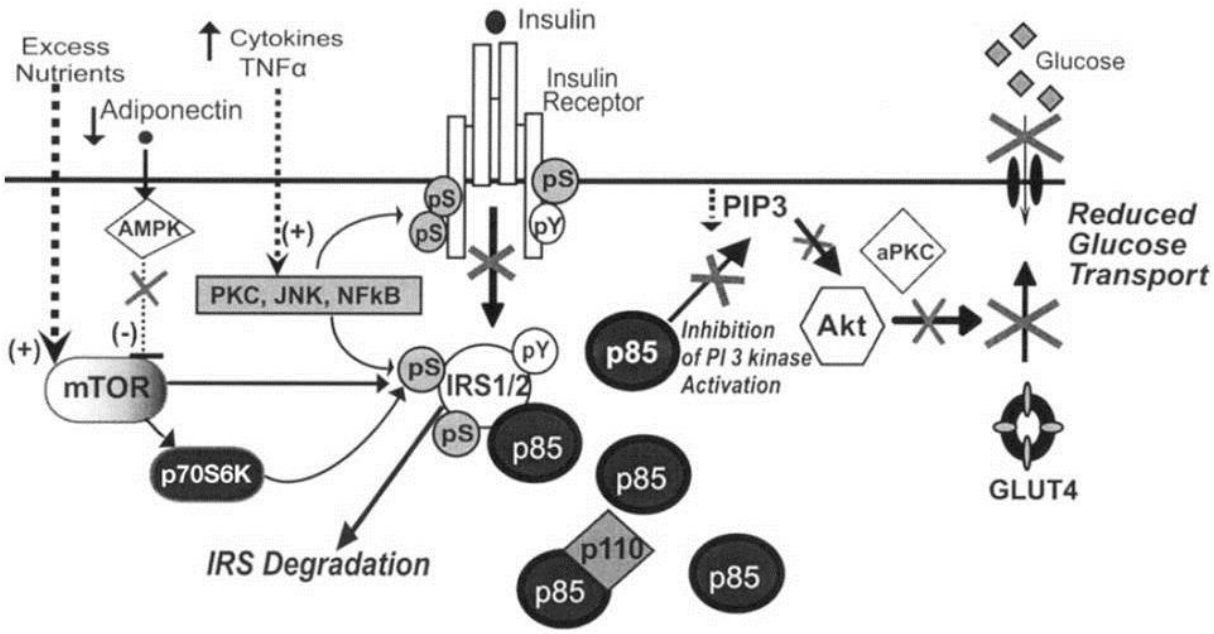

Figure 2: Summary of potential mechanisms for insulin resistance in skeletal muscle during late pregnancy in human gestational diabetes. Akt: v-akt murine thymoma viral oncogene homolog 1 (Proteinkinase B); AMPK: protein kinase, AMP-activated; GLUT4: glucose transporter 4, insulin-dependent; IRS1/2: insulin receptor substrate 1/2; JNK: jun N-terminale Kinasen; mTOR: mammalian target of rapamycin; NFκB: nuclear factor kappa B; p70S6K1: ribosomal protein S6 kinase 1, 70kDa, polypeptide 1; p85: regulatory subunit of phosphoinositol 3-kinase; p100: catalytic subunit of phosphoinositol 3-kinase; PI 3 kinase: phosphoinositol 3-kinase; PIP3: phosphoinositol-3,4,5-phosphate; PKC: protein kinase C; pS: phosphorylation of serine/threonine residues; pY: phosphorylation of tyrosine residues; TNFα: tumor necrosis factor α. Adapted from Barbour et al. [17].

1.4 Inflammatory and vascular changes in pregnancies complicated by pregravid obesity and GDM

Recent evidence suggests that chronic subclinical inflammation might be implicated in the pathogenesis of obesity-related comorbidities and GDM. Circulating pro-inflammatory cytokines like IL6 [20,28,29], TNF-α [18,30] and MCP-1 [31] were increased in obese and/or women with GDM, whereas anti-inflammatory IL10 levels were reduced in GDM subjects [32]. Several studies already found associations between acute phase proteins, like C-reactive protein (CRP), and pregravid BMI [20,31] or GDM risk [33]. Moreover, Challier et al. [29] demonstrated the increased gene expression of monocyte activation markers (CD14, CD68) and inflammatory cytokines (TNF-α and IL6) in peripheral blood mononucleated cells (PBMC) of obese maternal blood samples compared to lean subjects. Pregravid obesity and GDM are also well-established risk factors in the development of hypertensive complications during pregnancy [34]. Particularly the high prevalence of preeclampsia might be explained by chronic preexisting endothelial activation [35]. Endothelial-dependent vasodilation was

impaired in obese women and inversely related to maternal insulin and inflammatory cytokine levels compared to lean women [20,35]. Moreover, soluble intercellular cell adhesion molecule (sICAM) 1 and vascular cell adhesion molecule (sVCAM) 1 that were both associated with endothelial dysfunction and inflammatory processes, are increased in pregnancies with hyperglycemia [36,37].

1.5 Pre-, peri- and postnatal risk factors of obese and/or diabetic mothers and their offspring

Obese women are more likely affected by the 'metabolic syndrome of pregnancy' including hypertension, preeclampsia, disorders of the nutrient metabolism and inflammation [38]. Pregravid obesity is, besides maternal age, ethnicity and family history of diabetes, also the strongest predictor for GDM incidence [39]. In 2010, 3.7 % of pregnant women developed GDM in Germany [14]. In contrast, the prevalence of GDM retrieved from the multicentric large HAPO (Hyperglycemia and Adverse Pregnancy Outcome) study cohort was 16.1 % [9]. Based on the HAPO results, new standard procedures for the oral glucose tolerance test (OGTT) were embedded in the German maternity guidelines and thus, GDM incidence is expected to increase during the following years.

Importantly, pregravid obesity and GDM are also independent risk factors for fetal hyperinsulinemia, large for gestational age (LGA, birth weight > 90^{th} percentile) and macrosomic (birth weight > 4000 g) newborns suggesting both maternal metabolic conditions might influence fetal development through similar mechanism [9]. In this regard, the combination of obesity and GDM was strongly associated with the highest percentile of cord C-peptide levels, birth weight and neonatal body fat [9]. However, the HAPO study recently revealed that the associations of primary adverse outcomes and OGTT results were continuous without identifying a clear inflection point [40]. Accordingly, the HAPO study found a linear correlation between increasing maternal glucose levels and cord C-peptide levels, birth weight and neonatal fat mass concluding that even small changes in glucose levels may have consequences for the offspring development [40]. These results were supported by Landon et al. [41] showing the reduction in offspring birth weight, fat mass and frequency of LGA of the treated mild GDM group compared to the mild GDM control group with usual prenatal care. Both studies emphasized the dietary counselling and self-monitoring of blood glucose even in cases with moderate hyperglycemia.

In early pregnancy, maternal obesity and GDM increase the risk for congenital malformations, miscarriage and placental dysfunction [42,43]. The related health risks also

emphasize the need for specific pre- and perinatal obstetric care. The risk for elective and emergency Caesarean sections, hemorrhages and infections, neonatal requirement for intensive care and prolonged hospital stay is significantly increased in obese women compared to normal weight women [44,45]. Similarly, data from the German perinatal statistics showed that offspring delivered by obese women have higher odds ratios of fetal distress, including abnormal cardiotocography (CTG), green amniotic fluid and fetal acidosis during delivery [46]. The postnatal diabetic fetopathy may comprise of hypoglycemia in consequence of sudden interruption to maternal glucose concentrations as well as abnormalities of calcium and magnesium metabolism, cardiorespiratory function and bilirubin metabolism [43].

Women with GDM have a higher prevalence developing type 2 diabetes *post partum (pp).* The 15-year cumulative risk for *post partum* diabetes in women with GDM was 63.6 % indicating the highest risk for women who required insulin therapy (92.3 %) compared to women with dietary treatment (39.7 %) during pregnancy [47]. Especially for women who gained excessive weight during pregnancy, long-term weight retention contributes to the development of obesity and metabolic disorders in postnatal life [48,49]. Moreover, children born from obese and/or diabetic mothers are at higher risk for obesity and insulin resistance/type 2 diabetes from periods in childhood [8,10,50] through adolescence [10,51] up to adulthood [52,53].

1.6 Adipose tissue development

A considerable amount of evidence has emerged that early life phases are assigned to critical periods for adipose tissue development in humans. The increased proliferation and differentiation capacity of cells isolated from fetal adipose tissue depots and the early determination of adipocytes might establish the framework for later adipose tissue expansion [54]. Thus, the acquisition of adipocytes within perinatal and early postnatal life seems to be an irreversible process. Immature adipose tissue is firstly detectable in the fetus between the 14^{th} and 16^{th} week of gestation [55]. Firstly, mesenchymal cell aggregates form to specific tissue lobules. The vascularization begins at the same time before primitive, and later on definitive, fat lobules appear. In late second trimester, fat tissues are already present in all principle fat deposit areas. It is suggested, that the number of fat lobules within the adipose tissue remains constant from the 23^{rd} week of gestation, therefore, further adipose tissue growth is achieved by the continuous increase of the fat lobules in size (hypertrophy) [56].

The human infant is delivered with a body fat content of 10-14 % in relation to total body mass, that is mainly located in subcutaneous regions [57,58]. Within the 1^{st} year of life, body

fat mass increases up to 20 % assessed by skinfold thickness measurement [58]. There is now growing evidence that adipose tissue is more a multi-functional organ rather than an inert storage site for excess energy [59]. It has been demonstrated that the human adipose tissue, including adipocytes and stromal vascular fraction (SVF) cells, secretes more than 100 different adipokines, cytokines and chemokines exerting multiple effects at the local and systemic level [59].

Adipose tissues are mainly distinguished between subcutaneous adipose tissue, that includes the fat depots under the skin, and visceral adipose tissue that comprises fat around abdominal viscera and inside intra-abdominal solid organs. Recent data suggest that the amount and secretory profile of visceral adipose tissue, rather than subcutaneous adipose tissue, both play an important role in the pathophysiology of insulin resistance and cardiovascular complications [60].

1.7 Fetal programming of obesity and metabolic diseases

There is increasing evidence that intrauterine and early postnatal environment may impact lasting determination of adipose tissue development, cardiovascular and metabolic diseases [61]. The concept of nutritional perturbation during critical developmental periods, e.g. the maternal-fetal hyperglycemia and overfeeding, that promote the development of chronic diseases, is commonly referred to as “fetal” or “perinatal programming’’ **(Figure 3).**

Based on investigations by Barker and Hales et al. [62], the `thrifty phenotype hypothesis’ („Barker hypothesis“) firstly postulated that intrauterine malnutrition, resulting in low birth weight, was associated with metabolic syndrome and cardiovascular diseases in adult life. A systematic meta-analysis emerged that the increased prevalence for type 2 diabetes in children born either underweight or overweight pointed to a U-shaped relationship between birth weight and diabetes risk in later life [61].

Maternal obesity and GDM can be considered as the best-investigated examples for fetal programming so far. Dabelea et al. [63] found in their highly noted study of the Pima Indian population that the risk of diabetes was significantly higher in siblings that were delivered after the mother developed diabetes compared to those born before the mother's diagnosis. Pedersen et al. [64] originally postulated that maternal hyperglycemia results in fetal hyperinsulinemia leading to disproportional growth (macrosomia) and excessive adipose tissue development (Pedersen hypothesis). Subsequent experiments support this theory indicating that maternal-fetal hyperglycemia leads to perinatal hyperplasia and

overstimulation of pancreatic beta-cells, which might affect the insulin secretion in postnatal life. Moreover, increased insulin concentrations within the fetal hypothalamus might impact long-term regulation of body weight, food intake and intermediate metabolism [61]. With regard to the predisposition of cardiovascular diseases in the adulthood, observed alterations in the fetal vasculature of the diabetic placenta and their extension to the umbilical cord vascular cells and fetal heart may also reflect dysregulation in other developing macro- and microvascular endothelial systems of the fetus [65].

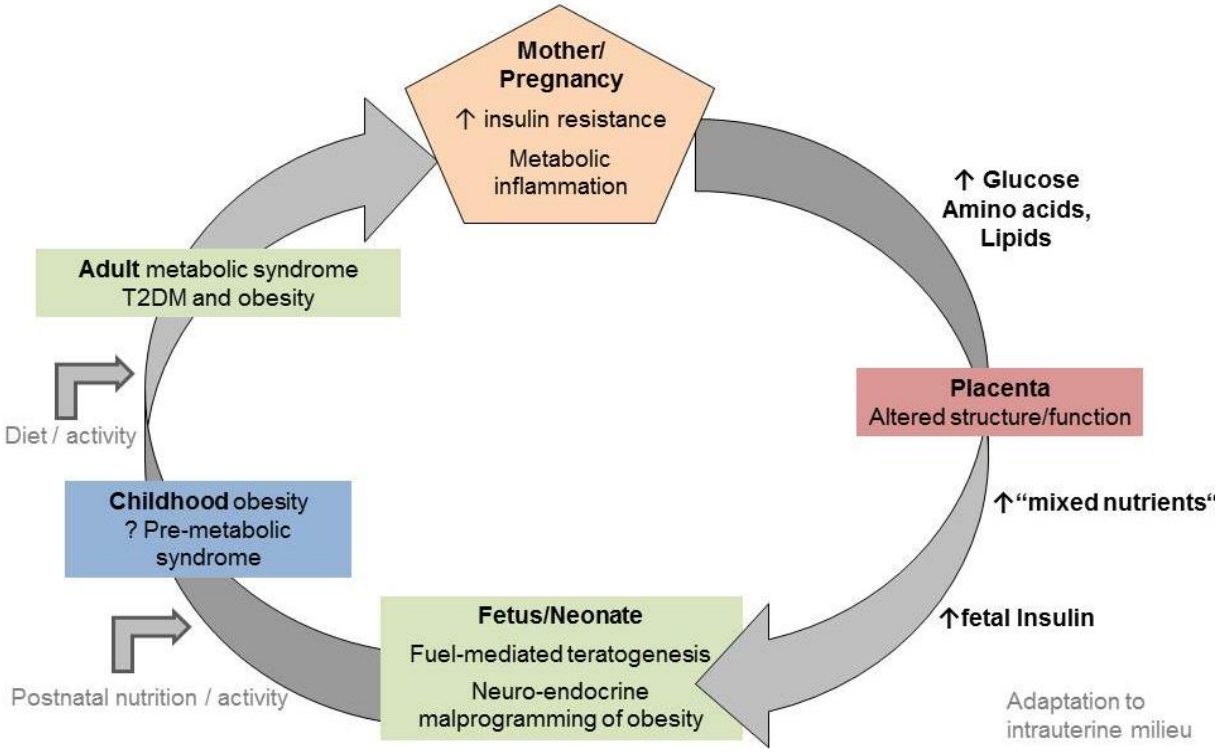

Figure 3: Model of fetal programming and the propagation of a vicious cycle. The intergenerational vicious cycle implicates that women with pregravid obesity and/or GDM delivered more frequently macrosomic females. They are more likely to become obese at childhood and reproductive age and give finally birth to large offspring themselves. T2DM: type 2 diabetes mellitus. Modified from Catalano et al. [38] and Plagemann et al. [61].

1.8 The human placenta

1.8.1 Development of human term placenta

The trophoblast determines large parts of the placenta and fetal membranes. It firstly appears as a single outer cell layer surrounding the embryoblast and the blastocoel of the blastocyst. Immediately after attachment to the uterine epithelium, the trophoblast cell lineage proliferates and differentiates into a cytotrophoblastic layer and an overlying

multinucleated syncytiotrophoblast [66]. The syncytiotrophoblast invades into the endometrial stroma and contact maternal vessels. Later, lacunar networks occurred within the syncytiotrophoblast and blood from eroded maternal vessels is moving within these networks. The remaining syncytiotrophoblast cells between the lacunae and the trabeculae are important for establishing the intervillous space. After successful implantation and initiation of placentation, extraembryonic mesodermal cells migrate to the top of the inner surface of the cytotrophoblast cells forming the chorion together [67].

At that time, cytotrophoblast cells penetrate into the syncytiotrophoblasts of the trabeculae and differentiate into extravillous cytotrophoblast cells. From the primitive basal plate, these cells form the cytotrophoblastic shell. A subset of extravillous cytotrophoblast cells (endovascular trophoblast) invade the decidual stroma and remodel maternal spiral arteries.

Another part of extravillous cytotrophoblasts (interstitial trophoblasts) invade the interstitium of the endometrium and recruit maternal arteries allowing the subsequent expansion of the villous region. Later, interstitial trophoblast cells terminally differentiated in multinucleated placental bed giant cells [66].

Several stages of villous development are discriminable. Primary villi are formed by evaginations of the syncytiotrophoblast (containing a cytotrophoblast core) into the trabeculae, by now intervillous space. Afterwards, extraembryomic mesodermal cells of the chorionic plate grow into the cytotrophoblast primary villi forming a mesenchymal core and turn them into secondary villi. Within the mesoderm, hematopoietic progenitors differentiate into different blood cells. Finally, for the maturation of tertiary villi, the development of placental capillaries is indicated [67].

The importance of accurate placental development is given in the pathology of preeclampsia or intrauterine growth restriction (IUGR). In preeclamptic pregnancies, the extra-villous trophoblasts fail to invade the spiral arteries in the maternal decidua leading to disturbed placentation. The preeclamptic placenta is therefore characterized by an increased uteroplacental vascular resistance and by placental hypoperfusion, resulting in fetal growth restriction [68]

1.8.2 Anatomy of the human placenta at term

At term, the human placenta is a circular, discoidal organ characterized by a diameter of 22 cm, a thickness of 2.5 cm and a weight of approximately 500 g [67]. Comprising of the direct contact of syncytiotrophoblast with maternal blood and the number of trophoblast layers, the mature placenta indicates hemomonochorial characteristics [69].

In the term placenta, the chorionic plate and the intervillous region, the main functional units of the placenta, represent the fetal part **(Figure 4).** The umbilical vessels branch radially into the fetal chorionic vessels forming the chorionic plate. They further give rise to 60-70 stem villi which mechanically stabilize the villous tree and support contracting forces within the blood vessels of the stem villous. A high degree of capillarization is provided by stem villous, branching into the terminal villi representing the final branches [67]. The basal plate denotes the maternal surface of the placenta. It comprises of fetal extravillous trophoblasts and cells derived from maternal uterine decidua. Placental septa subdivide the basal plate into 10-40 cotyledons consisting of 1-2 stem villi and their villous trees [67]. Circulating maternal blood enters the intervillous space via 80-100 endometrial spiral arteries in the decidua basalis. Special gaps in the cytotrophoblastic shell allow the endometrial arteries and veins to reach the intervillous space delimited by the anchoring villi. The maternal blood is temporarily located outside of the maternal circulation and bathes the villi, before it drains back through endometrial veins [69].

The placental villi are completely lined by the villous trophoblast, an epithelium-like two-layer. The mononucleated villous cytotrophoblast proliferate, differentiate and fuse to form the syncytiotrophoblast [66]. The syncytiotrophoblast is a multinucleated polar continuous layer with a basal membrane in contact with the underlying cytotrophoblast/ basement membrane, respectively, and a microvillous apical membrane facing maternal blood. The highly differentiated syncytiotrophoblast is characterized by failed proliferative and decreased transcriptional activity [67].

The placental barrier comprises of all cell layers separating the maternal blood of the intervillous space from the fetal blood in the vasculature in the villi. In the first trimester, the placental barrier consists of four layers: the syncytiotrophoblast, an intact layer of cytotrophoblasts, villous connective tissue and the endothelium of the fetal capillaries. In the second trimester, the particular cytotrophoblasts begin to separate due to fast expansion of villous surface consigning an incomplete layer. During the third trimester, the villous is characterized by occasional recurrent syncytial knots, which consist of nuclei aggregates forming multinucleated bulges in the syncytiotrophoblast layer. These aggregations continually shed from apical membrane into the maternal circulation [69]. Toward term, the mesenchymal core of each villous becomes more compact, and the fetal vessels come very proximal to the placental membrane. Moreover, age-dependent fibrin depositions form on the surfaces of villi, which might impair placental transfer.

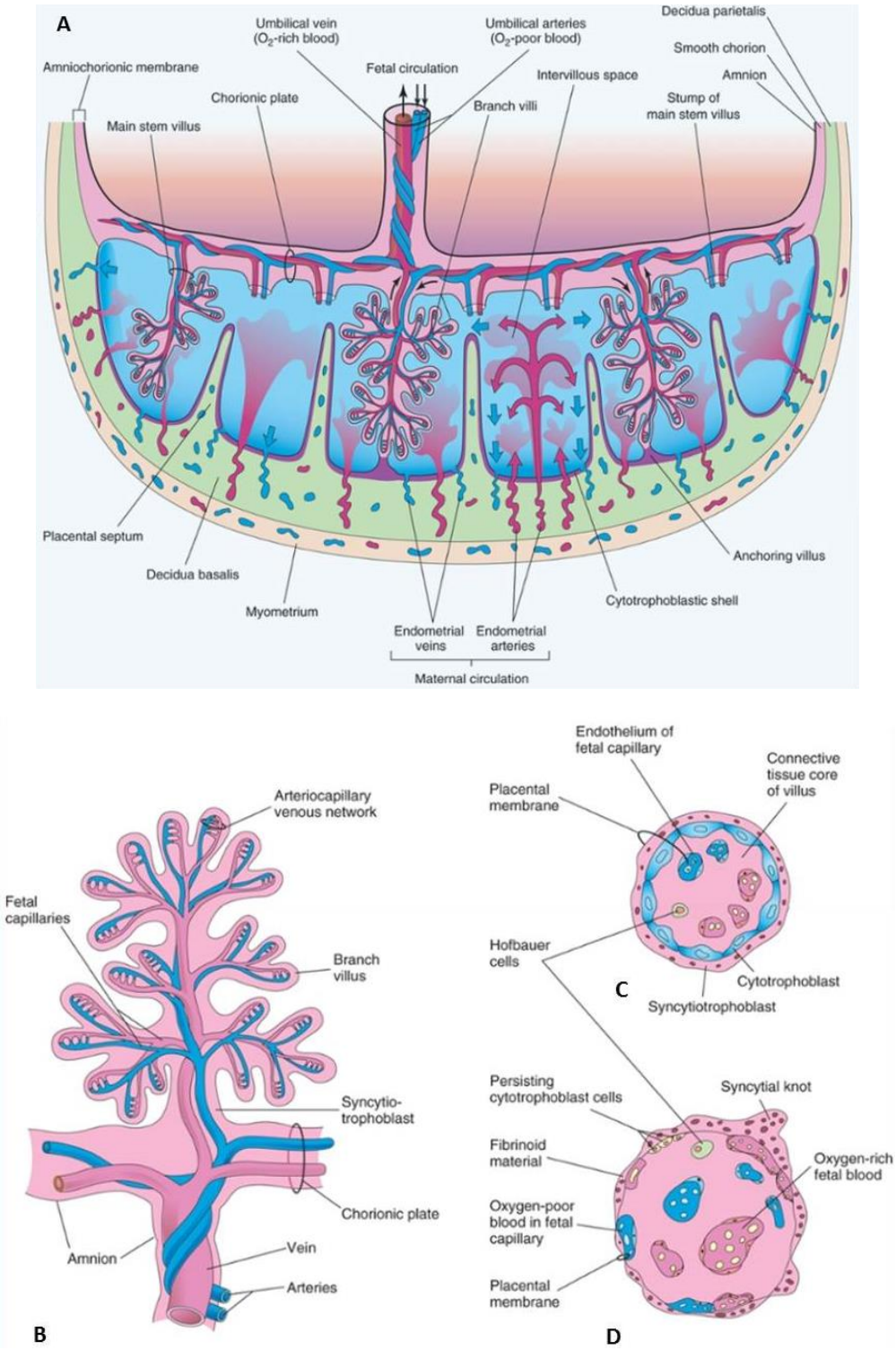

Figure 4: Schematic drawings of the placenta and the chorionic villous. **A)** Transverse section through a full-term placenta, showing the relation of the villous chorion to the decidua basalis, the fetal placental circulation, and the maternal placental circulation. The cotyledons are separated from each other by placental septa, projections of the decidua basalis. **B)** Stem chorionic villous showing its arterio-capillary-venous system. **C)** Section through a terminal chorionic villous at approximately 10 weeks. In the first trimester, the villous contains of an intact syncytiotrophoblast and cytotrophoblast layer forming the placental membrane. Numerous Hofbauer cells and the fetal capillaries are embedded in the villous mesenchyme. **D)** Section through a terminal chorionic villous at full term. The cytotrophoblast disappears from the villous wall and the thickness of the barrier decreases while the surface area increases. The fetal vessels have multiplied their branches and attach closer to the placental membrane. The syncytiotrophoblast nuclei group together in the syncytial knots. Adapted from Moore et al. [69].

1.8.3 Function of the placenta

The primary functions of the placenta can be subdivided into the following categories: transport/metabolism, endocrine functions and protection [66]. The placenta provides oxygen, macronutrients, vitamins and minerals to the fetus, whilst eliminating carbon dioxide and other waste products. The nutrient and waste transport across the syncytiotrophoblast layer is thought to be controlled by the polarized expression of specific transporters in the microvillous membrane (MVM) or basal membrane (BM) [70]. Jansson et al. [71] suggested that the placenta acts like a nutrient sensor supervising the transport functions according to maternal nutrient availability and fetal requirements.

The placenta itself can produce and release various hormones into maternal and/or fetal circulation, including oestrogens, progesterone, chorionic gonadotrophin and placental lactogen. They regulate embryonic development and mediate the required adaptations of the maternal physiology to support the pregnancy [72]. Different delivered growth factors, namely epidermal growth factor (EGF), insulin like growth factors 1 and 2 (IGF1/2), platelet-derived growth factor (PDGF) and cytokines impact maternal adjustment to pregnancy and placental development [66]. Secreted vasoactive peptides (e.g. endothelins) or nitric oxide (NO) might be involved in the control of placental blood flow. The syncytiotrophoblasts also play an essential role in restricting the exposure of the fetus to certain xenobiotics and maternal infections through the blood-placenta barrier [73].

1.8.4 Impact of the placenta in fetal programming

Due to its key role in fetal supply and regulation of fetal development, the placenta assumes an active role in fetal programming [74]. In pregnancies of women with maternal obesity and/or GDM, the placenta undergoes a variety of changes in morphology, hormone/cytokine production and nutrient transport pointing towards an adaptive process [75–77].

Many acquired adverse effects assigned to intrauterine environment might be regulated by epigenetic mechanism [78]. They comprise of modifications in gene activity and chromatin structure that are mitotically and meiotically inherited, however they are not associated to changes in the DNA sequence. The most important epigenetic processes include promoter DNA methylation and histone modification, interactions of micro (mi) RNA and messenger (m) RNA, as well as imprinting genes. Given the link between epigenetic regulatory mechanism and gene expression, it is suggested that environmental exposures can epigenetically impact placental mRNA expression that are associated with particular diseases or risk factors [78]. Moreover, there is an emerging role for placenta-derived miRNA as potential biomarkers for predicting GDM and adverse pregnancy outcomes [79]. With respect to pregnancy-associated diseases (e.g. preeclampsia, IUGR) and neonatal growth,

several environmental influences and maternal nutritional factors have been already linked to alterations in placental methylation [80]. Recently, variant changes in the placental global methylation levels were determined whether pregnancy was complicated by either gestational diabetes or obesity [81].

1.9 Placental abnormalities in pregnancies complicated by obesity and GDM

1.9.1 Placental inflammatory pathways

Alterations in morphologic placental structures might account for the increased risk of pregnancy complications in obese and/or diabetic women. Placentas of women with GDM are often enlarged, thick and plethoric while placental hypertrophy and decreased fetal-to-placental weight also accumulate with increasing BMI categories [75,82]. GDM was reported to alter the utero-placental vascular function via oxidative stress and inflammation [83]. Morphological changes observed in placentas of GDM women might often be inseparable from other maternal comorbidities like hypertension; therefore it is difficult to identify isolated hyperglycemic and insulinemic effects. Thus, diabetic placentas often display increased villous vasculature (chorangiosis) and villous immaturity that is characterized by centrally placed villous capillaries [84]. Other authors found fibrinoid necrosis, villous edema and cytotrophoblastic hyperplasia more frequently in placentas of GDM women [75]. In contrast to the recently described observations of GDM cases, studies investigating the independent impact of maternal obesity on placental microscopic structure are only poorly available [85]. However, with exception of enlarged muscularity of placental vessel walls, no further abnormal findings in the degree of placental maturity, vessel density, fibrin deposition or the formation of syncytial knots/ sprouts were detected in placentas of obese compared to lean women [28].

Similar to adipose tissue, the placenta is a source of adipokines and cytokines regulating energy homeostasis, proliferation and inflammatory processes through endocrine and paracrine mechanism [77]. Cytokines are pattern-specific mainly produced by placenta-specific resident macrophages (Hofbauer cells), trophoblast cells and vascular endothelium cells [86]. Therefore, placental cytokines were proposed to contribute to low-grade inflammation that was observed during late pregnancy compared to pregravid or early gestational stages [18]. Likewise to enhanced systemic inflammation that was found in pregnancies complicated with obesity and GDM **(see chapter 1.4),** higher levels of inflammatory cytokines (IL6, IL1, TNF-α and MCP-1) were expressed in corresponding

placentas [28,29]. Supporting these data, placental biopsies from obese and obese GDM subjects revealed differentially expressed genes assigned to inflammatory pathway and endothelial differentiation [30]. Moreover, Challier et al. [29] found an accumulation of macrophages in the villous stroma of obese women compared to lean controls although the results have been ambiguous [28].

1.9.2 Placental insulin and IGF signaling

In early pregnancy, the INSR is mainly expressed on the microvillous membrane of the syncytiotrophoblasts facing the maternal circulation. In contrast, the INSR in term placentas is predominantly located on fetal endothelial cells in the villous branching directing to the fetal circulation and on Hofbauer cells. This shift in INSR expression might reflect a change in the regulation of insulin effects from mother to fetus [86] The INSR location in later pregnancy stages also indicates an involvement of insulin in angiogenesis and glycogen synthesis [87]. IGF1R is predominantly expressed in cytotrophoblasts at early gestational stages, whereas the IGF1R expression at term placenta is mainly located at the basal membrane of syncytiotrophoblasts and moderately found on Hofbauer cells and endothelial cells. IGF1 und IGF2 regulate migration and invasion in first trimester trophoblasts, whereas they are largely involved in cytotrophoblast proliferation and amino acid transport at later stages. The relationship of fetal insulin and IGF2 levels with placental weight emphasizes their role in controlling placental growth [87]. Several studies found dysregulations in placental insulin and IGF signaling in diabetic women [88,89].

1.9.3 Placental macronutrient supply and transporters

Besides the amount and activity of transporters, the nutrient transfer is affected by several factors including maternal-fetal concentration gradient, blood flow, exchange surface and diffusion distance [76]. However, it seems that changes at the molecular level of transporters are counterbalanced by morphological changes. Consequently, changes in transporter expression *per se* will not necessarily predict the definite transport capacity *in vivo* and makes it difficult to estimate consequences for fetal growth [76].

1.9.3.1 *Placental glucose transport*

The growing fetus is strongly dependent on maternal glucose passing through the placenta, since the fetal glucose production from gluconeogensis is only minimal [76]. A maternal-fetal glucose concentration gradient can normally be observed throughout pregnancy [76]. The

prominent glucose transporter in the villous tissue is the glucose transporter 1 (GLUT1) that provides the glucose transport by facilitated diffusion and independently of insulin [90]. The asymmetrical distribution of GLUT1 in the syncytiotrophoblasts is indicated by higher expression on the MVM than on the BM while the transporter can be also found barely on cytotrophoblast and fetal endothelial cells [91]. The transport across the basal membrane was suggested to represent the rate-limiting step in the transplacental glucose transfer [91]. Unlike to type 1 diabetes, placental glucose transporting capacity of GLUT1 was not increased in GDM irrespective of offspring birth weight [76]. In contrast, GLUT3 protein is only expressed in arterial endothelial cells [91] and, more recently described, in microvillous membranes of villous syncytiotrophoblasts [92], but expression decreased with gestational age. Interestingly, GLUT4, the insulin-dependent GLUT isoform, was not found or only barely detected in intravillous stromal cells, suggesting only minor effects of insulin on maternal-fetal glucose transport.

1.9.3.2 *Placental lipid metabolism*

Normal fetal development is dependent on the supply of maternal fatty acids - especially on the essential linoleic and α-linolenic acid and long chain polyunsaturated fatty acids (LC-PUFAS). Thereby, the lipoproteinlipase (LPL) and endothelial lipase (LIPG) are responsible for the release of fatty acids from TG and phospholipids of maternal lipoproteins [90]. Various membrane-bound proteins, comprising of fatty acid binding protein plasma membrane (FABPpm), fatty acid translocase (CD36) and fatty acid transporters (FATP1-6) are expressed in trophoblasts. Distinct fatty acid binding proteins (FABP) bind to fatty acids in the cytosol providing the interaction with mitochondria, lipid droplets and nuclear transcription factors [93]. They also direct the fatty acid transport to the fetus across the BM by diffusion or facilitated by FATPs. During the first half of pregnancy, maternal cholesterol is sufficient to fulfill the fetal demands [94]. Later, there is an increased fetal cholesterol synthesis rate from gestational week 19 onwards, where fetal cholesterol synthesis via the Kandutsch-Russell pathway becomes important and maternally derived cholesterol only counts with 22-40 % to the fetal cholesterol pool [90,94]. Maternal cholesterol is mainly taken up by LDL- and very low-density lipoprotein (VLDL)-receptor-mediated endocytosis. Additionally, scavenger receptor (SR) class B1 induces cholesterol transfer from high-density lipoprotein (HDL), whereas VLDL is further bound by LDL-related protein (LRP) 1 [90]. ATP-binding cassette (ABC) transporters and SR-B1 are then mainly implicated in the cholesterol efflux to supply fetal lipoproteins [90].

Several authors assume that the placental uptake and transfer of fatty acids and cholesterol is modulated by maternal obesity and GDM. Correspondingly, Radaelli et al. [95] found significantly altered expression of genes involved in cholesterol and lipid biosynthetic pathways in placentas of obese GDM mothers. Other studies determined that the LPL activity and LIPG gene expression were significantly increased in placentas obtained from obese GDM women [26,96]. Nevertheless, several proteins that were involved in lipid transport, particularly CD36, FATP4, FABP4 and FABP5, were dysregulated in pregnancies complicated by maternal obesity and GDM [27,97]. Dubé et al. [26] found that LDL and VLDL receptor gene and protein expressions in villous placental tissues of obese GDM women were significantly elevated.

1.9.3.3 *Placental amino acid transfer and metabolism*

In normal pregnancies, almost all amino acids in the umbilical cord blood are higher concentrated compared to maternal circulation [98]. In addition, the concentration of free amino acids in the placenta exceeds those of maternal and fetal plasma, indicating the appropriate transfer of free amino acids across the placenta is indispensable for fetal growth. Recent studies showed, that 15-20 different amino acid carriers were expressed in the placenta with overlapping substrate specificity and distinct distribution at MVM and BM [90,93]. Studying the uptake of essential amino acids L-lysine, L-leucine and taurine into plasma membrane vesicles, only L-leucine uptake was increased in MVM vesicles isolated from diabetic syncytiotrophoblast plasma membranes [99]. Moreover, Jansson et al. [99,100] determined, that system A amino acid transporter isoform 2 (SLC38A2) activity and protein expression, localized in the MVM, was positively correlated with maternal pre-pregnancy BMI, diabetes and offspring birth weight. The mTOR was identified as positive regulator of placental amino acid transporters like system A and System L [90]. Several reports showed that insulin, IGF-1, leptin and amino acids may induce mTOR nutrient sensor signaling. Moreover, mTOR stimulate cell proliferation and growth via modulating proteins that were involved in protein synthesis. In this context, increased mTOR signaling was positively related to pregravid maternal BMI [100], GDM [101] and infant birth weight [100].

1.10 Concluding remarks

In recent years, inflammatory processes and metabolic disturbances, such as maternal adiposity and GDM, has been suggested to play important roles in mediating adverse pregnancy outcomes for mother and fetus, e.g. influencing fetal metabolism and

adipogenesis and having programming effects on offspring health. Therefore, new investigations are necessary to identify and differentiate factors in maternal obesity and GDM, which have a causal link or biomarker function with respect to these processes. Furthermore, it is still not understood, how deregulated signaling pathways and cellular processes are related to fetal adipogenesis or whether they point to potential analogue signaling pathways in fetal adipocytes or other cells that might influence the development of infant adipose tissue.

2 Aim of the study

There is increasing evidence, that obesity and related metabolic disorders are programmed during perinatal and early postnatal periods. Thus, the investigation of maternal and fetal plasma markers placental function and early adipose tissue growth parameters in relation to a later risk of obesity and the identification potential preventative measures against childhood obesity is strongly demanded. In the context of early adipose tissue markers, preperitoneal adipose tissue (PPA) assessed by ultrasonography has been proposed as a surrogate for visceral/intra-abdominal fat. Nevertheless, there is missing information about maternal and fetal metabolic biomarkers (e.g insulin and leptin) associated with the distribution of PPA and subcutaneous adipose tissues (SCA) in neonates and early infancy, especially in pregnancies with pregravid obesity and GDM. Considering the importance of the placenta for fetal growth, it is of great scientific interest to get molecular insight into placenta-mediated processes that are involved in metabolic programming effects of infant growth in general, and in adipose tissue development in particular. A few studies, recently studying global placental gene expression in GDM, reported on increased expression of inflammatory processes and endothelial dysfunctions as typical feature of GDM pregnancy, but did not consider maternal pregravid BMI without GDM. Therefore, the pilot study *GesA* (**Ges**tational diabetes mellitus, maternal **a**diposity and early childhood obesity) was conducted at the Chair of Nutritional Medicine (Prof. Dr. H. Hauner), Technische Universität München, Germany, to assess the impact of maternal pregravid obesity and the additive effect of GDM on childhood obesity. This *GesA* study offered the possibility to provide lacking comprehensive data for placental transcriptomic analysis between obese and lean subjects and their relationship to postnatal adipose tissue development. The aims of this PhD thesis were:

(1) Recruitment and characterization of pregnant obese women without and with GDM and normoglycemic lean women for the *GesA* study, as well as the collection of maternal and newborn blood and plasma samples and placental tissues.

(2) Examination of offspring body composition and fat distribution during year-1.

(3) Analyses of the relationship between maternal and newborn plasma factors and offspring adipose tissue distribution markers.

(4) Investigation of placental global gene expression with respect to maternal pregravid obesity and the additional impact of GDM compared to lean subjects.

(5) Identification of novel genes and associated signal pathways in the placenta, which are differentially regulated by maternal obesity with and without GDM and the evaluation of their link to postnatal adipose tissue growth up to year-1.

3 Study design, subjects and methods

3.1 General description of the study

The *GesA* study is a monocenter pilot trial with three parallel groups of pregnant and lactating women and their infants **(Figure 5)**. The study was primarily designed to examine the effect of pregravid obesity and GDM in pregnant women and breastfeeding mothers on placental gene expression and adipose tissue growth in their offspring. The study protocol was registered at the German clinical trials register (DRKS00004370) and approved by the ethical committee of the Technische Universität München (project number: 2629/09).

3.2 Primary and secondary endpoints

The measurement of the infant's fat mass assessed by skinfold thickness (SFT) measurements and by complementary ultrasonography was the primary outcome parameter of the study **(Figure 5).** Key secondary endpoints included (1) the assessment of infant growth parameters (body weight, height, head, arm and waist circumference), (2) the analysis of lipid, insulin, adipokine and cytokine concentrations in maternal and fetal blood samples and the determination of placental gene and protein expressions and (3) the relationship of plasma biomarkers and placental signaling parameters with offspring adipose tissue distribution markers.

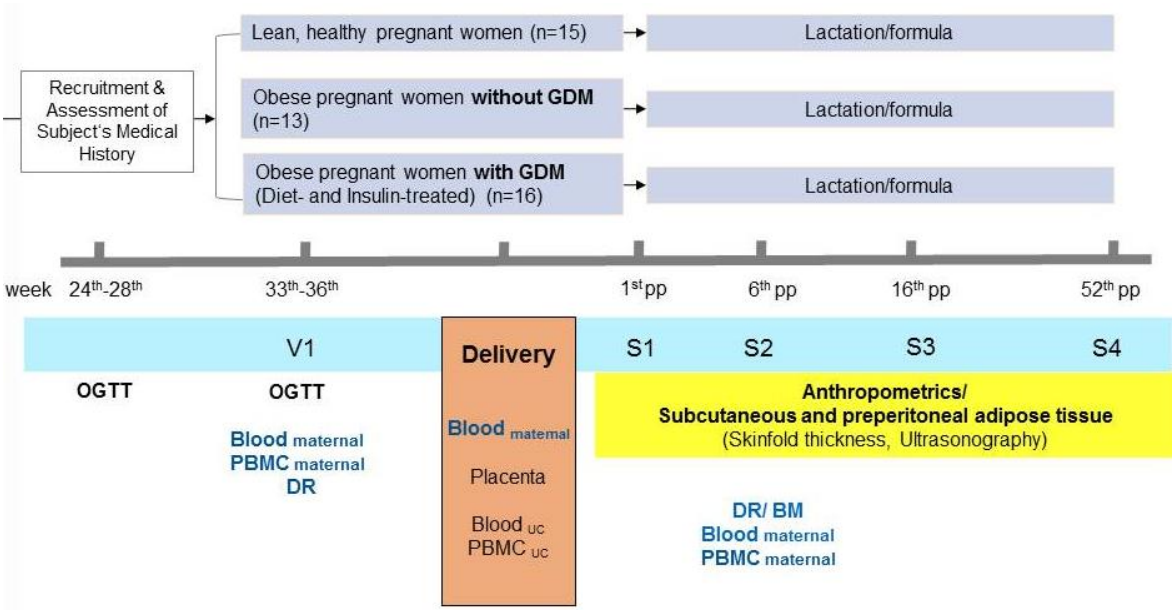

Figure 5: Study design of the *GesA* study. DR: dietary record; BM: breast milk; OGTT: oral glucose tolerance test; PBMC: peripheral blood mononuclear cells; pp: *post partum*; UC: umbilical cord

3.3 Recruitment and screening

Pregnant women were mainly recruited at the *Abteilung für Geburtshilfe und Perinatalmedizin der Frauenklinik,* Technische Universität München, Munich, Germany.

Further recruitment centers were the Department of Obstetrics and Gynaecology, Ludwig-Maximilians-University Munich, Germany and the *Medizinische Klinik und Poliklinik IV, Diabetes Zentrum - Campus Innenstadt, Klinikum der Universität München*, Munich, Germany. Inclusion and exclusion criteria are summarized in **Table 1**. Written informed consent was obtained from participants before their first appointment. The study group consisted of Caucasian pregnant women, who were divided into three groups according to their self-reported pregravid BMI and the result of the oral glucose tolerance tests in the 2nd and 3rd trimester: normoglycemic lean (BMI 18.5-25 kg/m^2; n = 15), obese women without GDM (BMI > 30 kg/m^2; n = 13), and obese women with GDM (BMI > 30 kg/m^2; diet-controlled n=7, insulin treated n = 9). Women underwent oral glucose tolerance test (OGTT) in the 2nd trimester and, in case of negative result, were retested in the 3rd trimester to confirm glucose tolerance and to re-evaluate group allocation. The diagnosis of GDM was defined according to HAPO criteria: fasting plasma glucose > 5.1 mmol/L (92 mg/dL), 1 h plasma glucose > 10.0 mmol/L (180 mg/dL), 2 h plasma glucose > 8.5 mmol/L (153 mg/dL). GDM is diagnosed if ≥ 1 of the thresholds was met or exceeded [40]. Besides monitoring their glucose levels, all GDM participants had dietary counseling and, if necessary, appropriate insulin treatment.

Table 1: Maternal and fetal inclusion and exclusion criteria (according to study protocol)

	Inclusion criteria	**Exclusion criteria**
Maternal	18 < Age < 43 years	Risk pregnancies like multiple pregnancy, rhesus incompatibility, hepatitis B/C infection, preeclampsia, HELLP syndrome or parity > 4
	Sufficient German language skills	Chronic hypertension
	Written informed consent	Type 1 oder type 2 diabetes
		Gastrointestinal disorders accompanied by maldigestion, malabsorption or elevated energy and nutritional requirements Known metabolic defects (e.g. phenylketonuria)
		Psychiatric diseases
		Alcohol abuse or smoking
Infant	Healthy newborn (according to newborn screening)	SGA (Birth weight < 10th percentile)
	Delivery between 37th and 42nd week of gestation	Birth deformities or morbidities
	APGAR > 7 (at 5 min)	Chromosome abnormality
		Metabolic defects

APGAR: abbreviation for **A**ppearance, **P**ulse, **G**rimace, **A**ctivity and **R**espiration (quick evaluation of a newborn's physical condition); HELLP: abbreviation for **H**emolysis, **EL**evated liver enzymes, **L**ow **P**latelet count; SGA: small for gestational age

3.4 Blood and tissue collection

Venous blood samples were obtained from fasted women during 33-36th week of gestation and before delivery (after insertion of an intravenous catheter). Neonatal blood was collected immediately after delivery from umbilical cord vein and artery. Furthermore, fasted venous maternal samples were obtained at week-6 after delivery. Blood samples were collected for the measurement of differential blood counts and HbA1c (EDTA KE monovettes, Sarstedt, Nurnbrecht, Germany), lipid profiles (Serum monovettes, Sarstedt) and glucose (EDTA-NaF monovettes, Sarstedt) at a certified laboratory **(see chapter 3.6).** Additional blood samples were obtained (EDTA KE monovettes, Sarstedt) and centrifuged (30 min, 1750 x g, room temperature) before respective plasma samples were stored at -80 °C for further analysis at the Chair of Nutritional Medicine.

After delivery, placentas were kept on 4°C and sample dissection was performed according to a standardized sampling protocol. The placenta was examined and abnormalities were thoroughly documented (e.g. completeness, infarcted or calcified areas and umbilical cord insertion) before the weight was determined **(Figure 6 A and B)**. In accordance with the preparation protocol, six placental tissue pieces were dissected from each of the four quadrants with 3 cm distance from the centre of the placenta while avoiding the sampling of macroscopic abnormalities **(Figure 6 C and D)**. Maternal basal plate and fetal chorionic plate were dissected from chorionic villous tissue and all three fractions, corresponding to the four quadrants of the placenta, were obtained separately (each 1 cm^3). All placenta samples were frozen in liquid nitrogen within 90 min after offspring delivery and stored at - 80 °C for further analysis.

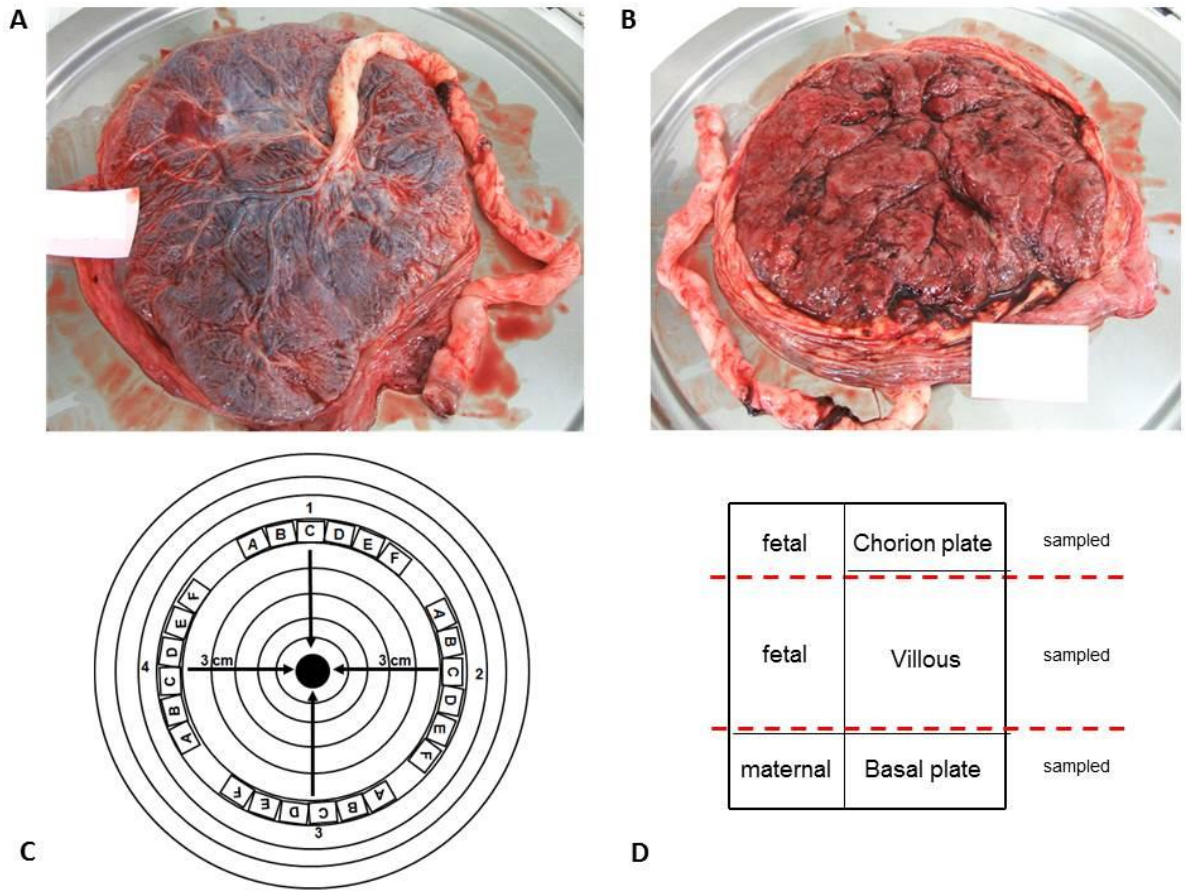

Figure 6: Human term placenta obtained from *GesA* study. A) Chorionic plate. **B)** Basal plate. **C)** Schematic picture with view on the chorionic plate showing the umbilical cord insertion in the middle of the placenta (black circle). The protocol requires sampling of six pieces (A-F) per quadrant (1 - 4). Samples A-E were snap-frozen in liquid nitrogen and samples F were formalin-fixed. **D)** Cross-sectional view through the placenta. Villous fraction was dissected from the chorionic and basal plate and all pieces were collected separately. Pictures A) and B) provided by Kirsten Uebel.

3.5 Infant growth and adipose tissue development

3.5.1 Infant anthropometric assessment

Anthropometric data and adipose tissue development measurements were performed as originally described by Hauner et al. [58]. Briefly, birth weight, height and head circumference were obtained from the obstetric protocol. At visit at week-6, month-4 and year-1 *pp*, the infant weight was measured at the study center to the nearest 10 g by a standardized infant scale (Babywaage Ultra MBSC-55; myweight ®, Erkelenz, Germany). Height was determined with a measuring stick (Säuglingsmessstab seca 207; Seca, Hamburg, Germany) to the nearest 0.1 cm while the infant was supine with stretched legs. The ponderal index (kg/m^3) was calculated according to the measured variables. Head circumference, arm circumference and waist circumference (only at year-1) were determined to the nearest 0.1 cm with a tape measure (Prym GmbH & Co. KG, Stolberg, Germany).

3.5.2 Infant fat mass and fat distribution assessed by SFT

SFT measurements were performed by only one researcher at day 2–5 *pp* in the obstetric clinic as well as at week-6, month-4 and year-1 *pp* in the study center. SFTs were determined in triplicates with a Holtain caliper (Holtain Ltd, Crosswell, Crymych, UK) at the infant`s left body axis at the following four sites: triceps, halfway between the acromion process and the olecranon process; biceps, 2 cm proximal to the skin crease of the elbow; subscapular, below the inferior angle of the left scapular and diagonal to the natural cleavage of the skin; suprailiac, along the midaxillary line above the iliac crest **(Figure 7).** Total body fat and lean mass were calculated via predictive SFT equations according to the method of Weststrate and Deurenberg [102]. Moreover, the description of subcutaneous body fat distribution was evaluated by the subscapular-triceps SFT ratio [103] and the percentage of trunk to total SFTs [104], applying the following equation:

(subscapular + suprailiac SFT) / (sum of 4 SFTs) x 100.

Figure 7: Skin fold thickness (SFT) assessment. A) Holtain Ltd. Caliper **B)** Suprailiacal and **C)** Tricipital SFT measurement at month-4 *pp*. Pictures B) and C) provided by Kirsten Uebel.

3.5.3 Infant fat mass and fat distribution assessed by ultrasonography

Ultrasound imaging, as described originally by Holzhauer et al. [105], and modified by Hauner et al. [58], was performed by two researchers, including one pediatrician, that was blinded to study group allocation, at week-1, week-6, month-4 and year-1 **(Figure 8 and Figure 9).** A high-resolution ultrasonographic system (Acuson Premium; Siemens Healthcare, Erlangen, Germany) with a 10-MHz linear probe (VFX 13–5; Siemens Healthcare, **Figure 8**) was applied. Abdominal subcutaneous and preperitoneal fat thickness was measured in sagittal planes as areas of 1-cm length below the xiphoid process **(Figure 10)**. Additionally, subcutaneous fat was determined in axial planes as areas of 1-cm length in the middle of the xiphoid process and the navel directly above the linea alba **(Figure 11)**.

A B

Figure 8: Ultrasonographic investigation. A) 10-MHz linear probe **B)** Assessment of preperitoneal and subcutaneous adipose tissue areas in sagittal plane at month-4 *pp*. Picture B provided by Kirsten Uebel.

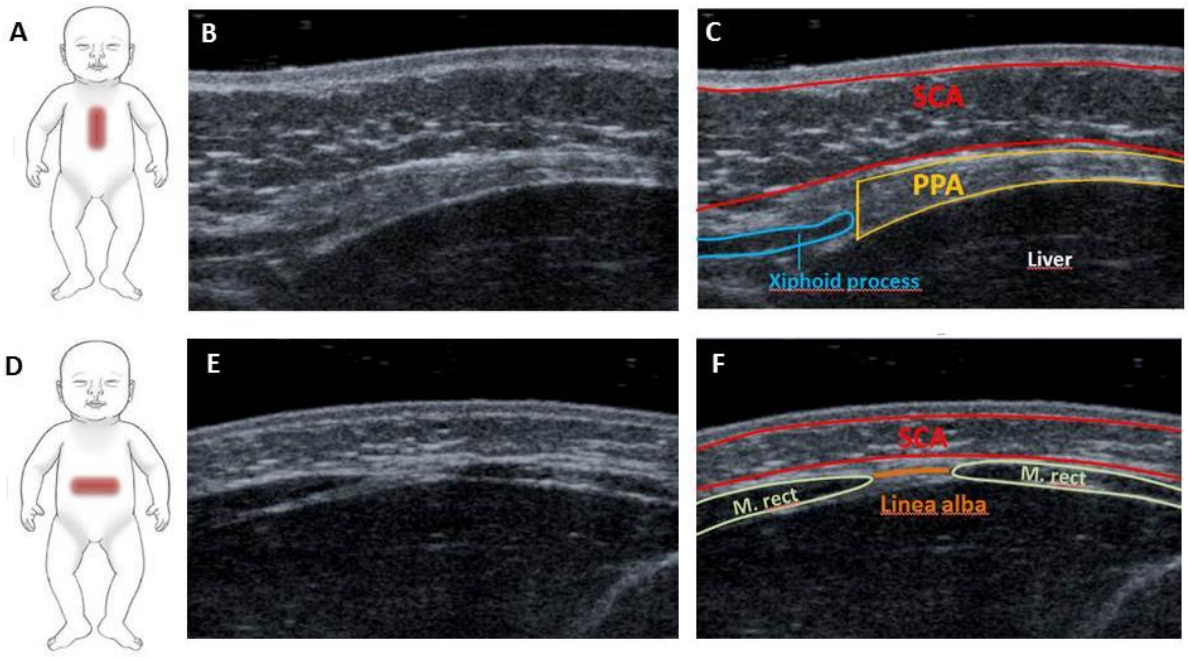

Figure 9: Examples for ultrasonograhic images assessed in the sagittal and axial plane. Schematic pictures demonstrate holding technique in sagittal **(A)** and axial **(D)** direction. The red line illustrates the direction of the linear probe. **B)** Example for picture taken in sagittal plane directing linear probe exactly along the linea alba. **E)** Example for picture in axial plane taken in the middle of the xiphoid process and the navel directly above the linea alba. **C)** and **F)** Respective pictures with labelling of the anatomic structures. M. rect: musculus rectus abdominis (light green); PPA: preperitoneal adipose tissue (yellow); SCA: subcutaneous adipose tissue (red). Pictures provided by Kirsten Uebel.

3.5.4 Evaluation of the ultrasound images

The areas of the infant's fat layers were determined in the sagittal and axial plane with the Osirix imaging software (Pixmeo; Genf, Switzerland; http://www.osirix-viewer.com). For

every age of investigation, the analysis was repeatedly performed in 6 different images (3 images of each plane) and the means were calculated.

3.5.4.1 *Assessment of preperitoneal fat*

The preperitoneal fat layer was only determined in the sagittal plane and was defined as area between the linea alba, forming the upper border, and the peritoneum, representing the lower border. The first reference point was set 0.5 cm caudal from the xiphoid process (sag cranial PPA) while the second measurement was conducted 1 cm caudal from the first reference point (sag caudal PPA) **(Figure 10).**

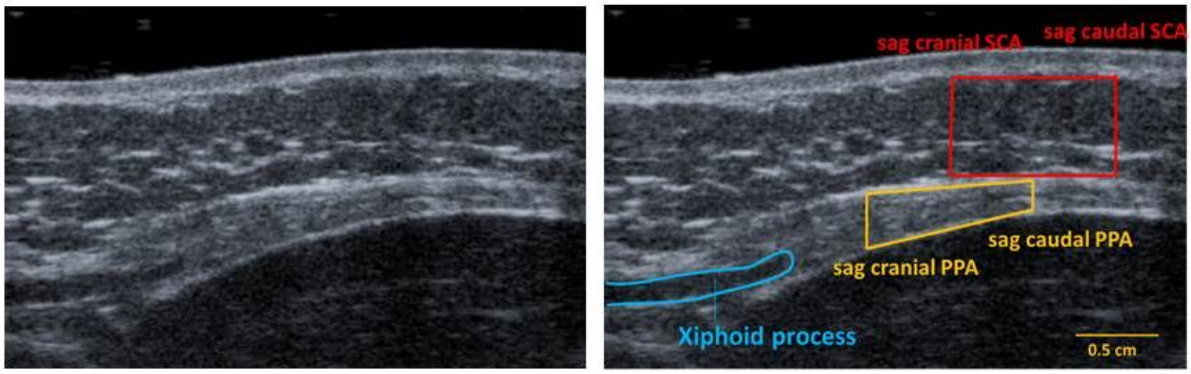

Figure 10: Example for the assessment of SCA (red) and PPA (yellow) adipose tissue in the sagittal plane. Subcutaneous and preperitoneal fat areas and reference points are indicated. PPA: preperitoneal adipose tissue (yellow); Sag: sagittal; SCA: subcutaneous adipose tissue (red). Pictures provided by Kirsten Uebel.

The area of preperitonal fat was calculated according to the formula for trapezoid areas.

$$\text{A sag PPA} = \frac{\text{sag cranial PPA [cm]} + sag\ caudal\ PPA\ [cm]}{2} \times 1\ [cm]$$

3.5.4.2 *Assessment of subcutaneous fat*

The subcutaneous fat was defined according to the echo-poor space between the cutis and the linea alba (M. rectus abdominis). The subcutaneous fat layer was determined in the sagittal and axial plane.

The starting point for determining subcutaneous fat layer in the sagittal plane is the xiphoid process, the lowest restriction of the sternum **(Figure 10)**. The first reference

point is set by definition 1 cm caudal from the xiphoid process (sag cranial SCA) and the second reference point is placed 1 cm caudal of the first reference point (sag caudal SCA).

$$A\ sag\ SCA = \frac{sag\ cranial\ SCA\ [cm] + sag\ caudal\ SCA\ [cm]}{2} \times 1\ [cm]$$

The evaluation in the axial plane was carried out directly above the linea alba (ax_m) as well as 1 cm on the right (ax_r) and on the left (ax_l) of the linea alba between the M. rectus abdominis and the cutis **(Figure 11).**

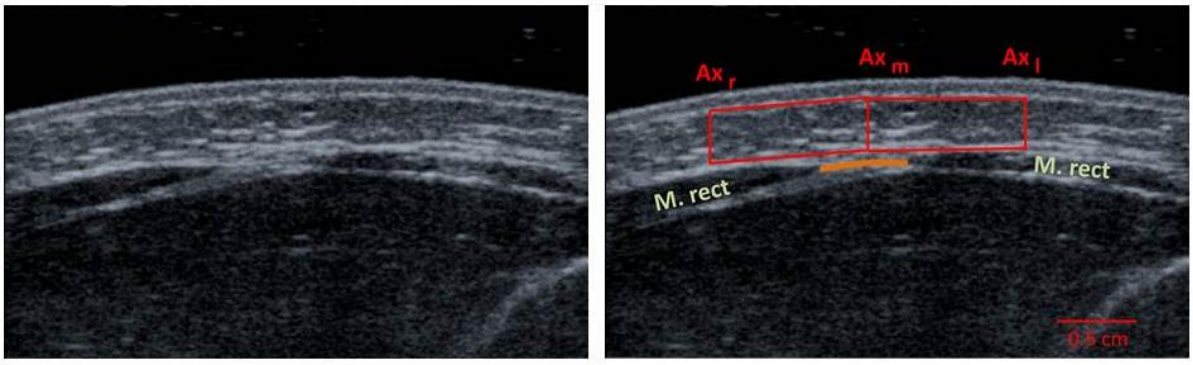

Figure 11: Example for the assessment of SCA (red) adipose tissue in the axial plane. Subcutaneous fat areas and reference points are indicated. ax_m: axial plane directly above the linea alba; ax_l: 1 cm on the left side in relation to ax_m; ax_r: 1 cm on the right side in relation to ax_m. M. rect: musculus rectus abdominis; SCA: subcutaneous adipose tissue. Pictures provided by Kirsten Uebel.

$$A\ ax\ SCA = \frac{(ax\ l\ [cm] + ax\ m\ [cm] \times 1\ [cm]) + (ax\ r\ [cm] + ax\ m\ [cm] \times 1\ [cm])}{4}$$

The ratio of preperitoneal to subcutaneous fat was calculated by using the area of preperitoneal fat layer divided by the mean of subcutaneous sagittal and axial fat layer.

$$\text{Ratio}\ \frac{\text{PPA}}{\text{SCA}} = \frac{\text{A sag PPA}}{\frac{\text{A sag SCA} + \text{A ax SCA}}{2}}$$

3.5.4.3 *Accuracy of ultrasonography assessment*

Based on finally 44 study participants, the ultrasonographic images of five infants, who underwent all four ultrasonography assessments (week-1, week-6, month-4 and year-1), were randomly chosen. The three images of each sagittal and axial plane were analyzed by a second, completely blinded, person. Accordingly, the evaluation of a total of 120 images from independent assessments was obtained. The interobserver variability was calculated by interclass correlation and further validated by the Bland Altman-plot [106].

3.6 Blood measurements

Maternal differential blood profiles obtained at 3rd trimester, before delivery and at week-6 *pp* were determined by flow cytometry and HbA1c was analyzed by immunoturbidimetry (TinaQuant, Roche Diagnostics, Mannheim, Germany). Serum lipid parameters, namely total, LDL and HDL cholesterol as well as TG were determined at all scheduled maternal sampling time points and from umbilical cord by using enzymatic methods (Roche Diagnostics). Corresponding maternal and umbilical cord plasma samples were kept for glucose assessment by the glucose oxidase method [107]. Plasma high sensitive CRP was only assessed in maternal samples at 3rd trimester by immunoturbidimetry (Roche Diagnostics). All measurements mentioned above were performed at Synlab, Munich, Germany.

Fasted maternal plasma and cord plasma insulin as well as fasted maternal plasma C-peptide were analyzed using a commercially available ELISA (Dako, Glostrup, Denmark). Maternal homeostasis model of assessment of insulin resistance (HOMA-IR) was determined according to the formula: HOMA-IR-index = [Insulin (µU/mL) x Glucose (mmol/L)] / 22.5. Maternal and cord plasma levels for leptin (R&D Systems, Minneapolis, MN, USA) as well as total adiponectin and HMW adiponectin (ALPCO, Salem, NH, USA) were determined by ELISA. The ratio of HMW to total adiponectin (S_A) was calculated for each plasma sample. Plasma IL6 was measured using the Quantikine High-sensitivity ELISA kit according to the manufacturer's instructions (R&D Systems). All calculated intra- and inter-assay coefficients of variation (CV) were less than 10 %.

3.7 RNA extraction

Placental villous biopsies of each of the four quadrants were ground in liquid nitrogen and 250 mg of each pooled placenta sample (4 x 65 mg villous tissue samples) were homogenized in Tri-Reagent® (Sigma-Aldrich, Taufkirchen, Germany). Subsequently, total RNA was extracted by the RNeasy Midi kit® (Qiagen, Hilden, Germany), including DNase I treatment in accordance with the manufacturer's instructions. The RNA concentration was

determined by measuring absorbance at 260 nm (NanodropTM 1000 Spectrophotomerter; Peqlab Biotechnology GmbH, Erlangen, Germany) and RNA integrity was assessed by Agilent 2100 Bioanalyzer (Agilent Technologies GmbH, Böblingen, Germany). Only samples with an RNA integrity number (RIN) above 6.5 were used for further analysis.

3.8 Microarray analysis

The microarray analysis was conducted on the Illumina® platform (Illumina, San Diego, CA, USA) in cooperation with Dr. Martin Irmler at the Institute of Experimental Genetics, Helmholtz Institute, Neuherberg, München.

Microarray profiling analysis was conducted from placentas of lean (n=9), obese (n=10) and obese insulin-treated GDM (n=8) women. 300 ng of total RNA were amplified using the Illumina® TotalPrep RNA Amplification kit (Ambion, Austin, TX, USA). Amplified cRNA was hybridised to HumanHT-12_v4 Expression BeadChips in the hybridisation oven (Illumina). Staining and scanning with the HiScan BeadArray Scanner was done according to the Illumina® expression protocol. Data were processed using the GenomeStudioV2010.1 software (gene expression module version 1.6.0) in combination with the HumanHT-12_V4_0_R2_15002873_B.bgx annotation file (Illumina). The background subtraction option was used and an offset was introduced to remove remaining negative expression values. CARMAweb was used for quantile normalisation [108]. Data were filtered before applying statistical methods for an average expression ≥ 30 in at least one study group. Statistical transcriptome analysis was conducted on $\log_2$-transformed data utilizing CARMAweb.
The hierarchical dendrogram and the Principle component analysis (PCA) of placental microarray data were conducted with all genes passing the initial expression filter ≥ 30 in at least one group on $\log_2$-transformed data (25722 genes). Both analyses were performed by the “R” statistical package (R Development Core Team, Auckland, New Zealand).

Genewise testing for differential expression was done employing the limma t-test and Benjamini-Hochberg multiple testing corrections. With regard to the obtained limited number of differentially regulated genes after using the false discovery rate (FDR), further analysis was continued with raw p-values. The following three pairwise group comparisons were conducted: (1) obese vs. lean group, (2) obese GDM vs. lean group and (3) obese GDM vs. obese group. The differentially expressed genes meeting the criteria for fold change (FC) ≥ 1.3 / ≤ -1.3 and p-value < 0.05 from pairwise comparisons were used for further pathway analysis.

The genes retrieved from the three comparisons were up-loaded into the web-based *Ingenuity Pathway Analysis* (IPA, Ingenuity Systems, Redwood City, California, USA,

www.ingenuity.com). IPA algorithmically generates networks according to their connectivity. The assigned score (negative log of p-values of Fisher tests) ranks the networks based to their relevance of supplied datasets. The discovered networks are presented as diagrams specifying the molecular relationships between genes. Genes are represented as colored nodes indicating the degree of up-regulation (red) or down-regulation (green). Genes represented in uncolored nodes are not differentially expressed in the uploaded data sets and were integrated into the generated networks based on the IPA knowledge memory showing their relevance to the particular network. The various shapes of the nodes represent the functional class of the genes and the biological relationships between the nodes are indicated by different lines. Edges are displayed with various labels that describe the nature of the relation between the nodes.

The Genomatix genome analyzer server (Genomatix, Munich, Germany; www.genomatix.de) was further applied for exploring signal transduction pathways, thus differentially regulated genes were uploaded into *Genomatix Pathway System (GePS)*. Significantly regulated pathways with p-values < 0.05 were thoroughly reported.

3.9 qPCR analysis

The differential expression of specific target genes was evaluated with the reverse transcription quantitative polymerase chain reaction (RT-qPCR). 10 ng total RNA of each sample were used per reaction applying the QuantiTect SYBR Green one-step-RT-PCR kit (Qiagen, Hilden, Germany) following the manufacturer's instruction. RT-qPCR was performed using the realplex^4 Mastercycler epgradient S (Eppendorf, Hamburg, Germany). The following amplification conditions were used: cDNA synthesis at 50 °C for 30 min terminated by reverse transcriptase enzyme inactivation at 95 °C for 15 min; 40 cycles of denaturation (95 °C for 15 s), annealing (60 °C for 30 s) and elongation (72 °C for 30 s), followed by a terminal melting curve. Cq-values were retrieved from the *CalqPlex* algorithm (realplex 2.0 software, Eppendorf), and analyzed according to the ΔΔCq-method [109]. The target genes were normalized using the geometric mean of β-actin (ACTB), and H2A histone family, member Z (H2AFZ). For RT-qPCR analysis, DNA oligonucleotides were obtained from metabion international AG (Planegg-Martinsried, Germany). Selected primer pairs should include an amplicon size of 80-150 base pairs (bp) and if possible, span exon-exon junctions. Primer length should be between 18-25 bp assigning a G-C base pair content of 40-70 %, a T_m (salt-adjusted) of 60-64 °C and a T_m (nearest neighbor) of 56–58 °C (OligoCalc; www.basic.northwestern.edu/biotools/oligocalc). The primer pairs were tested for self-complementarity (OligoCalc), heterodimer formation (IDT OligoAnalyzer (http://eu.idtdna.com/analyzer/applications/oligoanalyzer)) and target specificity (UCSC *in*

silico PCR; http://genome.ucsc.edu). Moreover, the specificity of the primers as well as their appropriate annealing temperature were ensured by melting curve analysis of the amplification products and agarose gel electrophoresis. RT-qPCR assays were controlled by non-template and (–)-RT assay controls for applied primers.

3.10 Western Blot analysis

Total protein extraction. Pooled villous placental tissues of the four quadrants were homogenized in radioimmunoprecipitation assay buffer (RIPA: 150 mM NaCl, 50 mM Tris, 1 mM EDTA, 1% Nonidet-P40, 0.2 % SDS, 0.25 % sodium deoxycholate; pH 7.4). Protease and phosphatase inhibitors were added as listed: protease inhibitor cocktail (Sigma-Aldrich, diluted 1:100 in RIPA puffer), 25 mM NaF, 20 nM Calyculin, 50 mM β-glycerol-phosphat Na_2, 1 mM EDTA. Samples were centrifuged (2000 x g, 2 min, 4 °C) to remove cell debris. The protein concentration was determined with the *Pierce® BCA protein Assay Kit* (Thermo Scientific, Rockford, IL, USA).

Nuclear protein extraction. Pooled villous placental tissues of the four quadrants were homogenized in homogenization buffer (10 mM HEPES (pH 7.9), 1.5 mM $MgCl_2$, 10 mM KCl, 20 mM NaF, 0.5 mM Dithiothreitol (DTT); with protease and phosphatase inhibitors as listed above) applying glass potters. After centrifugation (3300 x g, 15 min, 4 °C), the cell nuclei pellet was suspended in 40 µl low salt buffer (20 mM HEPES, 1.5 mM $MgCl_2$, 20 mM KCl, 0.2 mM EDTA, 20 mM NaF, 25 % glycerol [v/v], 0.5 mM DTT; with protease and phosphatase inhibitors as listed above), and subsequently mixed with 40 µl high salt buffer (20 mM HEPES, 1.5 mM $MgCl_2$, 1.2 M KCl, 0.2 mM EDTA, 20 mM NaF, 25 % glycerol [v/v], 0.5 mM DTT; with protease and phosphatase inhibitors as listed above). Afterwards, the mixture was agitated vigorously for 30 min at 4 °C and centrifuged (25000 x g, 30 min, 4 °C). The supernatant contain the nuclear protein extract and the protein concentration was further assessed by Bradford reagent (Bio-rad, Munich, Germany).

Western immunoblot. Protein samples were denatured in *Laemmli* buffer and separated by 10 % SDS-polyacrylamide gel. A standard protein ladder (PageRuler® prestained, Fermentas St. Leon-Rot, Germany) was used for all measurements. Separated protein samples were transferred to a 0.2 µm Protran™ nitrocellulose membrane (Whatman; GE Healthcare, Munich, Germany) using the semidry Fastblot B44 system or the tank blot Eco-Mini system (Biometra GmbH, Goettingen, Germany). Membranes were blocked in 2 % ECL advance blocking reagent (GE Healthcare, Munich, Germany) dissolved in tris-buffered saline (TBS; 20 mM Tris, 140 mM NaCl, pH 7.6) for 1 h. Subsequently, membranes were incubated overnight at 4 °C with the following primary antibodies, that were diluted in TBS-T (TBS + 0.1 % Tween 20) with 5% bovine serum albumin (BSA): rabbit anti-phospho-V-akt

Murine Thymoma Viral Oncogene Homolog 1 (AKT) XP and total AKT, rabbit anti-phospho-Glycogen synthase kinase 3 (GSK3β) and total GSK3β, anti-β-catenin XP, rabbit anti-Lamin A (for phosphorylated proteins 1:500, all other proteins 1.1000; Cell signaling, Frankfurt Germany) and mouse anti-Glyceraldehyde-3-phosphate dehydrogenase (GAPDH; 1:6000, AM4300, Ambion/Life technologies, Darmstadt, Germany). Then the membranes were incubated at room temperature for 1 h with secondary antibodies, goat anti-rabbit or goat anti-mouse conjugated with IRDye 800 and IRDye 680, respectively (1:10000, LI-COR Biosciences GmbH, Bad Homburg, Germany), that were diluted in TBS-T with 2% ECL. Signal detection and quantification of the fluorescence intensity were conducted with the Odyssey infrared imaging system applying the Odyssey Application Software 3.0 (LI-COR Biosciences GmbH). The integrated intensity of target proteins was normalized to GAPDH for total protein extracts and Lamin A for nuclear protein extracts.

3.11 Glycogen measurement

50 mg of the pooled villous placental tissues of the four quadrants were sonicated in 200 µL of NaOH (1 M) and incubated for 20 min at 60 °C. Subsequently, 1920 µL of cold 100 % ethanol and 74 µl saturated Na_2SO_4 were added. Samples were centrifuged at 10000 x g for 10 min at 4 °C and the supernatant was discarded. The pellet was resuspended in 100 µL H_2O and incubated at 60 °C for 10 min until it was completely dissolved. The pellet was washed with 900 µL of cold 100 % ethanol and centrifuged at 10000 x g for 10 min at 4 °C. The supernatant was again discarded and the pellet was resuspended in 100 µL H_2O at 60 °C for 10 min. An amyloglucosidase buffer mix was prepared with 0.6 mg/ml of amyloglucosidase (70 units/ mg, Sigma-Aldrich) in acetate buffer (0.25 M, pH 4.75). 400 µL of amyloglucosidase buffer mix were added to the samples and incubated overnight at 37 °C. Glucose concentration from supernatant was measured by the hexokinase method (DiaSys, Holzheim, Germany). 5 µl of sample and 200 µl reagents, mixed according to the manufacturer's protocol, were applied and the extinction was measured after 10 min at 334 nm. Glycogen was normalized to sample protein concentration assessed by Pierce® BCA Protein Assay Kit **(see chapter 3.10).**

3.12 Statistical analysis

For all statistical analyses, IBM SPSS statistics software was used (version 20.0; IBM corp.). Statistical support was given by PD Dr. Kurt Gedrich (Biochemistry Unit, Research Center for Nutrition and Food Sciences (ZIEL), Technische Universität München) and Dr. Tibor Schuster (Institute for Medical Statistics and Epidemiology, Klinikum rechts der Isar, Technische Universität München). One-way ANOVA with Sidak post hoc test was applied for

group comparison of normally distributed variables and data are presented as mean ± SD. In case of violation of the normality assumption, the Kruskal-Wallis test with Dunn's post hoc test was applied, and accordingly, data are presented as medians and interquartile ranges. The Exact Fisher test was used for qualitative measurements. Comparative statistical evaluation of infant growth and infant fat mass between the groups was performed by employing multiple linear regression models. The potential confounding factors offspring sex and pregnancy duration were taken into account when analyzing cord plasma parameters and the covariate infant age of investigation was additionally applied for respective anthropometric and adipose tissue growth assessments. Generally, infant parameters at week-6, month-4 and year-1 were adjusted for corresponding breastfeeding status.

Linear regression analyses were used to identify maternal and umbilical cord plasma parameters as well as placental values independently related to offspring adipose tissue distribution up to year-1. If necessary, logarithmically transformed variables were applied to accomplish normality of residuals. Values for the unadjusted analyses are presented, whereas the respective adjusted model considered the variables offspring sex, gestational duration, maternal pre-pregnancy BMI, area under the curve (AUC) $_{Glucose}$ (OGTT) and gestational weight gain (GWG). Applying adipose tissue markers at week-6, month-4 and year-1 as dependent variables, corresponding breastfeeding status was a further covariate.

Spearman correlation analysis was used to compare different growth and adipose tissue measures with each other at respective ages of investigation. Moreover, Spearman correlation analysis was applied to compare maternal and cord markers with each other and to compare maternal plasma inflammatory markers with placental cytokine/chemokine gene expression. The partial correlations were further conducted with the covariables maternal pre-pregnancy BMI, AUC $_{Glucose}$ (OGTT) and GWG for maternal markers and additionally with the variables infant sex and pregnancy duration for cord plasma markers. All statistical tests were performed two-sided and a p-value < 0.05 was considered as statistically significant.

4 Results

4.1 Maternal baseline characteristics

Baseline characteristic data of the study population are summarized in **Table 2**. Accordingly, obese participants with GDM were slightly older at study entry compared to obese women, but groups did not differ significantly in the amount of primiparous women. Both obese groups had similar pregravid weight and BMI, whereas the plasma glucose levels (fasted, 1h, 2h) during OGTT were significantly higher in the obese GDM group compared to the lean and obese subjects. Detailed OGTT results obtained from the study population are outlined in **Supplemental table 1**. Moreover, self-reported glucose measurements, begin of insulin therapy and daily amount of insulin units (at begin of treatment and before delivery) were recorded by the GDM group and are summarized in **Supplemental table 2.** Obese women with and without GDM had significantly increased systolic and diastolic blood pressure compared to lean women at 3rd trimester **(Table 2).** Alcohol and smoking habits before pregnancy were similar between all groups. Paternal parameters at study entry, namely weight, height, and BMI were not statistically different between the groups. Moreover, the participants were asked for their mother's anthropometric status before and during pregnancy to evaluate pattern of fetal programming in the maternal study population. Accordingly, the mothers of the enrolled lean and obese participants with and without GDM were comparable in pregravid BMI and GWG. Women belonging to the obese GDM group were heavier at birth compared to euglycemic counterparts but the result was not statistically significant ($p = 0.102$), and calculated ponderal index only approached significance ($p = 0.065$) **(Table 2).** Neither pregravid BMI nor GWG of participant's mothers was associated to their daughter's birth weight or ponderal index. However, the regression analysis showed that the pregravid BMI of the participant's mothers and the respective participant's pregravid BMI were significantly positively related ($\beta = 0.435$; $p = 0.006$, $n = 38$).

Table 2: Baseline characterization of study population

	Control group	Obese group	Obese GDM group	P-value[1]
N	**15**	**13**	**16**	
Age (y)	31.1 ± 3.1	28.5 ± 4.2	32.6 ± 4.8	**0.040** [c]
Primiparae (% [n])	86.7 [13]	76.9 [10]	56.2 [9]	0.299
Weight before pregnancy (kg)	59.0 (54.0-62.0)	105.0 (95.0-114.5)	101.0 (87-106.8)	**< 0.001** [a,b]
Height (cm)	169.9 ± 5.4	171.6 ± 4.9	170.0 ± 6.0	0.867
BMI before pregnancy (kg/m^2)	20.1 (19.5-22.0)	36.1 (32.2-38.3)	33.4 (31.1-36.1)	**< 0.001** [a,b]
RR systolic (mmHg)	111.5 ± 9.0	127.8 ± 16.0	123.0 ± 9.8	**0.002** [a,b]
RR diastolic (mmHg)	66.7 ± 7.5	79.2 ± 8.1	79.7 ± 10.0	**< 0.001** [a,b]
75 g OGTT				
Glucose fasted (mmol/L)	4.2 (3.9-4.4)	4.3 (4.0-4.6)	5.1 (4.4-5.6)	**< 0.001** [b,c]
Glucose 1h (mmol/L)	7.4 ± 0.9	7.3 ± 1.4	10.9 ±1.3	**< 0.001** [b,c]
Glucose 2h (mmol/L)	6.3 ± 1.0	6.5 ± 1.2	8.0 ± 1.6	**< 0.001** [b,c]
Area under curve	12.5 (11.9-13.2)	11.9 (11.6-14.1)	16.4 (16.0-18.1)	**< 0.001** [b,c]
Parental history of diabetes (% [n])	13.3 [2]	38.5 [5]	43.8 [7]	**0.181**
Smoking before pregnancy (% [n])	33.3 [5]	30.8 [4]	31.2 [5]	1.000
Alcohol consumption before pregnancy (% [n])	73.3 [11]	46.5 [6]	62.5 [10]	0.345
Paternal weight (kg)	82.9 ± 13.7	92.2 ± 19.1	86.9 ± 16.2	0.330
Paternal height (cm)	183.0 (179.0-194.0)	180.0 (175.0-188.5)	179.0 (175.0-187.0)	0.216
Paternal BMI (kg/m^2)	23.5 (22.2-26.8)	27.5 (24.0-31.0)	24.7 (23.2-29.8)	0.113
BMI of participant`s mother before pregnancy (kg/m^2)	21.1 (19.3-22.5)	22.2 (20.1-27.3)	22.(20.4-25.7)	0.170
GWG of participant`s mother (kg)	13.8 (12.8-16.3)	12.0 (9.0-20.0))	15.0 (9.4-27)	0.998
Maternal birth weight (g)	3300 (2960-3600)	3290 (3085-3465)	3590 (3248-3725)	0.102
Maternal birth height (cm)	50.0 (49.0-52.0)	52.0 (50.0-52.4)	51.5 (50.0-53.0)	0.673
Maternal ponderal index at birth (kg/m^3)	6.43 (6.00-6.96)	6.46 (6.10-6.66)	6.93 (6.34-7.30)	0.065

Data are presented as mean ± SD; otherwise skewed variables are presented as median followed by interquartile range. GWG: gestational weight gain; RR: blood pressure

[1] One-way ANOVA was performed with Sidak's post hoc test or nonparametric Kruskal-Wallis-test with Dunn's post hoc test.

[a] P-value < 0.05 obese vs. lean group; [b] p-value < 0.05 obese GDM vs. lean group; [c] p-value < 0.05 obese GDM vs. obese group. Significant values are presented in bold type.

Maternal metabolic characteristics obtained between week-33 and 36 of gestation (3rd trimester) are shown in **Table 3**. At baseline, obese women with and without GDM had significantly increased levels of fasting insulin and C-peptide levels compared to lean subjects and showed increased insulin resistance estimated by HOMA-IR-index. Plasma leptin levels of obese pregnant women were - irrespective of GDM - significantly higher while plasma HMW adiponectin levels and HMW-total adiponectin ratios (S_A) were significantly lower compared to the lean group. Concerning lipid profiling, total cholesterol levels were significantly decreased in obese subjects, but HDL cholesterol and TG levels did not differ between study groups. Regarding the determination of plasma inflammatory markers at 3rd

trimester, namely CRP and IL6, it was shown, that the three groups did not differ statistically in CRP levels in the post hoc analysis (ANOVA: p = 0.036); however, IL6 levels were found to be significantly elevated in both obese compared to the healthy lean group. Moreover, maternal CRP and IL6 showed a significantly positive correlation (r = 0.435, p = 0.006; **Supplemental Table 8**). In summary, both obese groups can be metabolically distinguished from lean subjects at baseline. Obese women mainly differed in glucose levels assessed by OGTT from their diabetic counterparts.

Table 3: Maternal fasted plasma parameters at 3rd trimester

	Control group	Obese group	Obese GDM group	P-value[1]
N	**15**	**12**	**13**	
Gestational age at blood sampling (weeks)	33.9 ± 1.4	34+3 ± 1.7	34+1 ± 1.0	0.836
Glucose (mmol/L)	4.10 ± 0.3	4.19 ± 0.40	4.39 ± 0.28	0.161
Insulin (µU/mL)	5.66 (4.76-10.05)	11.54 (9.28-20.54	13.99 (11.22-17.97)	**0.001** [a,b]
HOMA-IR-index	1.10 (0.86-1.79)	2.31 (1.98-4.15)	2.76 (2.08-3.63)	**0.001** [a,b]
C-peptide (ng/mL)	1.60 (1.42-2.23)	2.99 (2.05-3.51)	3.01 (2.64-3.14)	**0.001** [a,b]
HbA1c (%)	5.32 ± 0.31	5.45 ± 0.23	5.40 ± 0.28	0.474
Leptin (ng/mL)	9.30 (6.52-20.11)	46.03 (29.84-78.67)	42.24 (26.71-66.69)	**< 0.001** [a,b]
Total Adiponectin (µg/mL)	4.98 ± 1.02	4.14 ± 1.78	3.81 ± 1.39	0.071
HMW Adiponectin (µg/mL)	2.86 ± 0.82	2.06 ± 1.17	1.74 ± 0.91	**0.008** [b]
S_A	0.57 ± 0.1	0.48 ± 0.09	0.44 ± 0.07	**< 0.001** [a,b]
Total Cholesterol (mmol/L)	7.49 ± 1.51	6.28 ± 0.96	6.60 ± 0.96	**0.035** [a]
LDL Cholesterol (mmol/L)	4.86 ± 1.50	3.73 ± 0.87	3.92 ± 1.96	**0.039** [#]
HDL Cholesterol (mmol/L)	1.92 ± 0.49	1.73 ± 0.45	1.88 ± 0.28	0.524
TG (mmol/L)	2.53 ± 0.74	2.38 ± 0.57	2.76 ± 0.72	0.420
CRP (mg/L) [§]	3.80 (2.13-4.45)	7.05 (3.85-9.55)	6.30 (3.80-9.80)	**0.036**[#]
IL6 (pg/mL) [§]	0.50 ± 0.18	0.78 ± 0.26	0.81 ± 0.37	**0.012** [a,b]

CRP: C-reactive protein; HbA1c: hemoglobin A1c; HDL: high-density lipoprotein; HMW: high molecular weight; HOMA-IR: homeostasis model assessment-insulin resistance; LDL: low-density lipoprotein; S_A: HMW-total adiponectin ratio; TG: trigycerides.
Data are presented as mean ± SD; otherwise skewed variables are presented as median followed by interquartile range
[1] One-way ANOVA was performed with Sidak's post hoc test or nonparametric Kruskal-Wallis-test with Dunn's post hoc test.
[a] P-value < 0.05 obese vs. lean group; [b] p-value < 0.05 obese GDM vs. lean group. Significant values are presented in bold type.
[#] According to pairwise multiple comparison procedures (Sidak's post hoc test): p > 0.05
[§] One participant of the lean group was identified as outlier by the Grubbs test and was therefore excluded from the final CRP and IL6 statistical analysis.

Additionally to the assessment at 3rd trimester, differential blood cell count, HbA1c, plasma glucose and lipid profiles were analyzed prior to delivery and at week-6 *pp* **(Figure 12 and Figure 13; Supplemental table 3).** Fasted plasma glucose did not differ between groups at 3rd trimester **(Figure 12A).** At assessment, all GDM women already received insulin and diet therapy and the exclusively dietary-treated cases were particularly characterized by increased postprandial glucose levels, while fasted plasma glucose levels were often without indication of hyperglycemia **(Supplemental table 1).** At week-6 *pp*, especially the formerly insulin-treated women had elevated fasting plasma glucose levels (range from 4.3 to 6.1

mmol, mean: 5.2 mmol), whereas glucose levels of dietary-treated participants were lower (range from 4.1 to 4.6 mmol, mean: 4.3 mmol). Accordingly, plasma glucose levels at postnatal investigation did not significantly differ between the GDM group and their counterparts (p = 0.136), but showed a large interquartile range within the obese diabetic group representing the previous GDM degree **(Figure 12A).** HbA1c levels were similar between lean and obese participants with and without GDM at each scheduled examination **(Figure 12B).** Higher total and LDL cholesterol levels were also confirmed at delivery in the lean participants in comparison to the obese and obese GDM group **(Figure 13A and C).** TG levels were similar at delivery within the study population and elevated TG levels observed during pregnancy declined markedly after delivery (week-6 *pp*) irrespective of group allocation, but with the strongest decrease in the lean group **(Figure 13B).**

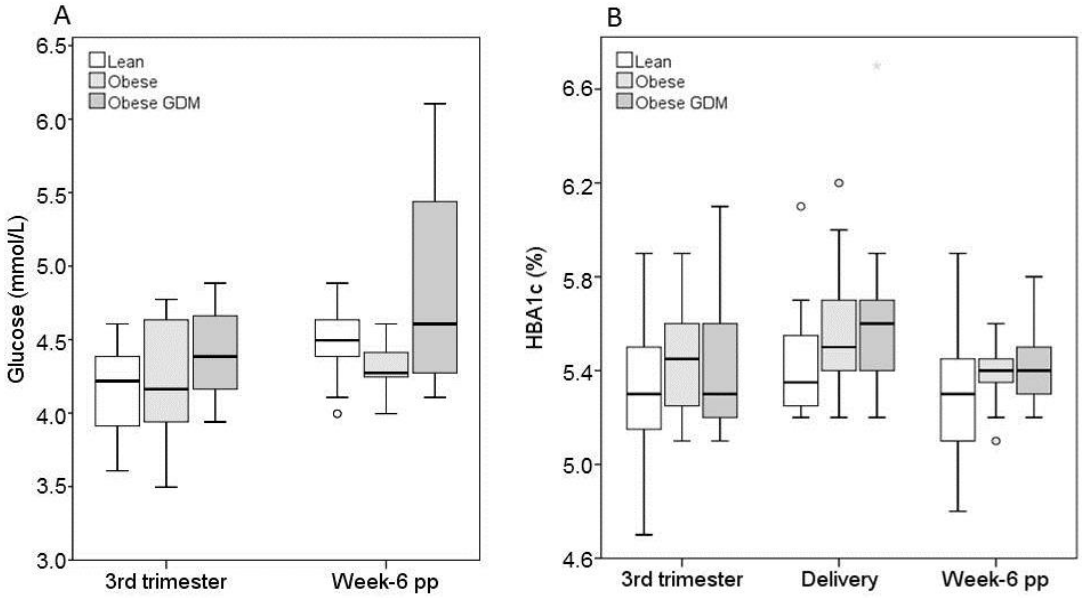

Figure 12: Longitudinal measurement of maternal plasma glucose and HbA1c levels from 3rd trimester to week-6 *pp*. A) Glucose samples from 3rd trimester and at week-6 *pp* were obtained in the fasted state. B) HbA1c levels are independent of fasted state and were also determined prior to delivery. Data are presented as boxplots. Bottom and top edges of the box represent the 25th and 75th percentiles. The horizontal line shows the median and the whiskers mark the maximum and minimum values. Outliers are presented as dots. The analysis was performed with samples of lean (n=15), obese (n=12) and obese GDM (n=13) women for 3rd trimester; with samples of lean (n=13), obese (n=13) and obese GDM (n=16) women at delivery and with samples of lean (n=15), obese (n=11) and obese GDM (n=9) women for week-6 *pp*.

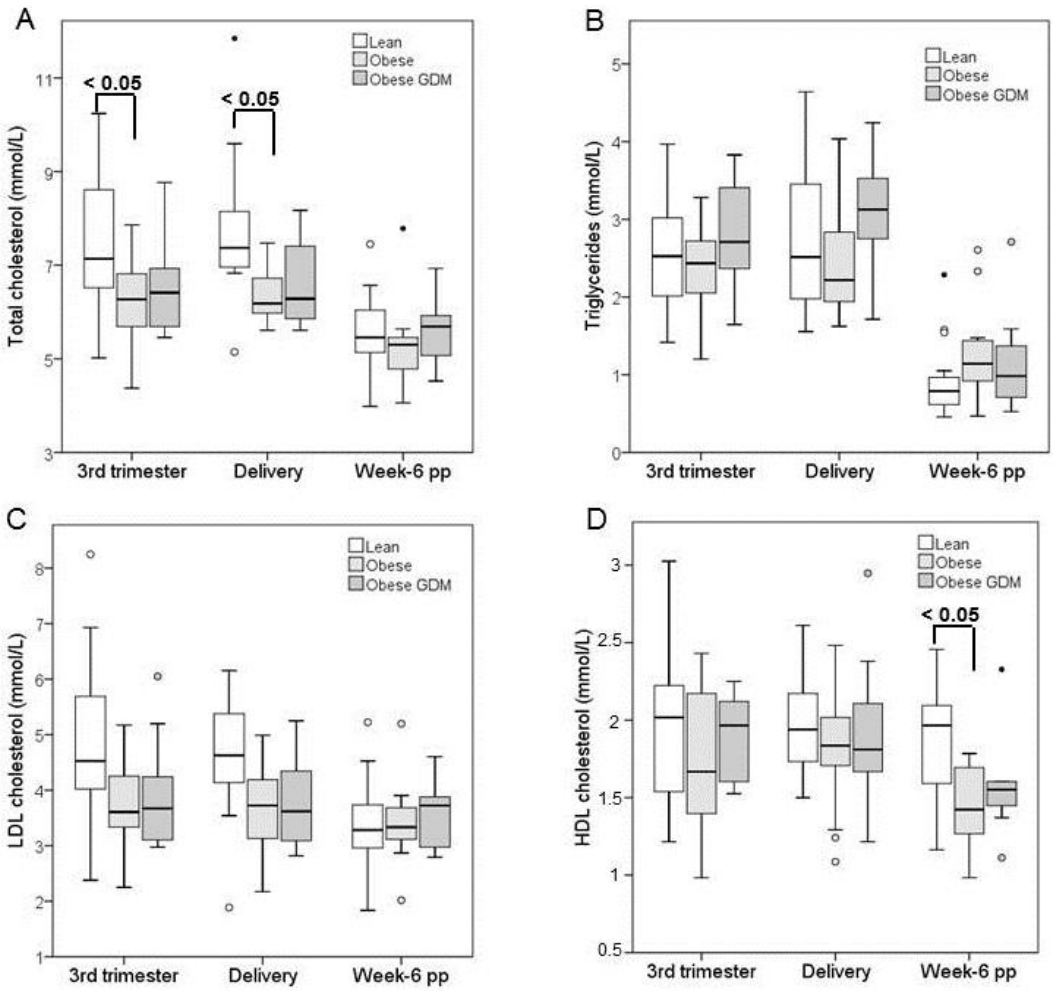

Figure 13: Longitudinal measurement of maternal lipid metabolism from 3rd trimester to week-6 pp. A) Total cholesterol, **B)** Triglycerides, **C)** LDL cholesterol (p-value from ANOVA at 3rd trimester: 0.039, Sidak-post hoc test: p-value > 0.05; p-value from ANOVA at delivery: 0.040, Sidak-post hoc test: p-value > 0.05) **D)** HDL cholesterol. Data are presented as boxplots. Bottom and top edges of the box represent the 25th and 75th percentiles. The horizontal line shows the median and the whiskers mark the maximum and minimum values. Outliers are presented as dots. Extremes are presented as asterisks. Analysis was performed with samples of lean (n=15), obese (n=12) and obese GDM (n=13) women for 3rd trimester; with samples of lean (n=13), obese (n=13) and obese GDM (n=16) women at delivery and with samples of lean (n=15), obese (n=11) and obese GDM (n=9) women for week-6 *pp*.

4.2 Birth outcomes

The birth outcomes are presented in **Table 4**. Pregnancy duration was significantly shorter in the obese GDM group compared to obese subjects. Gestational weight was significantly higher in lean women in comparison to both obese groups, but according to criteria of the Institute of Medicine (IOM), the majority of women exceeded - irrespective of study group allocation - the weight gain recommendation referred to their pregravid BMI. The mode of delivery did not differ between the three groups, but showed higher incidence of C-sections without previous labor in the obese GDM cases. High application of medications (analgesics) and/or peridual anesthesia (PDA) was observed throughout all groups, but did not differ significantly between lean, obese and obese GDM women. Notably, obese GDM women

delivered more frequently male offspring compared to the lean and obese participants, who showed more a homogenous distribution of infant sex within their groups. In each study group, similar incidence of LGA babies was observed, although the number of neonates born heavier than 4000 g was the highest in the obese GDM group. The placental weight and fetal-placental ratio did not differ significantly between the groups. With regard to the breastfeeding status at week-6 and month-4 and the introduction of solid food, no differences were found between the study groups.

Table 4: Birth outcomes

	Lean group	Obese group	Obese GDM group	P-value[1]
N	**15**	**13**	**16**	
Gestational age (days) [#]	278.2 ± 8.1	279.5 ± 8.2	271.3 ± 7.0	**0.012** [b]
GWG (kg) [# §]	16.8 ± 4.4	11.6 ± 5.6	12.1± 5.8	**0.022** [a,b]
GWG > IOM (% [n])	60 [9]	69.2 [9]	68.8 [11]	0.852
Induction of labor (% [n]) [#]	20 [3]	38.5 [5]	37.5 [6]	0.552
Medication (% [n]) [#]				
Analgesia	80 [12]	38.5 [5]	50.0 [8]	0.076
PDA	53.3 [8]	69.2 [9]	75.0 [12]	0.445
Mode of delivery (% [n]) [#]				
Spontaneous	60 [9]	46.2 [7]	37.5 [6]	0.483
C-section	40 [6]	53.8 [6]	62.5 [10]	
Blood loss at delivery (mL) [#]	350 (250-625)	400 (250-550)	400 (300-700)	0.826
Arterial pH [#]	7.31 (7.29-7.37)	7.25 (7.23-7.31)	7.29 (7.23-7.31)	**0.023** [a]
Base excess [#]	-4.7 ± -4.0	-5.5 ± -2.8	-4.0 ± -2.6	0.468
APGAR (5 min) [#]	10 (9-10)	10 (9-10)	10 (9-10)	0.938
Offspring male/female (n) [#]	8/7	8/5	13/3	0.275
LGA (% [n]) [#]	13.3 [2]	7.7 [1]	12.5 [2]	1.000
Birth weight > 4000g [#]	13.3 [2]	7.7 [1]	25.0 [4]	0.589
Weight percentile [#]	45.6 ± 24.6	57.6 ± 20.4	63.4 ± 23.9	0.110
Placental weight (g)	558 ± 80	561 ± 93	631 ± 151	0.145
Fetal-placental weight ratio	6.28 ± 0.93	6.66 ± 1.12	5.98 ± 1.22	0.261
Breastfeeding status at week-6 (% [n])				
Exclusively breastfed	66.7 [10]	53.8 [7]	28.6 [4]	0.257
Formula and breast milk	0 [0]	23.1 [3]	28.6 [4]	
Formula only	33.3 [5]	23.1 [3]	42.9 [6]	
Breastfeeding status at month-4 (% [n])				
Exclusively breastfed	53.3 [8]	46.2 [6]	42.9 [2]	0.304
Formula and breast milk	13.3 [2]	0[0]	28.6 [2]	
Formula only	33.3 [5]	53.8 [2]	28.6 [4]	
Introduction of solid food (months)	5.0 (5.0-6.0)	5.0 (4.0-6.0)	4.3 (4.0-5.8)	0.411

APGAR: **A**ppearance, **P**ulse, Grimace, **A**ctivity and **R**espiration (quick evaluation of a newborn's physical condition); C-section: Caesarean section; GWG: Gestational weight gain; IOM: Institute of Medicine [110]; LGA: Large for gestational age; PDA: peridual anesthesia

[#] Data were obtained from obstetric protocol.

[§] GWG was calculated as the last measured value at booking minus self-reported weight before pregnancy.

[1] One-way ANOVA was performed with Sidak's post hoc test or nonparametric Kruskal-Wallis-test with Dunn's post hoc test.

[a] P-value < 0.05 obese vs. lean group; [b] p-value < 0.05 obese GDM vs. lean group. Significant values are presented in bold type

4.3 Umbilical cord blood parameters

Table 5 shows the metabolic profiling performed in umbilical cord vein plasma. Cord plasma glucose levels did not differ between groups. In contrast, plasma insulin levels and HOMA-IR-indexes were significantly increased in the offspring delivered by obese GDM women compared to both normoglycemic groups. However, between the three study groups, no differences were observed for cord plasma HMW and total adiponectin or S_A. In addition, levels of cord total cholesterol, LDL, and HDL cholesterol as well as TG were similar between all groups.

Table 5: Umbilical cord plasma parameters

	Lean group	Obese group	Obese GDM group	P-value[1]	Adjusted p-value[2]
N	15	13	16		
Glucose (mmol/L)	4.46 ± 1.13	4.42 ± 1.03	4.60 ± 1.02	0.892	0.202
Insulin (µU/mL)	1.72 (1.08-5.14)	1.73 (1.33-3.97)	5.29 (4.21-8.33)	**0.023** [a,b]	**0.014** [a,b]
HOMA-IR-index	0.40 (0.22-1.23)	0.42 (0.23-0.74)	1.08 (0.81-1.52)	**0.021** [a,b]	**0.009** [a,b]
Leptin (ng/mL)	5.88 (2.15-9.70)	7.57 (4.56-16.65)	6.84 (4.76-11.58)	0.455	0.114
Total Adiponectin (µg/mL)	20.68 ± 6.23	20.82 ± 8.56	22.03 ± 7.33	0.977	0.685
HMW Adiponectin (µg/mL)	14.61 ± 5.15	14.28 ± 7.02	14.75 ± 5.80	0.860	0.884
S_A	0.70 ± 0.06	0.67 ± 0.06	0.65 ± 0.08	0.292	0.348
Total Cholesterol (mmol/L)	1.71 (1.31-1.90)	1.53 (1.36-1.71)	1.55 (1.32-1.73)	0.718	0.886
LDL Cholesterol (mmol/L)	0.54 (0.32-0.65)	0.52 (0.38-0.60)	0.47 (0.41-0.54)	0.905	0.271
HDL Cholesterol (mmol/L)	0.72 (0.67-1.03)	0.62 (0.60-0.96)	0.72 (0.57-0.88)	0.691	0.724
TG (mmol/L)	0.35 (0.27-0.52)	0.35 (0.26-0.45)	0.40 (0.25-0.46)	0.959	0.847

HDL: high-density lipoprotein; HMW: high molecular weight; HOMA-IR: homeostasis model assessment-insulin resistance; LDL: low-density lipoprotein; S_A: HMW-total adiponectin ratio; TG: triglycerides.
Data are presented as mean ± SD; otherwise skewed variables are presented as median followed by interquartile range (all such values)
[1] One-way ANOVA was performed with Sidak's post hoc test or nonparametric Kruskal-Wallis-test with Dunn's post hoc test.
[2] Statistical analyses for cord plasma parameters were performed by multiple linear regression models and p-values were adjusted for infant sex and pregnancy duration.
[a] P-value < 0.05 obese GDM vs. lean group; [b] p-value < 0.05 obese GDM vs. obese group. Significant values are presented in bold type.

4.4 Infant anthropometric assessment from birth to year-1

All infant anthropometrics collected from birth to year-1 are summarized in **Table 6** and the most important longitudinally determined anthropometric parameters, namely body weight and ponderal index, are displayed in

Figure 14. Anthropometric birth outcomes, meaning weight, height, ponderal index, head and arm circumference were similar for all groups. Infant body weight, ponderal index and head circumference at week-6 were no longer significantly increased in GDM offspring compared to lean counterparts after adjustment for offspring sex, pregnancy duration and age at investigation. No differences were observed between the three groups with regard to anthropometric parameters at week-4 and year-1 and total weight gain from birth to year-1

after adjustment for indicated confounders. However, weight gain from birth to week-6 was moderately significantly increased in obese compared to lean neonates.

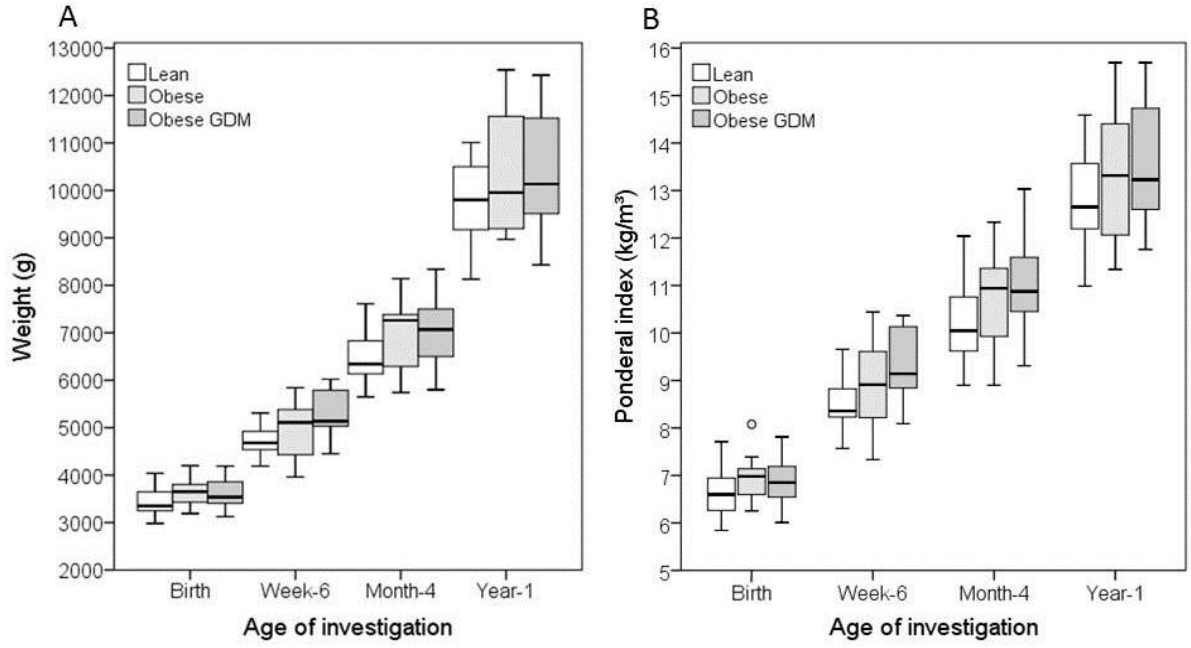

Figure 14: Longitudinal measurement of body weight (A) and ponderal index (B) at birth, week-6, month-4 and year-1 in infants delivered by lean and obese women with and without GDM. Data are presented as boxplots. Bottom and top edges of the box represent the 25th and 75t^{h} percentiles. The horizontal line shows the median and the whiskers mark the maximum and minimum values. Refer to **Table 6** to obtain the total numbers of infants that were included in the analysis for each study group.

Table 6: Anthropometric infant data from birth to year-1 of life

	Lean group	Obese group	Obese GDM group	P-value[1]	Adjusted p-value[2]
Age at investigation [d]					
Birth	1.0 ± 0.0 [15]	1.0 ± 0.0 [13]	1.0 ± 0.0 [16]	1.000	-
Week-6	43.2 ± 3.7 [15]	42.8 ± 2.0 [13]	43.1 ± 3.0 [12]	0.942	-
Month-4	113.0 (112-115.0) [15]	114.0 (111.0-115.0) [11]	115.0 (111.5-119.5) [13]	0.539	-
Year-1	367.0 (365.0-369.0) [15]	367.0 (363.5-374.5) [15]	367.0 (364.8-366.8) [14]	0.800	-
Weight [g]					
Birth	3,449 ± 332 [15]	3,651 ± 285 [13]	3,617 ± 333 [16]	0.201	0.169
Week-6	4,701 ± 330 [15]	4,963 ± 635 [13]	5,285 ± 517 [12]	**0.017** [b]	0.170
Month-4	6,468 ± 522 [15]	6,929 ± 829 [11]	7,066 ± 732 [13]	0.071	0.211
Year-1	9,786 ± 915 [15]	10,356 ± 1,273 [12]	10,392 ± 1,212 [14]	0.286	0.549
Weight gain [g]					
Δ Week-6- Birth	1,265 (1,095-1,480) [15]	1,480 (775-1,690) [13]	1,550 (1,361-1,892) [12]	**0.017** [b]	0.394
Δ Month-4 -Week-6	1,734 (1,390-2,100) [15]	2,070 (1,840-2,300) [11]	1,848 (1,460-2,100) [11]	0.112	**0.042** [a]
Δ Year-1- Month-4	3,318 ± 760 [15]	3,228 ± 801 [11]	3,329 ± 666 [13]	0.936	0.937
Δ Year-1 - Birth	6,337 ± 996 [15]	6,665 ± 1,220 [12]	6,765 ± 1,102 [14]	0.554	0.722
Lenght [cm]					
Birth	51.8 ± 1.5 [15]	52.5 ± 1.4 [13]	52.3 ± 1.5 [16]	0.299	0.264
Week-6	55.6 ± 0.9 [15]	56.0 ± 1.8 [13]	56.4 ± 1.4 [12]	0.360	0.738
Month-4	63.3 ± 1.2 [15]	64.4 ± 2.0 [11]	63.7 ± 1.4 [13]	0.226	0.177
Year-1	76.5 ± 2.3 [15]	77.5 ± 2.6 [12]	76.7 ± 2.7 [14]	0.551	0.666
Ponderal index [g/cm^3]					
Birth	6.65 ± 0.54 [15]	6.95 ± 0.48 [13]	6.81 ± 0.51 [16]	0.291	0.287
Week-6	8.45 ± 0.55 [15]	8.86 ± 1.03 [13]	9.36 ± 0.75 [12]	0.018 [b]	0.176
Month-4	10.21 ± 0.81 [15]	10.74 ± 1.06 [11]	11.04 ± 0.97 [13]	0.073	0.272
Year-1	12.80 ± 1.04 [15]	13.34 ± 1.38 [12]	13.52 ± 1.30 [14]	0.262	0.616
Head circumference [cm]					
Birth	34.0 (34.0-35.5) [15]	35.0 (34.5-36.5) [13]	35.5(34.0-36.0) [16]	0.072	0.410
Week-6	37.5 (37.0-38.8) [15]	38.3 (37.6-39.7) [13]	38.9 (37.7-40.0) [12]	**0.023** [b]	0.096
Month-4	41.1 ± 1.2 [15]	42.1 ± 1.7 [11]	42.0 ± 1.3 [13]	0.132	0.184
Year-1	45.6 ± 1.4 [15]	47.0 ± 1.6 [12]	47.1 ± 1.7 [14]	0.072	0.105
Arm circumference [cm]					
Birth	11.0 (10.5-11.4) [15]	11.0 (10.8-11.8) [13]	11.1 (10.8-11.5) [16]	0.518	0.759
Week-6	12.7 ± 0.7 [15]	12.7 ± 1.3 [13]	12.8 ± 0.8 [12]	0.153	0.368
Month-4	14.3 ± 1.0 [15]	14.7 ± 1.2 [11]	14.4 ± 1.2 [13]	0.679	0.689
Year-1	15.9 ± 1.2 [15]	16.2 ± 0.8 [12]	15.5 ± 1.3 [14]	0.291	0.201
Waist circumference [cm]					
Year-1	45.1 ± 2.4	45.6 ± 4.0	45.7 ± 3.0 [14]	0.859	0.897

Data are presented as mean ± SD; otherwise skewed variables are presented as median followed by interquartile range, n in brackets (all such values). Δ difference between indicated offspring ages

[1] One-way ANOVA was performed with Sidak's post hoc test or nonparametric Kruskal-Wallis-test with Dunn's post hoc test.

[2] Statistical analyses were performed by multiple linear regression models. P-values for parameters at week-1 were adjusted for infant sex, pregnancy duration and age at investigation. P-values at week-6, month-4 and year-1 were adjusted for infant sex, pregnancy duration, age at investigation and corresponding breastfeeding.

[a] P-value < 0.05 obese vs. lean group; [b] p-value < 0.05 obese GDM vs. lean group. Significant values are presented in bold type.

4.5 Infant fat mass assessment from week-1 to year-1

4.5.1 Assessment of skin fold thickness

In addition to the assessment of anthropometric data, subcutaneous adipose tissue was determined by SFT at 4 distinct body parts including trunk (subscapular, suprailial) and peripheral (biceps, triceps) measuring points **(Table 7)**. Adipose tissue growth pattern for SFT and total body fat were further displayed in **Figure 15.** The sum of 4 SFT at week-1 was significantly higher in the obese GDM group compared to the lean group, even after considering potential confounders, such as infant sex, pregnancy duration and age at investigation. At week-6, SFT and calculated total fat mass, equated to SFT, were statistically increased in the obese GDM offspring after adjusting for infant sex, pregnancy duration, age at investigation and breastfeeding status. In contrast, at month-4 and year-1, neither SFT nor total fat mass differ anymore between infants. Notably, although sum of all 4 SFT did not differ between groups at year-1, the trunk-total SFTs ratio was significantly increased in obese GDM offspring compared to lean and obese children, indicating changes in adipose tissue distribution with increased trunk fat in these infants at year-1. However, lean mass was similar between the groups at all ages investigated.

Table 7 : Infant adipose tissue growth assessed by skin fold thickness measurement from week-1 to year-1

	Lean group	Obese group	Obese GDM group	P-value[1]	Adjusted p-value[2]
Age at SFT investigation [d]					
Week-1	2.9 ± 0.7 [15]	2.7 ± 0.8 [13]	3.5 ± 1.2 [16]	0.059	-
Week-6	43.2 ± 3.7 [15]	42.8 ± 2.0[13]	43.1 ± 3.0 [12]	0.942	-
Month-4	113.0 (112-115.0) [15]	114.0 (111.0-115.0) [11]	115.0 (111.5-119.5) [13]	0.539	-
Year-1	367.0 (365.0-369.0) [15]	367.0 (363.5-374.5) [12]	367.0 (364.8-366.8) [14]	0.800	-
SFTs [mm]					
Week-1	18.9 ± 3.1 [15]	20.3 ± 2.6 [13]	21.6 ± 2.4 [16]	**0.031** [a]	**0.031** [a]
Week-6	25.2 ± 3.7 [15]	26.1± 5.1 [13]	30.4 ± 3.4 [12]	**0.007** [a,b]	**0.048** [a]
Month-4	30.7 ± 6.6 [15]	31.2 ± 4.3 [11]	33.6 ± 4.8 [13]	0.336	0.258
Year-1	29.0 ± 4.3 [15]	30.3 ± 4.6 [12]	29.7 ± 4.8 [14]	0.749	0.536
Fat mass [g] [3]					
Week-1	583 ± 139 [15]	660 ± 114 [13]	694 ± 117 [16]	**0.051**	**0.042** [a]
Week-6	1,008 ± 159 [15]	1,098 ± 285 [13]	1,307 ± 187 [12]	**0.004** [a,b]	**0.048** [a]
Month-4	1,581 ± 318 [15]	1,728 ± 327 [11]	1,847 ± 328 [13]	0.108	0.184
Year-1	2,260 ± 419 [15]	2,475 ± 536 [12]	2,444 ± 530 [14]	0.466	0.498
Lean mass [g] [3]					
Week-1	2,834 (2713-3031) [15]	2,996 (2899-3144) [13]	2,892 (2731-3173) [16]	0.221	0.399
Week-6	3,693 ± 244 [15]	3,850 ± 360 [13]	3,978 ± 375 [12]	0.089	0.417
Month-4	4,849 (4,551-5,232) [15]	5261 (4,611-5,702) [11]	5,199 (4,785-5,565) [13]	0.172	0.295
Year-1	7,526 ± 557 [15]	7,881 ± 789 [12]	7,948 ± 758 [14]	0.234	0.630
Subscapular-triceps SFT ratio [4]					
Week-1	0.89 ± 0.11 [15]	0.94 ± 0.13 [13]	0.96 ± 0.15 [16]	0.354	0.531
Week-6	0.90 ± 0.08 [15]	0.97 ± 0.15 [13]	0.98 ± 0.12 [12]	0.177	0.308
Month-4	0.95 ± 0.15 [15]	0.92 ± 0.16 [11]	0.96 ± 0.18 [13]	0.759	0.778
Year-1	0.87 (0.77-0.90) [15]	0.82 (0.74-0.89) [12]	0.89 (0.79-0.98) [14]	0.271	0.483
Trunk-total SFT (%) ratio [5]					
Week-1	47.4 ± 2.5 [15]	47.2 ± 3.3 [13]	48.1 ± 2.9 [16]	0.630	0.958
Week-6	48.4 ± 3.2 [15]	49.4 ± 3.4 [13]	49.1 ± 2.4 [12]	0.648	0.528
Month-4	49.0 ± 4.1 [15]	48.9 ± 2.4 [11]	49.6 ± 3.1 [13]	0.841	0.647
Year-1	45.1 ± 2.6 [15]	44.9 ± 2.6 [12]	48.5 ± 3.3 [14]	**0.002** [a,b]	**0.035** [a,b]

SFT: sum of the 4 skin fold thickness measurements (biceps + triceps + subscapular + suprailiac).
Data are presented as mean ± SD; otherwise, skewed variables are presented as median followed by interquartile range, n in brackets (all such values).
[1] One-way ANOVA was performed with Sidak's post hoc test or nonparametric Kruskal-Wallis-test with Dunn's post hoc test
[2] Statistical analyses were performed by multiple linear regression models. P-values for parameters at week-1 were adjusted for infant sex, pregnancy duration and age at investigation. P-values at week-6, month-4 and year-1 were adjusted for infant sex, pregnancy duration, age at investigation and corresponding breastfeeding status.
[a] P-value < 0.05 obese GDM vs. lean group; [b] p-value < 0.05 obese GDM vs. obese group. Significant values are presented in bold type.
[3] Fat mass and lean mass were estimated from the sum of 4 SFTs by using the equations of Weststrate and Deurenberg [102].
[4] Subscapular-triceps SFT ratio was calculated according to [103].
[5] Trunk-total SFT (%) ratio was evaluated by applying the equation (subscapular + suprailiac SFT) / (sum of 4 SFTs) x 100 [104].

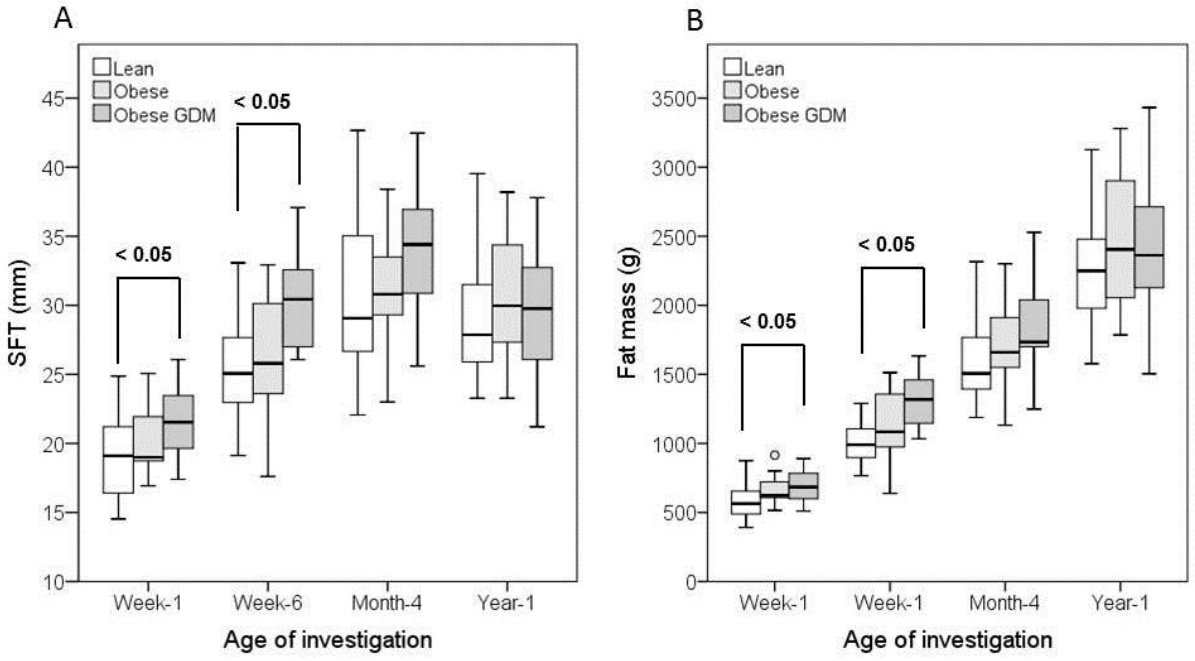

Figure 15: Longitudinal measurement of SFT (A) and fat mass (B) at week-1, week-6, month-4 and year-1 in infants delivered by lean and obese women with and without GDM. Data are presented as boxplots. Bottom and top edges of the box represent the 25th and 75t^{h} percentiles. The horizontal line shows the median and the whiskers mark the maximum and minimum values. Outliers are presented as dots. Refer to **Table 7** to obtain the total numbers of infants that were included in the analysis for each study group. SFT: sum of the 4 skin fold thickness measurements (biceps + triceps + subscapular + suprailiac).

4.5.2 Precision of ultrasonography

The interclass coefficient (ICC) between the two independent observers for the ultrasonographic analysis was 0.981 and the p-value < 0.001, indicating high correlation between independent assessments. In the Bland-Altman plot analysis, the mean of the differences (bias) between observers was -0.17 mm^2 and the *Limits of Agreement* were -0.65 mm^2 (mean -2 SD) and 0.31 mm^2 (mean +2 SD), representing no systematic inter-observer bias **(Figure 16).** Furthermore, there was no systemic underestimation or overestimation with respect to distinct fat depots.

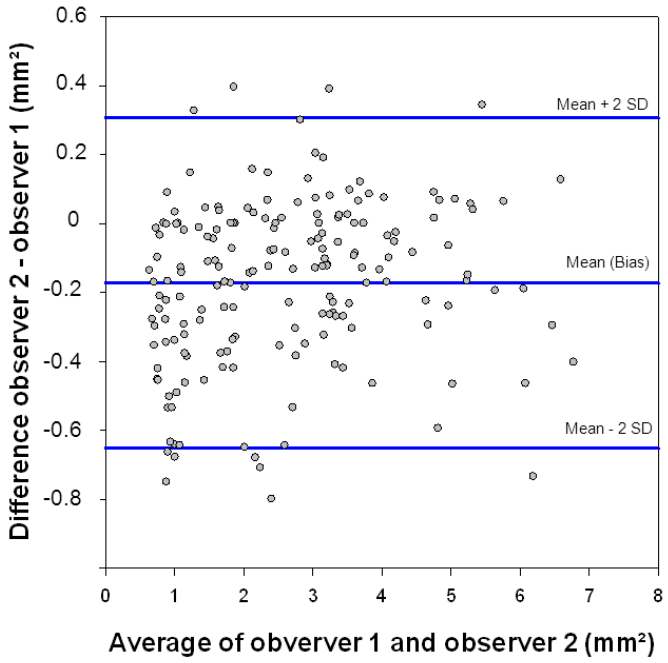

Figure 16: Inter-observer agreement for the ultrasonographic measurement of preperitoneal and subcutaneous fat was assessed by the Bland-Altman plot. 180 subcutaneous and preperitoneal adipose tissue areas were independently assessed by a second observer from 120 randomly chosen ultrasonographic images. The mean of the differences (bias) was -0.17 mm^2 and the Limits of Agreement were -0.65 mm^2 (mean -2 SD) and 0.31 mm^2 (mean + 2 SD). SD: standard deviation.

4.5.3 Assessment of abdominal ultrasonography

Complementary to the determination of SFT, abdominal ultrasonography was performed to discriminate between subcutaneous and preperitoneal adipose tissue. As indicated in **Table 8** and **Figure 17A**, SCA was significantly elevated in the newborns of obese mothers with GDM compared to the lean group after considering the confounders infant sex, gestational age and age at investigation. Likewise, PPA was significantly increased at week-1 compared to both, the normoglycemic lean and obese group **(Table 8** and **Figure 17B).** At the following scheduled ages of investigation at week-6, month-4 and year-1, the infants differed neither in SCA nor in PPA anymore. Moreover, the PPA-SCA ratios that were calculated at each assessment, were similar between the offspring of all study groups.

Table 8: Infant adipose tissue growth assessed by abdominal ultrasonography from week-1 to year-1 of life

	Lean group	Obese group	Obese GDM group	P-value[1]	Adjusted p-value[2]
Age at US investigation [d]					
Week-1	3.0 (2.3-4.0) [12]	3.0 (2.0-4.0) [12]	2.5 (2.0-4.0) [12]	0.813	-
Week-6	44.0 (42.0-46.0) [15]	43.0 (41.5-45.0.) [13]	43.5 (41.3-46.0) [12]	0.405	-
Month-4	113.0 (112-115.0) [15]	114.0 (111.0-115.0) [11]	115.0 (111.5-119.5) [13]	0.539	-
Year-1	367.0 (365.0-369.0) [15]	367.0 (363.5-374.5) [12]	367.0 (364.8-370.8) [14]	0.836	-
SCA (mm^2)					
Week-1	12.7 (9.5-15.4) [12]	16.7 (14.0-19.9) [12]	17.7 (16.8-19.4) [12]	**0.020** [a]	**0.014** [a]
Week-6	24.0 ± 6.6 [15]	26.5 ± 10.7 [13]	34.6 ± 7.9 [12]	**0.008** [a,b]	0.058 [a]
Month-4	41.3 ± 12.8 [15]	42.9 ± 9.4 [11]	45.6 ± 12.7 [13]	0.644	0.458
Year-1	24.6 (18.6-27.7) [15]	29.0 (26.8-36.2) [12]	34.2 (22.8-43.6) [14]	0.132	0.217
PPA (mm^2)					
Week-1	5.6 (4.9-7.9) [12]	7.9 (6.3-9.3) [12]	10.0 (8.9-12.2) [12]	**0.001** [a]	**0.001** [a,b]
Week-6	10.0 ± 2.7 [15]	11.4 ± 3.6 [13]	13.9 ± 2.9 [12]	**0.009** [a]	0.183
Month-4	13.5 (9.7-14.1) [15]	16.9 (12.1-18.6) [11]	15.6 (11.5-18.0) [13]	0.221	0.525
Year-1	17.5 ± 4.9 [15]	22.3 ± 7.0 [12]	20.8 ± 6.7 [14]	0.130	0.368
PPA-SCA ratio					
Week-1	0.24 (0.16-0.33) [12]	0.28 (0.17-0.36) [12]	0.28 (0.26-0.35) [12]	0.348	0.611
Week-6	0.20 (0.16-0.25) [15]	0.20 (0.16-0.30) [11]	0.21 (0.17-0.23) [13]	0.904	0.348
Month-4	0.17 ± 0.06 [15]	0.18 ± 0.08 [12]	0.18 ± 0.07 [14]	0.761	0.926
Year-1	0.29 (0.24-0.39) [15]	0.38 (0.24-0.51) [13]	0.32 (0.22-0.49) [12]	0.884	0.695

PPA: preperitoneal adipose tissue; SCA: subcutaneous adipose tissue (SCA and PPA were measured as areas of 1-cm length according to the method of Holzhauer et al. [105]. SCA indicates mean area from axial + sagittal plane); US: ultrasonography
Data are presented as mean ± SD; otherwise skewed variables are presented as median followed by interquartile range, n in brackets (all such values).
[1] One-way ANOVA was performed with Sidak's post hoc test or nonparametric Kruskal-Wallis-test with Dunn's post hoc test
[2] Statistical analyses were performed by multiple linear regression models. P-values for parameters at week-1 were adjusted for sex, pregnancy duration and age at investigation. P-values at week-6, month-4 and year-1 were adjusted for infant sex, pregnancy duration, age at investigation and corresponding breastfeeding status.
[a] P-value < 0.05 obese GDM vs. lean group; [b] p-value < 0.05 obese GDM vs. obese group. Significant values are presented in bold type.

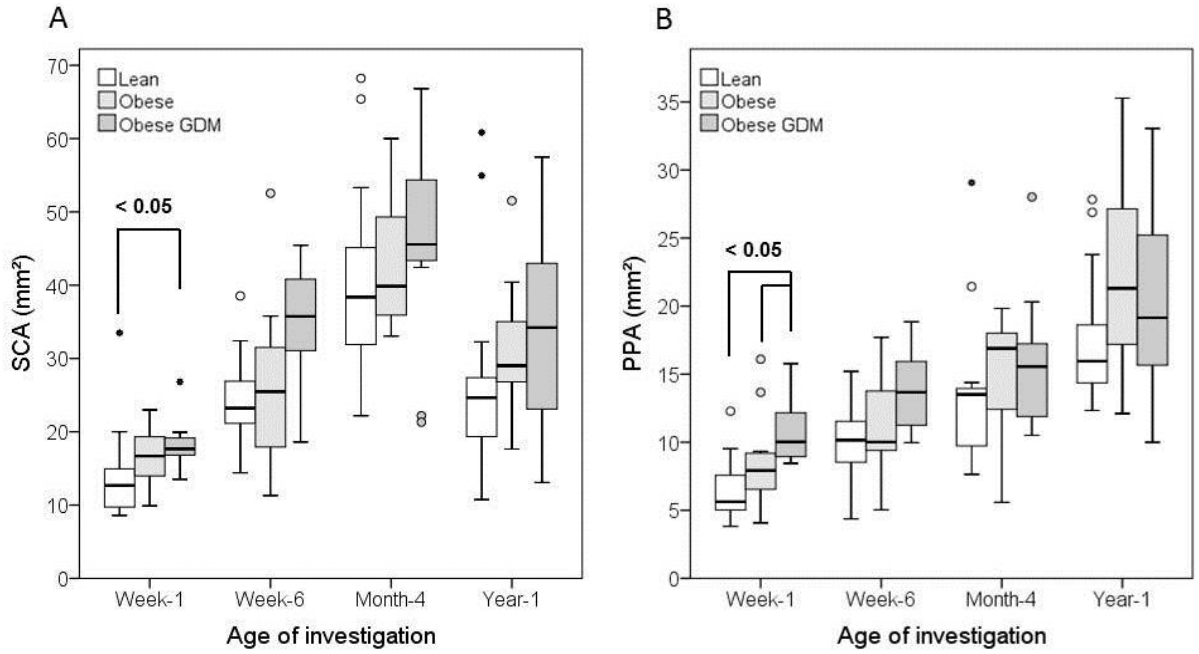

Figure 17: Longitudinal assessment of SCA (A) and PPA (B) at week-1, week-6, month-4 and year-1 in infants delivered by lean and obese women with and without GDM. Data are presented as boxplots. Bottom and top edges of the box represent the 25th and 75t^{h} percentiles. The horizontal line shows the median and the whiskers mark the maximum and minimum values. Outliers are presented as dots. Extremes are presented as asterisks. Refer to **Table 8** to obtain the total numbers of infants that were included in the analysis for each study group.

4.5.4 Correlation between anthropometric parameters and different measures of fat mass

To compare the anthropometric measures with SFT and abdominal fat distribution parameters (SCA, PPA), correlations between weight, ponderal index and particular adipose tissue parameters were conducted **(Table 9).** Body weight and ponderal index were significantly correlated with the sum of SFT, total fat mass and sonographic fat assessments (SCA and PPA) at all four ages of investigation. A strong correlation was also found between the both methods determining subcutaneous adipose tissue, namely SFT and ultrasonography. In early postnatal life at week-1 and week-6, PPA was correlated to anthropometric parameters and subcutaneous adipose tissue. With the beginning of the 3rd investigation at month-4, PPA correlated not any longer with subcutaneous adipose tissue neither determined by SFT nor ultrasonography. In contrast, PPA was further significantly associated with body weight and ponderal index at month-4 and at year-1. The PPA-SCA ratio did not correlate to body weight, ponderal index and subcutaneous fat determined by SFT at week-1 and week-6. In contrast, inverse relationships were found between sum of SFT and PPA-SCA ratio at month-4, while ponderal index, sum of SFT and fat mass showed a negative correlation with PPA-SCA ratio at the age of year-1.

Table 9: Spearman correlation between particular anthropometric and adipose tissue measurements at all ages investigated

	N	Body weight	Ponderal index	SFT	Fat mass	SCA	PPA
Week-1							
Ponderal index	44	**0.960 *** **	-	-	-	-	-
SFT	44	**0.578 *** **	**0.561 *** **	-	-	-	-
Fat mass	44	**0.814 *** **	**0.793 *** **	**0.931 *** **	-	-	-
SCA	36	**0.362 ***	0.323	**0.662 *** **	**0.605 ***	-	-
PPA	36	**0.434 *** **	**0.342 ***	**0.528 *** **	**0.552 *** **	**0.355 ***	-
PPA-SCA ratio	36	0.125	0.079	-0.068	0.006	-0.468	0.605

	N	Body weight	Ponderal index	SFT	Fat mass	SCA	PPA
Week-6							
Ponderal index	40	**0.975 *** **	-	-	-	-	-
SFT	40	**0.581 *** **	**0.607 *** **	-	-	-	-
Fat mass	40	**0.875 *** **	**0.886 *** **	**0.882 *** **	-	-	-
SCA	40	**0.507 *** **	**0.528 *** **	**0.777 *** **	**0.700 *** **	-	-
PPA	40	**0.533 *** **	**0.624 *** **	**0.584 *** **	**0.644 *** **	**0.627 *** **	-
PPA-SCA ratio	40	0.011	0.067	-0.228	-0.089	**-0.442 *** **	**0.349 ***

	N	Body weight	Ponderal index	SFT	Fat mass	SCA	PPA
Month-4							
Ponderal index	39	**0.976 * ****	-	-	-	-	-
SFT	39	**0.504 *** **	**0.515 *** **	-	-	-	-
Fat mass	39	**0.826 *** **	**0.820 *** **	**0.888 *** **	-	-	-
SCA	39	**0.542 *** **	**0.556 *** **	**0.785 *** **	**0.776 *** **	-	-
PPA	39	**0.400 ***	**0.391 ***	0.241	**0.378 ***	0.241	-
PPA-SCA ratio	39	0.026	0.013	**-0.321 ***	-0.181	**-0.497 *** **	**0.684 *** **

	N	Body weight	Ponderal index	SFT	Fat mass	SCA	PPA
Year-1							
Ponderal index	41	**0.957 *** **	-	-	-	-	-
SFT	41	**0.696 *** **	**0.743 *** **	-	-	-	-
Fat mass	41	**0.917 *** **	**0.913 *** **	**0.904 *** **	-	-	-
SCA	41	**0.577 *** **	**0.656 *** **	**0.682 *** **	**0.670 *** **	-	-
PPA	41	**0.328 ***	**0.364 ***	0.098	0.232	0.191	-
PPA-SCA ratio	41	-0.264	**-0.312 ***	**-0.597 *** **	**-0.460 *** **	**-0.675 *** **	**0.490 *** **

PPA: preperitoneal adipose tissue; SCA: subcutaneous adipose tissue; SFT: sum of the 4 skin fold thickness measurements (biceps + triceps + subscapular + suprailiac). *** P < 0.001; ** p < 0.01; * p < 0.05. Significant values are presented in bold type.

4.6 Correlation between metabolic markers in maternal and fetal plasma

Spearman and partial correlations were conducted to determine the association between different metabolic markers within maternal and fetal circulation, respectively **(Table 10).** At 3rd trimester, fasted maternal insulin levels were positively related to C-peptide and leptin levels in the unadjusted correlation (C-peptide: $r_1 = 0.757$ and leptin: $r_1 = 0.597$, $p < 0.001$) and after adjustment for maternal pre-pregnancy BMI, AUC $_{Glucose}$ (OGTT) and gestational weight gain ($r_2 = 0.735$, $p < 0.001$ and $r_2 = 0.380$, $p < 0.05$). Both, maternal insulin and C-peptide were significantly inversely associated to HMW, total adiponectin and S_A in the unadjusted analysis. Considering maternal confounders, however, only the negative correlation of C-peptide and total adiponectin was significant ($r_2 = -0.337$, $p < 0.05$).

Moreover, umbilical cord plasma insulin concentrations were significantly related to cord leptin levels in the unadjusted analysis ($r_1 = 0.464$ $p < 0.01$) and in the partial correlation analysis after adjustment for infant sex and pregnancy duration, maternal pre-pregnancy BMI, AUC $_{Glucose}$ (OGTT) and gestational weight gain ($r_2 = 0.388$ $p < 0.05$). However, neither insulin nor leptin levels were significantly associated with adiponectin (HMW, total and S_A) levels in umbilical cord plasma.

Table 10: Correlation between insulin, C-peptide and adiponectin levels from maternal and umbilical cord plasma, respectively.

Maternal plasma at 3rd trimester							
	N	**r**	**Insulin**	**C-peptide**	**HMW adiponectin**	**Total adiponectin**	**S_A**
C-peptide	42	r_1	**0.757*** **	-	-	-	-
		r_2	**0.735 *** **	-	-	-	-
HMW adiponectin	42	r_1	**-0.453 ****	**-0.447 ****	-	-	-
		r_2	-0.283	-0.294	-	-	-
Total adiponectin	42	r_1	**-0.423 ****	**-0.432 ****	**0.943 *** **	-	-
		r_2	-0.290	**-0.337 ***	**-0.944 *** **	-	-
S_A	42	r_1	**-0.458 ****	**-0.434 ****	**0.885 *** **	**0.774 *** **	-
		r_2	-0.25	-0.161	**0.779 *** **	**0.550 *** **	-
Leptin	42	r_1	**0.597 *** **	**0.498 ****	**-0.535 *** **	**-0.479 ****	**-0.539 *** **
		r_2	**0.380 ***	0.320	-0.257	-0.272	-0.163

HMW: high molecular weight; S_A: HMW-total adiponectin ratio; r: correlation coefficient. r_1: unadjusted Spearman correlation coefficient; r_2: partial correlation coefficient adjusted for covariates maternal pre-pregnancy BMI, AUC $_{Glucose}$ (OGTT) and gestational weight gain. *** $P < 0.001$; ** $p < 0.01$; * $p < 0.05$. Significant values are presented in bold type.

Continued table 10: Correlation between insulin, C-peptide and adiponectin levels from maternal and umbilical cord plasma, respectively.

			Umbilical cord plasma			
	N	**r**	**Insulin**	**HMW adiponectin**	**Total adiponectin**	**S_A**
HMW adiponectin	44	r_1	0.119	-	-	-
		r_2	0.064	-	-	-
Total adiponectin	44	r_1	0.121	**0.980 *****	-	-
		r_2	0.010	**0.984 *****	-	-
S_A	44	r_1	0.159	**0.704 *****	**0.591 *****	-
		r_2	0.150	**0.739 *****	**0.632 *****	-
Leptin	44	r_1	**0.464 ****	-0.039	-0.068	-0.124
		r_2	**0.388 ***	-0.041	-0.085	-0.103

HMW: high molecular weight; S_A: HMW-total adiponectin ratio; r: correlation coefficient. r_1: unadjusted Spearman correlation coefficient, r_2: partial correlation coefficient adjusted for covariates infant sex, pregnancy duration, maternal pre-pregnancy BMI, AUC $_{Glucose}$ (OGTT) and gestational weight gain. *** P < 0.001; ** p < 0.01; * p < 0.05. Significant values are presented in bold type.

4.7 Relation of maternal plasma markers to offspring fat distribution up to year-1

4.7.1 Relation of maternal plasma C-peptide and insulin levels to offspring fat distribution up to year-1

Multiple regression analyses were conducted to determine the association of maternal fasted C-peptide, insulin, adiponectin (HMW, total, S_A) and leptin levels with neonatal PPA, SCA and SFT at all ages investigated (**Figure 18**, **Figure 19** and **Supplemental table 4**).

For maternal C-peptide and insulin levels, a significantly positive relationship with infant PPA at week-1 was found in the unadjusted analysis and this association remained almost unchanged after adjustment for infant sex, pregnancy duration, pre-pregnancy BMI, OGTT-derived AUC $_{Glucose}$ and gestational weight gain (C-peptide: β_{adj} = 0.533; p = 0.001; insulin: β_{adj} = 0.444; p = 0.010) **(Figure 18).** Notably, no significant relationships were found for maternal insulin and C-peptide with subcutaneous adipose tissues, namely SCA and SFT.

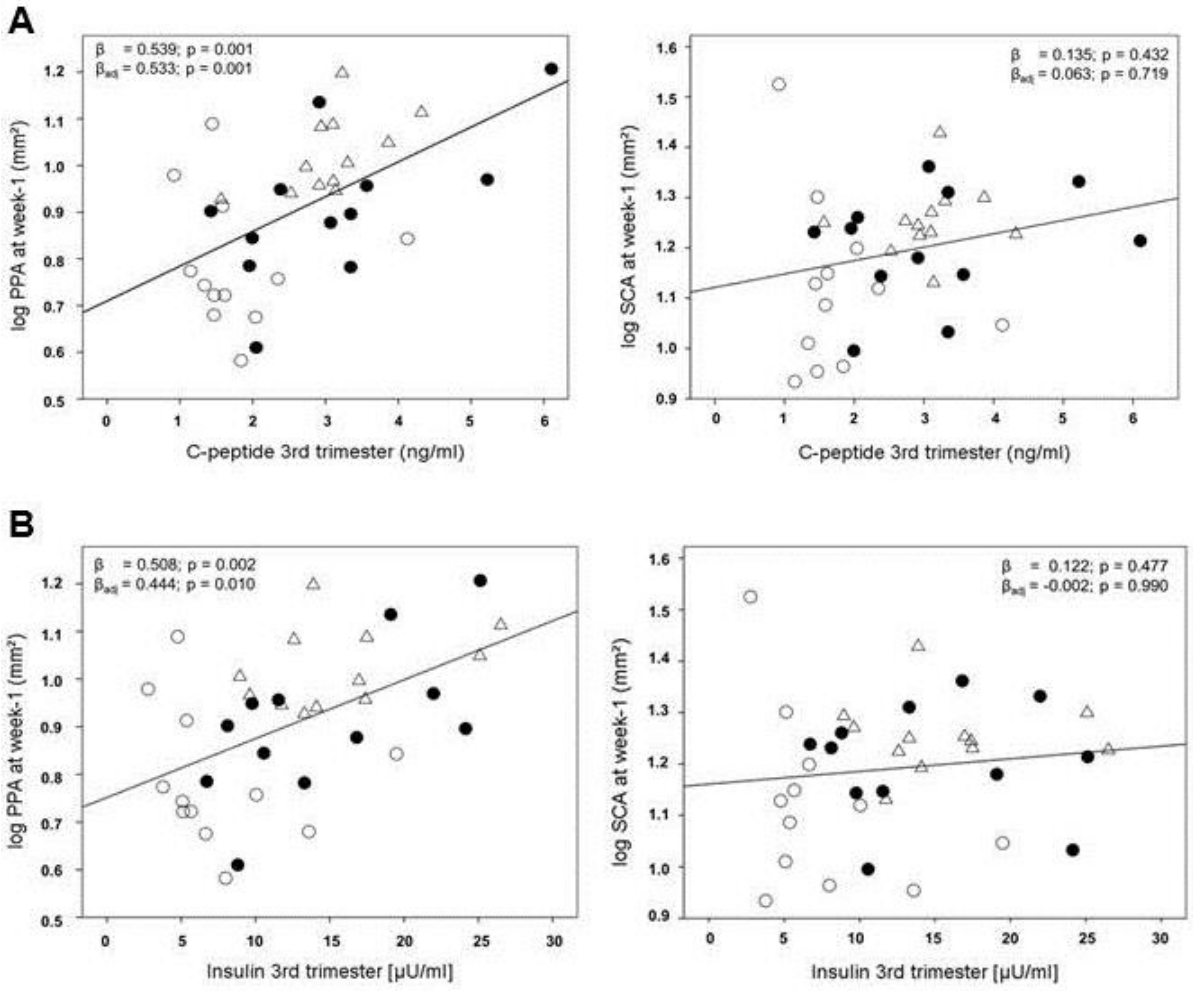

Figure 18: Regression of infant PPA and SCA at week-1 on maternal C-peptide and insulin levels at 3rd trimester. Maternal (A) C-peptide and (B) insulin are presented in relation to neonatal PPA and SCA, respectively. β: unadjusted standardized regression coefficient, β_{adj}: standardized regression coefficient adjusted for the covariates infant sex, pregnancy duration, maternal pre-pregnancy BMI, AUC $_{Glucose}$ (OGTT) and gestational weight gain. The plotted regression lines indicate the results of the unadjusted analyses (β). Log: logarithmic; PPA: preperitoneal adipose tissue; SCA: subcutaneous adipose tissue; open circles: lean group (n=12); black circles: obese group (n=12); open triangles: obese GDM group (n=12).

4.7.2 Relation of maternal plasma adiponectin and leptin levels to offspring fat distribution up to year-1

Interestingly, decreasing levels of maternal total adiponectin, HMW adiponectin, and S_A were significantly related to increased infant PPA at week-1 in the unadjusted analysis, whereas in the adjusted model, only maternal HMW adiponectin was still significantly related to newborn PPA (β_{adj} = -0.338; p = 0.038) **(Figure 19A-C**). Notably, maternal adiponectin levels at 3rd trimester were not significantly related to newborn SFT and SCA **(Figure 19** and **Supplemental table 4).** Regarding relationships between maternal biomarkers and PPA at later ages of investigation, maternal HMW, total adiponectin and S_A were still associated with PPA at week-6 in the unadjusted analysis (HMW adiponectin: β = -0.325; p = 0.041; total adiponectin: β = -0.318; p = 0.045; S_A: β = -0.326; p = 0.040), but no longer in the fully adjusted models (β_{adj}). The indicated maternal parameters were not further related to PPA at

month-4 and year-1 in both linear regressions, however the analysis showed that maternal HMW adiponectin and S_A were significantly positively related to infant SCA only at month-4 in the adjusted model (β_{adj} = 0.387; p = 0.041) **(Supplemental table 4).** In contrast to adiponectin, no such relationship was determined between maternal leptin levels and neonatal PPA in both analyses, but leptin levels were weakly related to SCA at week-1 in the unadjusted analysis (β = 0.332; p = 0.048) **(Figure 19D).**

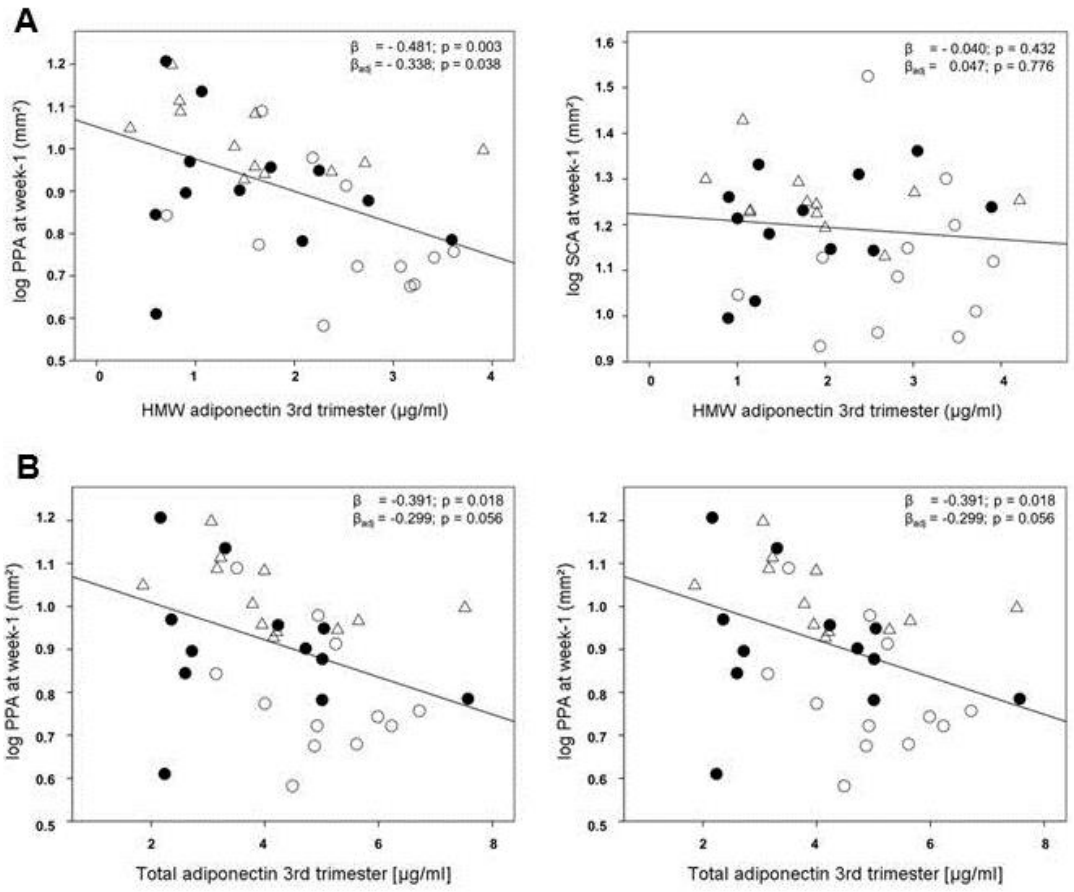

Figure 19: Regression of infant PPA and SCA at week-1 on maternal HMW, total adiponectin levels, HMW-total adiponcectin ratio (S_A) and leptin levels at 3rd trimester. Maternal (A) HMW adiponectin and (B) total adiponectin are presented in relation to neonatal PPA and SCA, respectively. β: unadjusted standardized regression coefficient; β_{adj}: standardized regression coefficient adjusted for the covariates infant sex, pregnancy duration, maternal pre-pregnancy BMI, $AUC_{Glucose}$ (OGTT) and gestational weight gain. The plotted regression lines indicate the results of the unadjusted analyses (β). HMW: high molecular weight; Log: logarithmic; PPA: preperitoneal adipose tissue; SCA: subcutaneous adipose tissue; open circles: lean group (n=12); black circles: obese group (n=12); open triangles: obese GDM group (n=12).

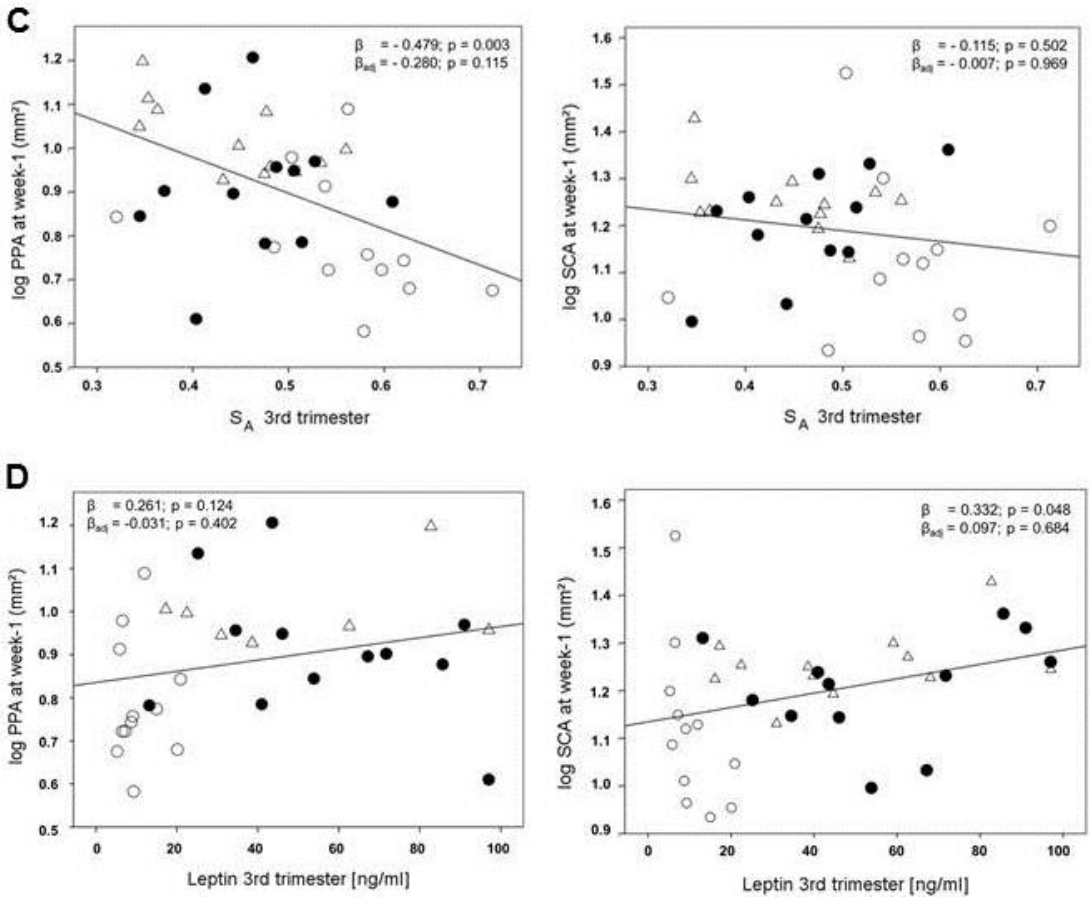

Continued Figure 19: Regression of infant PPA and SCA at week-1 on maternal HMW, total adiponectin levels, HMW-total adiponcectin ratio (S_A) and leptin levels at 3rd trimester. (C) S_A and (D) leptin are presented in relation to neonatal PPA and SCA, respectively. β: unadjusted standardized regression coefficient; β_{adj}: standardized regression coefficient adjusted for the covariates infant sex, pregnancy duration, maternal pre-pregnancy BMI, AUC $_{Glucose}$ (OGTT) and gestational weight gain. The plotted regression lines indicate the results of the unadjusted analyses (β). HMW: high molecular weight; Log: logarithmic; PPA: preperitoneal adipose tissue; S_A: HMW-total adiponectin ratio; SCA: subcutaneous adipose tissue; open circles: lean group (n=12); black circles: obese group (n=12); open triangles: obese GDM group (n=12).

4.7.3 Relation of maternal plasma CRP and IL6 levels to offspring fat distribution up to year-1

Further multiple regression analyses were conducted to assess the potential impact of maternal fasted systemic inflammatory markers (CRP and IL6) at 3rd trimester on infant adipose tissue growth up to year-1 **(Table 11).** For maternal CRP levels, a significantly positive relationship with infant PPA at week-1 and at week-6 (β = 0.461; p = 0.007 and β = 0.410; p = 0.012) as well as for SCA at year-1 (β = 0.367; p = 0.022) were only determined in the unadjusted analysis. In contrast, maternal plasma IL6 levels were significantly positively related to PPA at week-6 after adjustment for infant sex, pregnancy duration, pre-pregnancy BMI, OGTT-derived AUC $_{Glucose}$, gestational weight gain and breastfeeding status (β_{adj} = 0.333; p = 0.030).

Table 11: Regression of infant fat distribution parameter up to year-1 on maternal plasma CRP and IL6 levels at 3rd trimester

		Maternal plasma CRP					Maternal Plasma IL6				
		Unadjusted analysis		Adjusted analysis			Unadjusted analysis		Adjusted analysis		
	N	β	P-value	β	P-value	Adj model r^2	β	P-value	β	P-value	Adj model r^2
Week-1											
SFT	37	0.298	0.066	0.191	0.301	0.064; p = 0.234	0.086	0.601	0.007	0.967	0.031; p = 0.329
SCA	33	0.278	0.117	0.165	0.399	0.152; p = 0.109	0.159	0.377	0.101	0.567	0.139: p = 0.126
PPA	33	**0.461**	**0.007**	0.239	0.204	0.373; p= 0.043	0.218	0.222	0.171	0.339	0.125; p = 0.147
Week-6											
SFT	37	0.196	0.246	0.078	0.679	0.114; p = 0.159	0.102	0.549	0.040	0.811	0.077; p = 0.220
SCA	37	0.191	0.258	0.065	0.726	0.141: p = 0.117	0.010	0.953	0.078	0.634	0.144; p = 0.112
PPA	37	**0.410**	**0.012**	0.258	0.143	0.251; p = 0.027	0.273	0.102	**0.333**	**0.030**	**0.316; p = 0.009**
Month-4											
SFT	37	0.084	0.621	0.037	0.841	0.124; p = 0.142	0.123	0.468	0.177	0.277	0.158; p = 0.095
SCA	37	0.105	0.536	0.115	0.543	0.075; p = 0.237	0.148	0.382	0.216	0.196	0.116; p = 0.155
PPA	37	-0.069	0.680	-0.089	0.658	-0.100; p = 813	-0.052	0.755	-0.032	0.858	-0.106; p = 0.832
Year-1											
SFT	39	0.105	0.525	-0.014	0.942	-0.067; p = 0.704	0.117	0.480	0.145	0.414	-0.044; p = 0.616
SCA	39	**0.367**	**0.022**	0.247	0.196	0.045; p = 0.303	0.161	0.329	0.148	0.388	-0.016; p = 0.395
PPA	39	0.168	0.308	0.019	0.913	0.143.; p = 0.102	0.078	0.636	0.076	0.634	0.149; p = 0.094

β: standardized regression coefficient, r^2: coefficient of determination; SCA: subcutaneous adipose tissue; SFT: skin fold thickness, PPA: preperitoneal adipose tissue. Variables for adjusted analysis: infant sex, pregnancy duration, respective breastfeeding status, maternal pre-pregnant BMI, $AUC_{Glucose}$ (OGTT) and gestational weight gain. Significant values are presented in bold type.

4.8 Relation of umbilical cord plasma markers to offspring fat distribution up to year-1

4.8.1 Relation of cord plasma insulin to offspring fat distribution up to year-1

The relationship of umbilical cord levels with adipose tissue markers (SFT, SCA and PPA at all ages investigated) was explored by linear regression analysis. The infant covariables sex, pregnancy duration, respective breastfeeding status and additionally the maternal covariables pre-pregnancy BMI, $AUC_{Glucose}$ (OGTT) and gestational weight gain were considered in the adjusted model **(Table 12).** Thus, cord insulin levels were positively related to newborn SFT in the unadjusted analysis, not in the adjusted model (β_{adj} = 0.325; p = 0.071). Applying identical variables for further regression analyses, cord insulin levels also emerged as positive determinant for SCA and PPA development at week-1 in the unadjusted analysis **(Table 12)** and this independent relationship still remained after adjusting for indicated covariables (β_{adj} = 0.390; p = 0.039; β_{adj} = 0.436; p = 0.022). At week-6, umbilical cord insulin levels were further significantly related to SCA in the unadjusted analyses and the relationship of SFT and PPA with cord insulin approached significance (β = 0.294; p = 0.065 and β = 0.307; p = 0.054). However, no associations were found between cord insulin levels and fat distribution parameters at week-6, month-4 and year-1 in the fully adjusted analyses.

Table 12: Regression of fat distribution parameters up to year-1 on cord plasma insulin levels

	Cord plasma insulin					
		Unadjusted analysis		Adjusted analysis		
	N	β	P-value	β	P-value	Adjusted model r^2
Week-1						
SFT	44	**0.398**	**0.007**	0.325	0.071	**0.195; p = 0.026**
SCA	36	**0.464**	**0.004**	**0.390**	**0.039**	**0.310; p = 0.008**
PPA	36	**0.445**	**0.007**	**0.436**	**0.022**	**0.311; p = 0.008**
Week-6						
SFT	40	0.294	0.065	0.292	0.146	0.122; p = 0.127
SCA	40	**0.335**	**0.035**	0.241	0.217	0.163; p = 0.074
PPA	40	0.307	0.054	0.287	0.119	0.268; p = 0.014
Month-4						
SFT	39	0.281	0.084	0.196	0.335	0.080; p = 0.215
SCA	39	0.175	0.287	0.056	0.794	-0.044; p = 0.615
PPA	39	0.146	0.368	0.011	0.961	-0.090; p = 0.799
Year-1						
SFT	41	-0.072	0.653	-0.017	0.937	-0.080; p = 0.769
SCA	41	0.027	0.866	0.085	0.68	-0.034; p = 0.585
PPA	41	0.062	0.698	0.198	0.29	0.137; p = 0.099

β: standardized regression coefficient, r^2: coefficient of determination; PPA: preperitoneal adipose tissue; SCA: subcutaneous adipose tissue; SFT: sum of the 4 skin fold thickness measurements (biceps + triceps + subscapular + suprailiac). Variables for adjusted analysis: infant sex, pregnancy duration, respective breastfeeding status, maternal pre-pregnancy BMI, $AUC_{Glucose}$ (OGTT) and gestational weight gain. Significant variables are presented in bold type.

4.8.2 Relation of cord plasma leptin and adiponectin to offspring fat distribution up to year-1

Linear regression analyses were performed to assess the relationship of adipose tissue markers leptin and adiponectin in cord blood plasma with distinct growth parameters assessed at all ages investigated **(Table 13).** Cord leptin levels were highly related to SFT and SCA at week-1 and similar relationships were observed after considering infant sex, pregnancy duration, maternal pre-pregnancy BMI, $AUC_{Glucose}$ (OGTT) and gestational weight gain (SFT: $\beta_{adj} = 0.381$; p = 0.009; SCA: $\beta_{adj} = 0.416$; p = 0.007). At week-6, cord leptin levels emerged as significant positive variables only for SCA, but not SFT, in the unadjusted and adjusted analysis ($\beta_{adj} = 0.408$; p = 0.007). However, the positive relationship of cord insulin to SCA attenuated at month-4 ($\beta_{adj} = 0.298$, p = 0.091) and did not last until year-1. In contrast, PPA remained unrelated to cord leptin levels in both linear regression analyses at all ages investigated. In general, cord plasma HMW adiponectin and S_A were not significantly related to indicated newborn adipose tissue markers from week-1 up to year-1. However, a significant negative relationship of cord plasma S_A with PPA at year-1 was only found in the unadjusted analysis (β = -0.313, p = 0.047).

Table 13: Regression of adipose tissue distribution up to year-1 on cord plasma leptin and adiponectin levels

		Cord plasma leptin					Cord plasma HMW adiponectin					Cord Plasma S_A				
		Unadjusted analysis		Adjusted analysis			Unadjusted analysis		Adjusted analysis			Unadjusted analysis		Adjusted analysis		
	N	β	P-value	β	P-value	Adjusted model r^2	β	P-value	β	P-value	Adjusted model r^2	β	P-value	β	P-value	Adjusted model r^2
Week-1																
SFT	44	**0.463**	**0.002**	**0.381**	**0.009**	**0.270; p=0.006**	-0.008	0.959	0.007	0.904	0.120; p=0.094	-0.127	0.410	-0.056	0.721	0.123; p=0.090
SCA	36	**0.482**	**0.003**	**0.416**	**0.007**	**0.381; p=0.002**	0.204	0.232	0.146	0.351	0.233; p=0.034	0.014	0.936	-0.045	0.798	0.201; p=0.047
PPA	36	0.113	0.664	-0.053	0.748	0.174; p=0.068	0.099	0.565	0.181	0.254	0.208; p=0.043	-0.057	0.743	0.121	0.500	0.185; p=0.060
Week-6																
SFT	40	0.180	0.267	0.164	0.319	0.090; p=0.185	0.194	0.231	0.234	0.270	0.123; p=0.125	0.016	0.924	0.175	0.326	0.090; p=0.187
SCA	40	**0.404**	**0.010**	**0.408**	**0.007**	0.301; p=0.008	0.070	0.668	0.102	0.516	0.133; p=0.110	-0.098	0.546	0.039	0.822	0.125; p=0.123
PPA	40	0.027	0.868	0.001	0.998	0.209; p=0.038	-0.173	0.387	-0.112	0.450	0.223; p=0.030	-0.233	0.148	-0.022	0.893	0.209; p=0.038
Month-4																
SFT	39	0.050	0.765	0.122	0.722	0.067; p=0.245	0.300	0.063	0.225	0.175	0.107; p=0.159	0.254	0.119	0.305	0.077	0.144; p=0.102
SCA	39	0.215	0.188	0.298	0.091	0.047; p=0.298	0.155	0.345	0.083	0.638	-0.039; p=0.595	0.159	0.333	0.174	0.343	-0.016; p=0.508
PPA	39	0.044	0.789	0.051	0.779	-0.088; p=0.790	0.130	0.423	0.100	0.573	-0.080; p=0.759	0.093	0.567	0.148	0.426	-0.069; p=0.718
Year-1																
SFT	41	0.089	0.581	0.029	0.884	-0.079; p=0.767	0.062	0.698	0.088	0.616	-0.072; p=0.737	0.117	0.465	0.236	0.204	-0.028; p=0.558
SCA	41	0.066	0.680	-0.031	0.873	-0.039; p=0.604	-0.059	0.713	-0.046	0.788	-0.038; p=0.598	-0.098	0.977	0.124	0.500	-0.025; p=0.549
PPA	41	0.017	0.914	-0.072	0.651	0.142; p=0.093	-0.082	0.609	0.070	0.652	0.142; p=0.093	**-0.313**	**0.047**	-0.137	0.416	0.154; p=0.079

β: standardized regression coefficient; HMW: high molecular weight; PPA: preperitoneal adipose tissue; r^2: coefficient of determination. S_A: HMW-total adiponectin ratio; SCA: subcutaneous adipose tissue; SFT: sum of the 4 skin fold thickness measurements (biceps + triceps + subscapular + suprailiac). Variables for adjusted analysis: infant sex, pregnancy duration, respective breastfeeding status maternal pre-pregnancy BMI, $AUC_{Glucose}$ (OGTT) and gestational weight gain. Significant variables are presented in bold type.

4.9 Associations between offspring anthropometric parameters at birth and at year-1

The effect of neonatal anthropometric parameters on corresponding primary endpoint parameters at year-1 were evaluated by linear regression, while infant sex, pregnancy duration, breastfeeding status at month-4, pre-pregnancy BMI, AUC $_{Glucose}$ (OGTT) and gestational weight gain were included as variables in the adjusted analysis **(Table 14).** Values for PPA at week-1 emerged as positive independent determinants of PPA at year-1 in both analyses (β_{adj} = 0.486, p = 0.010). In contrast, no further significant relationships were observed between newborn body weight, ponderal index, SFT, SCA, and respective parameters assessed at year-1.

Table 14: Regression of year-1 growth and fat mass parameters on respective neonatal assessments

	Respective parameter at year-1					
		Unadjusted analysis		Adjusted analysis		
	N	β	P-value	β	P-value	Adjusted model r^2
Birth weight	41	0.294	0.062	0.179	0.289	0.149; p = 0.085
Birth ponderal index	41	0.248	0.117	0.161	0.342	0.130; p = 0.109
SFT at week-1	41	-0.012	0.939	-0.082	0.666	-0.074; p = 0.746
SCA at week-1	36	0.006	0.863	-0.260	0.227	-0.260; p = 0.277
PPA at week-1	36	**0.520**	**0.002**	**0.486**	**0.010**	**0.275; p = 0.027**

β: standardized regression coefficient; PPA: preperitoneal adipose tissue; r^2: coefficient of determination; SCA: subcutaneous adipose tissue; SFT: sum of the 4 skin fold thickness measurements (biceps + triceps + subscapular + suprailiac).
Variables for adjusted analysis: infant sex, pregnancy duration, breastfeeding status at month-4, maternal pre-pregnancy BMI, AUC $_{Glucose}$ (OGTT) and gestational weight gain. Significant variables are presented in bold type

4.10 Transcriptomic analysis of placental gene expression

4.10.1 Global gene expression and hierarchical clustering

Hierarchical dendrogram and PCA of placental microarray data were applied to identify if samples that were allocated to the same group, have similar global gene expression pattern. The samples that are clustered in similar areas within the two-dimensional plots show (a) similarities among the particular group members and (b) differences between study groups.

The results of the hierarchical dendrogram and the PCA are presented in **Supplemental Figure 1** and **2,** respectively. After applying all transcriptomic data with fluorescence values ≥ 30 in at least one group for the PCA calculation, placental samples obtained from lean and obese women with and without GDM only poorly grouped in similar areas within the two-dimensional scatterplot. Likewise, the hierarchical dendrogram revealed no clear clustering of samples into the group allocation according to pregravid BMI and OGTT.

After the compilation of all genes meeting the criteria for fold change (FC) ≥ 1.3 or ≤ -1.3 and p-value < 0.05 from pairwise comparisons, most differentially expressed genes were found in placentas of obese GDM cases compared to normoglycemic lean (454 genes) and obese subjects (469 genes). Thereof, 221 (48.7 %) and 160 genes (34.1 %) were up-regulated and further 233 (51.3 %) and 309 genes (65.9 %) were down-regulated in placentas of GDM women compared to lean and obese women, respectively. In contrast, only 152 genes were significantly regulated between normoglycemic lean and obese women **(Figure 20).** Thereof, 83 genes (54.6 %) were higher and 69 genes (45.4 %) were lower expressed in placentas of obese compared to lean participants.

Due to recurrent appearance of differentially regulated genes within the three pairwise comparisons, it was possible to identify distinct impacts of pregravid obesity and GDM on gene expression (**Supplemental table 5).** Out of 152 genes, 117 genes were found exclusively regulated in obese compared to lean subjects, whereas 35 genes showed similar fold changes in placentas of obese and obese GDM compared to lean subjects, respectively, suggesting a regulation through pregravid BMI, but independently of GDM incidence. Furthermore, 151 indicated genes were differentially expressed in placentas with GDM incidence compared to placentas of lean and obese participants. The regulation of these genes might represent the separate impact of GDM in comparison with normoglyemic women independently of pregravid BMI. Nevertheless, 318 and 303 genes were particularly regulated only in the obese GDM group compared to lean and obese women, respectively **(Supplemental table 5).**

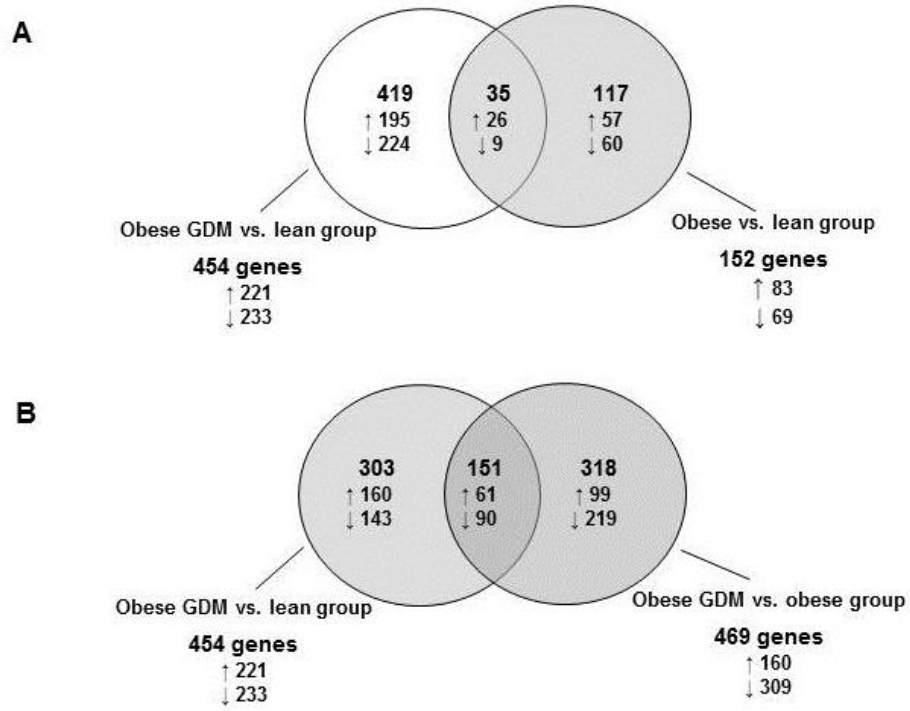

Figure 20: VENN diagrams representing the numbers of differentially regulated genes according to LIMMA statistical analysis from three comparisons - obese vs. lean group, obese GDM vs. lean group, and obese GDM vs. obese group. The differentially expressed genes meeting the criteria for FC ≥ 1.3 or ≤ -1.3 and p-value < 0.05 from pairwise comparisons are indicated. **A)** Common regulated genes in the obese and obese GDM group compared to the lean group. **B)** Common regulated genes in the obese GDM group compared to the lean and obese group. Analysis was performed in term placentas of lean (n=9), obese (n=10) and obese GDM (n=8) women.

4.10.2 Functional networks of differentially regulated genes

All differentially regulated genes from indicated pairwise comparisons were applied to generate functional networks with the 'IPA'-software. Each gene was mapped according to information retrieved from the 'Ingenuity Pathways Knowledge Base' (IPKB).

The three highest scored functional networks, including the assigned differentially regulated genes of all pairwise comparisons, are presented in **Supplemental table 6**. Furthermore, each top global molecular network is visualised in a diagram. The networks that were enriched by differentially expressed genes in the comparison of the lean and obese group comprise of 'Cell Death and Survival, Cellular Development, Cellular Growth and Proliferation', 'Cardiovascular System Development and Function, Organismal Development, Cellular Development' as well as 'Cellular Assembly and Organization, Post-Translational Modification, Hematological Disease'. From the comparison between samples that were obtained from the lean and obese GDM group, the highest scored-enriched networks were related to either 'Cancer, Connective Tissue Disorders, Organismal Injury and Abnormalities'

or ‘Cellular Growth and Proliferation’. The comparison between samples from the obese and obese GDM group revealed the top three enriched functional networks comprising of ‘Cardiovascular System Development and Function, Organismal Development, Gene Expression’ and ‘Cellular Development, Hematological System Development and Function, Hematopoiesis’ as well as ‘Connective Tissue Disorders’.

4.10.3 Placental pathway analysis of differentially regulated genes

To investigate potentially regulated signaling pathways between placentas obtained from lean and obese women with and without GDM, the ‘Genomatix GEPS’-program was applied, including canonical as well as signal transduction pathways from Genomatix Literature Mining.

Due to the small number of differentially regulated genes for each canonical pathway, the analysis was carried out with the signal transduction pathways from Genomatix Literature Mining **(Table 15).** Accordingly, genes implicated in *Lymphocyte specific protein tyrosine kinase*, *Fibroblast growth factor* and *Oncogenic pathways*, as well as in *Angiogenesis, Hypoxia inducible factor 1α, Nitric oxide* and *Lipid signaling,* were significantly regulated between placentas obtained from lean and obese women. The most significantly enriched pathways affected by maternal obesity with GDM included *Proliferation, Differentiation, Angiogenesis* as well as *Transforming growth factor β (TGF-β), Vascular endothelial growth facor (VEGF)* and *V AKT murine thymoma viral oncogene homolog 1 signaling* in comparison to both normoglycemic groups. Moreover, the Genomatix analysis revealed that differentially regulated genes assigned to *Low-density lipoprotein receptor related protein/ Wingless-int (wnt) type/ β-catenin signaling* were over-represented in the GDM cases compared to the lean and obese non-diabetic counterparts. In contrast, genes involved in *Paired like homeodomain 2, Matrix metalloproteinase and Thrombospondin signaling* were only significantly enriched in placentas of obese GDM in comparison to lean subjects. Furthermore, genes assigned to *Notch, Mothers against decapentaplegic (DPP) homolog* as well as *Retinoic acid receptor α signaling* were only differentially expressed between placentas of obese GDM and euglycemic obese women. Interestingly, the pathway analysis of this thesis did not provide significantly regulated pathways between the three groups that were related to immune system or inflammatory processes.

Table 15: Over-represented signal transduction pathways from pairwise comparisons analysed by the Genomatix Pathway System (GePS)

Pathway		List of observed genes	P-value
A) Obese vs. lean group			
Formly peptide receptor 1	2/15	LCP1[#], LYN[§]	4.97E-03
F Box and WD repeat domain containing 7	2/18	ILK[§], NOTCH1[#]	7.14E-03
Anaplastic lymphoma kinase	2/23	LYN[§], JUNB[§]	1.15E-02
Reelin	2/24	LDLR[§], NOTCH1[#]	1.25E-02
Progesteron receptor	2/27	PRL[§], ERRFI1[§]	1.57E-02
Lymphocyte specific protein tyrosine kinase	3/77	DPP4[§], G3BP1[§], LYN[§]	1.74E-02
Lipid	6/299	LDLR[§], HPSE[#], DPP4[§], FABP4[#], XDH[§], LYN[§]	1.89E-02
CD36 molecule (Thrombospondin receptor)	2/233	LDLR[§], LYN[§]	2.30E-02
Dual specificity tyrosine phosphorylation regulated kinase	2/37	SEPT4[#], NFATC1[§]	2.85E-02
Oncogenic	4/175	HILPDA[§], TSC22D1[§], ERRFI1[§], NOTCH1[#]	3.58E-02
Angiogenesis	3/159	NOTCH[#], HPSE[#], FLT1[§]	3.59E-02
Hypoxia inducible factor 1α	3/103	HILPDA[§], ILK[§], FLT1[§]	3.70E-02
Fibroblast growth factor (FGF)	4/247	HS6ST2[§], FGF12[#], HPSE[#],HES5[#]	3.78E-02
Hairy and enhancer of Split1	2/44	HES5[#], NOTCH1[#]	3.92E-02
FMS like receptor tyrosine kinase 3	2/44	LYN[§], FLT1[§]	3.92E-02
Nitric oxide	3/106	RGN[#], XDH[§], GAPDH[§]	3.98E-02
B) Obese GDM vs. lean group			
Proliferation	28/415	SPIN1[#], LRIG1[§], CHI3L1[§], CXCR7[§], CCND2[§], VCAN[§], IGFBP5[§], CD28[§], COL1A1[§], GAS6[§], CD9[§], PROK1[§], CSPG4[§], PITX2[§], PC[§], SDC1[#], F3[§], SLC3A2[#], WNT7A[#], NOX4[§], PRL[§], NIM1[#], EGFL7[§], S100A4[§], HGF[§], FGFR3[§], SPARC[§], JUNB[§]	3.26E-06
Paired like Homeodomain 2	5/15	CCND2[§], LEFTY2[§], PITX2[§], LEF1[§], PAWR[#]	3.82E-05
Transforming growth factor β	29/506	BAMBI[§], TGFBI[§], BMP5[§], VCAN[§], MATN2[§], DCN[§], PRRX1[§], COMP[§], LEFTY2[§], RUNX1T1[§], COL1A1[§], CTHRC1[§], TMEM119[§], ETS1[§], BMP4[§], FBLN2[§], ADAMTSL2[§], FMOD[§], PDZRN3[§], NOX4[§], KRT14[§], FSCN1[§], MGP[§], GULP1[#], TM4SF5[#], SPARC[§], JUNB[§], GREM2[#], ADAM12[#]	1.36E-04
Matrix Metalloproteinase	21/175	CLDN5[§], MMP23B[§], ETS1[§], CD9[§], ENPP2[§], FLNA[§], TIMP4[§], NOX4[§], FSCN1[§], TIMP2[#], S100A4[§], HGF[§], ADAM12[#]	1.14E-03
Wingless-int (wnt) type	23/451	LGR4[#], SPIN1[#], BAMBI[§], HOXC6[§], ANTXR1[§], CD97[#], RSPO2[§], NRARP[§], CTHRC1[§], PIGP[#], CD9[§], PITX2[§], PROM1[§], DKK3[§], BMP4[§], WNT7A[#], PDZRN3[§], LEF1[§], SSBP2[§], S100A4[§], PTK7[§], CDH11[§], GREM2[#]	1.54E-03
Differentiation	28/572	DES[§], HEY2[§], PLEKHM3[§], NEUROD2[#], SMARCD3[§], TGFBI[§], BMP5[§], NDN[§], IGFBP5[§], STK40[#], COL1A1[§], TCF21[§], TMEM119[§], ETS1[§], PROK1[§], PITX2[§], BMP4[§], WNT7A[#], PDZRN3[§], NOX4[§], PRL[§], KRT14[§], RARRES2[§], CXCL14[§], CDH11[§], FGFR3[§], JUNB[§], ADAM12[#]	2.19E-03
Thrombospondin 1	5/35	CD36[§], PRKCZ[#], THBS2[§], FSCN1[§], SPARC[§]	2.63E-03
Angiogenesis	11/159	SLCO2A1[#], ETS1[§], ENPP2[§], THBS2[§], F3[§], HPSE[#], APLNR[§], TIMP2[#], HGF[§], SPARC[§], MIR126[§]	4.70E-03
Low-density lipoprotein receptor related protein	8/115	DCN[§], THBS2[§], DKK3[§], SDC1[#], WNT7A[#], LEF1[§], PTH1R[§], GULP1[#]	1.47E-02
Lymphoid enhancer binding factor 1 (TCF/LEF)	7/115	VCAN[§], NRARP[§], PITX2[§], DKK3[§], SDC1[#], LEF1[§], FSCN1[§]	1.47E-02
V AKT murine thymoma viral oncogene homolog 1	13/238	PLEKHM3[§], IRS1[§], PRKCZ[#], GAS6[§], PROM1[§], SPON2[§], HPSE[#], NOX4[§], PKIB[#], PAWR[#], SPARC[§], PIK3CB[#], DSC2[#]	1.53E-02

Continued Table 15: Over-represented signal transduction pathways from pairwise comparisons analysed by the Genomatix Pathway System (GePS)

Pathway		List of observed genes	P-value
Vascular endothelial growth factor	10/164	HEY2[§], ETS1[§], PLVAP[§], HPSE[#], MGP[§], TIMP2[#], PTPRJ[#], HGF[§], SPARC[§], MIR126[§]	1.60E-02
Nodal	3/20	LEFTY2[§], PITX2[§], BMP4[§]	1.71E-02
Cadherin 2, Type 1, N Cadherin (Neuronal)	4/38	COL1A1[§], WNT7A[#], LEF1[§], CDH11[§]	2.06E-02
Cadherin 5, Type 2 (Vascular endothelium)	4/39	CLDN5[§], FLNA[§], MGP[§], PTPRJ[#]	2.25E-02
FBJ Murine osteosarcoma viral oncogene homolog B	2/9	FOSB[§], JUNB[§]	2.45E-02
Mitogen acticated protein kinase	23/542	ZFP36[§], FOSB[§], MKNK1[§], CHI3L1[§], IGFBP5[§], SELM[§], HSPA1A[§], P2RY6[#], STK40[#], COL1A1[§], CDK10[§], ETS1[§], PROK1[§], RASSF2[§], F3[§], SELE[§], NOX4[§], APLNR[§], MGP[§], CLCNKA[#], IER3[§], JUNB[§], MC5R[§]	2.71E-02
CD40 Ligand	4/42	CD28[§], SLAMF1[§], SELE[§], CD83[§]	2.87E-02
Dopamine receptor	3/26	ADRB2[§], FLNA[§], PAWR[#]	3.46E-02
Growth hormone receptor	3/27	IRS1[§], PRL[§], SOCS3[§]	3.82E-02
Glial cell line derived neurotrophic factor	4/46	LRIG1[§], PROK1[§], BMP4[§], GFRA2[§]	3.84E-02
β-catenin	14/330	LGR4[#], BAMBI[§], RSPO2[§], CSPG4[§], PITX2[§], DKK3[§], SLIT2[§], WNT7A[#], LEF1[§], FSCN1[§], S100A4[§], CDH11[§], GREM2[#], DSC2[#]	4.16E-02
Indian hedgehog	3/29	BMP4[§], PTH1R[§], FGFR3[§]	4.58E-02
Tissue inhibitor of Metalloproteinase	4/49	SDC1[#], TIMP4[§], TIMP2[#], HGF[§]	4.68E-02
Focal adhesion Kinase 1	9/171	COL1A1[§], CD9[§], ENPP2[§], CSPG4[§], SLC3A2[#], HPSE[#], EGFL7[§], TIMP2[#], TM4SF5[#]	4.91E-02
Caveolin	5/72	CD36[§], ETS1[§], F3[§], FLNA[§], ST3GAL5[§]	4.98E-02
C) Obese GDM vs. obese group			
Transforming growth factor β	36/506	EFEMP2[§], SLC25A4[#], BAMBI[§], RUNX1[§], KLF2[§], MECOM[§], FLRT3[§], TGFBI[§], BMP5[§], MATN2[§], COL1A2[§], DCN[§], DACH1[§], IGFBP7[§], COMP[§], RUNX1T1[§], COL1A1[§], CTHRC1[§], TMEM119[§], CLIC4[#], BMP4[§], FBLN2[§], FMOD[§], TAGLN[§], LAMA2[§], SDC2[§], TBX2[§], LTBP2[§], ID1[§], MGP[§], IGFBP3[§], FOXF1[§], SPARC[§], TSC22D1[#], GREM2[#], EBF1[§]	7.23E-07
Angiogenesis	16/159	CX3CL1[§], CEACAM1[§], EFNB2[§], IGFBP7[§], CLIC4[#], ENPP2[§], NOTCH1[§], THBS2[§], PTP4A3[§], PDGFRB[§], ID1[§], COL18A1[§], FLT1[#], SPARC[§], TFAP2A[#], CXCL12[§]	1.97E-05
Proliferation	28/415	CXCR7[§], ST6GAL1[§], MECOM[§], CCND2[§], CD274[#], PTGFR[§], COL1A1[§], SMARCA1[#], KLF5[#], GAS6[§], CSPG4[§], PROK1[§], NOTCH1[§], PITX2[§], MFGE8[§], RGN[§], PDGFRB[§], DBN1[§], SLC3A2[#], WNT7A[#], ID1[§], COL18A1[§], IGFBP3[§], FLT1[#], FGFR3[§], SPARC[§], CXCL12[§], EBF1[§]	3.90E-05
Notch	19/234	SEPT4[§], HEY2[§], RUNX1[§], EFNB2[§], HOXC6[§], SMARCD3[§], IRF6[#], NRARP[§], NOTCH1[§], THBS2[§], PROM1[§], MEG3[§], SDC2[§], HEYL[§], HES5[§], FOXF1[§], AES[#], SPARC[§], EBF1[§]	6.83E-05
Mothers against DPP homolog	21/288	EFEMP2[§], SLC25A4[#], BAMBI[§], RUNX1[§], MECOM[§], BMP5[§], COL1A2[§], DCN[§], DACH1[§], IGFBP7[§], RUNX1T1[§], COL1A1[§], BMP4[§], TAGLN[§], TBX2[§], ID1[§], IGFBP3[§], CDH11[§], SPARC[§], TSC22D1[#], GREM2[#]	1.33E-04
Vascular endothelial growth factor	14/164	HEY2[§], EFNB2[§], KLF2[§], VWF[§], IGFBP7[§], CLIC4[#], PTPRB[§], PLVAP[§], PDGFRB[§], MGP[§], COL18A1[§], FLT1[#], SPARC[§], CXCL12[§]	3.82E-04
Retinoic acid receptor α	6/41	RUNX1[§], RARB[§], RUNX1T1[§], KLF5[#], TGM2[#], IGFBP3[§]	1.27E-03
Axl receptor tyrosine kinase	3/10	MERTK[§], AXL[§], GAS6[§]	2.73E-03
Peroxisome proliferator activated receptor (PPAR) γ	9/99	CX3CL1[§], CEBPA[#], CD36[§], BAMBI[§], WNT7A[#], FOXO1[§], NR1H3[§], CX3CR1[§], TSC22D1[#]	2.77E-03
TEK tyrosine kinase	4/23	KLF2[§], COMP[§], PTPRB[§], FLT1[#]	4.45E-03

Continued Table 15: Over-represented signal transduction pathways from pairwise comparisons analysed by the Genomatix Pathway System (GePS)

Pathway		List of observed genes	P-value
Lysophosphatidic acid receptor	3/12	ENPP2[§], LPAR1[§], LPAR5[§]	4.80E-03
V AKT murine thymoma viral oncogene homolog 1	15/238	PDCD4[#], HTT[§], PHLDB1[§], AXL[§], MAPT[§], DMD[§], GAS6[§], PDPK1[#], PROM1[§], DDB1[#], FOXO1[§], PKIB[§], SPARC[§], CXCL12[§], PIK3CB[#]	5.10E-03
Retinoic acid receptor β	3/13	RBP1[§], JUN[§], RARB[§]	6.10E-03
Oncogenic	12/175	RUNX1[§], PDCD4[#], TRIM29[#], HOXC6[§], JUN[§], IGFBP7[§], NOTCH1[§], DKK3[§], SDC2[§], FGFR3[§], TSC22D1[#], PIK3CB[#]	6.19E-03
FMS like receptor tyrosine kinase 3	5/44	CEBPA[#], PDGFRB[§], LYN[#], FLT1[#], CXCL12[§]	9.72E-03
Phospholipase A2	6/63	VWF[§], XDH[#], ENPP2[§], PLA2G4C[§], PLA2G5[§], SLC6A4[#]	1.11E-02
Differentiation	27/572	CEBPA[#], HEY2[§], RUNX1[§], SMARCD3[§], TGFBI[§], BMP5[§], NDN[§], COL1A1[§], IRF6[#], SPRY1[§], TCF21[§], TMEM119[§], PROK1[§], NOTCH1[§], PITX2[§], BMP4[§], KRT19[#], TAGLN[§], WNT7A[#], ID1[§], RARRES2[§], HES5[§], AES[#], CDH11[§], FGFR3[§], TFAP2A[#], EBF1[§]	1.17E-02
Developmental	9/124	CEBPA[#], MECOM[§], IRF6[#], DMD[§], NOTCH1[§], BMP4[§], WNT7A[#], AES[#], TFAP2A[#]	1.20E-02
F Box and WD repeat Domain containing 7	3/18	JUN[§], KLF5[#], NOTCH1[§]	1.56E-02
Wingless-int (wnt) type	22/451	LGR4[#], ARMCX1[§], BAMBI[§], TRIM29[#], TNFRSF19[§], HOXC6[§], FLRT3[§], SMARCA1[#], IRF6[#], DSP[#], NRARP[§], CTHRC1[§], PITX2[§], PROM1[§], DKK3[§], BMP4[§], TPBG[#], WNT7A[#], SDC2[§], PTK7[§], CDH11[§], GREM2[#]	1.58E-02
Fibroblast growth factor (FGF)	14/247	ENPP1[§], FLRT3[§], CCND2[§], DACH1[§], PTGFR[§], SPRY1[§], BMP4[§], TFPI[§], TBX2[§], COL18A1[§], MC1R[§], HES5[§], CDH11[§], FGFR3[§]	1.62E-02
β-catenin	17/330	LGR4[#], ARMCX1[§], BAMBI[§], TRIM29[#], DSP[#], CSPG4[§], PITX2[§], DKK3[§], TPBG[#], TGM2[#], KCNIP3[§], WNT7A[#], SDC2[§], GLCE[#], COL11A1[§], CDH11[§], GREM2[#]	2.02E-02
Low-density lipoprotein receptor related protein	8/115	DCN[§], THBS2[§], DKK3[§], PDGFRB[§], WNT7A[#], SDC2[§], PTH1R[§], IGFBP3[§]	2.19E-02
Parathyroid hormone related protein	6/75	COL1A1[§], PRRT2[§], RAMP3[§], PTH1R[§], MGP[§], FGFR3[§]	2.46E-02
Phospholipase C	10/168	VWF[§], PTGFR[§], SPRY1[§], TGM2[#], PDGFRB[§], EDNRA[§], SPON1[§], PTH1R[§], LYN[#], FGFR3[§]	2.93E-02
Histone Deacetylase	6/79	RUNX1[§], KLF2[§], MECOM[§], HTT[§], KLF5[#], EDNRA[§]	3.08E-02
ATP Binding Cassette, Subfamily A (ABC1)	4/43	CD36[§], NR1H3[§], CETP[§], TFAP2A[#]	3.91E-02
Nitric oxide	7/106	IDO1[§], CD36[§], KLF2[§], XDH[#], DMD[§], RGN[§], COL18A1[§]	3.96E-02
Chemokine (C C Motif) Ligand 2	6/85	CX3CL1[§], JUN[§], CD274[#], COL1A1[§], CX3CR1[§], CXCL12[§]	4.18E-02
Hairy and enhancer of SPLIT1	4/44	HEY2[§], NOTCH1[§], HES5[§], AES[#]	4.20E-02

Shown are regulated pathways with Genomatix threshold p-value < 0.05. [#] up-regulated gene in pairwise comparison; [§] down-regulated gene in pairwise comparison. Analysis was performed in term placentas of lean (n=9), obese (n=10) and obese GDM (n=8) women.

4.10.4 Expression of genes involved in glucose, insulin and insulin growth factor signaling identified by microarray data sets

The mean group expressions (fluorescence), fold changes and p-values of genes involved in glucose, insulin and insulin growth factor signaling are presented in **Table 16.** No differences were found in the gene expression of the most important placental glucose transporter, GLUT1 and GLUT3, between samples from lean and obese women with and without GDM. The INSR was significantly up-regulated in placentas obtained from obese diabetic compared to both euglycemic groups (FC: 1.27 and 1.25 $p < 0.05$). In contrast, IRS1 was down-regulated in placentas of obese GDM compared to lean subjects (FC: -1.35 $p < 0.05$). Gene expression levels of IGF1 and IGF2 and their respective receptors were similar between all groups. However, IGFBP 3/5/7 gene expressions were significantly lower in placentas of obese GDM compared to normoglycemic lean and obese women (IGFBP3: FC: -1.27, $p < 0.05$ and -1.33, $p < 0.01$ and IGFBP5: FC: -1.32 and FC: -1.29, $p < 0.01$; IGFBP7: FC: -1.39, $p < 0.01$), whereas IGF2BP3 was up-regulated in the obese GDM compared to lean group (FC: 1.28 $p < 0.01$). Regarding the genes that are involved in the glycogen metabolism, only GSK3β expression was significantly increased in samples from obese compared to lean subjects (FC: 1.17, $p < 0.05$), whereas flucan (1,4-alpha-), branching enzyme 1 (glycogen branching enzyme, GBE1) was up-regulated in placentas of obese compared to diabetic women (FC: 1.23, $p < 0.01$).

The mean group expressions (fluorescence) and respective fold changes and p-values of risk genes for type 2 diabetes are shown in **Supplemental table 7.** Thus, the dual specificity phosphatase 9 (DUSP9) was expressed at a lower level in tissues from obese than lean subjects (FC: -1.24, $p < 0.05$). Furthermore, GLIS family zink finger 3 (GLIS3) was significantly up-regulated (FC: 1.36 and FC: 1.41, $p < 0.05$) and JAZF zink finger 1 (JAZF1) was down-regulated in placentas of obese GDM compared to both euglycemic groups (FC: 1.28 and FC: -1.27, $p < 0.01$). The paired related homeobox 1 (PRRX1) expression was significantly reduced in the obese GDM compared to lean group (FC: -1.54, $p < 0.05$). Moreover, tumor protein p53 inducible nuclear protein 1 (TP53INP1) gene expression was significantly lower in the placentas of obese compared to the lean and obese diabetic women (FC: -1.17 and FC: -1.24, $p < 0.05$).

Table 16: Mean group gene expression and corresponding regulations of glucose, insulin, insulin growth factor and glycogen signaling pathways identified by placental microarray analysis

Gene symbol	Gene name	L Mean expression	OB Mean expression	OB GDM Mean expression	FC OB vs L	FC OB GDM vs L	FC OB GDM vs OB
Glucose transporter							
SLC2A1	Solute carrier family 1 (facilitated glucose transporter 1)	8846	8464	9090	-1.05	1.03	1.07
SLC2A3	Solute carrier family 3 (facilitated glucose transporter 3)	1452	1357	1192	-1.07	-1.22	-1.14
Insulin signaling							
INSR	Insulin receptor	38	39	49	1.01	**1.27***	**1.25***
IRS1	Insulin receptor substrate 1	186	151	138	-1.23	**-1.35***	-1.09
IRS2	Insulin receptor substrate 2	596	640	678	1.07	1.14	1.06
PIK3R1	Phosphoinositide-3-kinase, regulatory subunit 1 (alpha)	36	31	36	-1.16	-1.00	1.15
PIK3R2	Phosphoinositide-3-kinase, regulatory subunit 2 (alpha)	748	782	756	1.04	1.01	-1.04
Insulin growth factor signaling							
IGF1	Insulin-like growth factor 1	58	56	63	-1.05	1.07	1.12
IGF2	Insulin-like growth factor 2	171	163	171	-1.05	-1.00	1.05
IGF1R	Insulin-like growth factor 1 receptor	42	44	41	1.04	-1.03	-1.07
IGF2R	Insulin-like growth factor 2 receptor	1082	1179	1129	1.09	1.04	-1.04
IGFBP1	Insulin-like growth factor binding protein 1	310	188	250	-1.83	-1.59	1.16
IGFBP2	Insulin-like growth factor binding protein 2	136	138	101	1.02	-1.34	-1.36
IGFBP3	Insulin-like growth factor binding protein 3	4472	4712	3530	1.05	**-1.27***	**-1.33****
IGFBP4	Insulin-like growth factor binding protein 4	589	589	549	1.00	-1.07	-1.07
IGFBP5	Insulin-like growth factor binding protein 5	3098	3024	2348	-1.02	**-1.32****	**-1.29****
IGFBP6	Insulin-like growth factor binding protein 6	50	50	44	1.01	-1.13	-1.13
IGFBP7	Insulin-like growth factor binding protein 7	857	842	603	-1.02	-1.42	**-1.39****
IGF2BP1	Insulin-like growth factor 2 binding protein 1	30	34	35	1.12	1.15	1.03
IGF2BP2	Insulin-like growth factor 2 binding protein 2	1182	1185	1302	1.00	1.10	1.10
IGF2BP3	Insulin-like growth factor 2 binding protein 3	1666	1847	2135	1.11	**1.28****	1.16
Glycogen metabolism							
GYG1	Glycogenin 1	565	519	558	-1.09	-1.01	1.08
GYG2	Glycogenin 2	46	46	40	-1.00	-1.14	-1.14
GSK3B	Glycogen synthase kinase 3 beta	468	548	522	**1.17***	1.12	-1.05
GYS1	Glycogen synthase 1 (muscle)	32	31	32	-1.06	1.00	1.06
PYGL	Phosphorylase, glycogen, liver	556	486	524	-1.14	-1.06	1.08
PYGB	Phosphorylase, glycogen, brain	134	139	135	1.03	1.01	-1.03
GBE1	Flucan (1,4-alpha-), branching enzyme 1 (glycogen branching enzyme)	362	330	407	-1.10	1.12	**1.23****

* P < 0.05, ** p < 0.01, significantly regulated genes are presented in bold type. Analysis was performed in term placentas of lean (n=9), obese (n=10) and obese GDM (n=8) women. GDM: gestational diabetes mellitus; FC: fold change; L: lean; OB: obese

4.10.5 Expression of genes involved in lipid and cholesterol transport and metabolism identified by the microarray data sets

To answer the question whether placental lipid and cholesterol transport and metabolism are affected by maternal obesity with and without GDM, differential expression of key genes was studied **(Table 17).** Accordingly, LIPG was significantly down-regulated in placentas of GDM women compared to euglycemic obese counterpart (FC: -1.40; $p < 0.05$). Regarding fatty acid transport, FABP4 expression was significantly higher in the obese compared to the lean group (FC: 1.37; $p < 0.05$), whereas FATP1 and FATP3 mRNA were significantly reduced in obese GDM compared to obese and lean women, respectively (FC: -1.23 and -1.15; $p < 0.05$). No differences were observed between study groups for acyl-CoA synthases and genes implicated in the TG biosynthesis. Only in the biosynthesis of saturated fatty acids, acetyl-coenzyme A carboxylase β (ACACB) expression was significantly reduced in the obese GDM compared to the obese group (FC: -1.29; $p < 0.01$). Based on genes categorized to β-oxidation, acyl-Coenzyme A dehydrogenase, C-4 to C-12 straight chain (ACADM), acyl-Coenzyme A dehydrogenase family, member 10 (ACAD10) and acyl-coenzyme A oxidase 2 (ACOX2) were significantly down-regulated in placentas of obese diabetic compared to euglycemic obese subjects, respectively (FC: -1.12, -1.14 and -1.26; all $p < 0.05$). In contrast, ACAD9 mRNA was significantly higher expressed in obese compared to lean counterparts (FC: 1.13; $p < 0.05$). The peroxisomal enoyl coenzyme A hydratase 1 (ECH1) gene that is additionally involved in β-oxidation processes, was up-regulated in obese GDM compared to lean subjects (FC: 1.14, $p < 0.05$). Furthermore, methylmalonyl CoA epimerase (MCEE), that is involved in the β-oxidation of uneven fatty acids, was significantly reduced in obese GDM compared to obese women (FC: -1.18; $p < 0.05$). The expression levels of the isoforms of peroxisome proliferator-activated receptors (PPARs), namely PPARA, PPARG and PPARD, were similar between the study groups.

Regarding cholesterol transfer and metabolism, a significant reduction of LDLR, sterol regulatory element binding transcription factor 2 (SREBF2) and 3-hydroxy-3-methylglutaryl-Coenzyme A reductase (HMGCR) mRNA levels was evident in the obese compared to the lean group (LDLR: FC: -1.36; $p < 0.05$; SREBF2: FC: -1.12 and HMGCR: FC: -1.13; $p < 0.05$). However, 3-hydroxy-3-methylglutaryl-Coenzyme A synthase 2 (HMGCS2) was significantly up-regulated in both obese groups compared to the lean women (FC: 1.67 and 2.26; $p < 0.01$). Moreover, Niemann-Pick disease, type C1 (NPC-1) and 24-dehydro-cholesterol reductase (DHCR24) expressions were significantly higher in GDM compared to lean and obese women, respectively (FC: 1.15 and 1.34, $p < 0.05$).

Table 17: Mean group gene expression and corresponding regulations of lipid and cholesterol signaling pathways identified by DNA microarray analysis

Gene symbol	Gene name	L mean expression	OB mean expression	OB GDM mean expression	FC OB vs L	FC OB GDM vs L	FC OB GDM vs OB
Triglyceride lipases							
LPL	Lipoprotein lipase	609	854	584	1.40	-1.04	-1.46
LIPE	Lipase, hormone-sensitive	30	29	31	-1.03	1.05	1.09
LIPG	Lipase, endothelial	594	660	471	1.11	-1.26	**-1.40***
Fatty acid transporters							
CD36	CD36 molecule (thrombospondin receptor)	1114	1279	1083	1.15	-1.03	-1.18
FABP1	Fatty acid binding protein 1, liver			< Background			
FABP2	Fatty acid binding protein 2, intestinal			< Background			
FABP3	Fatty acid binding protein 3, muscle and heart			< Background			
FABP4	Fatty acid binding protein 4, adipocyte	2112	2886	2279	**1.37***	1.08	-1.27
FABP5	Fatty acid binding protein 5 (psoriasis-associated)	1062	1256	1009	1.18	-1.05	-1.24
FABP6	Fatty acid binding protein 6, ileal			< Background			
FABP7	Fatty acid binding protein 7, brain	30	30	32	1.01	1.07	1.06
FABP9	Fatty acid binding protein 9, testis			< Background			
SLC27A1	Solute carrier family 27 (fatty acid transporter), member 1	121	127	104	1.05	-1.16	**-1.23***
SLC27A2	Solute carrier family 27 (fatty acid transporter), member 2	354	292	330	-1.21	-1.07	1.13
SLC27A3	Solute carrier family 27 (fatty acid transporter), member 3	462	469	410	1.02	**-1.13***	-1.15
SLC27A4	Solute carrier family 27 (fatty acid transporter), member 4			< Background			
SLC27A5	Solute carrier family 27 (fatty acid transporter), member 5	29	32	30	1.08	1.03	-1.05
SLC27A6	Solute carrier family 27 (fatty acid transporter), member 6	95	97	95	1.02	1.00	-1.02
Acyl-CoA Synthases							
ACSL1	Acyl-CoA synthetase long-chain family member 1	187	142	157	-1.32	-1.19	1.10
ACSL3	Acyl-CoA synthetase long-chain family member 3	949	924	953	-1.03	1.00	1.03
ACSL4	Acyl-CoA synthetase long-chain family member 4	81	78	85	-1.03	1.05	1.09
ACSL5	Acyl-CoA synthetase long-chain family member 5	164	184	167	1.12	1.02	-1.10
ACSL6	Acyl-CoA synthetase long-chain family member 6			< Background			
Acyl-CoA binding proteins							
DBI	Diazepam binding inhibitor (GABA receptor modulator, acyl-Coenzyme A binding protein)	1514	1366	1479	**-1.11***	-1.02	1.08
PECI	Peroxisomal D3,D2-enoyl-CoA isomerase	209	195	203	-1.07	-1.03	1.04

Continued Table 17: Mean group gene expression and corresponding regulations of lipid and cholesterol signaling pathways identified by DNA microarray analysis

Gene symbol	Gene name	L mean expression	OB mean expression	OB GDM mean expression	FC OB vs L	FC OB GDM vs L	FC OB GDM vs OB
TG Biosynthesis							
DGAT1	Diacylglycerol O-acyltransferase homolog 1	105	102	105	-1.02	-1.00	1.02
DGAT2	Diacylglycerol O-acyltransferase homolog 2	43	44	43	1.01	-1.00	-1.02
GPAM	Glycerol-3-phosphate acyltransferase, mitochondrial	70	72	72	1.03	1.04	1.01
LPIN1	Lipin 1	764	755	772	-1.01	1.01	1.02
LPIN2	Lipin 2	29	28	33	-1.03	1.13	1.16
MOGAT1	Monoacylglycerol O-acyltransferase 1			< Background			
MOGAT2	Monoacylglycerol O-acyltransferase 2			< Background			
β-Oxidation							
ACAA1	Acetyl-Coenzyme A acyltransferase 1 (peroxisomal 3-oxoacyl-Coenzyme A thiolase)	288	302	294	1.05	1.02	-1.03
ACAA2	Acetyl-Coenzyme A acyltransferase 2 (mitochondrial 3-oxoacyl-Coenzyme A thiolase)	232	247	246	1.06	1.06	1.00
ACADM	Acyl-Coenzyme A dehydrogenase, C-4 to C-12 straight chain	231	246	220	1.06	-1.05	**-1.12***
ACADS	Acyl-Coenzyme A dehydrogenase, C-2 to C-3 short chain	90	88	92	-1.01	1.02	1.04
ACADVL	Acyl-Coenzyme A dehydrogenase, very long chain	5249	5396	5539	1.03	1.06	1.03
ACADSB	Acyl-Coenzyme A dehydrogenase, short/branched chain	33	33	35	-1.00	1.08	1.08
ACAD8	Acyl-Coenzyme A dehydrogenase family, member 8	175	188	172	1.08	-1.01	-1.09
ACAD9	Acyl-Coenzyme A dehydrogenase family, member 9	323	366	386	**1.13***	1.19	1.05
ACAD10	Acyl-Coenzyme A dehydrogenase family, member 10	107	111	97	1.03	-1.10	**-1.14***
ACAD11	Acyl-Coenzyme A dehydrogenase family, member 11	460	501	510	1.09	1.11	1.02
ACOX1	Acyl-Coenzyme A oxidase 1, palmitoyl	288	285	302	-1.01	1.05	1.06
ACOX2	Acyl-Coenzyme A oxidase 2, branched chain	99	102	81	1.03	-1.22	**-1.26***
ACOX3	Acyl-Coenzyme A oxidase 3, pristanoyl	389	391	429	1.01	1.10	1.10
CPT1A	Carnitine palmitoyltransferase 1A (liver)	39	38	40	-1.02	1.02	1.04
CPT1B	Carnitine palmitoyltransferase 1B (muscle)	95	105	87	1.11	-1.10	-1.22
CPT1C	Carnitine palmitoyltransferase 1C	31	31	29	-1.00	-1.06	-1.06
CPT2	Carnitine palmitoyltransferase II	514	542	560	1.05	1.09	1.03
ECH1	Enoyl Coenzyme A hydratase 1, peroxisomal	1778	1916	2030	1.08	**1.14***	1.06

Continued Table 17: Mean group gene expression and corresponding regulations of lipid and cholesterol signaling pathways identified by DNA microarray analysis

Gene symbol	Gene name	L mean expression	OB mean expression	OB GDM mean expression	FC OB vs L	FC OB GDM vs L	FC OB GDM vs OB
ECHS1	Enoyl Coenzyme A hydratase, short chain, 1, mitochondrial	621	543	551	-1.14	-1.13	1.01
HADHA	Hydroxyacyl-Coenzyme A dehydrogenase/3-ketoacyl-Coenzyme A thiolase/enoyl-Coenzyme A hydratase, alpha subunit	145	148	143	1.02	-1.01	-1.04
HADHB	Hydroxyacyl-Coenzyme A dehydrogenase/3-ketoacyl-Coenzyme A thiolase/enoyl-Coenzyme A hydratase, beta subunit	269	267	270	-1.01	1.01	1.01
NDUFAB1	NADH dehydrogenase (ubiquinone) 1, alpha/beta subcomplex, 1, 8 kDa	1262	1175	1262	-1.07	-1.00	1.07
β-Oxidation of uneven fatty acids							
PCCA	Propionyl Coenzyme A carboxylase, alpha polypeptide	539	544	556	1.01	1.03	1.02
PCCB	Propionyl Coenzyme A carboxylase, beta polypeptide	778	794	868	1.02	1.12	1.09
MCEE	Methylmalonyl CoA epimerase	387	434	368	1.12	-1.05	**-1.18***
β-Oxidation of unsaturated fatty acids							
EHHADH	Enoyl-Coenzyme A, hydratase/3-hydroxyacyl Coenzyme A dehydrogenase	49	48	46	-1.03	-1.07	-1.04
ACADL	Acyl-Coenzyme A dehydrogenase, long chain	50	53	58	1.06	1.16	1.10
Biosynthesis of saturated fatty acids							
ACACB	Acetyl-Coenzyme A carboxylase beta	103	118	91	1.15	-1.13	**-1.29****
ACACA	Acetyl-Coenzyme A carboxylase alpha	232	217	231	-1.07	-1.00	1.06
FASN	Fatty acid synthase	671	648	712	-1.04	1.06	1.10
Biosynthesis of unsaturated fatty acids							
FADS1	Fatty acid desaturase 1 (FADS1), mRNA.	131	123	117	-1.07	-1.12	-1.05
FADS2	Fatty acid desaturase 2 (FADS2), mRNA.	33	33	31	1.01	-1.06	-1.07
ELOVL1	Elongation of very long chain fatty acids (FEN1/Elo2, SUR4/Elo3, yeast)-like 1	202	199	204	-1.01	1.01	1.02
ELOVL2	Elongation of very long chain fatty acids (FEN1/Elo2, SUR4/Elo3, yeast)-like 2	120	106	101	-1.13	-1.19	-1.06
ELOVL3	(ELOVL3), mRNA.	34	31	32	-1.08	-1.05	1.03
ELOVL4	Elongation of very long chain fatty acids (FEN1/Elo2, SUR4/Elo3, yeast)-like 4	89	80	74	-1.12	-1.21	-1.08
ELOVL5	ELOVL family member 5, elongation of long chain fatty acids (FEN1/Elo2, SUR4/Elo3-like, yeast)	253	245	251	-1.03	-1.01	1.03
ELOVL6	ELOVL family member 6, elongation of long chain fatty acids (FEN1/Elo2, SUR4/Elo3-like, yeast)	35	31	30	-1.11	-1.15	-1.03

Continued Table 17: Mean group gene expression and corresponding regulations of lipid and cholesterol signaling pathways identified by DNA microarray analysis

Gene symbol	Gene name	L mean expression	OB mean expression	OB GDM mean expression	FC OB vs L	FC OB GDM vs L	FC OB GDM vs OB
ELOVL7	ELOVL family member 7, elongation of long chain fatty acids (yeast) .	30	30	31	-1.00	1.03	1.03
SCD	Stearoyl-CoA desaturase (delta-9-desaturase)	323	294	326	-1.10	1.01	1.11
Peroxisomen proliferation-activator receptors							
PPARA	Peroxisome proliferator-activated receptor alpha			< Background			
PPARG	Peroxisome proliferator-activated receptor gamma	986	995	1020	1.01	1.03	1.02
PPARD	Peroxisome proliferative activated receptor, delta	224	202	206	-1.11	-1.09	1.02
Cholesterol transfer							
VLDLR	Very low-density lipoprotein receptor	165	162	158	-1.02	-1.05	-1.03
LDLR	Low-density lipoprotein receptor	1062	778	879	**-1.36***	-1.21	1.13
LDLRAP1	Low-density lipoprotein receptor adaptor protein 1	100	89	91	-1.13	-1.10	1.02
LRP1	Low-density lipoprotein-related protein 1	111	109	105	-1.02	-1.06	-1.04
LRP2	Low-density lipoprotein-related protein 2	148	133	152	-1.12	1.02	1.14
SCARB1	Scavenger receptor class B, member 1	1975	2121	2052	1.07	1.04	-1.03
ABCA1	ATP-binding cassette, sub-family A	1892	1964	1821	1.04	-1.04	-1.08
ABCG1	ATP-binding cassette, sub-family G	444	431	461	-1.12	1.04	1.07
NPC1	Niemann-Pick disease, type C1	812	831	933	1.02	**1.15***	1.12
Cholesterol metabolism							
SREBF1	Sterol regulatory element binding transcription factor 1	108	113	101	1.05	-1.07	-1.12
SREBF2	Sterol regulatory element binding transcription factor 2	39	35	37	**-1.12***	-1.06	1.06
ACAT1	Acetyl-Coenzyme A acetyltransferase 1	405	433	392	1.07	-1.03	-1.10
HMGCR	3-hydroxy-3-methylglutaryl-Coenzyme A reductase	389	343	396	**-1.13***	1.02	**1.16***
HMGCS1	3-hydroxy-3-methylglutaryl-Coenzyme A synthase 1 (soluble)	436	436	437	1.00	1.00	1.00
HMGCS2	3-hydroxy-3-methylglutaryl-Coenzyme A synthase 2 (mitochondrial)	113	189	255	**1.67****	**2.26****	1.35
MVK	Mevalonate kinase	43	39	42	-1.09	-1.03	1.07
PMVK	Phosphomevalonate kinase	144	144	140	1.00	-1.03	-1.03
DHCR24	24-dehydrocholesterol reductase	174	156	209	-1.12	1.20	**1.34***
DHCR7	7-dehydrocholesterol reductase	62	59	68	-1.04	1.11	1.15

* P < 0.05, ** p < 0.01, *** p < 0.001; significantly regulated genes are presented in bold type. Analysis was performed in term placentas of lean (n=9), obese (n=10) and obese GDM (n=8) women. GDM: gestational diabetes mellitus; FC: fold change; L: lean; OB: obese.

4.10.6 Gene expression of adipokines and adipokine receptors identified by the DNA microarray data sets

As indicated in **Table 18,** several adipokines and adipocytokines, originally described to be involved in adipose tissue biology, were abundantly expressed by villous placental tissues**.** Microarray analysis revealed that leptin (LEP), chemerin (RARRES2) and visfantin (NAMPT) were highly expressed in the examined samples. In contrast, adiponectin (ADIPOQ), omentin (ITLN1) and resistin (RETN) were only expressed at the level of background signal showing mean fluorescent signals between 25 and 34. Unlike the absent adiponectin mRNA detection, both adiponectin receptors (ADIPOR1 and 2) were abundantly expressed in all samples investigated, whereas the leptin receptor unexpectedly showed low mean expression between 38 and 90 depending on the probe set **(Table 18).** Chemerin was the only adipokine that was differentially regulated in placentas of GDM women, showing significantly lower expression in comparison to placentas obtained from lean and obese women (FC: -1.54 and -1.37; $p < 0.01$). Moreover, ADIPOR1 was significantly moderately increased in placentas of obese GDM compared to obese participants (FC: 1.12; $p < 0.05$).

Table 18: Mean group gene expression and corresponding regulations of adipokines and their receptors indentified by placental microarray analysis

Gene symbol	Gene name	L Mean expression	OB Mean expression	OB GDM Mean expression	FC OB vs L	FC OB GDM vs L	FC OB GDM vs OB
ADIPOQ	Adiponectin	31	34	33	1.11	1.07	-1.04
ADIPOR1	Adiponectin receptor 1	598	572	639	1.00	1.11	**1.12***
ADIPOR2	Adiponectin receptor 2	568	559	581	-1.02	1.02	1.04
LEP [#]	Leptin	1910	1622	3020	-1.18	1.58	1.86
LEP [#]	Leptin	1296	1126	1534	-1.15	1.18	1.36
LEPR	Leptin receptor	38	42	44	1.11	1.17	1.05
RARRES2	Retinoic acid receptor responder (Chemerin)	250	223	163	-1.12	**-1.54****	**-1.37****
NAMPT	Nicotinamide phospho-ribosyltransferase (Visfatin)	268	249	255	-1.08	-1.05	1.03
RETN	Resistin	< Background					
ITLN1	Intelectin 1 (Omentin)	28	30	32	1.05	1.14	1.08

[#] 2 probe sets were applied on the DNA Microrarray chip showing strong differential fluorescences and fold changes. * $P < 0.05$, ** $p < 0.01$; significantly regulated genes are presented in bold type. Analysis was performed in term placentas of lean (n=9), obese (n=10) and obese GDM (n=8) women. GDM: gestational diabetes mellitus; FC: fold change; L: lean; OB: obese.

4.10.7 Gene expression of immune cell marker and cytokine identified by the microarray data sets

The mean group expression (fluorescence), fold changes and p-values that were detected for immune cell markers, cytokines and chemokines are summarized in **Table 19.** All B and T cell markers (CD4, CD8, CD3, CD19 and CD20) were only marginally expressed in placental tissues; similarly, markers for dendritic cells, natural killer (NK) cells and granulocytes (CD11b, CD123, CD56, CD66b, CD11b, CD63) showed fluorescence signals only hardly exceeding the background signal level. In contrast, monocyte maturation and differentiation antigens CD14 and CD68 were abundantly expressed in the villous compartments representing the resident macrophages (Hofbauer cells). However, gene expression of above mentioned immune cell markers displayed no important regulations by maternal obesity and GDM (**Table 19)**. Regarding cytokine mRNA expression, no differences were found between CRP, TNF-α or IL6. However, IL1B expression was significantly decreased in obese GDM compared to lean women (FC: -1.29; $p < 0.05$), whereas IL6 expression was significantly lower in obese diabetic compared to obese participants (FC: -1.21; $p < 0.05$).

A further purpose was to evaluate placental inflammatory mediators and macrophage markers in relation to maternal peripheral inflammatory markers (**Supplemental table 8).** Accordingly, neither maternal plasma CRP nor IL6 levels correlated with placental cytokines and chemokine mRNA expressions (IL1B, IL6, IL8, CRP, TNF-α and MCP1) and macrophage markers (CD14, CD68).

Table 19: Mean group gene expression and corresponding regulations of immune cell marker and cytokines identified by placental DNA microarray analysis

Gene symbol	Gene name	L mean expression	OB mean expression	OB GDM mean expression	FC OB vs L	FC OB GDM vs L	FC OB GDM vs OB
T cell marker							
CD4	CD4 molecule	65	57	57	-1.14	-1.14	-1.00
CD8	CD8a molecule	31	30	37	-1.05	1.19	1.25
CD3	CD247 molecule	58	63	64	1.09	1.10	1.01
B cell marker							
CD19	CD19 molecule			< Background			
CD20	Membrane-spanning 4-domains, subfamily A, member 1	30	30	32	-1.01	1.06	1.07
Dentritic cells markers							
CD11c	Integrin, alpha X (complement component 3 receptor 4 subunit) (ITGAX)	50	51	49	1.00	-1.03	-1.03
CD123	Interleukin 3 receptor, alpha (IL3RA)	39	43	51	1.10	1.30	1.18
Macrophage/Monocyte marker							
CD14	CD14 molecule	6067	6135	5717	1.01	-1.06	-1.07
CD68	CD68 molecule	1346	1197	1200	-1.13	-1.12	1.00
CD33	CD33 molecule	100	98	84	-1.02	-1.18	-1.16
CD11b	Integrin, alpha M (complement component 3 receptor 3 subunit) (ITGAM)	127	109	110	-1.16	-1.16	1.00
NK cell markers							
CD56	Neural cell adhesion molecule 1			< Background			
Granulocyte markers							
CD66b	Carcinoembryonic antigen-related cell adhesion molecule 8 (CEACAM8), mRNA.	29	30	26	1.04	-1.12	-1.16
CD11b	Integrin, alpha M (complement component 3 receptor 3 subunit) (ITGAM)	127	109	110	-1.16	-1.16	1.00
CD63	CD63 molecule	2933	3030	3122	1.03	1.06	1.03
Interleukins/Chemokines							
IL1B	Interleukin 1, beta	77	66	60	-1.17	**-1.29***	-1.10
IL6	Interleukin 6 (interferon, beta 2)	114	128	105	1.12	-1.08	**-1.21***
IL8	Interleukin 8	177	122	123	-1.45	-1.44	1.01
TNF	Tumor necrosis factor (TNF superfamily, member 2)	33	31	34	-1.06	1.04	1.11
CRP	C-reactive protein, pentraxin-related	30	31	29	1.04	-1.04	-1.08
MCP1	Chemokine (C-C motif) ligand 2 (CCL2)	448	435	360	-1.03	-1.24	-1.21

* P < 0.05; significantly regulated genes are presented in bold type. Analysis was performed in term placentas of lean (n=9), obese (n=10) and obese GDM (n=8) women. GDM: gestational diabetes mellitus; FC: fold change; L: lean; OB: obese

4.10.8 Expression of genes involved in Wnt signaling identified by the microarray data sets

Given that the Genomatix pathway analysis revealed the over-representation of the *Low-density lipoprotein receptor related protein/ wnt type/ β-catenin* pathway in the placentas of obese diabetic mothers, the microarray data were thoroughly investigated for prominent genes that are implicated in Wnt/β-catenin signaling [111,112] **(Table 20).** Out of 19 known Wnt ligands in vertebrates, 9 ligands were expressed (fluorescence values ≥ 30) in the term placentas of the *GesA* study. By far, wingless-type MMTV integration site family (WNT) 3A was found to be the most abundantly expressed Wnt ligand. However, except for WNT7A (FC: OB GDM vs L: 1.78 and vs. OB: 1.81; $p < 0.001$), no further Wnt ligands were differentially expressed by maternal obesity with or without GDM. Regarding the expression of their receptors, all established 10 frizzled (FZD) receptors and their coreceptors low-density lipoprotein-related protein (LRP) 5/6 [111] were detectable in the villous tissues of the *GesA* study. However, FZD2 and FZD4 were significantly down-regulated in placentas of diabetic women compared to normoglycemic lean and obese groups (FZD2: FC: -1.26 and FC: -1.21; $p < 0.05$ and FZD4: -1.28; $p < 0.05$), whereas FDZ8 was lower expressed in obese compared to lean cases (FC: -1.20; $p < 0.01$). Moreover, downstream effectors in the canonical pathway [112], namely GSK3β and casein kinase (CSNK) 1A expressions were slightly increased in placentas of obese and obese diabetic subjects, respectively, whereas β-catenin was similarly expressed between all groups and adenomatosis polyposis coli (APC) was only rarely detectable within all samples. Notably, well-characterized transcriptional factors, like transcription factor (TCF) 4 and lymphoid enhancer-binding factor (LEF) 1 that are implicated in β-catenin-dependent transcriptional machinery [113], were also largely expressed but only showed a differential regulation for LEF1 in the placentas of the diabetic compared to lean mothers (FC: -1.27; $p < 0.05$). The expression of common Wnt/β-catenin signaling targets like v-myc myelocytomatosis viral oncogene homolog (MYC) or axin (AXIN) 2 [113] and trophoblast-specific targets like endogenous retroviral family W, env (C7, (ERVWE)) 1 and glial cells missing homolog (GCM) 1 [114] did not differ between the three groups. However, cyclin (CCN) D1 mRNA expression was significantly lower in placentas of diabetic mothers (FC: -1.20; $p < 0.05$) **(Table 20).**

Table 20: Mean group gene expression and corresponding regulations of Wnt signaling components and Wnt/β-catenin targets identified by DNA microarray analysis

Gene symbol	Gene name	L Mean expression	OB Mean expression	OB GDM Mean expression	FC OB vs L	FC OB GDM vs L	FC OB GDM vs OB
Wnt signaling components							
WNT1	Wingless-type MMTV integration site family, member 1			< Background			
WNT2	Wingless-type MMTV integration site family, member 2	355	341	309	-1.04	-1.15	-1.10
WNT2B	Wingless-type MMTV integration site family, member 2B	80	82	77	1.02	-1.05	-1.07
WNT3	Wingless-type MMTV integration site family, member 3	26	28	31	1.08	1.17	1.08
WNT3A	Wingless-type MMTV integration site family, member 3A	689	736	579	1.07	-1.19	-1.27
WNT4	Wingless-type MMTV integration site family, member 4			< Background			
WNT5A	Wingless-type MMTV integration site family, member 5A	118	125	132	1.05	1.12	1.06
WNT5B	Wingless-type MMTV integration site family, member 5B	47	40	37	**-1.17***	-1.26	-1.08
WNT6	Wingless-type MMTV integration site family, member 6	30	29	28	-1.02	-1.05	-1.03
WNT7A	Wingless-type MMTV integration site family, member 7A	89	87	158	-1.02	**1.78*****	**1.81*****
WNT7B	Wingless-type MMTV integration site family, member 7B			< Background			
WNT8A	Wingless-type MMTV integration site family, member 8A	34	33	32	-1.03	-1.05	-1.02
WNT8B	Wingless-type MMTV integration site family, member 8B			< Background			
WNT9A	Wingless-type MMTV integration site family, member 9A			< Background			
WNT9B	Wingless-type MMTV integration site family, member 9B	26	28	25	1.07	-1.02	-1.09
WNT10A	Wingless-type MMTV integration site family, member 10A			< Background			
WNT10B	Wingless-type MMTV integration site family, member 10B			< Background			
WNT11	Wingless-type MMTV integration site family, member 11	29	28	29	-1.06	-1.02	1.03
WNT16	Wingless-type MMTV integration site family, member 16			< Background			
DKK1	Dickkopf homolog 1 (Xenopus laevis)	336	297	261	-1.13	-1.29	-1.14
DKK3	Dickkopf homolog 3 (Xenopus laevis)	665	637	472	-1.04	**-1.41***	**-1.35****
FZD1	Frizzled homolog 1 (Drosophila)	116	114	100	-1.01	-1.15	-1.14
FZD2	Frizzled homolog 2 (Drosophila)	82	78	65	-1.05	**-1.26***	**-1.21***
FZD3	Frizzled homolog 3 (Drosophila)	63	62	68	-1.02	1.09	1.10
FZD4	Frizzled homolog 4 (Drosophila)	445	481	374	1.08	-1.19	**-1.28***
FZD5	Frizzled homolog 5 (Drosophila)	39	37	38	-1.05	-1.04	1.01
FZD6	Frizzled homolog 6 (Drosophila)	97	79	79	-1.23	-1.22	1.01
FZD7	Frizzled homolog 7 (Drosophila)	153	192	172	1.26	1.12	-1.12
FZD8	Frizzled homolog 8 (Drosophila)	34	29	32	**-1.20****	-1.08	1.12
FZD9	Frizzled homolog 9 (Drosophila)	57	62	63	1.08	1.10	1.03
FZD10	Frizzled homolog 10 (Drosophila)	34	39	35	1.13	1.04	-1.09

Continued Table 20: Mean group gene expression and corresponding regulations of Wnt signaling components and Wnt/β-catenin targets identified by DNA microarray analysis

Gene symbol	Gene name	L mean expression	OB mean expression	OB GDM mean expression	FC OB vs L	FC OB GDM vs L	FC OB GDM vs OB
LRP5	Low-density lipoprotein-related protein 5	397	342	369	-1.16	-1.08	1.08
LRP6	Low-density lipoprotein-related protein 6	40	44	40	1.09	-1.01	-1.10
DVL1	Dishevelled, dsh homolog 1 (Drosophila)	40	34	37	1.01	1.07	1.05
DVL2	Dishevelled, dsh homolog 2 (Drosophila)	129	126	130	-1.02	1.01	1.03
DVL3	Dishevelled, dsh homolog 3 (Drosophila)	983	1056	1030	1.07	1.05	-1.03
CDH11	Cadherin 11, type 2, OB-cadherin (osteoblast)	644	582	427	-1.11	**-1.51***	**-1.37***
GSK3B	Glycogen synthase kinase 3 beta	468	548	522	**1.17***	1.12	-1.05
APC	Adenomatosis polyposis coli			< Background			
APC2	Adenomatosis polyposis coli 2			< Background			
CSNK1A1	Casein kinase 1, alpha 1	111	115	126	1.03	**1.14***	1.10
TCF4	Transcription factor 4	284	306	239	1.08	-1.19	-1.28
LEF1	Lymphoid enhancer-binding factor 1	187	165	147	-1.13	**-1.27***	-1.13
Wnt signaling targets							
AXIN2	Axin 2	476	500	420	1.05	-1.13	-1.19
CCND1	Cyclin D1	1704	1673	1418	-1.02	**-1.20***	-1.18
ERVWE1	Endogenous retroviral family W, env(C7), member 1 (syncytin 1)	1903	1947	1990	1.02	1.05	1.02
GCM1	Glial cells missing homolog 1 (Drosophila)	3501	3146	3549	-1.11	1.01	1.13
MYC	V-myc myelocytomatosis viral oncogene homolog (avian)	195	161	173	-1.21	-1.13	1.07

* P < 0.05; ** p < 0.01; *** p < 0.001; significantly regulated genes are presented in bold type. Analysis was performed in term placentas of lean (n=9), obese (n=10) and obese GDM (n=8) women. GDM: gestational diabetes mellitus; FC: fold change; L: lean; OB: obese

4.11 Validation of target gene expressions by RT-qPCR

The confirmatory RT-qPCR analysis was conducted in the final number of placental villous tissues from lean (n=14), obese (n=13) and obese GDM (n=16) women. The applied primer pair sets are shown in the **chapter 8.1.** Additionally, the checklist for *M*inimum *I*nformation für Publication of RT-*q*PCR *E*xperiments (MIQE) is provided in **Supplemental table 9.**

4.11.1 Expression analysis of genes implicated in inflammatory processes

Pregravid obesity and GDM were recently reported to be associated with increased cytokine and chemokine expression in the placenta [29,30,115]. To accommodate the inflammatory aspect in the present study, five genes, already described as differentially expressed by maternal obesity and/or GDM [28], were analyzed **(Figure 21).** RT-qPCR analysis revealed that the gene expression of IL1β, TNF-α, MCP1 and LEP did not differ between the three

groups. However, IL8 mRNA expression was significantly decreased in placentas obtained from obese GDM subjects compared to the lean group (FC: -1.80; $p < 0.05$). Taken together the pairwise comparisons of immune cell markers and cytokine expressions obtained from microarray data **(chapter 4.10.7)** and RT-qPCR validations, the data did not provide evidence for altered expression of inflammatory markers in the placental villous compartment of obese women with and without GDM. Indeed, particular cytokines even indicated increased gene expression in the lean group.

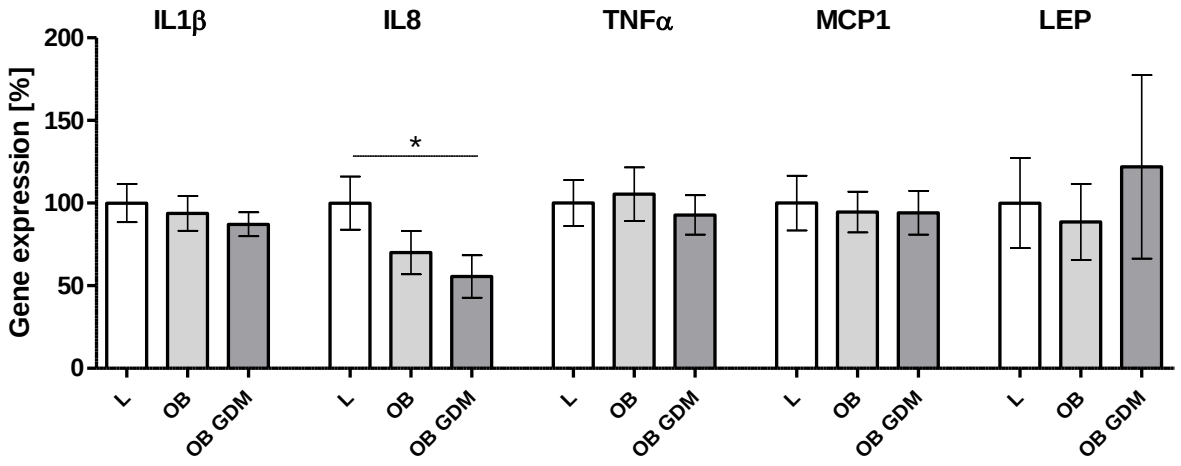

Figure 21: Expression analysis of genes implicated in inflammatory processes validated by RT-qPCR. Shown are the relative mean gene expression levels ± SEM after RT-qPCR with 10 ng of RNA for IL1β (C_q range 26.7-28.7), IL8 (C_q range 27.6-31.6), TNF-α (C_q range 28.4-31.3), MCP1 (C_q range 24.2-27.0) and LEP (C_q range 20.6-28.9). Validation was performed in term placentas of lean (n=14), obese (n=13) and obese GDM (n=16) women. Data were analyzed by ΔΔCq-method with normalization to ACTB and H2AFZ gene expression. Statistical analysis for gene expression was performed using One-Way ANOVA and Sidak's post hoc test or nonparametric Kruskal-Wallis-test with Dunn's post hoc test. Asterisks indicate significant differences between groups: * $p < 0.05$. GDM: gestational diabetes mellitus; IL1β: interleukin 1β; IL8: interleukin 8; L: lean; LEP: leptin; MCP: monocyte chemotactic protein-1; OB: obese; TNF-α: tumor necrosis factor α.

4.11.2 Expression analysis of genes implicated in angiogenesis

The incidence of endothelial dysfunctions in women with pregravid obesity and GDM is well established (see **chapter 1.4** and **1.9.1**). According to the pathway analysis, genes involved in angiogenic signaling were differentially expressed between placentas of lean, obese and obese GDM women. Thus, the RT-qPCR validation of mRNA expression was conducted for fms-related tyrosine kinase (FLT) 1 (vascular endothelial growth factor receptor 1) and prokineticin (PROK) 1 **(Figure 22)**. As already indicated by DNA microarray analysis, the RT-qPCR assessment showed that FLT1 mRNA expression was significantly decreased in placentas of normoglycemic obese women compared to lean and obese GDM subjects (FC: -1.52 and FC -1.94; $p < 0.05$). In contrast, the decrease in PROK1 mRNA expression in the placentas of the obese GDM group was not changed to a statistically significant extent

compared to the lean and obese group as predicted by microarray analysis (FC: -1.30 and FC: -1.31; $p > 0.05$).

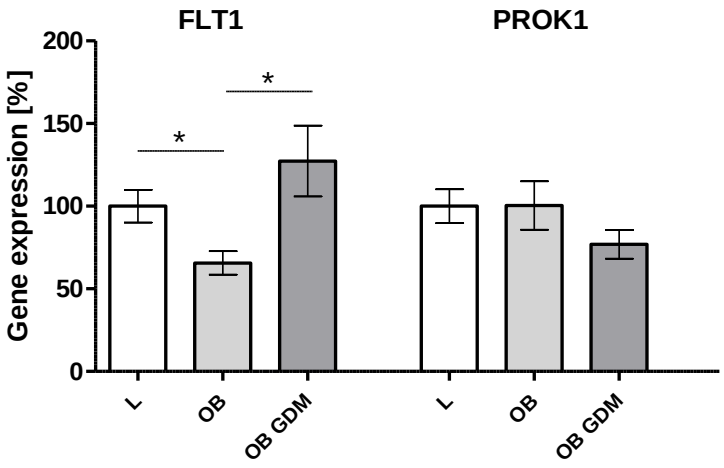

Figure 22: Expression analysis of genes implicated in angiogenesis validated by RT-qPCR. Shown are the relative mean gene expression levels ± SEM after RT-qPCR with 10 ng of RNA for FLT1 (C_q range 23.9-27.4) and PROK1 (C_q range 25.1-27.7). Validation was performed in term placentas of lean (n=14), obese (n=13) and obese GDM (n=16) women. Data were analyzed by ΔΔCq-method with normalization to ACTB and H2AFZ gene expression. Statistical analysis for gene expression was performed using One-Way ANOVA and Sidak's post hoc test or nonparametric Kruskal-Wallis-test with Dunn's post hoc test. Asterisks indicate significant differences between groups: * $p < 0.05$. FLT1: fms-related tyrosine kinase 1; GDM: gestational diabetes mellitus; L: lean; OB: obese; PROK1: prokineticin 1.

4.11.3 Expression analysis of genes implicated in ceramide synthesis

Due to hypothesized involvement in impaired insulin signal transduction [116,117], the serine palmitoyltransferase long chain base subunit 3 (SPTLC3) was chosen for RT-qPCR validation. According to the microarray data, the rate-limiting enzyme of the *de novo* synthesis of sphingolipids was found to be significantly up-regulated in placentas of obese GDM subjects compared to both euglycemic groups **(Supplemental table 5).** Considering the data from the RT-qPCR validation individually, it was obvious that the more severe GDM cases that were treated by insulin therapy, had significantly up-regulated placental SPTLC3 expressions compared to the lean women (FC: 1.45; $p < 0.05$, data not shown in the figure). However, the expression level was not significantly increased anymore in the combined group of insulin- and dietary-treated GDM women (FC: 1.19; $p > 0.05$) **(Figure 23)**.

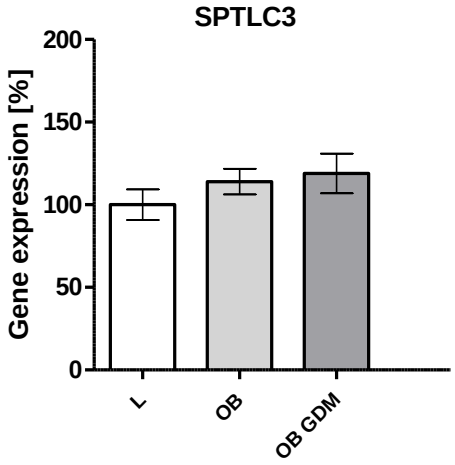

Figure 23: Expression analysis of SPTLC3 validated by RT-qPCR. Shown are the relative mean gene expression levels ± SEM after RT-qPCR with 10 ng of RNA for SPTLC3 (C_q range 20.3-22.6). Validation was performed in term placentas of lean (n=14), obese (n=13) and obese GDM (n=16) women. Data were analyzed by ΔΔCq-method with normalization to ACTB and H2AFZ gene expression. Statistical analysis for gene expression was performed using One-Way ANOVA and Sidak's post hoc test or nonparametric Kruskal-Wallis-test with Dunn's post hoc test. GDM: gestational diabetes mellitus; L: lean; OB: obese; SPTLC3: serine palmitoyltransferase long chain base subunit 3.

4.11.4 Expression analysis of genes implicated in Wnt signaling

The canonical and non-canonical Wnt signaling pathways are involved in the decidualisation process, trophoblast migration/invasion and placental differentiation [112]. According to the Genomatix pathway analysis, *Low-density lipoprotein receptor related protein/Wnt type/β-catenin* signaling was identified as differentially regulated pathway in the GDM cases compared to the non-diabetic counterparts **(Table 15 and Table 20).** Thus, four genes were chosen for RT-qPCR validation for their particular interest in the Wnt signaling (**Figure 24)**. As already indicated by microarray, mRNA expression analyses by RT-qPCR showed that the WNT7A expression was significantly increased in obese GDM group by FC of 1.51 and 1.53 compared to the lean and obese women ($p < 0.01$), respectively. In contrast, the Dickkopf homolog (DKK) 3 expression was significantly decreased in placental tissues of obese GDM subjects compared to the lean and obese women (FC: -1.33 and FC: -1.35; $p < 0.001$). The cadherin (CDH) 11 was found to be significantly decreased compared to the lean group (FC: -1.38; $p < 0.05$). In contrast, the parathyroid hormone (PTH) 1 receptor gene was significantly lower expressed in obese GDM compared to the obese group (FC: 1.50; $p < 0.01$).

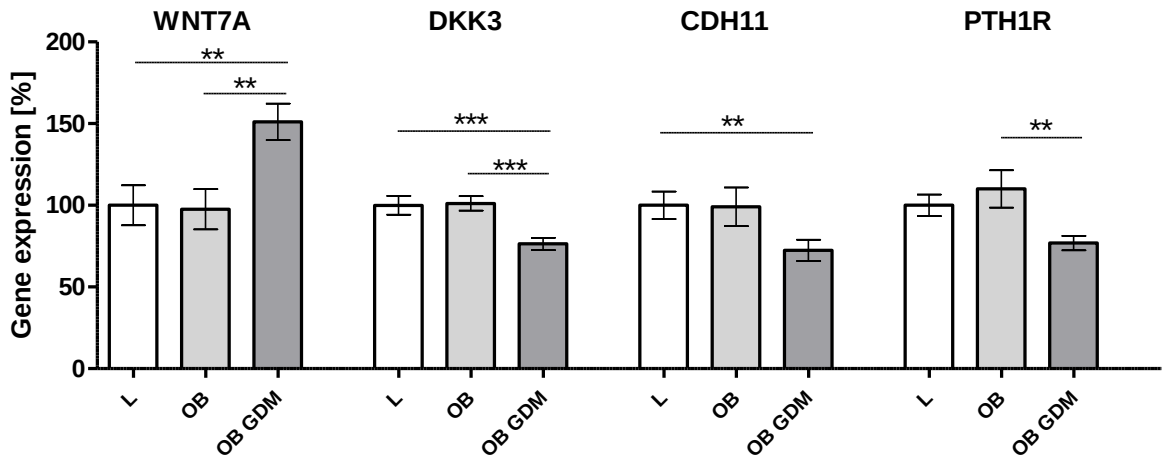

Figure 24: Expression analysis of genes implicated in the Wnt signaling pathway validated by RT-qPCR. Shown are the relative mean gene expression levels ± SEM after RT-qPCR with 10 ng of RNA for WNT7A (C_q range 25.2-28.1), DKK3 (C_q range 25.7 -27.0), PTH1R (C_q range 26.1-27.6) and CDH11 (C_q range 24.9-27.1). Validation was performed in term placentas of lean (n=14), obese (n=13) and obese GDM (n=16) women. Data were analyzed by ΔΔCq-method with normalization to ACTB and H2AFZ gene expression. Statistical analysis for gene expression was performed using One-Way ANOVA and Sidak's post hoc test or nonparametric Kruskal-Wallis-test with Dunn's post hoc test. Asterisks indicate significant differences between groups as: * $p < 0.05$; ** $p < 0.01$; *** $p < 0.001$. CDH11: cadherin 11; DKK3: dickkopf homolog 3; GDM: gestational diabetes mellitus; L: lean; OB: obese; PTH1R: parathyroid hormone 1 receptor; WNT7A: wingless-type MMTV integration site family 7A.

4.11.5 Comparison of gene expression data obtained by DNA microarray and RT-qPCR analysis

Figure 25 illustrates the correlation between the FC obtained from DNA microarray analysis and the FC retrieved from RT-qPCR validation. Accordingly, all 11 genes chosen for RT-qPCR analysis, each comprising of the FC of three pairwise comparisons (OB vs. L, OB GDM vs. L and OB GDM vs. OB), were plotted against their counterparts from DNA microarray data sets. The analysis indicated a significant positive correlation between the gene expression FC of the two different detection methods ($r = 0.865$; $p < 0.001$). In summary, the microarray and RT-qPCR data were consistent for the indicated genes emphasizing the robustness of the DNA microarray.

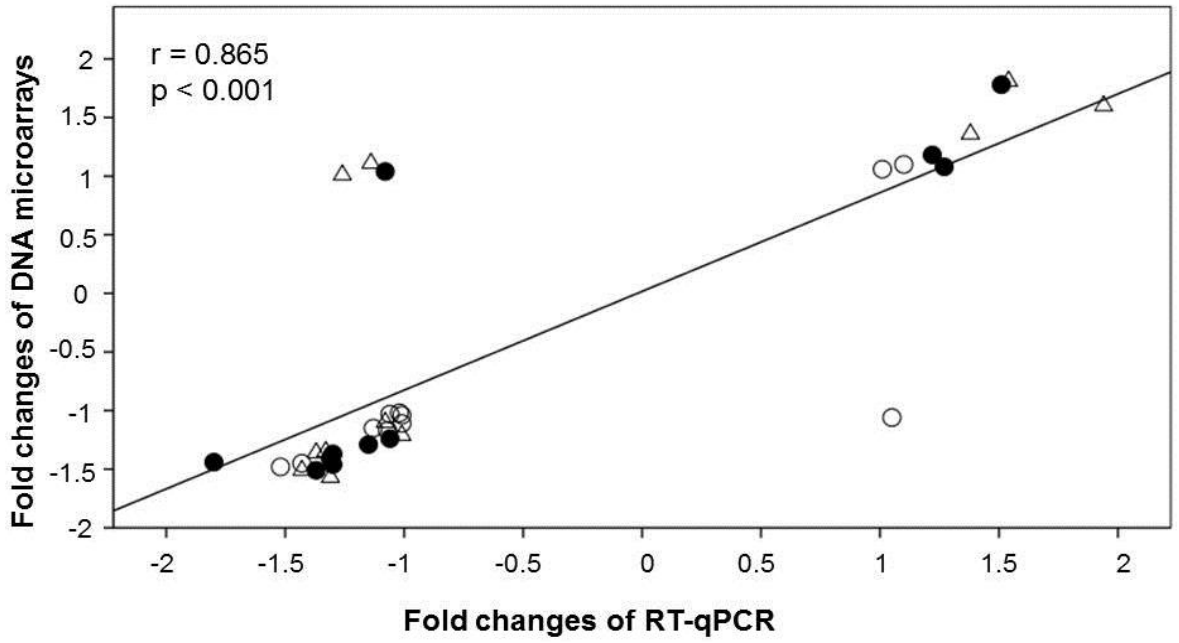

Figure 25: Correlation between FC of DNA microarray and RT-qPCR data. All 11 RT-qPCR experiments, including three pairwise comparisons of each target gene (final number of variables: 33) and their corresponding DNA microarray values were used for the correlation analysis. FC: fold change; r = Spearman correlation coefficient; RT-qPCR: reverse transcription quantitative polymerase chain reaction. Open circles: lean group, black circles: obese group, open triangles: obese GDM group.

4.12 Western blot analysis

4.12.1 Analysis of placental AKT and GSK3β protein expression

With respect to the down-stream signaling pathway of insulin and various growth/survival factors, the protein kinase AKT plays an essential role in controlling protein synthesis, glucose metabolism, angiogenesis, survival/apoptosis and proliferation [118]. After PI3K-dependent activation, AKT is subsequently phosphorylated at Thr 308 by the 3-phospho-inositide-dependent protein kinase (PDK) 1 and at Ser 473 by mTOR complex (mTORC) 2. AKT is directly involved in cell cycle regulation and controls indirectly proliferation processes by phosphorylation and inactivation of GSK3β at Ser 9. Another important AKT function is the regulation of the glycogen synthesis through phosphorylation and inactivation of GSK3α (Ser 21) and GSK3β (Ser 9). To examine as to whether maternal obesity and GDM also impact placental AKT and GSK3β activation status, both phosphorylated (Ser 473 for AKT and Ser 9 for GSK3β) and respective total protein levels were measured by Western immunoblot analysis. The results and representative blots are illustrated in **Figure 26** (entire blots of all measured samples are shown in **Supplemental figure 3**)**.** AKT phosphorylation at Ser 473 was significantly increased in placentas of obese GDM subjects compared to the lean and obese groups (FC: 1.43 and FC: 1.31, $p < 0.05$), whereas the total AKT protein levels were similar between groups**.** The pAKT-total AKT ratio (each normalized to GAPDH) was increased in placentas of obese GDM women, but only reached borderline significance

(p = 0.057). Moreover, GSK3β showed a significant increase in phosphorylation at Ser 9 in placentas obtained from obese GDM women compared to lean subjects (FC: 1.96; p < 0.001). However, total GSK3β protein levels were not regulated between groups and the ratio of pGSK3β to total GSK3β (each normalized to GAPDH) showed a significant increase in the obese GDM group (FC: 1.70, p < 0.01). The correlation analysis revealed a significant positive correlation between pAKT-total AKT ratio and pGSK3β-total GSK3β ratio in the unadjusted analysis (r_1 = 0.350, p = 0.025, **Figure 27**).

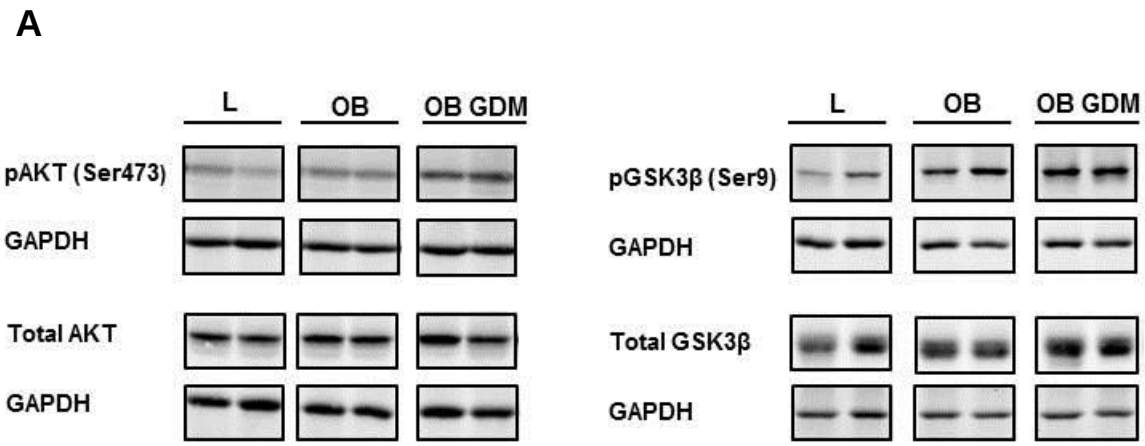

Figure 26: Analysis of pAKT (Ser 473), total AKT, pGSK3β (Ser 9) and total GSK3β in placental protein extracts of lean, obese and obese GDM women by Western blot. A) Representative Western blot images for pAKT, total AKT, pGSK3β and total GSK3β. 65 µg proteins per lane from term placental villous tissues were loaded on a 10 % polyacrylamide gel. SDS-PAGE was performed at 100 V for ~3 hrs followed by semi-dry blotting on a nitrocellulose membrane for 45 min at 200 mA. Detection was performed with rabbit anti-phospho-AKT XP (Ser473) (D9E) XP (#4060 Cell Signaling,1:500) and rabbit anti-AKT (#9272, Cell Signaling, 1:1000) and rabbit anti-phospho-GSK3β (#9336, Cell signaling; 1:500) and rabbit anti-GSK3β (#9315,Cell Signaling, 1:1000) and GAPDH (#AM4300, Ambion/Life technologies, 1:6000) using the Odyssey® Infrared Imaging System (LI-COR Biosciences GmbH). Densitometric analyses of pAKT, total AKT (both 60 kDa), pGSK3β, total GSK3β (both 46 kDa) and GADPH (37 kDa) were analyzed using the Odyssey application software v3.0, LI-COR Biosciences GmbH. Western Blot analysis was performed in placentas of lean (n=13), obese (n=13) and obese GDM (n=15) women.

B

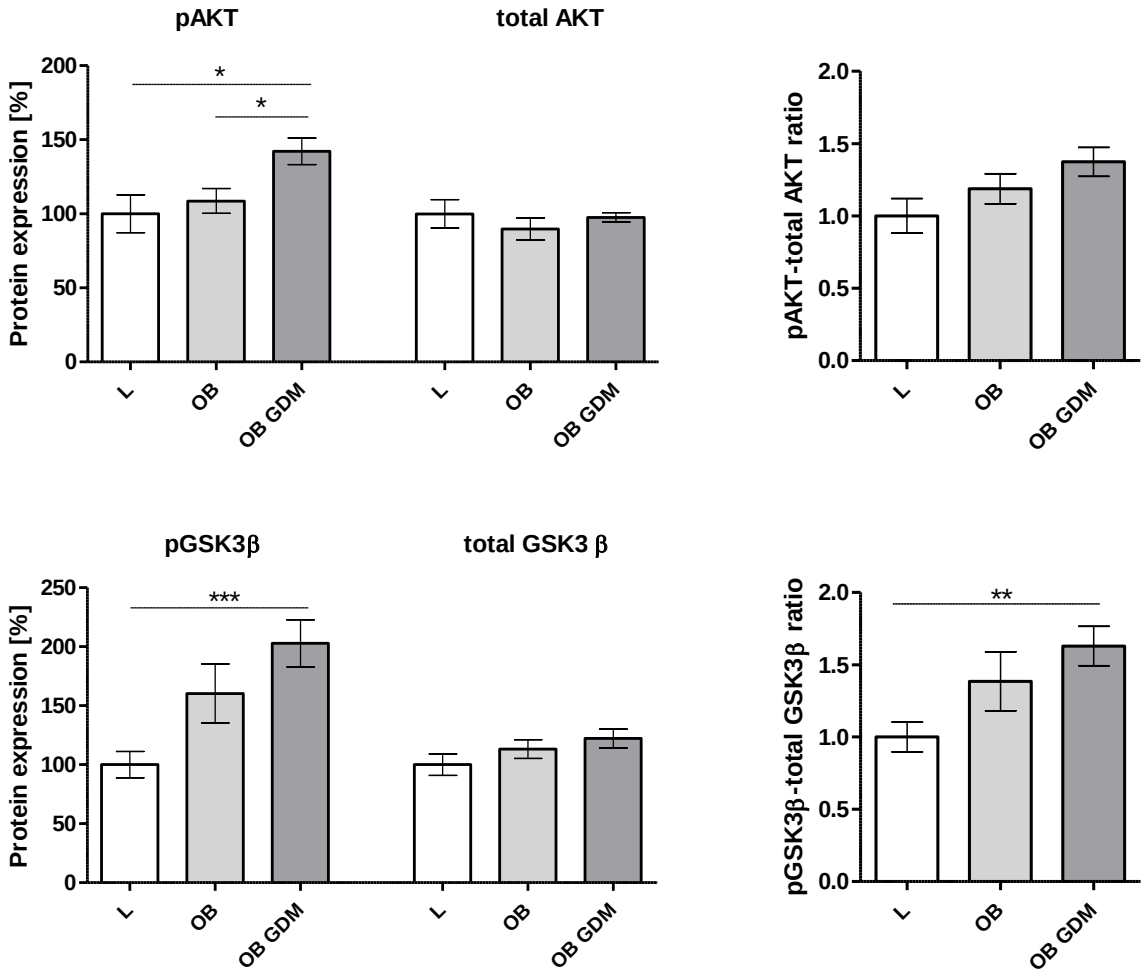

Continued Figure 26: Analysis of pAKT (Ser 473), total AKT, pGSK3β (Ser 9) and total GSK3β expression in placental protein extracts of lean, obese and obese GDM women by Western blot. B) Results of normalized pAKT, total AKT, pGSK3β and total GSK3β are shown as means ± SEM. Ratios of pAKT to total AKT and pGSK3β to total GSK3β (each normalized to GAPDH) are further displayed as means ± SEM. Statistical analysis was performed using One-Way ANOVA and Sidak's post hoc test or nonparametric Kruskal-Wallis-test with Dunn's post hoc test. Asterisks indicate significant differences between groups as indicated: *$p < 0.05$; ***$p < 0.001$. The entire blots are shown in **Supplemental figure 3.**

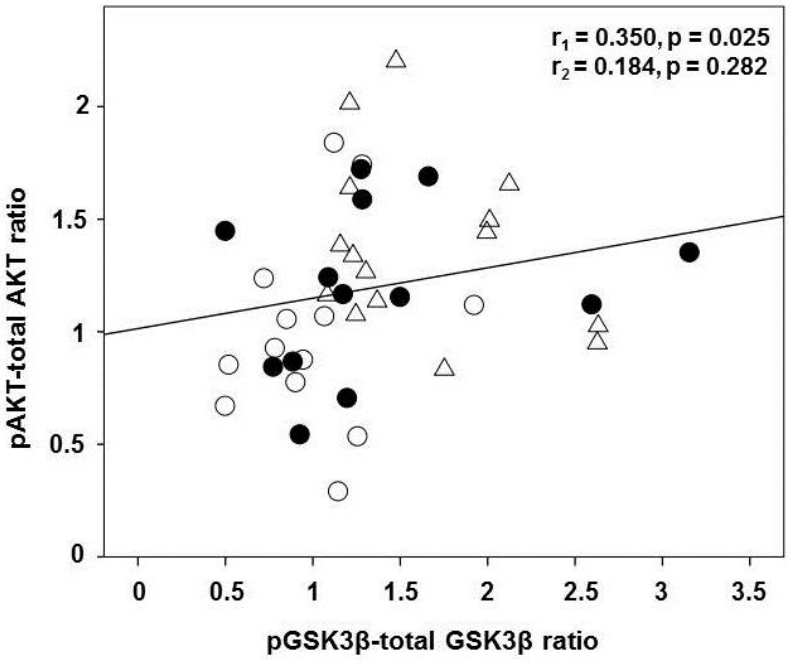

Figure 27: Correlation of phosphorylated AKT (Ser 473)-total AKT ratio and phosphorylated GSK3β (Ser 9)-total GSK3β ratio. r_1 = unadjusted Spearman correlation coefficient; r_2: partial correlation coefficient adjusted for covariates infant sex, pregnancy duration, maternal pregravid BMI, AUC $_{(Glucose)}$ OGTT and gestational weight gain. Open circles: lean group, black circles: obese group, open triangles: obese GDM group.

4.12.2 Detection of nuclear β-catenin

In the absence of a Wnt ligand in the canonical pathway, cytoplasmic β-catenin is mainly located to adherens junctions and complexed with APC, GSK3β, CSNK1A1 and scaffold protein axin. Within this complex, β-catenin is subsequently phosphorylated by CSNK1A1 and GSK3β, and finally degraded in the 26S proteasome [119]. After Wnt ligand binding to the frizzled (Fzd) receptor, a heterodimeric complex of Fzd and its coreceptor LRP is formed and bound by dishevelled (Dsh). Subsequently, GSK3β- and CSNK1G-dependent phosphorylations activate the LRP coreceptor and lead to the axin translocation to the receptor complex at the plasma membrane, disrupting the axin scaffold complex [119]. Moreover, Dsh is able to inhibit GSK3β activity resulting in reduced axin phosphorylation and β-catenin binding. Finally, stabilized β-catenin translocate to the nucleus functioning as a transcriptional co-regulator [119].

To verify the potential impact of increased GSK3β phosphorylation on β-catenin translocation, nuclear protein extracts from frozen placenta tissues were prepared**.** The nuclear extracts were controlled for cytosolic contamination measuring GAPDH protein expression. The results revealed that nuclear β-catenin protein expressions were significantly elevated in placentas of obese GDM compared to lean subjects (FC: 1.47; $p < 0.05$) **(Figure 28; Supplemental figure 3).**

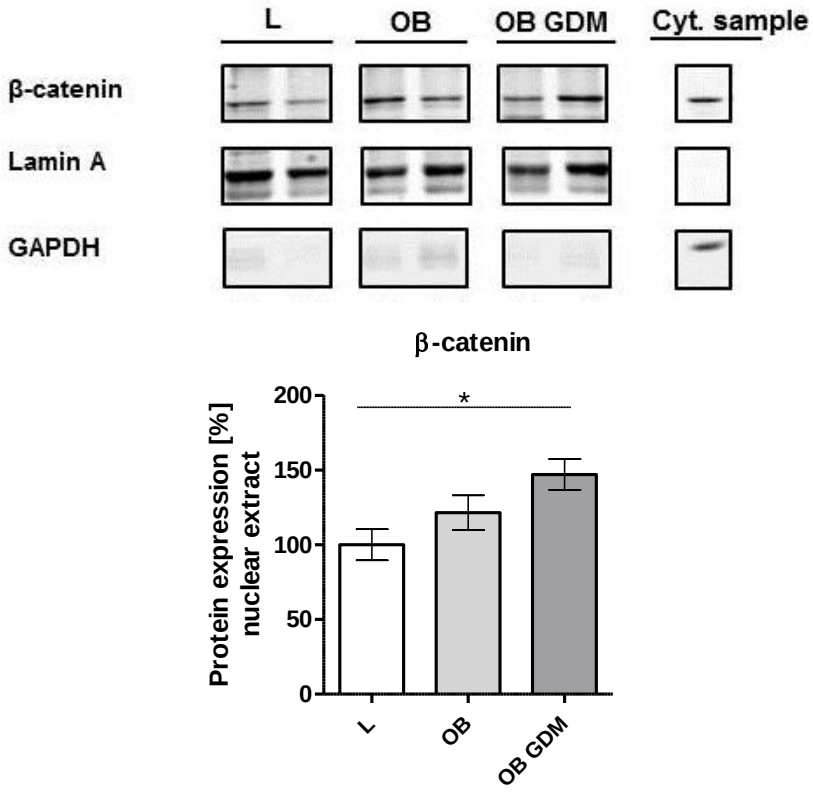

Figure 28: Analysis of β-catenin expression in placental nuclear protein extracts of lean, obese and obese GDM women by Western blot. Representative Western blot images for β-catenin are shown Cyt: cytosolic samples (control sample for Lamin A and GAPDH protein expression). 15 µg proteins per lane from term placental villous tissues were loaded on a 10 % polyacrylamide gel. SDS-PAGE was performed at 100 V for ~3 hrs followed by wet blotting on a nitrocellulose membrane for 4-4.5 hrs at 150 mA (4°C). Detection was performed with rabbit anti-β-Catenin (D10A8) XP (# 8480, Cell signaling, 1:1000), Lamin A (# 2032, Cell signaling, 1:1000) and GAPDH (# AM4300, Ambion/Life technologies, 1:6000) using the Odyssey® Infrared Imaging System (LI-COR Biosciences GmbH). Densitometric analyses of β-Catenin (92 kDa), Lamin A (70 kDa) and GADPH (37 kDa) were analyzed using the Odyssey application software v3.0, LI-COR Biosciences GmbH. Western Blot analysis was performed in placentas of lean (n=12), obese (n=13) and obese GDM (n=15) women. Results of normalized β-catenin are shown as means ± SEM. The nuclear extracts were controlled for cytosolic contamination measuring GAPDH protein expression. Statistical analysis was performed using One-Way ANOVA and Sidak's post hoc test. Asterisks indicate significant differences between groups as indicated: * $p < 0.05$. The entire blots are shown in **Supplemental figure 3.**

4.13 Measurement of placental glycogen concentration

The glycogen synthase (GYS) is constitutively phosphorylated by casein kinase 2 (CSNK2A1 and CSNK2A2) at Ser 656, providing initial priming for a strict phosphorylation sequence by GSK3β (Ser 652, Ser 648, Ser 644, Ser 640), that successively inhibited the GYS activity [120]. In the presence of an insulin signal, the GSK3β activity is indirectly blocked via AKT-mediated phosphorylation at Ser 9. Consequently, the decreased phosphorylation of GYS by GSK3β increases the glycogen synthesis. The described mechanism links GSK3β in the pathway from insulin to glucose disposal in turns of glycogen [120].

To determine the impact of GSK3β phosphorylation on glycogen concentration in the placentas, glycogen was extracted from villous tissues and normalized to respective protein

concentration. The analysis revealed that glycogen concentrations were significantly increased in placentas obtained from obese diabetic women compared to lean and obese participants (31.9 vs. 24.4 and 24.3 µg glycogen/mg protein; $p < 0.05$) **(Figure 29).** Moreover, the positive relationship between the placental pGSK3β-total GSK3β ratio and glycogen concentration reached significance in the unadjusted analysis ($\beta = 0.309$; $p = 0.049$).

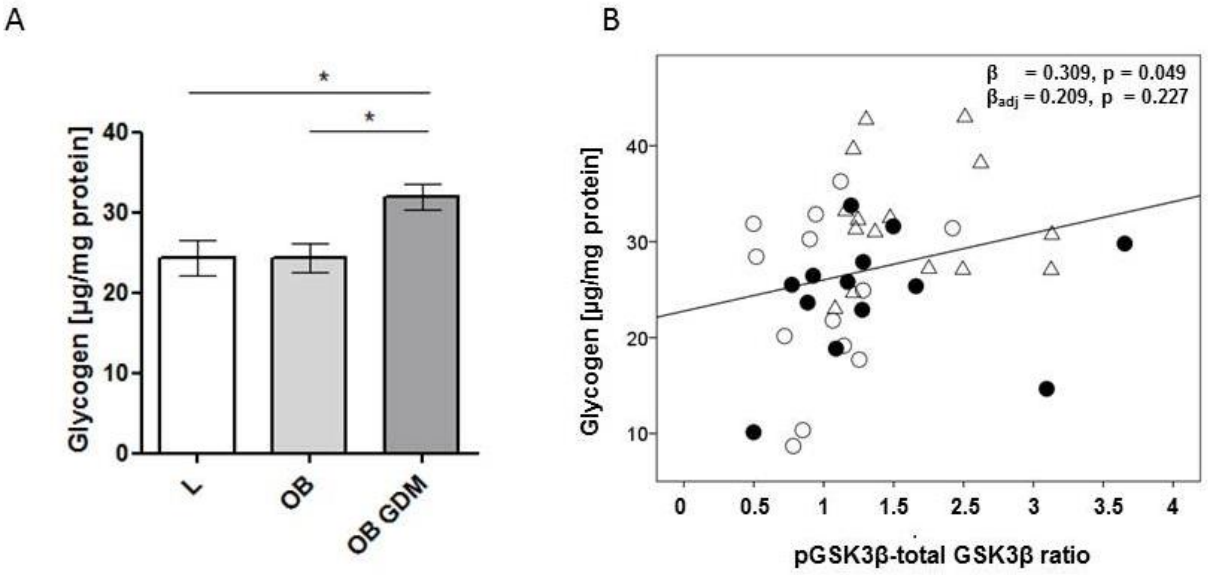

Figure 29: Analysis of the glycogen concentration in term placentas and the relation of pGSK3β-total GSK3β ratio to glycogen concentration. A) Glycogen was extracted from villous placental tissues and normalized to protein concentration. **B)** Regression analysis of villous placental glycogen concentration on pGSK3β-total GSK3β ratio measured by western blot. β: standardized regression coefficient. Variables for adjusted analysis: infant sex, pregnancy duration, maternal pregravid BMI, AUC ($_{Glucose}$) OGTT and gestational weight gain. Open circles: lean group, black circles: obese group, open triangles: obese GDM group.

4.14 Placental gene and protein expression in relation to offspring adipose tissue distribution up to year-1

Considering the importance of the placenta for fetal growth, the aim of this study was to analyse molecular placenta-mediated processes with respect to offspring adipose tissue growth. Thus, linear regression analysis was used to explore the relationship between differentially regulated target genes (WNT7A, DKK3, PTH1R, CDH11 and FLT1) and offspring SFT, SCA and PPA from week-1 up to year-1 **(Table 21).** Accordingly, placental WNT7A mRNA levels were positively related to neonatal PPA at week-1 in the unadjusted analysis and further after adjusting for infant sex, pregnancy duration, maternal pre-pregnancy BMI, AUC $_{Glucose}$ (OGTT) and gestational weight gain. However, performing the linear regressions with mRNA expression levels for DKK3, PTH1R, CDH11 and FLT1,

respectively, no significant relationships were found between these placental gene expression levels and fat distribution parameters up to year-1 in the unadjusted and fully adjusted analyses (**Table 21**).

The relationship of differentially regulated placental protein levels and infant adipose tissue growth was further assessed by linear regression **(Table 22).** Values for placental pAKT-total AKT ratios emerged as positive independent determinants of PPA at week-1 in the unadjusted analysis and also after adjustment for infant sex, pregnancy duration, pre-pregnancy BMI, $AUC_{Glucose}$ (OGTT) and gestational weight gain. Moreover, the pAKT-total AKT ratios were significantly positively related to SFT at week-6 in the unadjusted analysis and to SFT at month-4 in both linear regression analyses. For the pGSK3β-total GSK3β ratios, a significantly positive relationship with infant PPA at week-1 was only found in the unadjusted analysis. However, in both analysis models, no significant relationships were determined between placental nuclear β-catenin protein levels and adipose tissue distribution parameters at all ages investigated.

Table 21: Regression of infant fat distribution parameter up to year-1 on placental gene expressions WNT7A, DKK3, CDH11, PTH1R and FLT1

		WNT7A					DKK3					CDH11				
		Unadjusted analysis		Adjusted analysis			Unadjusted analysis		Adjusted analysis			Unadjusted analysis		Adjusted analysis		
	N	β	P-value	β	P-value	Adj model r^2	β	P-value	β	P-value	Adj model r^2	β	P-value	β	P-value	Adj model r^2
Week-1																
SFT	43	0.285	0.064	0.198	0.223	0.100; p = 0.131	-0.080	0.610	0.042	0.221	0.063; p = 0.216	-0.216	0.163	-0.024	0.897	0.062; p = 0.219
SCA	35	0.167	0.338	0.109	0.504	0.169; p = 0.078	0.064	0.715	0.369	0.059	0.258: p = 0.023	-0.183	0.293	0.148	0.453	0.173: p = 0.075
PPA	35	**0.405**	**0.016**	**0.355**	**0.028**	**0.257; p= 0.023**	-0.104	0.554	0.030	0.885	0.115; p = 0.149	-0.128	0.462	-0.141	0.486	0.130; p = 0.126
Week-6																
SFT	39	0.190	0.246	0.090	0.601	0.048; p = 0.297	-0.307	0.058	-0.135	0.503	0.053; p = 0.282	-0.010	0.951	-0.028	0.884	0.040; p = 0.320
SCA	39	0.146	0.376	-0.013	0.937	0.110: p = 0.154	-0.103	0.532	0.241	0.211	0.154; p = 0.089	-0.022	0.893	0.057	0.762	0.112; p = 0.149
PPA	39	0.036	0.826	-0.106	0.769	0.214; p = 0.038	-0.075	0.649	0.319	0.076	0.281; p = 0.013	0.055	0.741	0.080	0.651	0.208; p = 0.042
Month-4																
SFT	38	0.008	0.961	0.003	0.987	0.010; p = 0.418	-0.132	0.429	-0.019	0.929	0.010; p = 0.417	0.004	0.979	0.057	0.779	0.012; p = 0.409
SCA	38	-0.134	0.422	-0.222	0.246	-0.057; p = 0.660	0.005	0.978	0.190	0.398	-0.080; p = 0.744	0.224	0.176	0.374	0.076	0.006; p = 0.431
PPA	38	0.170	0.300	0.082	0.656	-0.033; p = 0.573	-0.124	0.452	0.060	0.784	-0.037; p = 0.590	-0.171	0.299	-0.244	0.238	0.007; p = 0.427
Year-1																
SFT	40	-0.127	0.434	-0.102	0.575	-0.073; p = 0.736	-0.023	0.889	-0.028	0.899	-0.083; p = 0.774	0.232	0.150	0.266	0.209	-0.031; p = 0.568
SCA	40	-0.053	0.745	-0.104	0.569	-0.070; p = 0.723	-0.212	0.190	-0.218	0.314	-0.047; p = 0.632	-0.097	0.551	-0.055	0.796	-0.079; p = 0.757
PPA	40	-0.058	0.724	-0.120	0.459	0.148.; p = 0.091	0.006	0.970	0.078	0.689	0.139; p = 0.104	0.249	0.122	0.264	0.162	0.186; p = 0.054

β: standardized regression coefficient; r^2: coefficient of determination; CDH11: cadherin 11; DKK3: dickkopf homolog 3; SCA: subcutaneous adipose tissue; SFT: sum of the 4 skin fold thickness measurements (biceps + triceps + subscapular + suprailiac); PPA: preperitoneal adipose tissue; WNT7A: wingless-type MMTV integration site family, member 7A. Variables for adjusted analysis: infant sex, pregnancy duration, respective breastfeeding status, maternal pre-pregnant BMI, $AUC_{Glucose}$ (OGTT) and gestational weight gain. Significant variables are presented in bold type.

Continued table 21: Regression of infant fat distribution parameter up to year-1 on placental gene expressions WNT7A, DKK3, CDH11, PTH1R and FLT1

		PTH1R					FLT1				
		Unadjusted analysis		Adjusted analysis			Unadjusted analysis		Adjusted analysis		
	N	β	P-value	β	P-value	Adj model r^2	β	P-value	β	P-value	Adj model r^2
Week-1											
SFT	43	**-0.320**	**0.036**	0.236	0.164	0.111; p = 0.112	0.071	0.650	0.081	0.644	0.067; p = 0.205
SCA	35	-0.111	0.527	0.105	0.56	0.166; p = 0.081	0.134	0.442	0.223	0.251	0.195: p = 0.056
PPA	35	-0.058	0.740	-0.095	0.606	0.123; p= 0.136	0.162	0.351	0.121	0.547	0.126; p = 0.132
Week-6											
SFT	39	**-0.367**	**0.021**	-0.322	0.078	0.132; p = 0.118	0.163	0.321	0.130	0.495	0.053; p = 0.280
SCA	39	-0.221	0.177	-0.071	0.695	0.114: p = 0.146	0.211	0.197	0.107	0.558	0.119; p = 0.137
PPA	39	-0.121	0.464	0.004	0.982	0.203; p = 0.045	0.035	0.832	-0.080	0.647	0.208; p = 0.042
Month-4											
SFT	38	-0.307	0.061	-0.198	0.284	0.047; p = 0.302	0.037	0.825	0.042	0.827	0.011; p = 0.413
SCA	38	-0.161	0.333	-0.048	0.806	-0.104; p = 0.826	0.072	0.667	0.032	0.875	-0.105; p = 0.830
PPA	38	-0.060	0.716	0.018	0.923	-0.040; p = 0.598	-0.026	0.877	-0.256	0.184	0.019; p = 0.386
Year-1											
SFT	40	-0.110	0.501	-0.159	0.402	-0.060; p = 0.684	-0.085	0.603	-0.058	0.769	-0.081; p = 0.765
SCA	40	-0.289	0.071	-0.303	0.104	0.006; p = 0.427	-0.058	0.721	-0.018	0.929	-0.081; p = 0.764
PPA	40	-0.030	0.855	-0.146	0.388	0.154 p = 0.084	-0.084	0.605	-0.126	0.474	0.147; p = 0.092

β: standardized regression coefficient; FLT1: fms-related tyrosine kinase 1; r^2: coefficient of determination; SCA: subcutaneous adipose tissue; SFT: sum of the 4 skin fold thickness measurements (biceps + triceps + subscapular + suprailiac); PPA: preperitoneal adipose tissue; PTH1R: parathyroid hormone 1 receptor. Variables for adjusted analysis: infant sex, pregnancy duration, respective breastfeeding status, maternal pre-pregnant BMI, $AUC_{Glucose}$ (OGTT) and gestational weight gain. Significant variables are presented in bold type

Table 22: Regression of infant fat distribution parameter up to year-1 on placental pAKT-total AKT ratio, pGSK3β-total GSK3β ratio and nuclear β-catenin

		pAKT-total AKT ratio					pGSK3β-total GSK3β ratio					n-β-catenin				
		Unadjusted analysis		Adjusted analysis			Unadjusted analysis		Adjusted analysis			Unadjusted analysis		Adjusted analysis		
	N	β	P-value	β	P-value	Adj model r^2	β	P-value	β	P-value	Adj model r^2	β	P-value	β	P-value	Adj model r^2
Week-1																
SFT	41	0.254	0.109	0.167	0.312	0.120; p = 0.108	0.219	0.169	0.071	0.676	0.098; p = 0.146	0.099	0.545	0.039	0.827	0.122; p = 0.110
SCA	33	-0.071	0.696	-0.018	0.464	0.230; p = 0.042	0.115	0.523	-0.027	0.874	0.215: p = 0.051	0.129	0.473	0.075	0.696	0.234: p = 0.040
PPA	33	**0.415**	**0.016**	**0.375**	**0.027**	**0.217; p= 0.050**	**0.391**	**0.024**	0.278	0.130	0.132; p = 0.136	0.194	0.278	-0.042	0.834	0.161; p = 0.098
Week-6																
SFT	37	**0.350**	**0.034**	0.295	0.081	0.118; p = 0.152	0.091	0.592	0.012	0.950	0.019; p = 0.391	0.219	0.193	0.035	0.859	0.111; p = 0.163
SCA	37	0.299	0.072	0.225	0.177	0.129: p = 0.133	0.037	0.828	-0.092	0611	0.080; p = 0.225	0.346	0.036	0.151	0.421	0.192; p = 0.061
PPA	37	0.294	0.078	0.194	0.220	0.210; p = 0.049	0.103	0.545	-0.043	0.802	0.169; p = 0.083	0.099	0.559	-0.288	0.120	0.240; p = 0.031
Month-4																
SFT	37	**0.427**	**0.008**	**0.369**	**0.034**	**0.121; p = 0.147**	0.045	0.792	0.051	0.800	-0.028; p = 0.549	0.025	0.889	0.020	0.925	0.098; p = 0.200
SCA	37	0.224	0.182	0.193	0.366	-0.079; p = 0.733	-0.075	0.658	-0.125	0.550	-0.110; p = 0.834	0.116	0.506	0.106	0.633	0.025; p = 0.377
PPA	37	0.203	0.222	-0.371	0.053	-0.007; p = 0.474	-0.228	0.168	-0.334	0.076	0.047; p = 0.302	0.261	0.124	0.213	0.342	-0.019; p = 0.514
Year-1																
SFT	38	0.270	0.101	0.234	0.182	0.025; p = 0.368	0.059	0.727	0.105	0.582	-0.025; p = 0.541	-0.021	0.900	-0.034	0.882	-0.103; p = 0.811
SCA	38	0.239	0.149	0.157	0.381	-0.039; p = 0.591	0.088	0.528	-0.048	0.803	-0.064; p = 0.685	0.198	0.241	0.206	0.348	-0.006; p = 0.473
PPA	38	0.075	0.656	0.037	0.819	0.124; p = 0.136	0.295	0.072	0.218	0.209	0.168; p = 0.079	0.092	0.587	-0.149	0.468	0.111; p = 0.163

AKT: V-akt murine thymoma viral oncogene homolog 1; β: standardized regression coefficient; GSK3β: Glycogen synthase kinase 3β; β: r^2: coefficient of determination; SCA: subcutaneous adipose tissue; SFT: sum of the 4 skin fold thickness measurements (biceps + triceps + subscapular + suprailiac); PPA: preperitoneal adipose tissue. Variables for adjusted analysis: infant sex, pregnancy duration, respective breastfeeding status, maternal pre-pregnant BMI, $AUC_{Glucose}$ (OGTT) and gestational weight gain. Significant variables are presented in bold type.

5 Discussion

The rising incidence of obesity within the obstetrical population emphasizes the need for appropriate preterm intervention and medical care to diminish the obesity prevalence in the offspring [4]. Perturbations of normal pattern at critical periods of placental development may result in altered function and fetal malprogramming. Therefore, maternal metabolic changes and inflammatory processes might target the placental structure and physiology leading to long-lasting impact on offspring health and disease [74]. Thus, the *GesA* study investigated the impact of maternal obesity with and without GDM on maternal and cord plasma biomarkers as well as on global gene expression profiles and signal pathways in the placenta, which might be related to the early adipose tissue development in the offspring.

Major findings of this PhD thesis were that the intrauterine hyperglycemia had a brief impact on neonatal SFT, SCA and PPA of the diabetic offspring, which seemed to diminish during the 1st year *pp*. Importantly, maternal C-peptide and HMW adiponectin levels, obtained at 3rd trimester, were found to be potentially predictive for elevated PPA in early infancy and newborn PPA was significantly related to PPA development at year-1. In contrast, maternal CRP and IL6 levels were only barely related to adipose tissue growth up to year-1.
The placentas of obese GDM women showed the most striking alterations in global gene expression compared to euglycemic lean and obese women, respectively. Notably, the placentas of obese women with and without GDM did not display increased inflammatory processes and cytokine expression. The hypothesis of the inflamed placenta in pregnancies complicated by maternal obesity and/or GDM is not a stringent necessity and might be accounted for the selection of relatively `healthy´ women apart from their obesity and GDM. However, the observed alterations in insulin and Wnt/β-catenin signaling in placentas of obese women with GDM might point to changes in trophoblast differentiation/villous immaturity and angiogenic processes. Furthermore, linear regression analysis revealed that the placental pAKT-total AKT protein ratio and the WNT7A mRNA levels were positively related to early infant SFT and PPA. This strongly suggests that insulin signaling and Wnt/β-catenin signaling can be important modulators of placental functions which might impact factors that are important for fetal and newborn subcutaneous and preperitoneal adipose tissue growth.

5.1 Impact of maternal obesity with and without GDM on offspring adipose tissue development up to year-1

5.1.1 Diabetic offspring had increased SFT, PPA and SCA at week-1

BMI and ponderal index are often provided as obesity markers, but recently performed correlation analyses indicated, that they only account for 15 % of the variance of obesity in the newborns [121]. Thus, for newborns and toddlers, it is important to apply further non-invasive methods to estimate adipose tissue composition. With the use of special equations, it is possible to relate the skinfold thickness to consistent body fat mass and percentage of body weight [102]. A few recently published studies have used bioelectrical impedance analysis (BIA) to estimate body composition and to differentiate between fat and lean mass, but this method can not specifically measure the relative quantities and distribution of SCA and PPA [122,123]. This study is the first reporting the comparative longitudinally assessment of SFT and complementary abdominal ultrasonography of SCA and PPA from birth to year-1 *pp* in offspring of normoglycemic lean mothers and obese mothers with and without GDM. One major finding was that abdominal SCA and PPA areas were significantly higher at week-1 and SFT was significantly elevated until week-6 in infants born to obese women with GDM compared to offspring born to lean mothers.

Preperitoneal fat is, together with intraperitoneal and retroperitoneal fat, a component of the visceral adipose tissue. Mook-Kanamori et al. [124] were the first who retrospectively compared different computer tomography (CT) scans of non-obese children (median age 7.9 years) and evaluated whether preperitoneal fat thickness is a good approximations for visceral fat. Afterwards, the authors directly compared CT measurements with ultra-sonographic assessment of abdominal fat distribution in non-obese children (median age 9.5 years). They concluded that preperitoneal fat assessed by ultrasonography is a useful surrogate for visceral fat in children and is considered as a valid method for measuring infant abdominal fat distribution in epidemiological and clinical research. Recently, Holzhauer et al. [105] developed a standardized protocol to measure the thickness of subcutaneous and preperitoneal fat of 2-year-old children and verified its reliability. This method was slightly modified by Hauner et al. [58] and extended for infants from week-6 to year-1 *pp*, but was not applied proximal after birth. The importance of investigating specific changes in early adipose tissue distribution, as performed in the present study, is supported by recent insights into distinct neonatal fat depots assessed by magnetic resonance tomography (MRT) [125,126]. The authors described significantly increased intra-hepatocellular lipids in newborns in relation to pregravid BMI and GDM, but conflicting results have been reported regarding the effect of maternal obesity on abdominal fat in neonates [125,126]. Brumbaugh et al. [125] did not find a difference in intra-abdominal fat per body length in infants of obese mothers with GDM, whereas Modi et al. [126] showed the correlation of maternal pre-pregnancy BMI with

abdominal fat in newborns, but did not discriminate between subcutaneous and intra-abdominal fat.

5.1.2 Gestational weight gain had no impact on infant adipose tissue development

It was confirmed that obese women, regardless of GDM, gained significantly less weight than lean women [127,128]. According to IOM criteria [110], obese women (BMI > 30 kg/m^2) should gain less than 9 kg, whereas weight gain of normal weight women (18.5 kg/m^2 < BMI < 25 kg/m^2) should be limited to 16 kg during pregnancy. Mean weight gain in all 3 groups exceeded these recommendation, showing even more than two-thirds of obese women with and without GDM and 60 % of lean women exceeded the advocated weight-gain limit. Regarding the impact of GWG as confounder in the linear regression models, this factor was neither associated to neonatal SFT and SCA nor PPA development. However, excessive maternal GWG is considered as risk factor for rapid neonatal weight gain [129] and childhood obesity [130]. Moreover, GWG was significantly related to persisting obesity risk through adolescence [131,132] and to adult BMI z-scores [133]. Notably, lifestyle intervention studies, that were performed during pregnancy in euglycemic obese women, could partly restrict GWG, but had no effect on pregnancy-associated comorbidities, birth weight or macrosomia rate emphasising the need for obesity therapies prior to pregnancy [134,135]. Only a few studies addressed the improvement of maternal metabolic markers in their intervention studies. However, Wolff et al. [136] showed that the restriction of GWG by intensive dietary consultations was accompanied by reduced serum leptin, insulin and blood glucose levels in the obese participants over in the course of pregnancy.

5.1.3 Differences in infant growth pattern attenuated during the 1st year

The findings on adipose tissue growth and distribution during the 1st year are consistent with data from several studies reporting that overweight at birth in GDM offspring diminished during year-1 *pp* [8,137,138]. Interestingly, these studies found that infant overweight re-emerged at the age of 2–3 years. In this context, GDM and decreased maternal insulin sensitivity (IS $_{OGTT}$ index) levels were reported to be independent predictors for both slower infant weight gain at month-6 *pp* [139] and reduced SFT at year-1 [140]. In contrast, other investigators showed increased body weight and weight-length ratio in 6-month-old children in relation to pregravid obesity and gestational weight gain or found persistent increased SFT at year-1 in LGA offspring born to GDM mothers [129,141].

Apart from maternal variables, cord plasma markers emerged as important predictors for weight and fat mass growth in early childhood; thus, elevated cord blood leptin levels were identified as being related to slower infant weight gain up to month-6 [139], year-2 [142] and year-3 [143]. Leptin is involved in the maintenance of energy homoeostasis via hypothalamic

neuron signaling [144]. It was speculated that early postnatal leptin-sensitive periods might decrease food intake and increase energy utilization [139]. However, the present study found no significant relationship of cord plasma leptin to growth markers at year-1. It was further shown that cord insulin levels were inversely related to infant weight gain at year-2 [145], but not to infant weight gain up to primary endpoint or adipose tissue parameters at year-1 in the *GesA* study. Altogether, it is tempting to speculate that increased intrauterine and perinatal insulin levels initiated a temporarily prolonged increase in adipose tissues in GDM offspring up to week-6, a postnatal time period where GDM offspring insulin have already returned to a normal level. Afterwards, during subsequent time up to year-1, weight and adipose tissue growth normalized, as these insulin-mediated effects faded away. However, a long-term impact of maternal and fetal hyperglycemia on later infancy and adolescence obesity risk is still plausible as indicated by epidemiological studies [10,51,146]. In addition, in a recently published study, a high infant BMI at year-1 and early rapid infant weight gain were considered as risk factors for the development and persistence of overweight during later childhood at the age of 7-9 years [147]. It was suggested, that the number of fat cells is already determined during childhood and adolescence, while the number of adipocytes remain constant in adults. This hypothesis was confirmed by studies reporting on the highest proliferation (thymidine kinase activity) of precursor cells in the adipose tissue during the sensitive developmental time window of early postnatal period and preadolescent stages (reviewed in [54]).

Notably, neonatal PPA correlated significantly to respective growth parameters and subcutaneous adipose tissues, but from month-4 on, no significant relationships persisted. The weak correlation of both subcutaneous with preperitoneal adipose tissues at month-4 and year-1 indicate the co-existence of two independently growing fat depots in the late postnatal period investigated. Correspondingly, neonatal PPA at week-1 was an independent predictor for PPA at the infant age of 1 year, whereas significant associations between birth weight, ponderal index, SFT, SCA and their year-1 accordant measurements were lacking. The data on PPA may reflect intrauterine influences on early particular adipose tissue compartments which may also have sustainable adverse effects at later stages in infancy or childhood. This proposed relationship warrants being evaluated in future studies. In this context, increased PPA was recently determined as cardiovascular risk factor in obese children [148] and non-obese adults [149,150]. Therefore it will be interesting to analyse in future studies whether increased PPA at birth might be not only indicative for later obesity risk, but also for cardiovascular risk in adulthood.

5.2 Obese women were characterized by hyperinsulinemia, but only offspring of obese diabetic mothers displayed fetal hyperinsulinemia

Maternal hyperinsulinemia is well characterized in women with gestational diabetes [95,96,151] but also in euglycemic obese pregnant women [20,29,122] resulting from impaired peripheral and hepatic insulin sensitivity compared to lean women [17]. In concordance with these reports, significantly elevated fasted insulin levels were found in both groups of obese participants with and without GDM in comparison to lean women at 3rd trimester. It can be assumed that hyperinsulinemia of obese participants without GDM compensate the persisting pathological insulin resistance, maintaining successfully normal levels of fasting and postprandial glucose levels similar to lean women. In contrast, high insulin levels observed in plasma of obese GDM women represent an inadequate β-cell response that is insufficient to overcome pathological insulin resistance, resulting in maternal hyperglycemia.

In this thesis, maternal plasma C-peptide was measured as surrogate for pancreatic insulin secretion, thereby discriminating plasma insulin levels from potential exogenous insulin interferences. The increased C-peptide levels further confirmed the enhanced insulin secretion in both obese groups. A novel relationship found in this study showed that maternal C-peptide and insulin levels emerged as positive determinants for infant PPA at week-1. This strongly supports the assumption that maternal insulin levels are important regulators of maternal metabolism that might impact fetal and newborn PPA growth [152].

The results of this thesis are compatible with the hypothesis proposed by Pedersen et al. [64], indicating that fetal hyperinsulinemia is an adaptive process resulting from elevated maternal glucose levels [9], and that fetal insulin is associated with neonatal fat mass and growth due to the role of insulin in adipogenesis and stimulation of IGF1 production [9,153]. Even if Landon et al. [41] did not find different rates of elevated cord blood C-peptide levels in the treated mild GDM group compared to the mild GDM control group with only usual prenatal care, the parameters birth weight, fat mass and frequency of LGA were reduced in the treated GDM group. This study emphasized the need for dietary counselling and self-monitoring of blood glucose even in cases with moderate hyperglycemia. In line with the present study, two other authors observed no fetal hyperinsulinemia in pregnancies of obese women without GDM [88,154]. In contrast, Catalano et al. [122] reported increased insulin levels and total fat mass in newborns from obese mothers, thus proclaiming insulin resistance *in utero* without maternal hyperglycemia. Thereby, the OGTT was only performed in the 2nd trimester and a subsequent glucose tolerance challenge in late pregnancy was not performed to exclude GDM in these obese women [122], whereas in the present study, the glucose tolerance was further re-evaluated in late pregnancy [152].

More recently, research interest has started to focus particularly on analyzing the distribution and accumulation of distinct fat depots in the body and their relationship to fetal metabolic

biomarkers. The present data indicate that cord plasma insulin was positively related to neonatal SFT and fat mass that is in line with the results reported by Brunner et al. [145]. Importantly, for the first time, the present results showed that cord insulin levels further emerged as independent predictors for PPA and SCA at week-1 *pp* [152]. Interestingly, Tamura et al. [155] have already shown that insulin levels are strongly related to preperitoneal and abdominal subcutaneous fat in 9-15-year old children. Furthermore, Cnop et al. [156] reported that insulin sensitivity was inversely correlated with visceral, but not with subcutaneous fat in adults.

5.3 Cholesterol metabolism during late pregnancy and in the placenta was altered in obese women without GDM

The present study found longitudinally decreased total and LDL cholesterol levels at 3rd trimester and at delivery in obese women compared to lean subjects [152]. Here, results are in line with recently published reports showing significantly lower total and LDL cholesterol levels in obese women with and without GDM [21,26,27]. However, reports on umbilical cord total and LDL cholesterol levels are not uniform, sometimes showing even opposing levels in relation to the mother [27,157]. In the present study, the mean TG levels were similar between the groups at 3rd trimester and at delivery. Although there are further studies indicating no significant alterations in TG levels by GDM [158] or BMI category [159,160], increased TG levels comprising all trimesters have also been found in obese and/or diabetic compared to normal-weight women [22,27].

As previously reported by Meyer et al. [160] and Scifres et al. [159], obese women exhibited higher TG, total and LDL cholesterol levels at the beginning of pregnancy compared to their lean counterparts. However, their change in maternal lipids per gestational week was decreased, reaching similar or even slightly lower maximum TG and cholesterol levels towards term. Accordingly, the *GesA* study confirmed lower levels of total and LDL cholesterol in obese women with and without GDM at 3rd trimester and at delivery. Furthermore, at week-6 *pp*, the present data of this study showed that lipid levels of obese women returned to higher mean levels after delivery compared to lean mothers. Even though overweight/obese pregnant women might show lower weekly lipid increase, they were shown to be at higher risk for the formation of small, dense LDL particles compared to the control group [22,160]. Thus, the shift to the atherogenic TG-rich LDL-III subclasses in obese women might reflect both, the increased hepatic TG lipase activity and the facilitated transfer of TG into LDL due to insulin resistance [22,160]. Little is known about other regulatory mechanism of lipid metabolism in pregnancies of obese and diabetic women, which could help to explain divergent outcomes in publications. However, lipid metabolism is also driven by steroid hormones (particularly estradiol) and sex hormone binding globulins which were

found to be reduced in obese and/or diabetic pregnant women [19,160] and might additionally explain the extent of dyslipidemia compared to normal pregnancies. Regarding abnormal fetal growth, several observations assume that, apart from maternal glucose levels, TG levels were in particular positively correlated to abdominal circumference at 3rd trimester [25] and birth weight [24,161,162].

Besides the placental glucose transport, particular attention was directed towards placental fatty acid and cholesterol transport with the goal of understanding fetal growth under abnormal metabolic (e.g. diabetic) conditions. In general, only a few genes assigned to lipid and cholesterol metabolism were found in this thesis to be differentially expressed in placentas of obese women with and without GDM. Another study revealed that key genes of lipid transport and metabolism were mainly enhanced in obese GDM compared to the lean control group [30]. However, *lipid metabolism* was identified in this thesis as differentially regulated pathway between placentas of lean and obese, but not obese diabetic women. Notably, the most dysregulated placental genes assigned to cholesterol metabolism were found in the comparison of lean and obese women. It can be speculated, that the observed differences in maternal cholesterol levels at 3rd trimester and before delivery affected the gene expression in placentas of obese women. Nevertheless, the *GesA* study did not reflect alterations in cord plasma cholesterol or TG levels between groups.

5.4 Maternal obesity was characterized by hyperleptinemia, but absent differences in placental leptin expression and cord leptin levels

As expected, maternal leptin levels were significantly increased in obese subjects of the *GesA* study and they correlated with pregravid BMI and insulin resistance [122,154,163]. In contrast, data of the present study did not confirm differences in cord blood leptin levels obtained from offspring of lean and obese women with and without GDM [122]. Because the delivery of placental leptin into fetal circulation is negligible, cord leptin levels are considered as appropriate markers indicating newborn fat storage [164]. Thus, the present study [152] reinforced recently published data showing the positive relationship of cord blood leptin with birth weight, ponderal index and fat mass [142,165,166]. Of note, cord leptin levels were furthermore identified as a novel important parameter that was associated with abdominal SCA, but not with PPA, in newborns. Particularly, cord leptin levels accounted for the highest variance in neonatal subcutaneous adipose tissue assessed by SFT and abdominal ultrasonography compared to respective body weight and ponderal index. Leptin is mainly expressed and secreted by subcutaneous adipose tissue that represents the largest adipose tissue compartment in newborns [167]. This might therefore explain the failed correlation between cord leptin and PPA at all ages investigated. Alike, Cnop et al. [156] found that leptin levels in adults were stronger related to subcutaneous than to visceral fat amounts.

In this study, the identified positive correlation between cord insulin and leptin was in line with Pratley et al. [168], who recently showed the positive regulation of leptin mRNA expression levels by insulin in adult abdominal subcutaneous adipose tissue. Similar to the data of this thesis, other authors reported that fetal insulin resistance (HOMA-IR-index) was positively related to cord leptin levels [122,169].

In the placenta, leptin is expressed in syncytiotrophoblasts, extravillous trophoblasts and fetal vascular endothelial cells and is released in large parts into maternal circulation, whereas only 5 % of placental leptin is delivered into the fetal circulation [164]. Short and long leptin receptor isoforms are mainly expressed at syncytiotrophoblasts [164]. In this study, mRNA levels of LEP and its receptor did not differ significantly between the groups, but in particular, the leptin expression in placentas of obese GDM women showed a large variance within the study group. In contrast, many other studies found increased leptin gene and protein expressions in placentas of obese and GDM subjects [170,171], whereas others did not confirm this result [172]. Leptin has been shown to favor the trophoblast invasion by regulating various trophoblastic growth factors. Thereby, the adipokine also stimulates the synthesis of extracellular matrix proteins (e.g. fibronectin), promotes the migration of the extravillous cytotrophoblasts into the decidual stroma and increases the trophoblast metalloproteinase secretion (e.g. MMP-2 and MMP-9) [173]. Leptin is as well ascribed various roles in placental proliferative and apoptotic processes by inhibiting caspase-3 activity, turning the cells towards a G2/M phase and up-regulating cyclin D1 expression in first-trimester trophoblast BeWo and JEG-3 cells [174]. Synergistically, leptin also stimulates the amino acid uptake and protein synthesis supporting placental growth [101]. Recently, the pleiotropic hormone has also been reported to be involved in placental angiogenic differentiation, increasing the VEGF secretion in trophoblast cells *in vitro* [173].

5.5 Decreased maternal adiponectin levels in obese pregnant women might have affected the placental physiology and infant adipose tissue growth

In pregnant women, it is well known that HMW and total adiponectin are closely related to glycemia, insulin sensitivity and beta-cell function [175,176]. The present study demonstrated that obese mothers, characterized by hyperinsulinemia and increased HOMA-IR-index, had decreased HMW adiponectin and S_A levels at 3rd trimester [152]. This is in line with recent data from animal and clinical studies reporting insulin as being a negative regulator of adiponectin, preferentially HMW adiponectin oligomer, secretion [177]. Moreover, TNF-α and other pro-inflammatory mediators can reduce the adiponectin transcription in adipocytes [17]. In contrast to maternal circulation, total and HMW adiponectin levels in cord plasma were

explainable by neither maternal obesity nor GDM in the present study which was in concordance with other reports [122,169,175]. Although several studies observed umbilical cord total and HMW adiponectin to be associated with neonatal weight, ponderal index and body fat [175,178–180], a relationship of umbilical cord total and HMW adiponectin with anthropometric or abdominal adipose tissue parameters did not emerge at any age investigated. In conclusion, the regulation of fetal adiponectin might be different from adult metabolism, nevertheless the present data were in accordance with the few studies in which no significant association between insulin sensitivity and adiponectin levels in neonates was found [122,169,179]. Cord plasma adiponectin levels are reported to increase significantly with gestational age [181] and the fetal plasma analysis of the *GesA* samples confirmed three to four times higher adiponectin levels at term compared to maternal circulation [175]. Besides expression in fetal white and brown adipocytes, adiponectin was recently detected in several fetal tissues derived from distinct embryonic germ layers, e.g. certain skeletal muscle fibers, smooth muscles of arterial walls, connective tissues and the epidermis [181].

Conflicting results have been published in reference to the question as to whether adiponectin mRNA expression is detectable in the placenta [151,182–184]. The microarray analysis of this thesis confirmed recent reports of failed placenta adiponectin expression suggesting that adiponectin, in particular derived from maternal circulation, impacts placental physiology and fetal development [117,181,185]. In line with Meller et al. [185] and Kleibslova et al. [151], both abundantly expressed adiponectin receptors (ADIPOR1 and ADIPOR2) were not differentially regulated by pregravid obesity and GDM.

The present study provided a novel inverse relationship between maternal HMW adiponectin levels at 3rd trimester and infant PPA at week-1. This strongly suggests that HMW adiponectin levels are important regulators of maternal metabolism that might impact fetal and newborn PPA growth [152]. These results were supported by findings from animal models indicating that chronic maternal adiponectin infusion down-regulates placental amino acid transporters and decreases offspring growth [186]. In the same vein, Benaitreau et al. [187] described anti-proliferative effects of adiponectin on JEG-3 and BeWo cells in vitro suggesting further mechanism involved in placental and fetal growth. However, placental adiponectin signaling has only been poorly investigated up to the present. In the proposed model by Aye et al. [117], adiponectin signaling in the placenta is supposed to act differentially in contrast to maternal tissues through impairing the insulin signaling and attenuating the amino acid transport, which might modulate fetal growth. Accordingly, adiponectin signals via p38 mitogen-activated protein kinase (MAPK) and PPARα activation. PPARα induces the gene expression of sphingolipid metabolizing enzymes, e.g. the key enzyme SPTLC3, finally stimulating the ceramide biosynthesis [117]. Ceramides attenuate

insulin downstream effects like the mTOR signaling, resulting in the inhibition of placental amino acid transport [117]. Interestingly, the present thesis described for the first time that SPTLC3 gene expression was significantly increased in placentas of obese GDM women in the microarray analysis. This result could only be validated by RT-qPCR for placentas of insulin-treated GDM compared to lean women, but not for placentas of mild dietary-treated diabetic cases. Whether adiponectin is further involved in the immunomodulation at the feto-maternal interface, trophoblast migration/differentiation and angiogenesis, as recently published, warrants further research [173].

5.6 Placental inflammatory pathways were not affected by pregravid obesity with and without GDM

Recently, many studies reported that hyperglycemia, hyperinsulinemia and maternal obesity have been associated with gestational hypertension, preeclampsia and feto-placental endothelial dysregulation [34]. Although within normal ranges, the present pilot study confirmed that obese women had, irrespectively of GDM, significantly higher systolic and diastolic blood pressure at 3rd trimester [20], which might also alter the vascular reactivity of feto-placental and umbilical vessels.

The microarray analysis and respective pathway assessment of the *GesA* samples revealed that genes implicated in angiogenesis were differentially regulated in all pairwise comparisons, respectively. In addition, genes involved in VEGF signaling and angiogenic pathways were also differentially expressed between the obese groups with and without GDM. Radaelli et al. [30] similarly found genes involved in endothelial differentiation that were deregulated between placentas of obese and obese GDM women. Due to the location of INSR in late pregnancy, increased fetal insulin levels might stimulate endothelial cell proliferation and branching angiogenesis in diabetic pregnancies [87]. Leach et al. [65] found that the increased numbers of capillaries was attended by enhanced expression of VEGF-A and its receptor VEGFR-2 in the endothelium and syncytiotrophoblast, whereas increased VEGFR-1 (FLT1) expression is restricted to the trophoblast. In this thesis, a significant increase of FLT1 gene expression was confirmed in placentas of obese diabetic women compared to euglycemic obese subjects by the microarray data and RT-qPCR analysis [30,188]. It has been reported that FLT1 functions as an endogenous VEGF inhibitor. Moreover, FLT1 was also up-regulated in the pathogenesis of placentas of preeclamptic compared to normotensive women [68] that is assumed to be triggered by high uteroplacental vascular resistance resulting in abnormal expression of angiogenic factors. PROK1, the endocrine gland-derived vascular endothelial growth factor, is expressed in syncytiotrophoblast, cytotrophoblasts, fetal endothelial cells and macrophages [85]. The microarray data from the *GesA* study showed a significant decrease in placentas of GDM

compared to lean women, which could not be validated in the RT-qPCR analysis. Interestingly, PROK1 was reported to up-regulate placental expression of IL8 *in vitro* and was already postulated as inflammatory response marker [85]. This report might be in line with significantly decreased IL8 gene expression in the placentas of obese GDM women of the present study.

Notably, several genes (e.g. laeverin (LVRN), pappalysin (PAPPA) 2, LEP, FLT1, pregnancy specific beta-1-glycoprotein (PSG) 1) and signaling pathways (angiogenesis, VEGF, TGF-β) have been found differentially expressed in obese women with and without GDM of the present study and in women with preeclampsia [68]. Nevertheless, it should be emphasized, that women with clinical manifestation of preeclampsia and HELLP (**H**emolysis, **EL**evated liver enzymes, **L**ow **P**latelet count) syndrome were excluded from the *GesA* study; however, vascular perturbations can be implicated in both pathogenesis and may contribute to disproportional fetal development and increased risk for cardiovascular diseases in later life.

It is widely accepted, that maternal obesity and GDM are related to systemic and placental inflammatory processes [28,29,115]. The displayed differential blood cell counts showed no appreciable differences in leukocytes, lymphocytes or granulocytes at 3rd trimester or before delivery. Similarly, Challier et al. [29] revealed no changes in the amount of granulocytes and monocytes before delivery, while Wolf et al. [189] found leukocyte counts positively related to GDM risk. To further evaluate the inflammatory hypothesis in the *GesA* study, IL6 and the liver-derived acute-phase protein CRP, which is mainly stimulated by cytokines such as TNF-α and IL6 [33], were analyzed in maternal plasma at 3rd trimester. Thus, moderate, but significantly higher plasma IL6 levels were confirmed in obese and obese GDM subjects [28,122]. In contrast, elevated circulating maternal CRP levels were confirmed in obese women with and without GDM [20,31,122], but differences did not reach statistical significance in the present study. However, Qiu et al. [33] found that the maternal CRP levels were a predictive risk factor for GDM incidence independently of pregravid BMI. Moreover, Ramsay et al. [20] certified that maternal CRP levels correlate positively with endothelial dysfunctions and linked the obesity-driven inflammation to vascular deregulations.

Interestingly, only a few genes were found to be dysregulated in placentas of obese women with and without GDM that were clearly involved in inflammatory processes. However, the transcriptomic analysis by Radaelli et al. [30] showed that genes of the inflammatory response represented the largest cluster of deregulated genes in diabetic placentas. However, the present RT-qPCR analysis confirmed the microarray profiling results showing that important cytokines (MCP1, TNF-α, IL1β, leptin) had similar expression between groups, whereas IL8 levels were even decreased in placentas of obese GDM women, which was in contrast to recently published data by Roberts et al. [28]. IL8 is mainly expressed by

trophoblast cells and provide a chemotactic and activating factor for neutrophils [190]. However, the gene expression of diverse neutrophil markers assumed no differences in this particular cell population between the groups of the *GesA* study, and Roberts et al. [28] confirmed the similar amounts of placental villous neutrophils in obese and normal weight subjects of their own study. Shimoya et al. [190] showed that the mode of delivery did not affect the amount of placental IL8 secretion; however, placentas exhibiting infections had higher secretion of this chemokine. The IL8 production was found to be increased with proceeding pregnancy [190] and it could be speculated whether a reduced IL8 expression in the obese GDM group was related to a shorter gestational age in these particular placentas. Nevertheless, it should be emphasized that the recently reported increase in cytokine and chemokine expression, indicating inflammatory pathways in the placenta, are mostly retrieved from gene expression data analysis and allows drawing only insufficient conclusions to placental cytokine production/secretion. Differences to other recently published reports might be explained by the strict exclusion criteria and differences in the patient groups of the *GesA* study (e.g. BMI of obese women, comorbidities). However, despite some indications for maternal peripheral inflammation with moderately elevated IL6 and CRP levels in both obese groups, the present microarray analysis and RT-qPCR validation provide no evidence for inflamed term placentas of `healthy´ women apart from obesity and GDM. To estimate the fetal systemic inflammatory conditions and their potential link to adipose tissue growth, data from cord inflammatory markers might be necessary, but were not measured in the present thesis. However, Challier et al. [29] reported that inflammatory markers like CD14, CD68, egf-like module containing, mucin-like, hormone receptor-like (EMR) 1, TNF-α and IL6 were not differentially expressed in PBMC from the umbilical cord blood of neonates born to obese compared to lean women, suggesting that the inflammatory status was restricted to the maternal and placental compartments. The linear regression analysis of the present data provide only minor evidence for maternal plasma IL6 and CRP levels as determinants for offspring adipose tissue growth up to year-1. In contrast, results from animal studies recently indicated that elevated IL6 levels in the fetal and maternal circulation of obese dams caused a fetal malprogramming of the neuropeptide Y neuron development in the arcuate nucleus [191]. The authors assume that the control of body weight and energy homeostasis might be deregulated by the adverse maternal environment and might therefore account for observed higher body weight in the offspring [191]. However, to date, convincing data showing the relationship between maternal and/or fetal inflammatory conditions and human neonatal adipose tissue distribution are still lacking.

5.7 Placental insulin and Wnt signaling were differentially regulated in obese women with GDM

The INSR gene expression, retrieved from the present DNA microarray analysis, was significantly higher in placentas of obese diabetic rather than normoglycemic lean and obese women. In contrast, Colomiere et al. [88] found a decreased expression of INSR in obese insulin-controlled GDM, but not in diet-controlled GDM women, compared to obese mothers without GDM. The authors further reported on defective insulin signaling by decreased PI3Kp85 and GLUT4 mRNA levels in the obese GDM subjects with insulin therapy, which, however, was not confirmed by the data presented in this thesis. Even if the IRS1 gene expression in the obese diabetic was found to be lower than in the lean women of the present study, increased placental pAKT and pGSK3β protein expression may argue for increased insulin signaling in the placentas of obese GDM mothers. Notably, several IGFBP transcripts (IGFBP 3/5/7) were down-regulated in the obese GDM group that was in line with Grissa et al. [89] reporting that IGFBP3 mRNA expression was down-regulated in placentas of diabetic mothers. It can be speculated that differentially expressed IGFBPs influence the bioavailability of IGF1/2 and modulate the placental, and probably the fetal, growth.

In the present study, significantly increased pAKT (Ser 473) levels were selectively determined in placentas of obese women with GDM, whereas the calculated pAKT-total AKT ratio only approached significance. Jansson et al. [100] already found increased placental AKT (Thr 308) phosphorylation in relation to pregnancies with high pregravid maternal pre-pregnancy BMI, but the authors neither considered maternal/fetal glucose nor respective insulin levels for their correlation analysis. Importantly, despite maternal hyperinsulinemia in normoglycemic obese subjects, placental pAKT (and pAKT-total AKT ratio) remained at the level of lean women. Given that applied villous placenta for the analysis derived from fetal tissues, fetal hyperinsulinemia was exclusively observed in the obese GDM group and might therefore be involved in increased AKT phosphorylation. GSK3β is a well-known downstream target of AKT that is inhibited by phosphorylation at Ser 9, and a significant positive correlation between pAKT-total AKT ratio and pGSK3β-GSK3β ratio protein expression was confirmed. Importantly, Wnt ligands can - independently of canonical pathway - also induce AKT phosphorylation at Ser 473 and subsequently GSK3β phosphorylation at Ser 9 [192] or mediate phosphorylation of Akt/mTOR components via non-canonical pathways [193]. Jansson et al. [100] already referred to the positive relationship between placental pAKT (Thr 308) and offspring birth weight and a novel relationship found in this thesis extended this report for placental pAKT (Ser 473)-total AKT ratio and the neonatal PPA adipose tissue marker. Similarly, WNT7A expression emerged as positive determinants for newborn PPA. This strongly proposes that placental insulin and/or Wnt/β-catenin pathways might be

involved in the regulation of factors or mechanisms effecting offspring subcutaneous and preperitoneal adipose tissue growth in early life.

The placental pGSK3β-total GSK3β ratio showed a significant positive correlation with glycogen concentrations confirming their direct link in the signaling pathway. In concordance with Desoye et al. [194], the placental glycogen concentration was significantly increased in diabetic placentas of the *GesA* study. However, most of the key genes involved in glycogen metabolism were not differentially expressed in the DNA microarray data sets. Only GSK3β expression was significantly increased in placentas of obese compared to lean subjects. Moreover, the GBE1 expression was up-regulated in placentas of diabetic compared to normoglycemic obese women which was in line with findings from Radaelli et al. [95]. It has been recently reported, that cytotrophoblast and syncytiotrophoblast cells only contain minor glycogen amounts and that the glycogen synthesis is not induced by hyperglycemia or insulin in these cells [194]. In contrast, glycogen is stored in larger parts in the feto-placental vasculature, including endothelial cells, smooth muscle cells and pericytes. It is speculated by Desoye et al. [194] that GLUT1 and GLUT3 transporters increase glucose uptake from the feto-placental circulation into the endothelial cells where glucose is deposited as glycogen. In contrast to other fetal tissues, the placenta might be the only organ incrementing glycogen content during the diabetic situation [194]. The placenta may buffer excess fetal glucose levels, but in cases of exhausted storage capacity, persisting fetal hyperglycemia - as well documented in the present cord plasma samples of diabetic mothers - might develop [194].

Besides the involvement in glycogen and protein synthesis, GSK3β plays a prominent role in β-catenin signaling. Experiments in extravillous first trimester trophoblast cells showed that different growth factors can mediate anti-apoptotic and migratory effects via phosphorylation of AKT, GSK3β and β-catenin [192,195]. In this thesis, the microarray analysis revealed that the Wnt signaling pathway was over-represented by the set of differentially expressed genes in the placentas of diabetic compared to lean and obese mothers. Therefore, this pathway was chosen for further RT-qPCR validation and protein signaling analysis. WNT7A gene expression was already described in first and third trimester cytotrophoblasts [111] and form together with WNT3A and WNT7B part of the vascular Wnt ligands [196]. DKK3 belongs to the dickkopf homolog family of four members (DKK1-4) and DKKL (DKK-like) 1. They encode secreted proteins that typically modulate Wnt/β-catenin signaling. Despite the fact that DKK1 is described as main Wnt antagonist via direct interaction with Wnt co-receptors LRP5/6, evidence was found for a similar modulating role for DKK3 [197]. Recently, a study showed that DKK3 could act as negative regulator of WNT7A in PC12 cells [198]. In the present study, both, increased WNT7A and lower DKK3 expression in the diabetic placentas might be implicated in the activation of canonical Wnt signaling. It was found that placental CDH11

showed gene expression dynamics throughout pregnancy with a continual increase from early to mid-pregnancy and a subsequent significant decrease in gene expression at term [199]. The results from Uusküla et al. [199], which indicated that CDH11 gene expression was up-regulated in diabetic term placentas compared to the euglycemic control group, were not confirmed by the data of this thesis. However, one has to consider that compared to the present study design, women with GDM were not allocated by BMI in the study of Uusküla et al. [199]. Getsios et al. [200] reported an important role for CDH11 in promoting the terminal differentiation and fusion of mononucleate cytotrophoblasts. Thus, the decreased CDH11 expression in placentas of diabetic women of the *GesA* study might be in line with recently reported abnormalities in villous maturation of placentas of GDM women [201]. Moreover, CDH11 was described as pro-apoptotic tumor suppressor, suggesting a role for extra-nuclear β-catenin sequestration in intercellular junctions leading to decreased β-catenin-mediated transcriptional activity in common carcinomas [202]. Therefore, the decreased CDH11 expression might be linked to the increased accumulation of nuclear β-catenin in the placentas of obese GDM women.

Apart from the described potential effect of β-catenin location and Wnt signaling on trophoblast proliferation and differentiation, one can speculate on the perturbations of β-catenin location and Wnt signaling in endothelial cells. It can be assumed from increased nuclear β-catenin levels in the obese GDM group that the impaired involvement in adherens junctions enlarges the pool of free β-catenin, which in turn, increases the downstream β-catenin signaling. In this context, Leach et al. [203] already found in placentas of women with type 1 diabetes that insulin affected the feto-placental vascular function by impairing the expression of VE-cadherin und β-catenin at intercellular junctions. Thus, these authors suggested that the loss of VE-cadherin and β-catenin expression from adherens junctions induced the VEGF-mediated proliferative signal response of endothelial cells. This might finally explain the lack in endothelial barrier integrity and contribute to vascular proliferation and increased capillary length recently reported in placentas of women with GDM or type 1 diabetes [75,203]. The findings of Leach et al. might be in concordance with the present pathway analysis indicating that placental angiogenic and integrin pathways were differentially regulated in obese women with and without GDM.

In the *GesA* study, the PTH1R transcript was firstly described in the placenta and was found to be down-regulated in obese GDM women. The PTH1R was already shown to be expressed in bone and vascular smooth muscle (VMSC) [204]. *In vitro,* PTH1R was indicated to inhibit the WNT7A-induced collagen expression in VSMCs. Moreover, PTH1R activation was shown to decrease vascular oxidative stress and β-catenin protein accumulation and nuclear signaling [204]. According to decreased PTH1R expression in the diabetic placental tissues of the *GesA* study, a favoring role in WNT7A-dependent signaling pathways and β-

catenin signaling in these placentas can be suggested. However, further research has to be undergone to determine the functional relationship of PTH1R and Wnt signaling in the placenta, particularly in the placental vasculature. Furthermore, histological and immunohistochemical analyses of the placental vasculature are necessary to evaluate whether there are changes in vascular morphology between the study groups.

Despite the well-characterized Wnt signaling components in the placenta, information is still lacking concerning Wnt/β-catenin-dependent target genes in this tissue. Thus, typical transcriptional target genes, mostly identified in colon carcinoma, e.g. Axin and MYC, were not differentially regulated between the groups. Matsuura et al. [114] identified GCM1 and ERVWE1 as Wnt/β-catenin targets in the choriocarcinoma BeWo cell line that are implicated in cell fusion processes, but a differential regulation was not confirmed in the present microarray analysis.

5.8 Comparison of the present placental DNA microarray analysis with recently published transcriptomic data

In comparison to the microarray analysis by Enquobahrie et al. [188] and Radaelli et al. [30,95], the assessment perfomed in this thesis identified overall lower fold changes after particular group comparisons, and FDR values only barely reached significant levels; therefore a less stringent threshold for significant levels (raw p-value < 0.05) was used. Reasons for different outcomes might be based on selection of study cases and their individual differences of expression pattern. Thus, compared to the study population of Enquobahrie et al. [188], the *GesA* study used more stringent exclusion criteria (e.g. preeclampsia and chronic hypertension, different ethnicities) to minimize bias in gene regulation due to other pregnancy complications. Further reasons for weaker regulations compared to other studies may be implicated in the mode of delivery, but given that each group had a similar ratio of spontaneous deliveries to C-sections, other published placental microarray analyses were only conducted in placentas obtained from C-sections [30,95]. However, previous studies with heterogeneous mode of deliveries confirmed no influence of labor on global gene expression results [188]. Moreover, the application of different microarray chips, platforms and protocols should not be underestimated regarding minor overlap between different published microarray data. However, obtained microarray and RT-qPCR data from placental RNA samples of the *GesA* study demonstrated a significant and convincing correlation between the two techniques, fortifying the accurate performance of DNA microarrays. Notably, different ratios of up- and down-regulated genes were identified in the respective pairwise comparisons of this thesis. Thus, nearly equal counts of up- and down-regulated genes were found in placentas of obese and obese GDM women each in the comparison with the lean counterparts. In contrast, approximately two-thirds of genes were

down-regulated in obese GDM compared to normoglycemic obese subjects. Zhao et al. [205] also identified a similar ratio of up- to down-regulated genes in placentas of the GDM group in comparison to the group without GDM even if the authors examined only a very low number of placenta samples in each group.

5.9 Strengths and limitations of the present study

An important strength of the present pilot study was the intensive metabolic characterization of the participants, while typical metabolic perturbations were confirmed and emphasized between the distinct groups. Another essential aspect was the complementary assessment of offspring adipose tissue by SFT and ultrasonography. Body weight and BMI only insufficiently explain the variance in adipose tissue amounts, but are often used to categorize overweight and obesity. Nevertheless, the discrimination between subcutaneous and preperitoneal/visceral fat is important for evaluating metabolic and cardiovascular risk factors. Beneficially, various biosamples were collected from maternal and fetal circulation (3rd trimester, prior to delivery, cord blood (PBMC, plasma, erythrocytes)), from feto-placental interface (placenta, cord), and from postnatal period (maternal blood samples at week-6, breast milk at week-6, anthropometrics, SFT, US), to obtain a comprehensive description of a critical window during fetal development. The collected data are also important for the correlation analysis between maternal/fetal biomarkers and offspring adipose tissue growth. Strength of the study was further the high number of placental transcriptomic analyses performed on the majority of participants, followed by a high RT-qPCR validation rate in all samples available. However, the microarray analysis represented the global gene expression changes observed in placental villous tissues, thus, it can only be speculated, which cell types within the placenta were responsible for the different expression of the particular transcripts.

A limitation might be also the missing consideration of lean GDM cases, but due to the strong interest in pregravid obesity, the aim was to evaluate the additional effect of GDM on differential placental gene expression and offspring adipose tissue growth. Further limitations comprise of the recruitment at registration date (early 3rd trimester) in the obstetric clinic, so that participants could not be selected according to standardized delivery mode. Therefore, the potential impact of delivery mode and/or medications could not be excluded. Due to study protocol, it was not possible to enroll most of the participants prior to 32th week of gestation, thus, the feasibility to analyze early biomarkers, indicating the onset of GDM, was not given. To investigate the potential long-term impact of fetal programming, it might be necessary to extent the follow-up period to re-investigate offspring adipose tissue growth in later childhood/adolescence. This pilot study was not powered for analyzing sex differences in the

placenta, cord blood or anthropometric/adipose tissue growth parameters. Nevertheless, sex-adjusted analysis was carried out to minimize confounder effects.

5.10 Conclusion

In conclusion, this PhD thesis showed that maternal pregravid obesity combined with GDM, led to offspring neonatal hyperinsulinemia and increased offspring fat mass until week-6, whereas pregravid obesity did not. More importantly, adiposity risk in the obese GDM group attenuated during the first year of life. Furthermore, maternal C-peptide and HMW adiponectin levels were identified as potential predictors for distinct PPA growth in early infancy, which may be indicative for adiposity risk at later stages. Recently, increased PPA was determined as cardiovascular risk factor in obese children and obese/non-obese adults. Therefore, increased PPA at birth might be not only indicative of later obesity risk, but also for cardiovascular risk in adulthood.

Consequently, it is suggested that dietary and lifestyle intervention studies during pregnancy are evaluated by means of analyzing maternal and offspring metabolic markers in combination with ultrasonographic data of offspring abdominal adipose tissues at different stages in order to identify reliable predictors for adiposity risk. This should contribute to a better understanding of how treatment of pregravid obesity and GDM in pregnant women can be improved to reduce offspring adiposity risk.

The present microarray analysis provided the placental gene expression profiles and diverse signaling pathways that are altered by maternal pregravid obesity with and without GDM. The most striking alterations in placental gene expression were found in obese GDM women compared to euglycemic lean and obese women. This result is in concordance with differential fetal outcomes and early adipose tissue growth observed in GDM offspring. A very important aspect of the study indicates that the placentas of obese women with and without GDM are not necessarily inflamed and the selection of relatively `healthy´ obese women without severe complications during pregnancy might favor this result. However, the activation of insulin and Wnt signaling pathways in the placenta were exclusively found in diabetic subjects and might result from fetal hyperinsulinemia. The shifted location of β-catenin from adherens junctions to the nucleus is suggested and might favor the trophoblast and/or endothelial proliferation in diabetic placentas, which is in line with proliferative and angiogenic pathways that were found enriched by the set of differentially expressed transcripts in the microarray analysis. There are grounds for speculation that deregulated insulin and Wnt signaling pathways in the placenta indicate analogue signaling pathways in fetal adipocytes that can influence infant adipose tissue growth. Another effort needs to be targeted on understanding differentially regulated placental gene functions in obese pregnant women with and without GDM and their impact on fetal adaption.

5.11 Further perspectives

In this PhD thesis, placental tissue samples from fetal, intervillous and maternal compartments of the four quadrants were also collected for future histological investigations **(see chapter 3.4)**. The histological analysis might be very suitable to detect the localization and cell type of protein expressions with immunohistochemical techniques or to examine gene expressions according to the *in situ*-hybridization technique. In this context, the morphological analysis can be important to confirm alterations in vessel formation and angiogenic processes that might be related to observed deregulations in Wnt signaling. Using the choriocarcinoma cells lines BeWo and JEG-3, one can assess whether the changes in the Wnt signaling pathway, as described in this thesis, are caused by changes in glucose and insulin concentrations.

For future studies, placental miRNAs, isolated from study participants during this thesis, will be helpful regarding the molecular characterization of the mRNA-miRNA network in the placenta. Moreover, the isolation of miRNA from maternal and umbilical cord plasma will be necessary to determine circulating miRNA biomarkers, which might be associated with offspring adipose tissue.

6 References

1. WHO - World Health Organization: *Obesity and overweight: http://www.who.int/mediacentre/factsheets/fs311/en/*; 2013.
2. Flegal KM: Prevalence of Obesity and Trends in the Distribution of Body Mass Index Among US Adults, 1999-2010. *JAMA* 2012, 307:491-497.
3. Kurth B: Erste Ergebnisse aus der „Studie zur Gesundheit Erwachsener in Deutschland“ (DEGS). *Bundesgesundheitsbl* 2012, 55:980-990.
4. Fisher SC, Kim SY, Sharma AJ, Rochat R, Morrow B: Is obesity still increasing among pregnant women? Prepregnancy obesity trends in 20 states, 2003-2009. *Prev Med* 2013, 56:372-378.
5. Max-Rubner-Institut Bundesforschungsinstitut für Ernährungs und Lebens-mittel: *Nationale Verzehrsstudie II - Ergebnisbericht, Teil 1.*; 2008.
6. Ogden CL, Carroll MD, Kit BK, Flegal KM: Prevalence of childhood and adult obesity in the United States, 2011-2012. *JAMA* 2014, 311:806-814.
7. Wenig CM: The impact of BMI on direct costs in Children and Adolescents: empirical findings for the German Healthcare System based on the KiGGS-study. *Eur J Health Econ* 2012, 13:39-50.
8. Schaefer-Graf UM, Pawliczak J, Passow D, Hartmann R, Rossi R, Buhrer C, Harder T, Plagemann A, Vetter K, Kordonouri O: Birth weight and parental BMI predict overweight in children from mothers with gestational diabetes. *Diabetes Care* 2005, 28:1745-1750.
9. Catalano PM, McIntyre HD, Cruickshank JK, McCance DR, Dyer AR, Metzger BE, Lowe LP, Trimble ER, Coustan DR, Hadden DR, Persson B, Hod M, Oats JJN: The Hyperglycemia and Adverse Pregnancy Outcome Study: Associations of GDM and obesity with pregnancy outcomes. *Diabetes Care* 2012, 35:780-786.
10. Boerschmann H, Pfluger M, Henneberger L, Ziegler A, Hummel S: Prevalence and Predictors of Overweight and Insulin Resistance in Offspring of Mothers With Gestational Diabetes Mellitus. *Diabetes Care* 2010, 33:1845-1849.
11. American Diabetes Association.: Diagnosis and classification of diabetes mellitus. *Diabetes Care* 2013, 36 Suppl 1:S67-74.
12. Cnop M, Welsh N, Jonas J, Jorns A, Lenzen S, Eizirik DL: Mechanisms of pancreatic beta-cell death in type 1 and type 2 diabetes: many differences, few similarities. *Diabetes* 2005, 54 Suppl 2:S97-107.
13. Herder C, Roden M: Genetics of type 2 diabetes: pathophysiologic and clinical relevance. *Eur J Clin Invest* 2011, 41:679-692.
14. Kleinwechter H, Schäfer-Graf U, Bührer C, Hoesli I, Kainer F, Kautzky-Willer A, Pawlowski B, Schunck K, Somville T, Sorger M: *Evidenzbasierte Leitlinie zu Diagnostik, Therapie u. Nachsorge der Deutschen Diabetes-Gesellschaft (DDG) und der Deutschen Gesellschaft für Gynäkologie und Geburtshilfe (DGGG)*; 2011.
15. Butte NF: Carbohydrate and lipid metabolism in pregnancy: normal compared with gestational diabetes mellitus. *Am J Clin Nutr* 2000, 71:1256S-1261S.
16. Bonet B, Viana M, Sánchez-Vera I: Intermediary metabolism in pregnancies complicated by destational diabetes. In *Textbook of Diabetes and Pregnacy, Second Edition*:35-40.
17. Barbour LA, McCurdy CE, Hernandez TL, Kirwan JP, Catalano PM, Friedman JE: Cellular mechanisms for insulin resistance in normal pregnancy and gestational diabetes. *Diabetes Care* 2007, 30 Suppl 2:S112-119.
18. Kirwan JP, Hauguel-de Mouzon S, Lepercq J, Challier J, Huston-Presley L, Friedman JE, Kalhan SC, Catalano PM: TNF-alpha is a predictor of insulin resistance in human pregnancy. *Diabetes* 2002, 51:2207-2213.
19. Herrera E, Ortega-Senovilla H: Disturbances in lipid metabolism in diabetic pregnancy – Are these the cause of the problem? *Best Practice & Research Clinical Endocrinology & Metabolism* 2010, 24:515-525.

20. Ramsay JE, Ferrell WR, Crawford L, Wallace AM, Greer IA, Sattar N: Maternal Obesity Is Associated with Dysregulation of Metabolic, Vascular, and Inflammatory Pathways. *The Journal of Clinical Endocrinology & Metabolism* 2002, 87:4231-4237.
21. Vahratian A, Misra VK, Trudeau S, Misra DP: Prepregnancy Body Mass Index and Gestational Age-Dependent Changes in Lipid Levels During Pregnancy. *Obstet Gynecol* 2010, 116:107-113.
22. Qiu C, Rudra C, Austin M.A., Williams MA: Association of Gestational Diabetes Mellitus and Low-density Lipoprotein (LDL) Particle Size. *Physiol. Res.* 2007, 56:571-578.
23. Catalano PM, Hauguel-de Mouzon S: Is it time to revisit the Pedersen hypothesis in the face of the obesity epidemic? *American Journal of Obstetrics and Gynecology* 2011, 204:479-487.
24. Di Cianni G, Miccoli R, Volpe L, Lencioni C, Ghio A, Giovannitti MG, Cuccuru I, Pellegrini G, Chatzianagnostou K, Boldrini A, Del Prato S: Maternal triglyceride levels and newborn weight in pregnant women with normal glucose tolerance. *Diabet Med* 2005, 22:21-25.
25. Schaefer-Graf UM, Graf K, Kulbacka I, Kjos SL, Dudenhausen J, Vetter K, Herrera E: Maternal Lipids as Strong Determinants of Fetal Environment and Growth in Pregnancies With Gestational Diabetes Mellitus. *Diabetes Care* 2008, 31:1858-1863.
26. Dube E, Ethier-Chiasson M, Lafond J: Modulation of Cholesterol Transport by Insulin-Treated Gestational Diabetes Mellitus in Human Full-Term Placenta. *Biology of Reproduction* 2013, 88:16.
27. Dube E, Gravel A, Martin C, Desparois G, Moussa I, Ethier-Chiasson M, Forest J, Giguere Y, Masse A, Lafond J: Modulation of Fatty Acid Transport and Metabolism by Maternal Obesity in the Human Full-Term Placenta. *Biology of Reproduction* 2012, 87:14.
28. Roberts K, Riley S, Reynolds R, Barr S, Evans M, Statham A, Hor K, Jabbour H, Norman J, Denison F: Placental structure and inflammation in pregnancies associated with obesity. *Placenta* 2011, 32:247-254.
29. Challier J, Basu S, Bintein T, Minium J, Hotmire K, Catalano P, Hauguel-de Mouzon S: Obesity in Pregnancy Stimulates Macrophage Accumulation and Inflammation in the Placenta. *Placenta* 2008, 29:274-281.
30. Radaelli T, Varastehpour A, Catalano P, Hauguel-de Mouzon S: Gestational Diabetes Induces Placental Genes for Chronic Stress and Inflammatory Pathways. *Diabetes* 2003, 52:2951-2958.
31. Madan JC, Davis JM, Craig WY, Collins M, Allan W, Quinn R, Dammann O: Maternal obesity and markers of inflammation in pregnancy. *Cytokine* 2009, 47:61-64.
32. Kuzmicki M, Telejko B, Zonenberg A, Szamatowicz J, Kretowski A, Nikolajuk A, Laudanski P, Gorska M: Circulating Pro- and Anti-inflammatory Cytokines in Polish Women with Gestational Diabetes. *Horm Metab Res* 2008, 40:556-560.
33. Qiu C, Sorensen TK, Luthy DA, Williams MA: A prospective study of maternal serum C-reactive protein (CRP) concentrations and risk of gestational diabetes mellitus. *Paediatr Perinat Epidemiol* 2004, 18:377-384.
34. Carpenter MW: Gestational Diabetes, Pregnancy Hypertension, and Late Vascular Disease. *Diabetes Care* 2007, 30:S246–250.
35. Stewart FM, Freeman DJ, Ramsay JE, Greer IA, Caslake M, Ferrell WR: Longitudinal Assessment of Maternal Endothelial Function and Markers of Inflammation and Placental Function throughout Pregnancy in Lean and Obese Mothers. *Journal of Clinical Endocrinology & Metabolism* 2006, 92:969-975.
36. Lowe LP, Metzger BE, Lowe WL, Dyer AR, McDade TW, McIntyre HD: Inflammatory Mediators and Glucose in Pregnancy: Results from a Subset of the Hyperglycemia and Adverse Pregnancy Outcome (HAPO) Study. *Journal of Clinical Endocrinology & Metabolism* 2010, 95:5427-5434.
37. Mordwinkin NM, Ouzounian JG, Yedigarova L, Montoro MN, Louie SG, Rodgers KE: Alteration of endothelial function markers in women with gestational diabetes and their fetuses. *J Matern Fetal Neonatal Med* 2013, 26:507-512.

38. Catalano PM: Obesity, insulin resistance, and pregnancy outcome. *Reproduction* 2010, 140:365-371.
39. Torloni MR, Betrán AP, Horta BL, Nakamura MU, Atallah AN, Moron AF, Valente O: Prepregnancy BMI and the risk of gestational diabetes: a systematic review of the literature with meta-analysis. *Obesity Reviews* 2009, 10:194-203.
40. Coustan DR, Lowe LP, Metzger BE, Dyer AR: The Hyperglycemia and Adverse Pregnancy Outcome (HAPO) study: paving the way for new diagnostic criteria for gestational diabetes mellitus. *American Journal of Obstetrics and Gynecology* 2010, 202:654.e1–6.
41. Landon MB, Spong CY, Thom E, Carpenter MW, Ramin SM, Casey B, Wapner RJ, Varner MW, Rouse DJ, Thorp JM, Sciscione A, Catalano P, Harper M, Saade G, Lain KY, Sorokin Y, Peaceman AM, Tolosa JE, Anderson GB: A Multicenter, Randomized Trial of Treatment for Mild Gestational Diabetes. *N Engl J Med* 2009, 361:1339-1348.
42. Denison FC, Roberts KA, Barr SM, Norman JE: Obesity, pregnancy, inflammation, and vascular function. *Reproduction* 2010, 140:373-385.
43. Nold JL, Georgieff MK: Infants of diabetic mothers. *Pediatric Clinics of North America* 2004, 51:619-637.
44. Heslehurst N, Simpson H, Ells LJ, Rankin J, Wilkinson J, Lang R, Brown TJ, Summerbell CD: The impact of maternal BMI status on pregnancy outcomes with immediate short-term obstetric resource implications: a meta-analysis. *Obesity Reviews* 2008, 9:635-683.
45. Poobalan AS, Aucott LS, Gurung T, Smith WCS, Bhattacharya S: Obesity as an independent risk factor for elective and emergency caesarean delivery in nulliparous women - systematic review and meta-analysis of cohort studies. *Obesity Reviews* 2009, 10:28-35.
46. Briese V, Voigt M, Wisser J, Borchardt U, Straube S: Risks of pregnancy and birth in obese primiparous women: an analysis of German perinatal statistics. *Arch Gynecol Obstet* 2011, 283:249-253.
47. Ziegler A, Wallner M, Kaiser I, Rossbauer M, Harsunen MH, Lachmann L, Maier J, Winkler C, Hummel S: Long-Term Protective Effect of Lactation on the Development of Type 2 Diabetes in Women With Recent Gestational Diabetes Mellitus. *Diabetes* 2012, 61:3167-3171.
48. Fraser A, Tilling K, Macdonald-Wallis C, Hughes R, Sattar N, Nelson SM, Lawlor DA: Associations of gestational weight gain with maternal body mass index, waist circumference, and blood pressure measured 16 y after pregnancy: the Avon Longitudinal Study of Parents and Children (ALSPAC). *American Journal of Clinical Nutrition* 2011, 93:1285-1292.
49. Mamun AA, Kinarivala M, O'Callaghan MJ, Williams GM, Najman JM, Callaway LK: Associations of excess weight gain during pregnancy with long-term maternal overweight and obesity: evidence from 21 y postpartum follow-up. *American Journal of Clinical Nutrition* 2010, 91:1336-1341.
50. Catalano PM, Farrell K, Thomas A, Huston-Presley L, Mencin P, Mouzon SH de, Amini SB: Perinatal risk factors for childhood obesity and metabolic dysregulation. *American Journal of Clinical Nutrition* 2009, 90:1303-1313.
51. Gillman MW, Rifas-Shiman S, Berkey CS, Field AE, Colditz GA: Maternal Gestational Diabetes, Birth Weight, and Adolescent Obesity. *PEDIATRICS* 2003, 111:e221–226.
52. Clausen TD, Mathiesen ER, Hansen T, Pedersen O, Jensen DM, Lauenborg J, Damm P: High Prevalence of Type 2 Diabetes and Pre-Diabetes in Adult Offspring of Women With Gestational Diabetes Mellitus or Type 1 Diabetes: The role of intrauterine hyperglycemia. *Diabetes Care* 2007, 31:340-346.
53. Clausen TD, Mathiesen ER, Hansen T, Pedersen O, Jensen DM, Lauenborg J, Schmidt L, Damm P: Overweight and the Metabolic Syndrome in Adult Offspring of Women with Diet-Treated Gestational Diabetes Mellitus or Type 1 Diabetes. *Journal of Clinical Endocrinology & Metabolism* 2009, 94:2464-2470.
54. Hauner H, Brunner S, Amann-Gassner U: The role of dietary fatty acids for early human adipose tissue growth. *American Journal of Clinical Nutrition* 2013, 98:549S–555S.

55. Poissonnet C, Burdi A, Bookstein F: Growth and development of human adipose tissue during early gestation. *Early Human Development* 1983, 8:1-11.
56. Poissonnet CM, Burdi AR, Garn SM: The chronology of adipose tissue appearance and distribution in the human fetus. *Early Hum Dev* 1984, 10:1-11.
57. Catalano PM, Thomas A, Huston-Presley L, Amini SB: Increased fetal adiposity: A very sensitive marker of abnormal in utero development. *American Journal of Obstetrics and Gynecology* 2003, 189:1698-1704.
58. Hauner H, Much D, Vollhardt C, Brunner S, Schmid D, Sedlmeier E, Heimberg E, Schuster T, Zimmermann A, Schneider KM, Bader BL, Amann-Gassner U: Effect of reducing the n-6:n-3 long-chain PUFA ratio during pregnancy and lactation on infant adipose tissue growth within the first year of life: an open-label randomized controlled trial. *American Journal of Clinical Nutrition* 2012, 95:383-394.
59. Hauner H: Secretory factors from human adipose tissue and their functional role. *Proc Nutr Soc* 2005, 64:163-169.
60. Hamdy O, Porramatikul S, Al-Ozairi E: Metabolic obesity: the paradox between visceral and subcutaneous fat. *Curr Diabetes Rev* 2006, 2:367-373.
61. Plagemann A: Maternal diabetes and perinatal programming. *Early Human Development* 2011, 87:743-747.
62. Hales CN, Barker DJ: Type 2 (non-insulin-dependent) diabetes mellitus: the thrifty phenotype hypothesis. *Diabetologia* 1992, 35:595-601.
63. Dabelea D, Hanson RL, Lindsay RS, Pettitt DJ, Imperatore G, Gabir MM, Roumain J, Bennett PH, Knowler WC: Intrauterine exposure to diabetes conveys risks for type 2 diabetes and obesity: a study of discordant sibships. *Diabetes* 2000, 49:2208-2211.
64. Pedersen J (Ed): *The pregnant diabetic and her newborn:problems and management.* Baltimore: The Williams and Wilkins Company; 1967.
65. Leach L: Placental Vascular Dysfunction in Diabetic Pregnancies: Intimations of Fetal Cardiovascular Disease? *Microcirculation* 2011, 18:263-269.
66. Gude NM, Roberts CT, Kalionis B, King RG: Growth and function of the normal human placenta. *Thrombosis Research* 2004, 114:397-407.
67. Huppertz B: The anatomy of the normal placenta. *Journal of Clinical Pathology* 2008, 61:1296-1302.
68. Sitras V, Paulssen R, Grønaas H, Leirvik J, Hanssen T, Vårtun Å, Acharya G: Differential Placental Gene Expression in Severe Preeclampsia. *Placenta* 2009, 30:424-433.
69. Moore KL: *Developing Human: Clinically Oriented Embryology*: Elsevier - Health Sciences Division; 2011.
70. Enders, Blankenship: Comparative placental structure. *Adv Drug Deliv Rev* 1999, 38:3-15.
71. Jansson T, Powell TL: IFPA 2005 Award in Placentology Lecture. Human placental transport in altered fetal growth: does the placenta function as a nutrient sensor? -- a review. *Placenta* 2006, 27:S91-7.
72. Lewis R, K. Cleal J, Godfrey K (Eds): *Reproductive and developmental toxicology: The placental role in fetal programming.* Amsterdam, Boston: Elsevier; 2011.
73. Kitano T, Iizasa H, Hwang I, Hirose Y, Morita T, Maeda T, Nakashima E: Conditionally immortalized syncytiotrophoblast cell lines as new tools for study of the blood-placenta barrier. *Biol Pharm Bull* 2004, 27:753-759.
74. Myatt L: Placental Adaptive Responses and Fetal Programming. *The Journal of Physiology* 2006, 572:25-30.
75. Gauster M, Desoye G, Tötsch M, Hiden U: The Placenta and Gestational Diabetes Mellitus. *Curr Diab Rep* 2012, 12:16-23.
76. Desoye G, Shafrir E, Hauguel-de Mouzon S: The placenta in diabetic pregnancy:Placental transfer of nutrients. In *Textbook of Diabetes and Pregnacy, Second Edition*:47-56.
77. Hauguel-de Mouzon S, Guerremillo M: The Placenta Cytokine Network and Inflammatory Signals. *Placenta* 2006, 27:794-798.

78. Maccani MA, Marsit CJ: Epigenetics in the Placenta. *American Journal of Reproductive Immunology* 2009, 62:78-89.
79. Zhao C, Dong J, Jiang T, Shi Z, Yu B, Zhu Y, Chen D, Xu J, Huo R, Dai J, Xia Y, Pan S, Hu Z, Sha J, Zhang C: Early Second-Trimester Serum MiRNA Profiling Predicts Gestational Diabetes Mellitus. *PLoS ONE* 2011, 6:e23925.
80. Novakovic B, Saffery R: The ever growing complexity of placental epigenetics - role in adverse pregnancy outcomes and fetal programming. *Placenta* 2012, 33:959-970.
81. Nomura Y, Lambertini L, Rialdi A, Lee M, Mystal EY, Grabie M, Manaster I, Huynh N, Finik J, Davey M, Davey K, Ly J, Stone J, Loudon H, Eglinton G, Hurd Y, Newcorn JH, Chen J: Global Methylation in the Placenta and Umbilical Cord Blood From Pregnancies With Maternal Gestational Diabetes, Preeclampsia, and Obesity. *Reprod Sci* 2013, 21:131-137.
82. Wallace J, Horgan G, Bhattacharya S: Placental weight and efficiency in relation to maternal body mass index and the risk of pregnancy complications in women delivering singleton babies. *Placenta* 2012, 33:611-618.
83. Roberts DJ, Raspollini Maria R.: Histopathology of placenta. In *Textbook of Diabetes and Pregnacy, Second Edition*:41-46.
84. Madazl&inodot, R&inodot, za, Tuten A, Calay Z, Uzun H, Uludag S, Ocak V: The Incidence of Placental Abnormalities, Maternal and Cord Plasma Malondialdehyde and Vascular Endothelial Growth Factor Levels in Women with Gestational Diabetes Mellitus and Nondiabetic Controls. *Gynecol Obstet Invest* 2008, 65:227-232.
85. Denison FC, Battersby S, King AE, Szuber M, Jabbour HN: Prokineticin-1: A Novel Mediator of the Inflammatory Response in Third-Trimester Human Placenta. *Endocrinology* 2008, 149:3470-3477.
86. Desoye G, Hauguel-de Mouzon S: The Human Placenta in Gestational Diabetes Mellitus: The insulin and cytokine network. *Diabetes Care* 2007, 30:S120–126.
87. Hiden U, Glitzner E, Hartmann M, Desoye G: Insulin and the IGF system in the human placenta of normal and diabetic pregnancies. *Journal of Anatomy* 2009, 215:60-68.
88. Colomiere M, Permezel M, Riley C, Desoye G, Lappas M: Defective insulin signaling in placenta from pregnancies complicated by gestational diabetes mellitus. *European Journal of Endocrinology* 2008, 160:567-578.
89. Grissa O, Yessoufou A, Mrisak I, Hichami A, Amoussou-Guenou D, Grissa A, Djrolo F, Moutairou K, Miled A, Khairi H, Zaouali M, Bougmiza I, Zbidi A, Tabka Z, Khan NA: Growth factor concentrations and their placental mRNA expression are modulated in gestational diabetes mellitus. Possible interactions with macrosomia. *BMC Pregnancy Childbirth* 2010, 10:7.
90. Larqué E, Ruiz-Palacios M, Koletzko B: Placental regulation of fetal nutrient supply. *Current Opinion in Clinical Nutrition and Metabolic Care* 2013, 16:292-297.
91. Illsley NP: Glucose transporters in the human placenta. *Placenta* 2000, 21:14-22.
92. Brown K, Heller DS, Zamudio S, Illsley NP: Glucose transporter 3 (GLUT3) protein expression in human placenta across gestation. *Placenta* 2011, 32:1041-1049.
93. Jones H, Powell T, Jansson T: Regulation of Placental Nutrient Transport – A Review. *Placenta* 2007, 28:763-774.
94. Baardman ME, Erwich JJH, Berger RM, Hofstra RM, Kerstjens-Frederikse WS, Lütjohann D, Plösch T: The origin of fetal sterols in second-trimester amniotic fluid: endogenous synthesis or maternal-fetal transport? *American Journal of Obstetrics and Gynecology* 2012, 207:202.e19–25.
95. Radaelli T, Lepercq J, Varastehpour A, Basu S, Catalano PM, Hauguel-de Mouzon S: Differential regulation of genes for fetoplacental lipid pathways in pregnancy with gestational and type 1 diabetes mellitus. *American Journal of Obstetrics and Gynecology* 2009, 201:209.e1–10.
96. Gauster M, Hiden U, van Poppel M, Frank S, Wadsack C, Hauguel-de Mouzon S, Desoye G: Dysregulation of Placental Endothelial Lipase in Obese Women With Gestational Diabetes Mellitus. *Diabetes* 2011, 60:2457-2464.

97. Scifres CM, Chen B, Nelson DM, Sadovsky Y: Fatty Acid Binding Protein 4 Regulates Intracellular Lipid Accumulation in Human Trophoblasts. *Journal of Clinical Endocrinology & Metabolism* 2011, 96:E1083–1091.
98. Desforges M, Sibley CP: Placental nutrient supply and fetal growth. *Int. J. Dev. Biol.* 2010, 54:377-390.
99. Jansson T, Ekstrand Y, Bjorn C, Wennergren M, Powell TL: Alterations in the Activity of Placental Amino Acid Transporters in Pregnancies Complicated by Diabetes. *Diabetes* 2002, 51:2214-2219.
100. Jansson N, Rosario FJ, Gaccioli F, Lager S, Jones HN, Roos S, Jansson T, Powell TL: Activation of Placental mTOR Signaling and Amino Acid Transporters in Obese Women Giving Birth to Large Babies. *Journal of Clinical Endocrinology & Metabolism* 2013, 98:105-113.
101. Perez-Perez A, Maymo JL, Gambino YP, Guadix P, Duenas JL, Varone CL, Sanchez-Margalet V: Activated translation signaling in placenta from pregnant women with gestational diabetes mellitus: possible role of leptin. *Horm Metab Res* 2013, 45:436-442.
102. Westrate J, Deurenberg P: Body composition in children: proposal for a method for calculating body fat percentage from total body desity or skinfold-thickness measurements. *American Journal of Clinical Nutrition* 1989:1104-1115.
103. Haffner SM, Stern MP, Hazuda HP, Pugh J, Patterson JK: Do upper-body and centralized adiposity measure different aspects of regional body-fat distribution? Relationship to Non-Insulin-Dependent Diabetes Mellitus, Lipids and Lipoproteins. *Diabetes* 1987, 36:43-51.
104. Weststrate JA, Deurenberg P, van Tinteren H: Indices of body fat distribution and adiposity in Dutch children from birth to 18 years of age. *Int J Obes* 1989, 13:465-477.
105. Holzhauer S, Zwijsen RML, Jaddoe VWV, Boehm G, Moll HA, Mulder PG, Kleyburg-Linkers VA, Hofman A, Witteman JCM: Sonographic assessment of abdominal fat distribution in infancy. *Eur J Epidemiol* 2009, 24:521-529.
106. Bland JM, Altman DG: Statistical methods for assessing agreement between two methods of clinical measurement. *Lancet* 1986, 1:307-310.
107. Bankar SB, Bule MV, Singhal RS, Ananthanarayan L: Glucose oxidase--an overview. *Biotechnol Adv* 2009, 27:489-501.
108. Rainer J, Sanchez-Cabo F, Stocker G, Sturn A, Trajanoski Z: CARMAweb: comprehensive R- and bioconductor-based web service for microarray data analysis. *Nucleic Acids Research* 2006, 34:W498–503.
109. Livak KJ, Schmittgen TD: Analysis of Relative Gene Expression Data Using Real-Time Quantitative PCR and the $2^{-\Delta\Delta CT}$ Method. *Methods* 2001, 25:402-408.
110. Rasmussen KM: *Weight gain during pregnancy: Reexamining the guidelines.* Washington, DC: National Academies Press; 2009.
111. Sonderegger S, Husslein H, Leisser C, Knöfler M: Complex Expression Pattern of Wnt Ligands and Frizzled Receptors in Human Placenta and its Trophoblast Subtypes. *Placenta* 2007, 28:S97–102.
112. Sonderegger S, Pollheimer J, Knöfler M: Wnt Signalling in Implantation, Decidualisation and Placental Differentiation – Review. *Placenta* 2010, 31:839-847.
113. Heuberger J, Birchmeier W: Interplay of Cadherin-Mediated Cell Adhesion and Canonical Wnt Signaling. *Cold Spring Harbor Perspectives in Biology* 2010, 2:a002915.
114. Matsuura K, Jigami T, Taniue K, Morishita Y, Adachi S, Senda T, Nonaka A, Aburatani H, Nakamura T, Akiyama T: Identification of a link between Wnt/β-catenin signalling and the cell fusion pathway. *Nat Comms* 2011, 2:548.
115. Magee TR, Ross MG, Wedekind L, Desai M, Kjos S, Belkacemi L: Gestational diabetes mellitus alters apoptotic and inflammatory gene expression of trophobasts from human term placenta. *J Diabetes Complications* 2014.
116. Schmitz-Peiffer C: Targeting Ceramide Synthesis to Reverse Insulin Resistance. *Diabetes* 2010, 59:2351-2353.
117. Aye I, Powell T, Jansson T: Review: Adiponectin – The missing link between maternal adiposity, placental transport and fetal growth? *Placenta* 2013, 34:S40–45.

118. Manning BD, Cantley LC: AKT/PKB signaling: navigating downstream. *Cell* 2007, 129:1261-1274.
119. Daugherty RL, Gottardi CJ: Phospho-regulation of -Catenin Adhesion and Signaling Functions. *Physiology* 2007, 22:303-309.
120. Sutherland C: What Are the bona fide GSK3 Substrates? *International Journal of Alzheimer's Disease* 2011, 2011:1-23.
121. Catalano PM, Tyzbir ED, Allen SR, McBean JH, McAuliffe TL: Evaluation of fetal growth by estimation of neonatal body composition. *Obstet Gynecol* 1992, 79:46-50.
122. Catalano PM, Presley L, Minium J, Hauguel-de Mouzon S: Fetuses of Obese Mothers Develop Insulin Resistance in Utero. *Diabetes Care* 2009, 32:1076-1080.
123. Sewell MF, Huston-Presley L, Super DM, Catalano P: Increased neonatal fat mass, not lean body mass, is associated with maternal obesity. *Am J Obstet Gynecol* 2006, 195:1100-1103.
124. Mook-Kanamori D, Holzhauer S, Hollestein L, Durmus B, Manniesing R, Koek M, Boehm G, van der Beek E, Hofman A, Witteman J, Lequin M, Jaddoe V: Abdominal Fat in Children Measured by Ultrasound and Computed Tomography. *Ultrasound in Medicine & Biology* 2009, 35:1938-1946.
125. Brumbaugh DE, Tearse P, Cree-Green M, Fenton LZ, Brown M, Scherzinger A, Reynolds R, Alston M, Hoffman C, Pan Z, Friedman JE, Barbour LA: Intrahepatic Fat Is Increased in the Neonatal Offspring of Obese Women with Gestational Diabetes. *The Journal of Pediatrics* 2012, 162:930-936.e1.
126. Modi N, Murgasova D, Ruager-Martin R, Thomas EL, Hyde MJ, Gale C, Santhakumaran S, Dore CJ, Alavi A, Bell JD: The influence of maternal body mass index on infant adiposity and hepatic lipid content. *Pediatr Res* 2011, 70:287-291.
127. Straughen JK, Trudeau S, Misra VK: Changes in adipose tissue distribution during pregnancy in overweight and obese compared with normal weight women. *Nutr Diab* 2013, 3:e84.
128. Ehrenberg HM, Huston-Presley L, Catalano PM: The influence of obesity and gestational diabetes mellitus on accretion and the distribution of adipose tissue in pregnancy. *Am J Obstet Gynecol* 2003, 189:944-948.
129. Deierlein AL, Siega-Riz AM, Adair LS, Herring AH: Effects of Pre-Pregnancy Body Mass Index and Gestational Weight Gain on Infant Anthropometric Outcomes. *The Journal of Pediatrics* 2011, 158:221-226.
130. Olson CM, Strawderman MS, Dennison BA: Maternal Weight Gain During Pregnancy and Child Weight at Age 3 Years. *Matern Child Health J* 2009, 13:839-846.
131. Oken E, Rifas-Shiman SL, Field AE, Frazier AL, Gillman MW: Maternal Gestational Weight Gain and Offspring Weight in Adolescence. *Obstetrics & Gynecology* 2008, 112:999-1006.
132. Laitinen J, Jääskeläinen A, Hartikainen A, Sovio U, Vääräsmäki M, Pouta A, Kaakinen M, Järvelin M: Maternal weight gain during the first half of pregnancy and offspring obesity at 16 years: a prospective cohort study. *BJOG: An International Journal of Obstetrics & Gynaecology* 2012, 119:716-723.
133. Schack-Nielsen L, Michaelsen KF, Gamborg M, Mortensen EL, Sørensen TIA: Gestational weight gain in relation to offspring body mass index and obesity from infancy through adulthood. *Int J Obes Relat Metab Disord* 2009, 34:67-74.
134. Guelinckx I, Devlieger R, Mullie P, Vansant G: Effect of lifestyle intervention on dietary habits, physical activity, and gestational weight gain in obese pregnant women: a randomized controlled trial. *American Journal of Clinical Nutrition* 2010, 91:373-380.
135. Vinter CA, Jensen DM, Ovesen P, Beck-Nielsen H, Jorgensen JS: The LiP (Lifestyle in Pregnancy) Study: A randomized controlled trial of lifestyle intervention in 360 obese pregnant women. *Diabetes Care* 2011, 34:2502-2507.
136. Wolff S, Legarth J, Vangsgaard K, Toubro S, Astrup A: A randomized trial of the effects of dietary counseling on gestational weight gain and glucose metabolism in obese pregnant women. *Int J Obes Relat Metab Disord* 2008, 32:495-501.
137. Whitaker RC, Pepe MS, Seidel KD, Wright JA, Knopp RH: Gestational Diabetes and the Risk of Offspring Obesity. *PEDIATRICS* 1998, 101:e9.

138. Silverman BL, Rizzo T, Green OC, Cho NH, Winter RJ, Ogata ES, Richards GE, Metzger BE: Long-term prospective evaluation of offspring of diabetic mothers. *Diabetes* 1991, 40 Suppl 2:121-125.
139. Parker M, Rifas-Shiman SL, Belfort MB, Taveras EM, Oken E, Mantzoros C, Gillman MW: Gestational Glucose Tolerance and Cord Blood Leptin Levels Predict Slower Weight Gain in Early Infancy. *The Journal of Pediatrics* 2011, 158:227-233.
140. Hamilton JK, Odrobina E, Yin J, Hanley AJ, Zinman B, Retnakaran R: Maternal Insulin Sensitivity During Pregnancy Predicts Infant Weight Gain and Adiposity at 1 Year of Age. *Obesity* 2009, 18:340-346.
141. Vohr BR, McGarvey ST: Growth patterns of large-for-gestational-age and appropriate-for-gestational-age infants of gestational diabetic mothers and control mothers at age 1 year. *Diabetes Care* 1997, 20:1066-1072.
142. Brunner S, Schmid D, Hüttinger K, Much D, Brüderl M, Sedlmeier E, Kratzsch J, Amann-Gassner U, Bader BL, Hauner H: Effect of reducing the n-6/n-3 fatty acid ratio on the maternal and fetal leptin axis in relation to infant body composition. *Obesity* 2013, 22:217-224.
143. Boeke CE, Mantzoros CS, Hughes MD, L. Rifas-Shiman S, Villamor E, Zera CA, Gillman MW: Differential associations of leptin with adiposity across early childhood. *Obesity* 2013, 21:1430-1437.
144. Morton GJ, Schwartz MW: Leptin and the Central Nervous System Control of Glucose Metabolism. *Physiological Reviews* 2011, 91:389-411.
145. Brunner S, Schmid D, Hüttinger K, Much D, Heimberg E, Sedlmeier E, Brüderl M, Kratzsch J, Bader BL, Amann-Gassner U, Hauner H: Maternal insulin resistance, triglycerides and cord blood insulin in relation to post-natal weight trajectories and body composition in the offspring up to 2 years. *Diabet. Med.* 2013, 30:1500-1507.
146. Hillier TA, Pedula KL, Schmidt MM, Mullen JA, Charles M, Pettitt DJ: Childhood obesity and metabolic imprinting: the ongoing effects of maternal hyperglycemia. *Diabetes Care* 2007, 30:2287-2292.
147. Péneau S, Rouchaud A, Rolland-Cachera M, Arnault N, Hercberg S, Castetbon K: Body size and growth from birth to 2 years and risk of overweight at 7–9 years. *International Journal of Pediatric Obesity* 2011, 6:e162–169.
148. Polat TB, Urganci N, Caliskan KC, Akyildiz B: Correlation of abdominal fat accumulation and stiffness of the abdominal aorta in obese children. *J Pediatr Endocrinol Metab* 2008, 21:1031-1040.
149. Liu KH, Chan YL, Chan WB, Kong WL, Kong MO, Chan JCN: Sonographic measurement of mesenteric fat thickness is a good correlate with cardiovascular risk factors: comparison with subcutaneous and preperitoneal fat thickness, magnetic resonance imaging and anthropometric indexes. *Int J Obes Relat Metab Disord* 2003, 27:1267-1273.
150. Tadokoro N, Murano S, Nishide T, Suzuki R, Watanabe S, Murayama H, Morisaki N, Saito Y: Preperitoneal fat thickness determined by ultrasonography is correlated with coronary stenosis and lipid disorders in non-obese male subjects. *Int J Obes Relat Metab Disord* 2000, 24:502-507.
151. Kleiblova P, Dostalova I, Bartlova M, Lacinova Z, Ticha I, Krejci V, Springer D, Kleibl Z, Haluzik M: Expression of adipokines and estrogen receptors in adipose tissue and placenta of patients with gestational diabetes mellitus. *Molecular and Cellular Endocrinology* 2010, 314:150-156.
152. Uebel K, Pusch K, Gedrich K, Schneider KM, Hauner H, Bader BL: Effect of maternal obesity with and without gestational diabetes on offspring subcutaneous and preperitoneal adipose tissue development from birth up to year-1. *BMC Pregnancy Childbirth* 2014, 14:138.
153. Regnault N, Botton J, Heude B, Forhan A, Hankard R, Foliguet B, Hillier TA, Souberbielle J, Dargent-Molina P, Charles M: Higher Cord C-Peptide Concentrations Are Associated With Slower Growth Rate in the 1st Year of Life in Girls but Not in Boys. *Diabetes* 2011, 60:2152-2159.

154. Ferraro ZM, Qiu Q, Gruslin A, Adamo KB: Characterization of the insulin-like growth factor axis in term pregnancies complicated by maternal obesity. *Human Reproduction* 2012, 27:2467-2475.
155. Tamura A, Mori T, Hara Y, Komiyama A: Preperitoneal fat thickness in childhood obesity: association with serum insulin concentration. *Pediatr Int* 2000, 42:155-159.
156. Cnop M, Landchild MJ, Vidal J, Havel PJ, Knowles NG, Carr DR, Wang F, Hull RL, Boyko EJ, Retzlaff BM, Walden CE, Knopp RH, Kahn SE: The concurrent accumulation of intra-abdominal and subcutaneous fat explains the association between insulin resistance and plasma leptin concentrations. Distinct metabolic effects of two fat compartments. *Diabetes* 2002, 51:1005-1015.
157. Sivakumar K, Bari MF, Adaikalakoteswari A, Guller S, Weickert MO, Randeva HS, Grammatopoulos DK, Bastie CC, Vatish M: Elevated Fetal Adipsin/Acylation-Stimulating Protein (ASP) in Obese Pregnancy: Novel Placental Secretion via Hofbauer Cells. *The Journal of Clinical Endocrinology & Metabolism* 2013, 98:4113-4122.
158. Schaefer-Graf UM, Meitzner K, Ortega-Senovilla H, Graf K, Vetter K, Abou-Dakn M, Herrera E: Differences in the implications of maternal lipids on fetal metabolism and growth between gestational diabetes mellitus and control pregnancies. *Diabetic Medicine* 2011, 28:1053-1059.
159. Scifres CM, Catov JM, Simhan HN: The impact of maternal obesity and gestational weight gain on early and mid-pregnancy lipid profiles. *Obesity (Silver Spring)* 2013, 22:932-938.
160. Meyer BJ, Stewart FM, Brown EA, Cooney J, Nilsson S, Olivecrona G, Ramsay JE, Griffin BA, Caslake MJ, Freeman DJ: Maternal Obesity Is Associated With the Formation of Small Dense LDL and Hypoadiponectinemia in the Third Trimester. *The Journal of Clinical Endocrinology & Metabolism* 2013, 98:643-652.
161. Whyte K, Kelly H, O'Dwyer V, Gibbs M, O'Higgins A, Turner MJ: Offspring birth weight and maternal fasting lipids in women screened for gestational diabetes mellitus (GDM). *Eur J Obstet Gynecol Reprod Biol* 2013, 170:67-70.
162. Son GH, Kwon JY, Kim YH, Park YW: Maternal serum triglycerides as predictive factors for large-for-gestational age newborns in women with gestational diabetes mellitus. *Acta Obstet Gynecol Scand* 2010, 89:700-704.
163. Qiu C, Williams MA, Vadachkoria S, Frederick IO, Luthy DA: Increased maternal plasma leptin in early pregnancy and risk of gestational diabetes mellitus. *Obstet Gynecol* 2004, 103:519-525.
164. Hauguel-de Mouzon S, Lepercq J, Catalano P: The known and unknown of leptin in pregnancy. *American Journal of Obstetrics and Gynecology* 2006, 194:1537-1545.
165. Karakosta P, Chatzi L, Plana E, Margioris A, Castanas E, Kogevinas M: Leptin levels in cord blood and anthropometric measures at birth: a systematic review and meta-analysis. *Paediatric and Perinatal Epidemiology* 2011, 25:150-163.
166. Schubring C, Siebler T, Kratzsch J, Englaro P, Blum WF, Triep K, Kiess W: Leptin serum concentrations in healthy neonates within the first week of life: relation to insulin and growth hormone levels, skinfold thickness, body mass index and weight. *Clin Endocrinol (Oxf)* 1999, 51:199-204.
167. Hube F, Lietz U, Igel M, Jensen PB, Tornqvist H, Joost HG, Hauner H: Difference in leptin mRNA levels between omental and subcutaneous abdominal adipose tissue from obese humans. *Horm Metab Res* 1996, 28:690-693.
168. Pratley RE, Ren K, Milner MR, Sell SM: Insulin increases leptin mRNA expression in abdominal subcutaneous adipose tissue in humans. *Mol Genet Metab* 2000, 70:19-26.
169. Luo Z, Nuyt A, Delvin E, Fraser WD, Julien P, Audibert F, Girard I, Shatenstein B, Deal C, Grenier E, Garofalo C, Levy E: Maternal and fetal leptin, adiponectin levels and associations with fetal insulin sensitivity. *Obesity* 2013, 21:210-216.
170. Varastehpour A, Radaelli T, Minium J, Ortega H, Herrera E, Catalano P, Hauguel-de Mouzon S: Activation of phospholipase A2 is associated with generation of placental lipid signals and fetal obesity. *J Clin Endocrinol Metab* 2006, 91:248-255.

171. Uzelac P, Li X, Lin J, Neese L, Lin L, Nakajima S, Bohler H, Lei Z: Dysregulation of Leptin and Testosterone Production and Their Receptor Expression in the Human Placenta with Gestational Diabetes Mellitus. *Placenta* 2010, 31:581-588.
172. Farley D, Choi J, Dudley D, Li C, Jenkins S, Myatt L, Nathanielsz P: Placental Amino Acid Transport and Placental Leptin Resistance in Pregnancies Complicated by Maternal Obesity☆. *Placenta* 2010, 31:718-724.
173. D'Ippolito S, Tersigni C, Scambia G, Di Simone N: Adipokines, an adipose tissue and placental product with biological functions during pregnancy. *BioFactors* 2012, 38:14-23.
174. Magarinos MP, Sanchez-Margalet V, Kotler M, Calvo JC, Varone CL: Leptin Promotes Cell Proliferation and Survival of Trophoblastic Cells. *Biology of Reproduction* 2007, 76:203-210.
175. Ballesteros M, Simon I, Vendrell J, Ceperuelo-Mallafre V, Miralles RM, Albaiges G, Tinahones F, Megia A: Maternal and Cord Blood Adiponectin Multimeric Forms in Gestational Diabetes Mellitus: A prospective analysis. *Diabetes Care* 2011, 34:2418-2423.
176. Retnakaran R, Connelly PW, Maguire G, Sermer M, Zinman B, Hanley AJG: Decreased high-molecular-weight adiponectin in gestational diabetes: implications for the pathophysiology of Type 2 diabetes. *Diabet Med* 2007, 24:245-252.
177. Wang Y, Lam KSL, Yau M, Xu A: Post-translational modifications of adiponectin: mechanisms and functional implications. *Biochem. J.* 2008, 409:623-633.
178. Weyermann M, Beermann C, Brenner H, Rothenbacher D: Adiponectin and Leptin in Maternal Serum, Cord Blood, and Breast Milk. *Clinical Chemistry* 2006, 52:2095-2102.
179. Basu S, Laffineuse L, Presley L, Minium J, Catalano PM, Hauguel-de Mouzon S: In Utero Gender Dimorphism of Adiponectin Reflects Insulin Sensitivity and Adiposity of the Fetus. *Obesity* 2009, 17:1144-1149.
180. Inoue M, Itabashi K, Nakano Y, Nakano Y, Tobe T: High-Molecular-Weight Adiponectin and Leptin Levels in Cord Blood Are Associated with Anthropometric Measurements at Birth. *Horm Res* 2008, 70:268-272.
181. Corbetta S: Adiponectin Expression in Human Fetal Tissues during Mid- and Late Gestation. *Journal of Clinical Endocrinology & Metabolism* 2005, 90:2397-2402.
182. Lappas M, Yee K, Permezel M, Rice GE: Release and regulation of leptin, resistin and adiponectin from human placenta, fetal membranes, and maternal adipose tissue and skeletal muscle from normal and gestational diabetes mellitus-complicated pregnancies. *J Endocrinol* 2005, 186:457-465.
183. Caminos JE, Nogueiras R, Gallego R, Bravo S, Tovar S, Garcia-Caballero T, Casanueva FF, Dieguez C: Expression and regulation of adiponectin and receptor in human and rat placenta. *J Clin Endocrinol Metab* 2005, 90:4276-4286.
184. McDonald EA, Wolfe MW: Adiponectin Attenuation of Endocrine Function within Human Term Trophoblast Cells. *Endocrinology* 2009, 150:4358-4365.
185. Meller M, Qiu C, Vadachkoria S, Abetew DF, Luthy DA, Williams MA: Changes in placental adipocytokine gene expression associated with gestational diabetes mellitus. *Physiol Res* 2006, 55:501-512.
186. Rosario FJ, Schumacher MA, Jiang J, Kanai Y, Powell TL, Jansson T: Chronic maternal infusion of full-length adiponectin in pregnant mice down-regulates placental amino acid transporter activity and expression and decreases fetal growth. *The Journal of Physiology* 2012, 590:1495-1509.
187. Benaitreau D, Dieudonne M, Santos ED, Leneveu M, Mazancourt Pd, Pecquery R: Antiproliferative Effects of Adiponectin on Human Trophoblastic Cell Lines JEG-3 and BeWo. *Biology of Reproduction* 2009, 80:1107-1114.
188. Enquobahrie DA, Williams MA, Qiu C, Meller M, Sorensen TK: Global placental gene expression in gestational diabetes mellitus. *American Journal of Obstetrics and Gynecology* 2009, 200:206.e1-13.
189. Wolf M, Sauk J, Shah A, Vossen Smirnakis K, Jimenez-Kimble R, Ecker JL, Thadhani R: Inflammation and glucose intolerance: a prospective study of gestational diabetes mellitus. *Diabetes Care* 2004, 27:21-27.

190. Shimoya K, Matsuzaki N, Taniguchi T, Kameda T, Koyama M, Neki R, Saji F, Tanizawa O: Human placenta constitutively produces interleukin-8 during pregnancy and enhances its production in intrauterine infection. *Biol Reprod* 1992, 47:220-226.
191. Sanders TR, Kim DW, Glendining KA, Jasoni CL: Maternal obesity and IL6 lead to aberrant developmental gene expression and deregulated neurite growth in the fetal arcuate nucleus. *Endocrinology* 2014:en20131968.
192. Sonderegger S, Haslinger P, Sabri A, Leisser C, Otten JV, Fiala C, Knofler M: Wingless (Wnt)-3A Induces Trophoblast Migration and Matrix Metalloproteinase-2 Secretion through Canonical Wnt Signaling and Protein Kinase B/AKT Activation. *Endocrinology* 2009, 151:211-220.
193. Maltzahn J von, Bentzinger CF, Rudnicki MA: Wnt7a–Fzd7 signalling directly activates the Akt/mTOR anabolic growth pathway in skeletal muscle. *Nat Cell Biol* 2011, 14:186-191.
194. Desoye G, Korgun ET, Ghaffari-Tabrizi N, Hahn T: Is fetal macrosomia in adequately controlled diabetic women the result of a placental defect?--a hypothesis. *J Matern Fetal Neonatal Med* 2002, 11:258-261.
195. Dash PR, Whitley GSJ, Ayling L, Johnstone AP, Cartwright JE: Trophoblast apoptosis is inhibited by hepatocyte growth factor through the Akt and beta-catenin mediated up-regulation of inducible nitric oxide synthase. *Cell. Signal.* 2005, 17:571-580.
196. Cheng S, Shao J, Halstead LR, Distelhorst K, Sierra O, Towler DA: Activation of Vascular Smooth Muscle Parathyroid Hormone Receptor Inhibits Wnt/ -Catenin Signaling and Aortic Fibrosis in Diabetic Arteriosclerosis. *Circulation Research* 2010, 107:271-282.
197. Hoang BH, Kubo T, Healey JH, Yang R, Nathan SS, Kolb EA, Mazza B, Meyers PA, Gorlick R: Dickkopf 3 inhibits invasion and motility of Saos-2 osteosarcoma cells by modulating the Wnt-beta-catenin pathway. *Cancer Res* 2004, 64:2734-2739.
198. Caricasole A: Functional Characterization of WNT7A Signaling in PC12 Cells: Interaction with a FZD5/LRP6 receptor complex and modulation by dickkopf proteins. *Journal of Biological Chemistry* 2003, 278:37024-37031.
199. Uusküla L, Männik J, Rull K, Minajeva A, Kõks S, Vaas P, Teesalu P, Reimand J, Laan M, Zenclussen AC: Mid-Gestational Gene Expression Profile in Placenta and Link to Pregnancy Complications. *PLoS ONE* 2012, 7:e49248.
200. Getsios S, MacCalman CD: Cadherin-11 modulates the terminal differentiation and fusion of human trophoblastic cells in vitro. *Developmental Biology* 2003, 257:41-54.
201. Madazli R, Tuten A, Calay Z, Uzun H, Uludag S, Ocak V: The incidence of placental abnormalities, maternal and cord plasma malondialdehyde and vascular endothelial growth factor levels in women with gestational diabetes mellitus and nondiabetic controls. *Gynecol Obstet Invest* 2008, 65:227-232.
202. Li L, Ying J, Li H, Zhang Y, Shu X, Fan Y, Tan J, Cao Y, Tsao SW, Srivastava G, Chan ATC, Tao Q: The human cadherin 11 is a pro-apoptotic tumor suppressor modulating cell stemness through Wnt/β-catenin signaling and silenced in common carcinomas. *Oncogene* 2011, 31:3901-3912.
203. Leach L, Gray C, Staton S, Babawale MO, Gruchy A, Foster C, Mayhew TM, James DK: Vascular endothelial cadherin and beta-catenin in human fetoplacental vessels of pregnancies complicated by Type 1 diabetes: associations with angiogenesis and perturbed barrier function. *Diabetologia* 2004, 47:695-709.
204. Cheng S, Shao J, Halstead LR, Distelhorst K, Sierra O, Towler DA: Activation of Vascular Smooth Muscle Parathyroid Hormone Receptor Inhibits Wnt/ -Catenin Signaling and Aortic Fibrosis in Diabetic Arteriosclerosis. *Circulation Research* 2010, 107:271-282.
205. Zhao Y, Wang D, Zhang L, Zhang F, Wang D, Zhang W: Genomic expression profiles of blood and placenta reveal significant immune-related pathways and categories in Chinese women with gestational diabetes mellitus. *Diabetic Medicine* 2011, 28:237-246.
206. Landvik N, Tekpli X, Anmarkrud K, Haugen A, Zienolddiny S: Molecular characterization of a cancer-related single nucleotide polymorphism in the pro-inflammatory interleukin-1B gene. *Mol. Carcinog.* 2012, 51:E168–175.

207. Nakatsu MN, Ding Z, Ng MY, Truong TT, Yu F, Deng SX: Wnt/ -Catenin Signaling Regulates Proliferation of Human Cornea Epithelial Stem/Progenitor Cells. *Investigative Ophthalmology & Visual Science* 2011, 52:4734-4741.
208. Bustin SA, Benes V, Garson JA, Hellemans J, Huggett J, Kubista M, Mueller R, Nolan T, Pfaffl MW, Shipley GL, Vandesompele J, Wittwer CT: The MIQE Guidelines: Minimum Information for Publication of Quantitative Real-Time PCR Experiments.
209. Ruijter JM, Ramakers C, Hoogaars WMH, Karlen Y, Bakker O, van den Hoff MJB, Moorman AFM: Amplification efficiency: linking baseline and bias in the analysis of quantitative PCR data. *Nucleic Acids Research* 2009, 37:e45.
210. Pfaffl MW, Tichopad A, Prgomet C, Neuvians TP: Determination of stable housekeeping genes, differentially regulated target genes and sample integrity: BestKeeper--Excel-based tool using pair-wise correlations. *Biotechnol Lett* 2004, 26:509-515.

7 Abbreviation

ABC	ATP-binding cassette
ACTB	β-actin
ADIPOR1/2	Adiponectin receptor 1/2
AKT	V-akt murine thymoma viral oncogene homolog 1 (Proteinkinase B)
AMPK	Protein kinase, AMP-activated, alpha 1 catalytic subunit (PRKAA1)
APC	Adenomatous polyposis coli
APGAR	**A**ppearance, **P**ulse, Grimace, **A**ctivity, **R**espiration
ApoB100	Apolipoprotein B100
AUC	Area under the curve
ax	Axial
β	Standardized regression coefficient
BeWo	Human placental choriocarcinoma cell line
BIA	Bioelectrical impedance analysis
BM	Basal membrane
BMI	Body mass index
CCND1	Cyclin D1
CD	Cluster of differentiation
CD36	Fatty acid translocase
CDH11	Cadherin 11 (OB cadherin)
CSNK1A/1G/2A	Casein kinase 1A/1G/2A
CRP	High sensitive C-reactive protein
CT	Computer tomography
CTG	Cardiotocography
CV	Coefficient of variation
DNA	Deoxyribonucleic acid
DKK 1/3	Dickkopf 1/ 3 homolog (Xenopus laevis)
DKKL1	Dickkopf-like 1
DPP	Decapentaplegic
Dsh	Dishevelled
DTT	Dithiothreitol
ECL	Electrochemiluminescence
EDTA	Ethylene-Diamine-Tetra-Acetic acid
EGF	Epidermal growth factor
ELISA	Enzyme-linked immunoabsorbent assay
EMR1	EGF-like module containing, mucin-like, hormone receptor-like 1
ERVWE1	Endogenous retroviral family W, env(C7), member 1 (syncytin 1)
FABP	Fatty acid binding protein
FABPpm	Fatty acid binding protein plasma membrane
FATP	Fatty acid transporters
FC	Fold change
FDR	False discovery rate
FLT1	Fms-related tyrosine kinase 1 (vascular endothelial growth factor receptor 1
FZD	Frizzled
GAPDH	Glyceraldehyde-3-phosphate dehydrogenase

GBE1	Flucan (1,4-alpha-), branching enzyme 1 (glycogen branching enzyme)
GCM1	Glial cells missing homolog 1 (Drosophila)
GDM	Gestational diabetes mellitus
GePS	Genomatix Pathway System
GesA	**Ges**tational diabetes mellitus and **a**diposity in early adipose tissue development
GLUT 1-4	Glucose transporter 1-4
GSK3β	Glycogen synthase kinase 3β
GWG	Gestational weight gain
GYS	Glycogen synthase
H2AFZ	H2A histone family, member Z
HAPO	Hyperglycemia and Adverse Pregnancy Outcome
HbA1c	Hemoglobin A1c
HDL	High density lipoprotein
HELLP	**H**emolysis, **EL**evated liver enzymes, **L**ow **P**latelet count
HEPES	4-(2-Hydroxyethyl)piperazine-1-ethanesulfonic acid
HMW	High molecular weight (adiponectin)
HOMA-IR	Homeostasis model of assessment of insulin resistance
hPGH	Human placental growth hormone
hPL	Human placental lactogen
ICC	Interclass coefficient
IGF1/ 2	Insulin like growth factor-1/ 2
IGF1R	Insulin like growth factor 1 receptor
IGFBP	Insulin like growth factor binding protein
IL1B/ 6/ 8	Interleukine 1B
IOM	Institute of Medicine
IPA	Ingenuity pathway analysis
INFγ	Interferon γ
INSR	Insulin receptor
IRS1	Insulin receptor substrate 1
IUGR	Intrauterine growth restriction
JEG-3	Human placental choriocarcinoma cell line
kDa	Kilo Dalton
L	Lean group
LC-PUFA	Long chain polyunsaturated fatty acid
LDL	Low-density lipoprotein
LEP	Leptin
LGA	Large for gestational age
LIPG	Endothelial lipase
LPL	Lipoproteinlipase
LRP 1/ 5/ 6	Low-density lipoprotein receptor-related protein 1/ 5 /6
m	messenger
M. rect.	Musculus rectus abdominis
MAPK1	Mitogen-activated protein kinase 1 (p38)
MCF-7	Michigan Cancer Foundation-7 (breast cancer cell line)
MCP1	Monocyte chemotactic protein-1, Chemokine (C-C motif) ligand 2 (CCL2)
MIQE	Minimum information for publication of quantitative real-time PCR
miRNA	Micro-RNA
MMP 2/9	Metalloproteinase 2/9

mRNA	Messenger RNA
MRT	Magnetic resonance tomography
mTOR	Mammalian target of rapamycin
MVM	Microvillous membrane
MYC	V-myc myelocytomatosis viral oncogene homolog (avian)
NFκB	Nuclear factor κB
NO	Nitric oxide
OB	Obese
OGTT	Oral glucose tolerance test
p	Phospho
p70S6K1	Ribosomal protein S6 kinase 1, 70kDa, polypeptide 1 (RPS6KB1)
PBMC	Peripheral blood mononuclear cell
PC12	Cell line from ratadrenal gland phaeochromocytoma
PCA	Principle Component Analysis
PDA	Peridual anesthesia
PDGF	Platelet-derived growth factor
PDK1	3-phospho-inositide-dependent protein kinase 1
PI3K	Phosphoinositol-3-kinase
pp	Post partum
PPA	Preperitoneal adipose tissue
PPARα/ γ/ δ	Peroxisome proliferator-activated receptor α/ γ/ δ
PROK1	Prokineticin 1
PTH1R	Parathyroid hormone 1 receptor
r	Correlation coefficient
r^2	Coefficient of determination
RIN	RNA integrity number
RIPA	Radioimmunoprecipitation assay buffer
RNA	Ribonucleic acid
RR	blood pressure (Riva-Rocci)
RT	Reverse transcription
RT-qPCR	Reverse transcription quantitative polymerase chain reaction
sag	Sagittal
SCA	Subcutaneous
SD	Standard deviation
SDS	Sodium dodecyl sulfate
SEM	Standard deviation of the mean
Ser	Serine
SFT	Sum of the 4 skin fold thickness measurements (biceps + triceps + subscapular + suprailiac)
SGA	Small for gestational age
sICAM1	Soluble intercellular adhesion molecule-1
SPTLC3	Serine palmitoyltransferase, long chain base subunit 3
SR-BI	Scavenger receptor class BI
STAT1	Signal-transducer/activator of transcription protein 1
sVCAM1	Soluble vascular cell adhesion molecule-1
SVF	Stromal vascular fraction
T2DM	Type 2 diabetes mellitus
TBS	Tris-buffered saline
TBST	Tris-buffered saline + Tween 20 (0.1 %)
TG	Triglycerides

TGF-β	Transforming growth factor β
Thr	Threonine
Tris	Tris(hydroxymethyl)aminomethane
TNF-α	Tumor necrosis factor α
Tyr	Tyrosine
US	Ultrasonography
VE	Vascular endothelial
VEGF	Vascular endothelial growth factor
VEGFR2	Vascular endothelial growth factor receptor 2
VLDL	Very low-density lipoprotein
VMSC	Vascular smooth muscle
Wnt	Wingless-Int
WNT3A/ 7A/ 7B	Wingless-type MMTV integration site family, member 3A/ 7A/ 7B

8 Materials

8.1 Primer sequences for RT- qPCR experiments

Gene symbol		Primer sequence 5‘-3‘	Accession number	Primer location in exon	Amplicon length (bp)	T (°C)
ACTB	fw	CCTGGAGAAGAGCTACGAGCTG	NM_001101.3	3-4	107	60
	rev	GACTCCATGCCCAGGAAGGAAGG				
CCL2 (MCP1)	fw	TCGCTCAGCCAGATGCAATCAATG	NM_002982.3	1-2	127	60
	rev	ACAGCTTCTTTGGGACACTTGC				
CDH11	fw	GTCAGAGACAACCGAGATAACACAGC	NM_001797.2	11-12	101	60
	rev	TCGCTGATCACTATGGGCAGAAG				
DKK3	fw	TGGAAGAGATGGAGGCAGAAGAA	NM_015881.5	2-3	101	60
	rev	CGTGTCTGTGTTGGTCTCATT				
FLT1	fw	GTCTGCTTCTCACAGGATCTAGTTC	NM_002019.4	1-2	112	60
	rev	CTGCATTGGAGATGCAGTGTCT				
H2AFZ	fw	CACCGCAGAGGTACTTGAACTG	NM_002106.3	3-4	139	60
	rev	ACCACCAGCAATTGTAGCCTTG				
IL1β [206]	fw	ATGGCCCTAAACAGATGAAGT	NM_000576.2	3-4	153	60
	rev	GCATCTTCCTCAGCTTGTCC				
IL8 [28]	fw	CTGGCCGTGGCTCTCTTG	NM_000584.3	1-2	76	60
	rev	TAGCACTCCTTGGCAAAACTG				
LEP	fw	ACACGCAGTCAGTCTCCTCCAA	NM_000230.2	2-3	130	60
	rev	TGGAAGGCATACTGGTGAGGAT				
PROK1	fw	AGCCACAAGGTCCCCTTCTTC	NM_032414.2	2-3	113	60
	rev	TTCAAGTCCATGGAGCAGCGGTA				
PTH1R	fw	AGTCTTCGGCTGGGGTCTGCC	NM_000316.2	10-11	109	60
	rev	CCACTTTTTGTTCCCGGAGC				
SPTLC3	fw	TGAGCCCACCGATAGCAGAGCAA	NM_018327.2	9-10	81	60
	rev	TCTGCAGCCCTTGAGTGGTCC				
TNF-α [28]	fw	GGAGAAGGGTGACCGACT	NM_000594.3	4	69	60
	rev	TGCCCAGACTCGGCAAAG				
WNT7A [207]	fw	CATAGGAGAAGGCTCACAAATGG	NM_004625.3	2-3	155	60
	rev	CGGCAATGATGGCGTAGGT				

8.2 Antibodies

Item	Company	City	Country
Akt Rabbit Antibody	Cell Signaling / New England Biolabs GmbH	Frankfurt am Main	Germany
Anti GAPDH mAntibody	Ambion / Life technologies	Darmstadt	Germany
GSK-3β (27C10) Rabbit mAntibody	Cell Signaling / New England Biolabs GmbH	Frankfurt am Main	Germany
Lamin A/C Rabbit Antibody	Cell Signaling / New England Biolabs GmbH	Frankfurt am Main	Germany
Phospho-Akt (Ser473) (D9E) XP® Rabbit mAntibody	Cell Signaling / New England Biolabs GmbH	Frankfurt am Main	Germany
Phospho-GSK-3β (Ser9) Rabbit Antibody	Cell Signaling / New England Biolabs GmbH	Frankfurt am Main	Germany
β-Catenin (D10A8) XP® Rabbit mAntibody	Cell Signaling / New England Biolabs GmbH	Frankfurt am Main	Germany
IRDye800CW goat anti-rabbit	LI-COR Biosciences GmbH	Bad Homburg	Germany
IRDye680CW goat anti-mouse	LI-COR Biosciences GmbH	Bad Homburg	Germany

8.3 Consumables

Item	Company	City	Country
96-well plate	Nunc / Thermo-Fisher Scientific	Langenselbold	Germany
Biosphere® filter tips (10, 100, 1000 µl)	Sarstedt AG & Co. KG	Nümbrecht	Germany
Cool rack 96-wells	Eppendorf AG	Hamburg	Germany
Corning® Costar® "stripette", disposable pipettes 2; 5; 10; 25; 50 ml	Corning® Inc., Sigma-Aldrich Chemie GmbH	München	Germany
Corning® Costar® reagent reservoirs	Corning® Inc., Sigma-Aldrich Chemie GmbH	München	Germany
Cotton gloves	Zefa-Laborservice GmbH	Harthausen	Germany
Dewar flask	KGW-Isotherm	Karlsruhe	Germany
Disposable pipettes 2; 5; 10; 25; 50 ml	Falcon™, BD Biosciences Heidelberg Germany	Heidelberg	Germany
Dissection scissors	Fine Science	Heidelberg	Germany
Einbettkassetten, Histosette® I, M498	VWR International GmbH	Darmstadt	Germany
Eppendorf Combitips plus	Eppendorf AG	Hamburg	Germany
Eppendorf Multipette® plus	Eppendorf AG	Hamburg	Germany
Eppendorf Xplorer®, multi-channel, 50 – 1200 µL, grün	Eppendorf AG	Hamburg	Germany
Forceps	Fine Science	Heidelberg	Germany
Gel chamber, sled, comb	UniEquip GmbH	Planegg	Germany
Glass plates, clips, rubber, chamber, combs	Biometra GmbH	Göttingen	Germany
Glassware (beakers, cylinders, funnels)	Diagonal GmbH &Co KG	Münster	Germany
Heat sealing film	Eppendorf AG	Hamburg	Germany
Laboratory aluminum foil	Carl Roth GmbH & Co. KG	Karlsruhe	Germany
Microtube boxes for freezing	Zefa-Laborservice	Harthausen	Germany
Microtube PP, 1,5 ml	Paul Böttger OHG	Bodenmais	Germany
Microtube PP, 2 ml	Diagonal GmbH & Co. KG	Münster	Germany
Mortar	Morgan Technical Ceramics - Haldenwanger	Waldkraiburg	Germany
Nitrile exam gloves	Kimberley-Clark Health Care	Zaventem	Belgium
Parafilm®	Pechiney Plastic Packaging	Chicago	IL, USA
Pasteur pipettes	glass Zefa-Laborservice GmbH	Harthausen	Germany
Pestle	Morgan Technical Ceramics - Haldenwanger	Waldkraiburg	Germany
Pipettes 10; 200, 1000 µl	Gilson Intl. B.V.	Limburg	Germany
Pipettes 2,5; 10; 100, 1000 µl	Eppendorf AG	Hamburg	Germany
Pipetting aid	Gilson Intl. B.V.	Limburg	Germany
Plastic beakers	Vitlab	Großostheim	Germany
Plastic ware (beakers, cylinders, funnels)	Diagonal GmbH &Co KG	Münster	Germany
Protran BA 83 Whatman™ (0.2 µm)	GE Healthcare Life sciences	Freiburg	Germany

Item	Company	City	Country
Reaction tubes, 0.2 ml	Zefa-Laborservice GmbH	Harthausen	Germany
Reaction tubes, 0.5 ml	Brand GmbH & Co. KG	Wertheim	Germany
Reaction tubes, 2 ml (safe-lock)	Eppendorf AG	Hamburg	Germany
Safety goggles	UVEX Winter Holding	Fürth	Germany
Scalpel	B. Braun Melsungen	Melsungen	Germany
S-Monovetten® (Serum, Serum-Gel, Hämatologie, Glucose)	Sarstedt AG & Co. KG	Nümbrecht	Germany
Spatula	Carl Roth GmbH & Co. KG	Karlsruhe	Germany
Tips, blue 1000 µl	Brand GmbH & Co. KG	Wertheim	Germany
Tips, white, 10 µl	Brand GmbH & Co. KG	Wertheim	Germany
Tips, yellow, 100 µl	Brand GmbH & Co. KG	Wertheim	Germany
Transferpette® Multi-channel, 30-300 µl	Brand GmbH & Co. KG	Wertheim	Germany
Tube racks	Brand GmbH & Co. KG	Wertheim	Germany
Tubes, 15 ml Greiner	Bio-One GmbH	Frickenhausen	Germany
Tubes, 50 ml Greiner	Bio-One GmbH	Frickenhausen	Germany
Twin.tec real-time PCR plates 96	Eppendorf AG	Hamburg	Germany
Water bottle	Vitlab	Großostheim	Germany
Whatman paper	Carl Roth GmbH & Co. KG	Karlsruhe	Germany

8.4 Machines

Item	Company	City	Country
10-MHz linear probe (VFX 13–5)	Siemens Healthcare	Erlangen	Germany
7900HT Fast Real-Time PCR System	Applied Biosystems GmbH	Darmstadt	Germany
Agilent 2100 Bioanalyzer	Agilent Technologies GmbH	Böblingen	Germany
Caliper	Holtain Limited	Crosswell, Crymych	United Kingdom
Centrifuge 5415 R	Eppendorf AG	Hamburg	Germany
Centrifuge 5424	Eppendorf AG	Hamburg	Germany
Centrifuge 5430	Eppendorf AG	Hamburg	Germany
Centrifuge 5810	Eppendorf AG	Hamburg	Germany
DNA/RNA UV-Cleaner UVC/T-M-AR	UniEquip GmbH	Planegg	Germany
Electrophoresis power supply CONSORT E861	Consort bvba	Turnhout	Belgium
Freezer "ThermoForma" -80°C	Thermo Fisher Scientific	Schwerte	Germany
Freezer "ThermoScientific HeraFreeze" -80°C	Thermo Fisher Scientific	Schwerte	Germany
Freezer -20 °C Liebherr premium	Liebherr GmbH	Biberach	Germany
Fridge 4 °C Liebherr	Liebherr GmbH	Biberach	Germany
Heat sealer	Eppendorf AG	Hamburg	Germany
Heraeus Megafuge 1.0 R Heraeus	Thermo Scientific	Waltham	MA, USA
High-resolution ultrasonographic system, Acuson Premium	Siemens Healthcare	Erlangen	Germany
HiScan BeadArray Scanner	Illumina	San Diego	CA, USA
Homogenizer ("Dispergierwerkzeug")	Miccra (ART Labortechnik)	Mühlheim	Germany
Hybridisation oven	Illumina	San Diego	CA, USA
Ice machine AF 100	Scotsman ice systems	Milan	Italy
Infant scale (Babywaage Ultra MBSC-55)	Myweight®	Erkelenz	Germany
Measuring stick (Säuglingsmessstab seca 207)	Seca	Hamburg	Germany
Measuring tape	Prym GmbH & Co. KG	Stolberg	Germany
Mini Centrifuge GMC-060	LMS Group	Tokyo	Japan
Mini scale EW3000-2M	Kern GmbH	Balingen	Germany
Mini scale PE360	Mettler-Toledo	Ingolstadt	Germany
ND-1000 Spectrophotometer	Peqlab biotechnology GmbH	Erlangen	Germany
Odyssey® Infrared Imaging System	LI-COR Biosciences GmbH	Bad Homburg	Germany
Power pack P25 T	Biometra GmbH	Göttingen	Germany
Printer	Intas Science Imaging InstrumentsGmbH	Göttingen	Germany
Realplex4 Mastercycler epgradient S	Eppendorf AG	Hamburg	Germany

Item	Company	City	Country
S20-K SevenEasy™ pH meter	Mettler-Toledo	Ingolstadt	Germany
Scale, max 820 g	Sartorius AG	Göttingen	Germany
Sonificator UW 2070	Bandelin electronic GmbH & Co.KG	Berlin	Germany
Spectrophotometer infinite M2000	Tecan Austria GmbH	Gröding	Germany
Thermocycler T3000	Biometra GmbH	Göttingen	Germany
Thermomixer comfort	Eppendorf AG	Hamburg	Germany
UV-VIS gel electrophoresis detection system	Intas Science Imaging Instruments GmbH	Göttingen	Germany
Vortexer "Vortex Genie 2"	Bender-Hobein	Gera	Germany
Vortexer 2x^3	Velp Scientifica	Usmate	Italy

8.5 Software

Item	Company	City	Country
2100 Expert Software vB.02.06.SI418	Agilent Technologies GmbH	Böblingen	Germany
Comprehensive R based Microarray Analysis web frontend (CarmaWeb)	Institute for Genomics and Bioinformatics, Graz University of Technology	Graz	Austria
GenesisWeb	Institute for Genomics and Bioinformatics, Graz University of Technology	Graz	Austria
Genomatix genome analyzer server	Genomatix Software GmbH	Munich	Germany
GenomeStudio™ Software v2010.1	Illumina	San Diego	CA, USA
IBM SPSS statistics software;version 20.0	IBM Deutschland GmbH	Ehningen	Germany
Ingenuity pathway analysis (IPA)	Ingenuity Systems, Inc.	Redwood City	CA, USA
Intas GDS	Intas Science Imaging Instruments GmbH	Göttingen	Germany
LinRegPCR v12.16	Dr. J.M. Ruijter, Academic Medical Center	Amsterdam	Netherlands
Microsoft Office	Microsoft Deutschland GmbH	Unterschleißheim	Germany
NanoDrop ND-1000 v3.7.1	PEQLAB Biotechnologie GmbH (Thermo Scientific)	Erlangen	Germany
Odyssey application software v3.0	LI-COR Biosciences GmbH	Bad Homburg	Germany
Osirix imagining software, Advanced open source PACS Workstation DICOM Viewer	Pixmeo	Genf	Switzerland
Prism v5.0	GraphPad Software, Inc.	La Jolla	CA, USA
R package version 2.15.3	R Development Core Team	Auckland	New Zealand
Realplex v2.0	Eppendorf AG	Hamburg	Germany
Tecan i-control v1.7.1.12	Tecan Austria GmbH	Gröding	Germany

8.6 Chemicals

Item	Company	City	Country
1 kb DNA ladder	New England Biolabs GmbH	Frankfurt am Main	Germany
2-(4-(2-Hydroxyethyl)- 1-piperazinyl)-ethansulfonsäure (HEPES) ($C_8H_{18}N_2O_4S$)	Carl Roth GmbH & Co. KG	Karlsruhe	Germany
Acetic acid (100 %) ($C_2H_4O_2$)	Merck KGaA	Darmstadt	Germany
Acrylamide/ Bisacrylamide "Roti-Gelektrophorese"	Carl Roth GmbH & Co. KG	Karlsruhe	Germany
Agarose, pegGOLD universal	Peqlab biotechnology GmbH	Erlangen	Germany
Ammoniumpersulphate (APS) ($(NH_4)_2S_2O_8$)	Bio-Rad Laboratories GmbH	München	Germany
Amyloglucosidase, 70 units/mg	Sigma-Aldrich Chemie GmbH	Taufkirchen	Germany
BCA protein assay kit	Pierce / Thermo Fisher Scientific	Bonn	Germany
Boric acid (H_3BO_3)	Merck KGaA	Darmstadt	Germany
Bovine serum albumine, Albumin Fraction V, pH 5.2, > 97 %	Carl Roth GmbH & Co. KG	Karlsruhe	Germany
Bradford protein assay dye reagent	Bio-Rad Laboratories GmbH	München	Germany
Bromophenolblue	Merck KGaA	Darmstadt	Germany
Calyculin A ($C_{50}H_{81}N_4O_{15}P$)	Enzo life sciences	Lörrach	Germany

Item	Company	City	Country
Carbon dioxide ("dry ice", CO_2)	TKD GmbH	Fraunberg-Tittenkofen	Germany
Chloroform ($CHCl_3$)	Carl Roth GmbH & Co. KG	Karlsruhe	Germany
Coomassie Brilliant Blue G 250	SERVA Electrophoresis GmbH	Heidelberg	Germany
Dithiotreitol (DTT) ($C_4H_{10}O_2S_2$)	AppliChem GmbH	Darmstadt	Germany
DNA-Oligonucleotides (PCR primer)	Metabion	Martinsried	Germany
ECL Advance™ blocking agent	GE Healthcare Life sciences	Freiburg	Germany
Ethanol (C_2H_6O)	J.T. Baker, Mallinckrodt	Deventer	Netherlands
Ethanol, vergällt (C_2H_6O)	CLN GmbH	Niederhummel	Germany
Ethidium bromide ($C_{21}H_{20}BrN_3$)	Carl Roth GmbH & Co. KG	Karlsruhe	Germany
Gene Ruler, 50 bp ladder	Fermentas GmbH	St. Leon-Rot	Germany
Glycerol ($C_3H_8O_3$)	Carl Roth GmbH & Co. KG	Karlsruhe	Germany
Glycerol 2-phosphate disodium salt hydrate ($C_3H_7Na_2O_6P \cdot xH2O$)	Sigma-Aldrich Chemie GmbH	Taufkirchen	Germany
Glycine ($C_2H_5NO_2$)	Merck KGaA	Darmstadt	Germany
Hydrochloric acid (HCl)	Carl Roth GmbH & Co. KG	Karlsruhe	Germany
Magnesium chloride ($MgCl_2$)	Merck KGaA	Darmstadt	Germany
Methanol (CH_4O)	Merck KGaA	Darmstadt	Germany
Nitrogen, liquid (N_2)	Linde Gas	Unterschleißheim	Germany
Nonidet P-40 ($C_{33}H_{60}O_{10}$ (n=9))	Sigma-Aldrich Chemie GmbH	Taufkirchen	Germany
Orange G	Sigma-Aldrich Chemie GmbH	Taufkirchen	Germany
p70 S6 Kinase Control Cell Extracts	Cell Signaling / New England Biolabs GmbH	Frankfurt am Main	Germany
PageBlue™ Protein staining solution	Fermentas GmbH	St. Leon-Rot	Germany
Pageruler, prestained	Fermentas GmbH	St. Leon-Rot	Germany
Paraplast®	Carl Roth GmbH & Co. KG	Karlsruhe	Germany
Potassium chloride (KCl)	Carl Roth GmbH & Co. KG	Karlsruhe	Germany
Protease inhibitor cocktail	Sigma-Aldrich Chemie GmbH	Taufkirchen	Germany
Rnase-Zap®	Sigma-Aldrich Chemie GmbH	Taufkirchen	Germany
Roti-Histofix 4 %, pH 7, phosphate-buffered formaldehyde solution	Carl Roth GmbH & Co. KG	Karlsruhe	Germany
Sodium acetate ($C_2H_3NaO_2$)	Carl Roth GmbH & Co. KG	Karlsruhe	Germany
Sodium chloride (NaCl)	Merck KGaA	Darmstadt	Germany
Sodium dodecyl-sulphate (SDS) ($NaC_{12}H_{25}SO_4$)	Carl Roth GmbH & Co. KG	Karlsruhe	Germany
Sodium floride (NaF)	Carl Roth GmbH & Co. KG	Karlsruhe	Germany
Sodium hydroxide (NaOH)	Merck KGaA	Darmstadt	Germany
Sodium sulphate (Na_2SO_4)	Merck KGaA	Darmstadt	Germany
Sodium-deoxycholate ($C_{24}H_{39}NaO_4$)	Sigma-Aldrich Chemie GmbH	Taufkirchen	Germany
Tetramethylethylenediamine (TEMED) ($C_6H_{16}N_2$)	Merck KGaA	Darmstadt	Germany
Titriplex® Ethylenediaminetetraacetic acid (EDTA) ($C_{10}H_{16}N_2O_8$)	Merck KGaA	Darmstadt	Germany
TRI Reagent® RNA Isolation Reagent	Sigma-Aldrich Chemie GmbH	Taufkirchen	Germany
TRIS (Tris-aminomethan) ($C_4H_{11}NO_3$)	AppliChem GmbH	Darmstadt	Germany
ε-Amino-n-caproic acid ($C_6H_{13}NO_2$)	Sigma-Aldrich Chemie GmbH	Taufkirchen	Germany

8.7 Kits

Item	Company	City	Country
Agilent RNA 6000 Nano Kit	Agilent Technologies	Waldbronn	Germany
C-peptide ELISA Kit	Dako	Glostrup	Denmark
Expression BeadChips Human HT-12 v4- Kit	Illumina	San Diego	CA, USA
Glucose (HK) Assay Kit	Sigma-Aldrich Chemie GmbH	Taufkirchen	Germany
High Sensitive Quantikine HS ELISA	R & D Systems	Minneapolis	MN, USA
HMW and Total adiponectin ELISA	Alpco	Salem	NH, USA
HotStarTaq® PCR Kit	Qiagen	Hilden	Germany
Human Leptin DuoSet	R & D Systems	Minneapolis	MN, USA
Illumina® TotalPrep™ RNA Amplification kit	Ambion	Austin	TX, USA
Insulin ELISA Kit	Dako	Glostrup	Denmark
mRNeasy® Midi Kit	Qiagen	Hilden	Germany
Omniscript® reverse transcription kit	Qiagen	Hilden	Germany
QuantiTect® SYBR® Green PCR kit	Qiagen	Hilden	Germany
RNase-free DNase Set	Qiagen	Hilden	Germany

9 Appendix

9.1 Supplemental figures

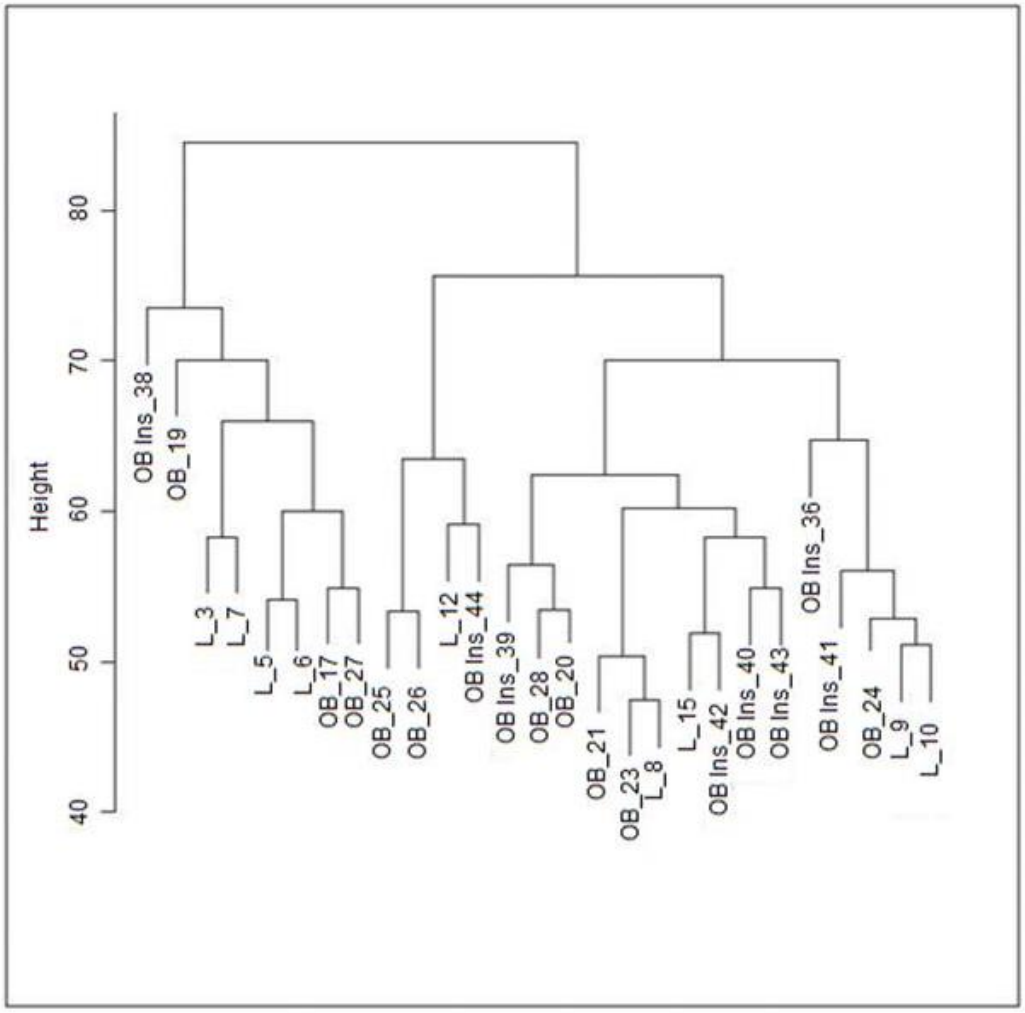

Supplemental figure 1: Hierarchical dendrogram of placental microarray data. The analysis was conducted with all genes passing the initial expression filter **≥** 30 in at least one group (25722 genes) on log_2-transformed data. Analysis and imaging were performed by "R" statistical package. L: lean; OB: obese; OB Ins: obese GDM (insulin therapy). Analysis was performed in term placentas of lean (n=9), obese (n=10) and obese GDM (n=8) women.

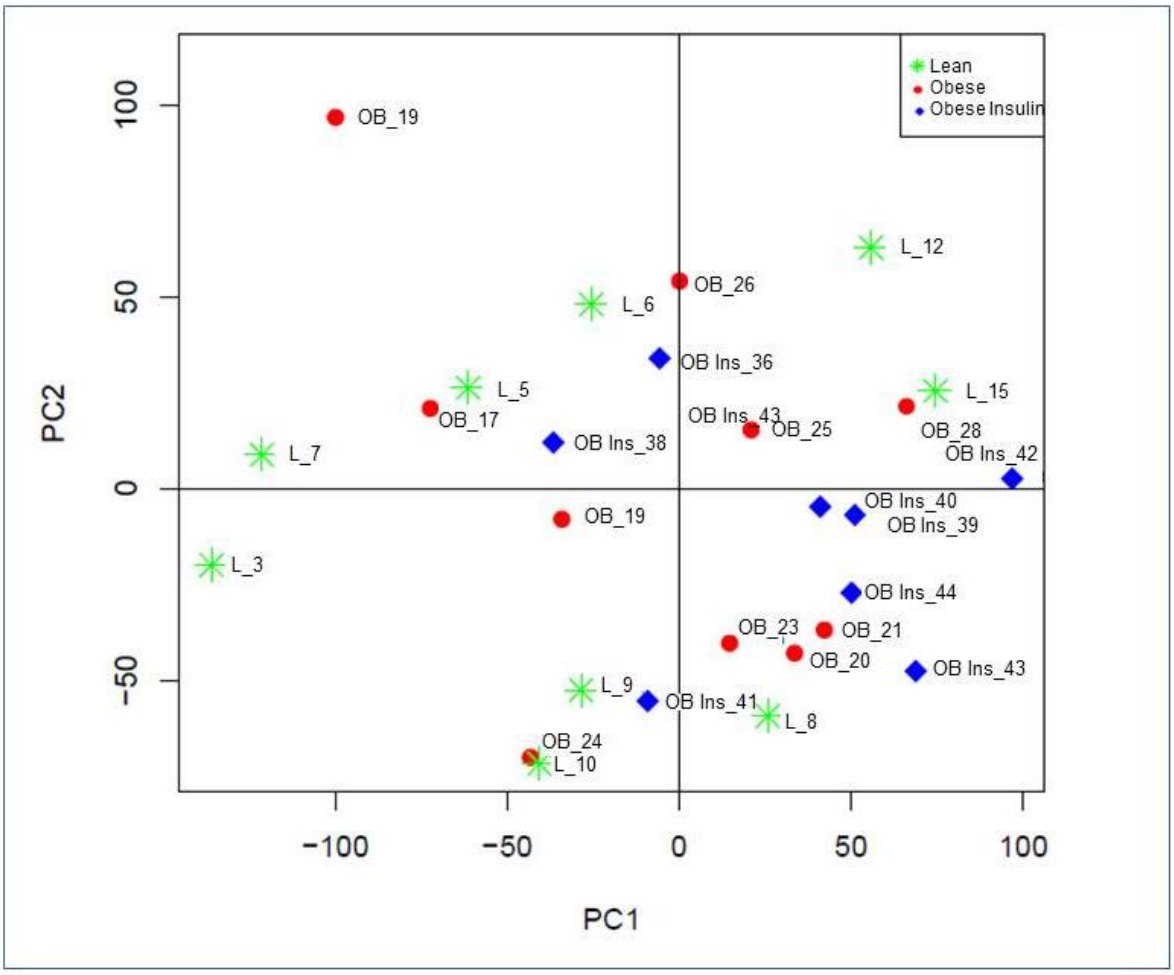

Supplemental figure 2: Principle component analysis of placental microarray data. The variance explained by the first principal components and the projections of the selected samples to the principal component (PC) 1 and PC2 are shown in the PCA scatter blot. The analysis was conducted with all genes passing the initial expression filter ≥ 30 in at least one group (25722 genes) on log_2-transformed data. Analysis and imaging were performed by "R" statistical package. L: lean; OB: obese; OB Ins: obese GDM (insulin therapy). Analysis was performed in term placentas of lean (n=9), obese (n=10) and obese GDM (n=8) women.

Supplemental figure 3: Western immunblots from all samples **A)** pGSK3β (Ser 9), **B)** total GSK3β, **C)** pAKT (Ser 473), **D)** total AKT, **E)** nuclear β-catenin. Blots were normalized to GAPDH (37 kDa) and Lamin A (70 kDa, only additionally for total β-catenin). Cyt: cytosolic samples (control sample for Lamin A and GAPDH protein expression); M: Membrane; L: Lean, OB: Obese. * Equal amounts of one of the *GesA* samples were applied on all 4 blots, respectively, to ensure equal blot development for different membranes. The groups L, OB and OB GDM and respective sample numbers are presented below the membranes. The individual parts of the membranes which include the specific protein bands used for the collage **(Figure 26 and 28)** are highlighted by respective frames. Positions of specific proteins of the molecular weight marker (M) are depicted at the margin of the membranes.

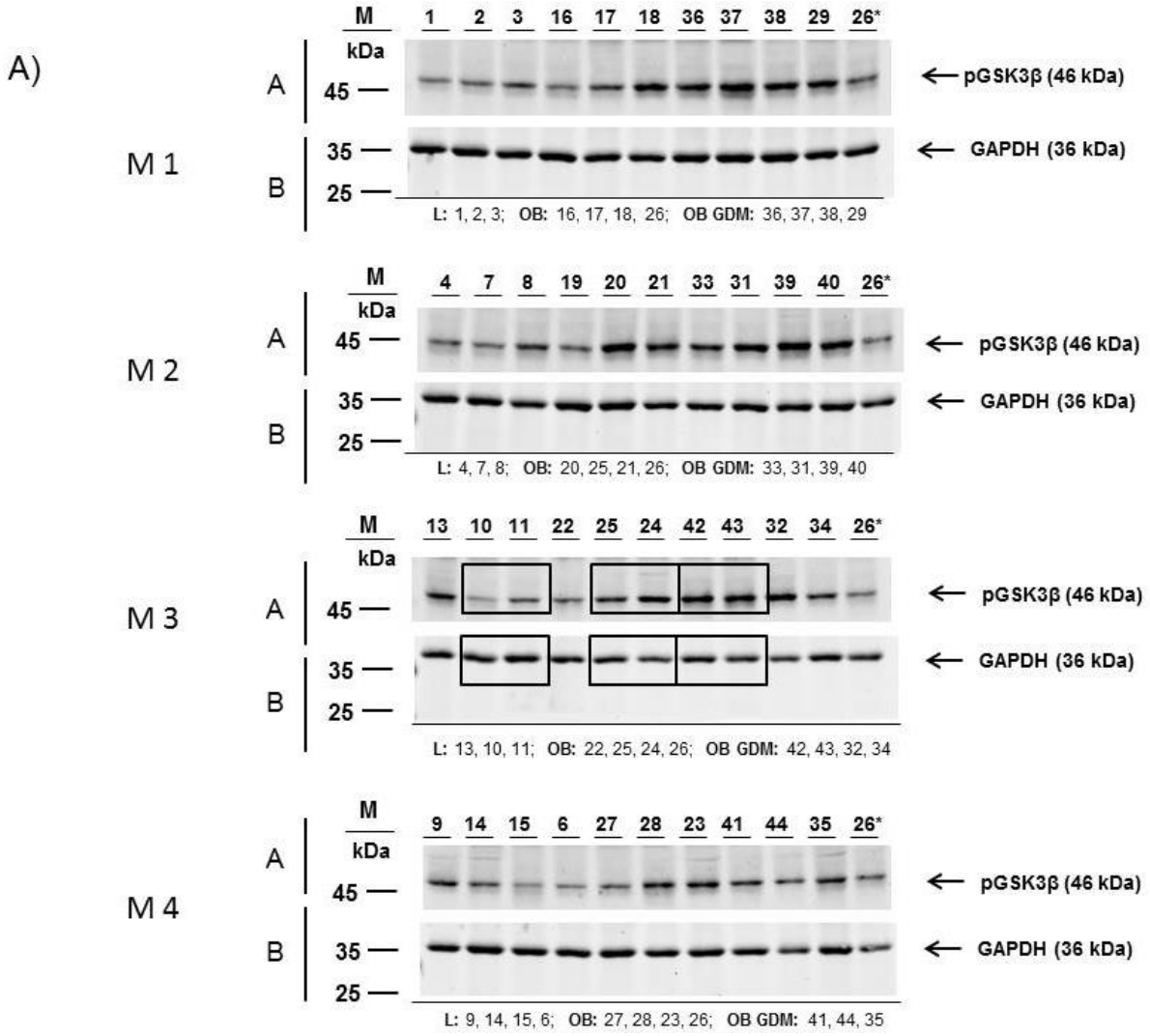

Continued supplemental figure 3

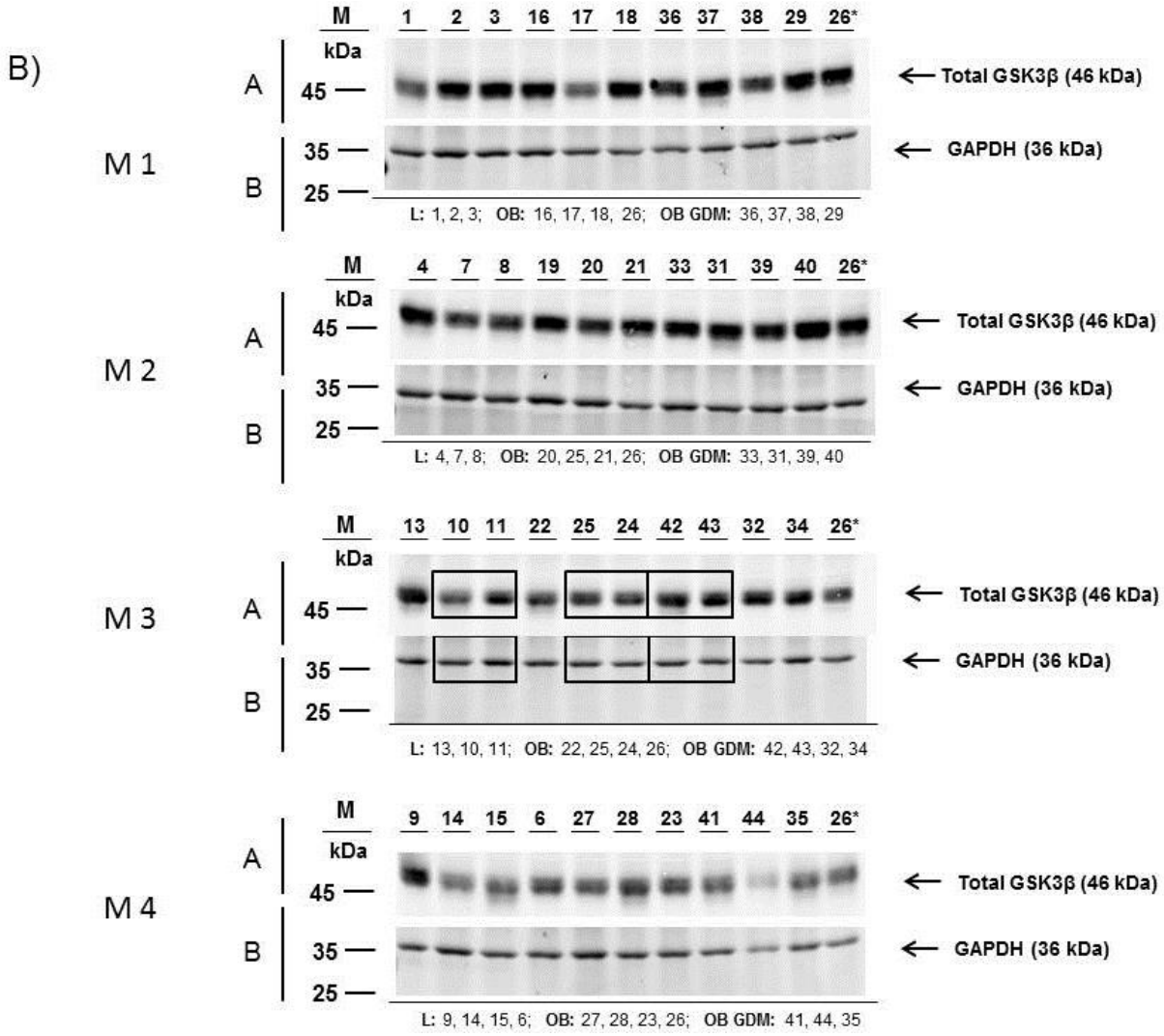

Continued supplemental figure 3

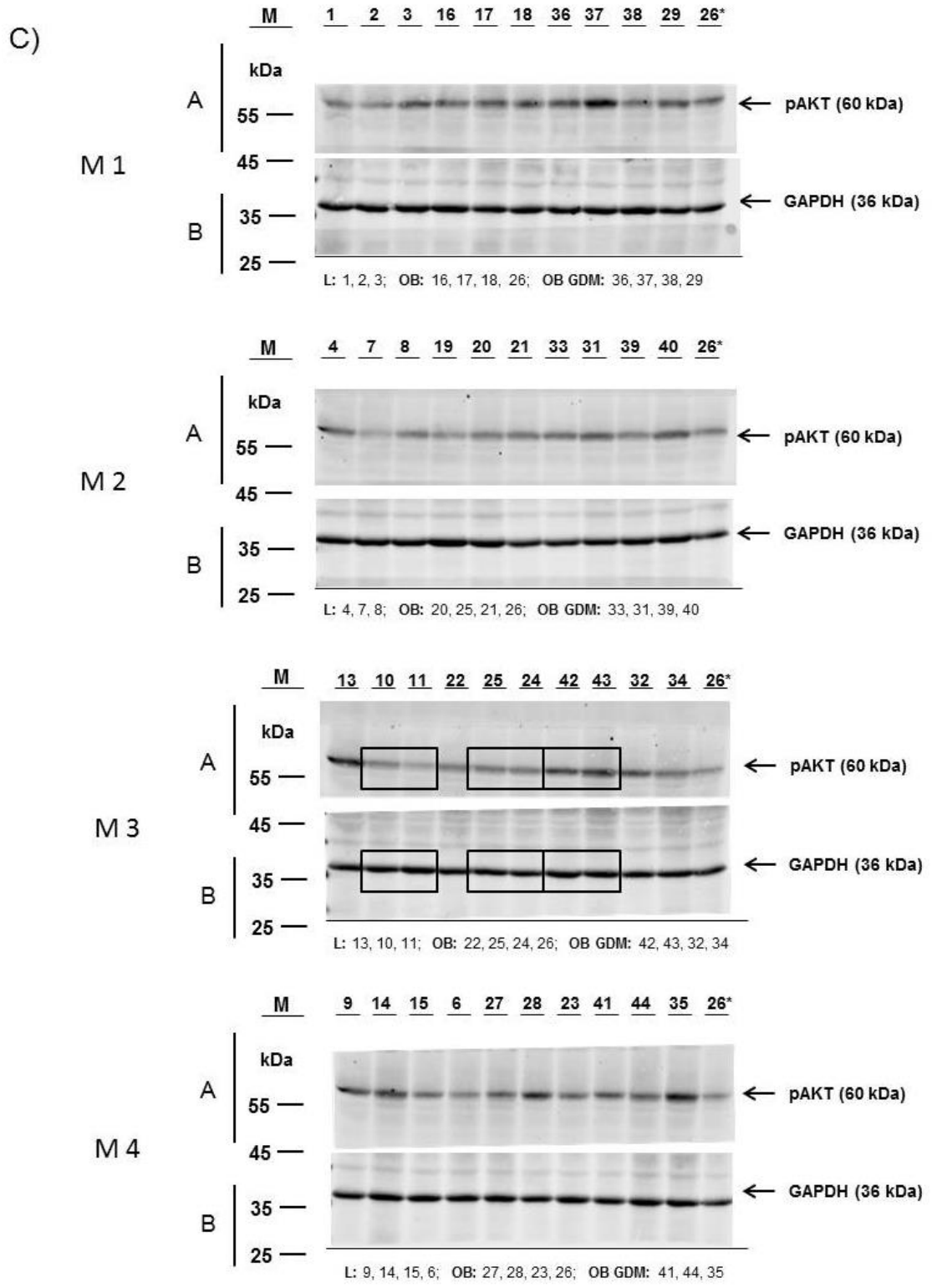

Continued supplemental figure 3

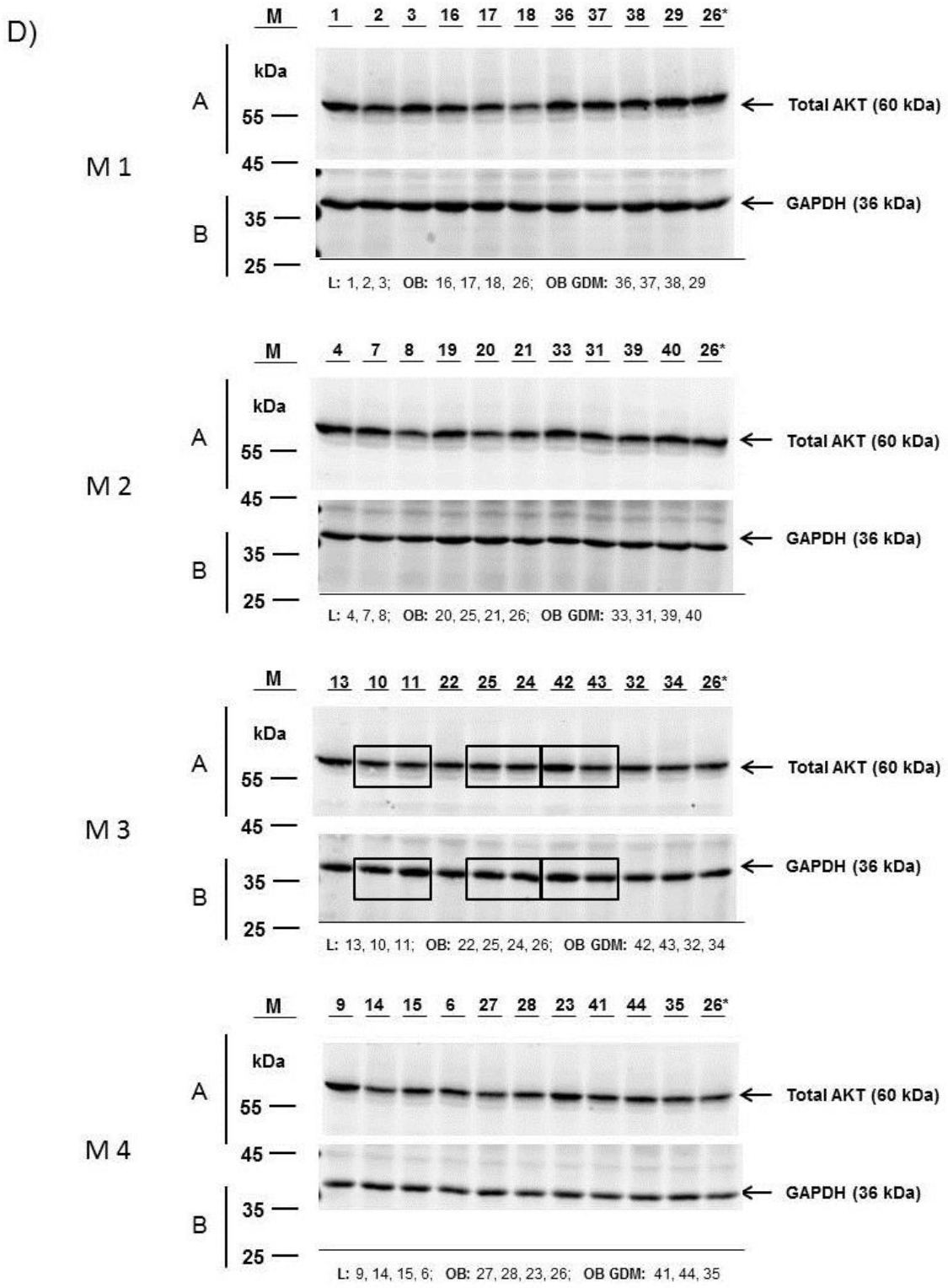

Continued supplemental figure 3

E)

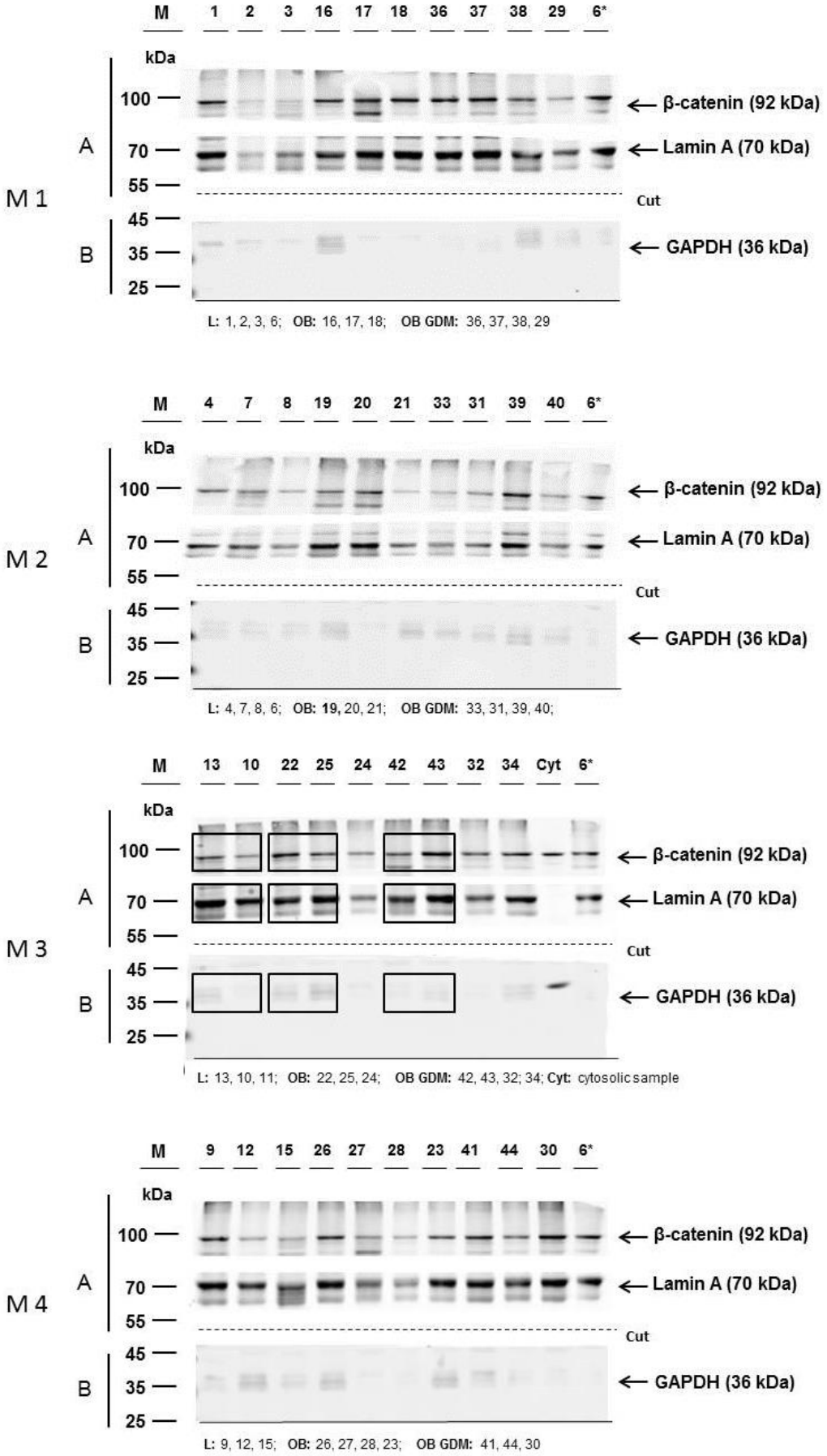

9.2 Supplemental tables

Supplemental table 1: Group allocation according to glucose levels obtained from OGTT at 3rd trimester

Group	Participant	Fasted (mmol/L)	1h (mmol/L)	2h (mmol/L)
Lean	L_1	4.50	6.22	5.72
Lean	L_2	4.33	7.22	6.05
Lean	L_3	4.22	7.05	6.77
Lean	L_4	4.22	6.77	6.05
Lean	L_5	4.00	7.38	5.66
Lean	L_6	4.55	5.94	6.44
Lean	L_7	4.38	7.10	7.88
Lean	L_8	3.61	7.55	6.49
Lean	L_9	3.66	7.38	5.55
Lean	L_10	3.94	8.27	7.49
Lean	L_11	3.89	9.38	4.77
Lean	L_12	3.77	7.60	6.60
Lean	L_13	4.61	7.27	7.16
Lean	L_14	4.38	8.88	7.33
Lean	L_15	4.00	7.10	4.55
Obese	OB_16	4.66	6.22	6.49
Obese	OB_17	4.72	9.49	7.99
Obese	OB_18	4.00	4.50	8.44
Obese	OB_19	4.16	9.21	7.99
Obese	OB_20	4.00	7.05	5.61
Obese	OB_21	4.33	7.49	7.16
Obese	OB_22	4.38	8.88	5.99
Obese	OB_23	4.00	6.44	4.83
Obese	OB_24	4.38	6.83	5.49
Obese	OB_25	4.77	7.88	6.72
Obese	OB_26	3.50	7.10	5.99
Obese	OB_27	4.16	8.44	7.22
Obese	OB_28	3.89	5.27	4.55
Obese+GDM (Diet)	GDM_29	**5.11**	9.71	6.66
Obese+GDM (Diet)	GDM_30	4.16	**10.27**	7.99
Obese+GDM (Diet)	GDM_31	4.72	9.55	**8.82**
Obese+GDM (Diet)	GDM_32	4.38	**10.38**	7.66
Obese+GDM (Diet)	GDM_33	3.94	**9.99**	6.88
Obese+GDM (Diet)	GDM_34	4.50	**11.49**	**9.44**
Obese+GDM (Diet)	GDM_35	**5.61**	**11.54**	7.66
Obese+GDM (Insulin)	GDM_36	4.44	9.44	**8.66**
Obese+GDM (Insulin)	GDM_37	**5.72**	**10.99**	5.22
Obese+GDM (Insulin)	GDM_38	**6.44**	**13.99**	**10.82**
Obese+GDM (Insulin)	GDM_39	4.44	**10.10**	6.66
Obese+GDM (Insulin)	GDM_40	**6.38**	**10.82**	7.94
Obese+GDM (Insulin)	GDM_41	**5.33**	**10.27**	6.55
Obese+GDM (Insulin)	GDM_42	**5.16**	**10.71**	7.55
Obese+GDM (Insulin)	GDM_43	**5.44**	**13.60**	**11.27**
Obese+GDM (Insulin)	GDM_44	**5.27**	9.71	7.71

Glucose level exceeding the HAPO criteria [40] are presented in bold type

Supplemental table 2: Overview on diet / insulin therapy and self-reported glucose measurements in the obese GDM group

No.	GDM treatment	Begin of insulin therapy (gest. week)	IE insulin/day (begin of treatment)	IE insulin/day (before delivery)	Self-reported mean glucose (mmol/L)				Evaluation of glucose levels
					fasted	Postp. after breakfast	Postp. after lunch	Postp. after dinner	
GDM_29	Diet		-	-	4.61	-	-	-	negative results
GDM_30	Diet		-	-	4.27	5.00#	4.88#	5.38#	negative results
GDM_31	Diet		-	-	3.89	-	-	-	negative results
GDM_32	Diet	-	-	-	4.61	5.66#	-	-	negative results
GDM_33	Diet	-	-	-	4.88	-	-	-	negative results
GDM_34	Diet	-	-	-	4.16	6.60#	6.16#	6.11#	negative results
GDM_35	Diet	-	-	-	4.77	5.66#	7.88#	7.22#	partly elevated, irregular measurements
GDM_36	Diet/Insulin	- 28	n/a	72	6.05	11.04#	-	-	labile diabetes, under strict medical survey, protocols not available
GDM_37	Diet/Insulin	34	20	23	4.33	6.22#	5.83#	6.05#	negative results
GDM_38	Diet/Insulin	34	4	12	5.00	6.88#	6.88#	6.83#	borderline elevated in fasted state
GDM_39	Diet/Insulin	26	10	44	-	-	-	-	labile diabetes, under strict medical survey, protocols not available
GDM_40	Diet/Insulin	31	10	16	5.27	6.94#	7.05#	6.94#	elevated in fasted state
GDM_41	Diet/Insulin	34	31	46	4.77	6.77§	6.05§	6.11§	negative results
GDM_42	Diet/Insulin	38	6	6	4.55	5.38§	5.88§	5.99§	negative results
GDM_43	Diet/Insulin	15	12	176	4.94	5.88§	5.94§	6.27§	borderline elevated in fasted state
GDM_44	Diet/Insulin	32	25	43	4.72	7.55#	7.27#	7.10#	borderline elevated after breakfast (and lunch)

Recommendation: Fasted < 5.00 mmol/L.
Recommendation: Postprandial (postp.): 1 h < 7.70 mmol/L or 2h < 6.66 mmol/L (dependent on counseling by dietician/diabetologist)

Measurement 1 h postprandial.; § Measurement 2 h postprandial

Supplemental table 3: Differential blood cell count from maternal samples obtained at 3rd trimester, delivery and at week-6 *pp*

Immune cell marker	Lean group	Obese group	Obese GDM group	P-value
3rd trimester				
N	**15**	**12**	**13**	
Leukocytes / nl	9.0 (8.6-11.0)	9.7 (7.9-10.9)	9.9 (8.3-11.8)	0.655
Lymphocytes (%)	20.1 ± 4.7	22.2 ± 5.1	19.6 ± 4.3	0.375
Monocytes (%)	6.6 ± 1.9	6.6 ± 1.8	6.2 ± 1.6	0.794
Neutrophil granolocytes (%)	69.4 (63.0-75.6)	66.7 (63.8-73.6)	74.7 (67.2-77.0)	0.145
Eosinophil granulocytes (%)	1.1 ± 0.6	1.1 ± 0.6	0.9 ± 0.6	0.614
Basophil granulocytes (%)	0.3 (0.0-0.3)	0.2 (0.0-0.3)	0.2 (0.1-0.3)	0.675
Delivery				
N	**13**	**13**	**16**	
Leukocytes / nl	11.2 ± 4.5	10.7 ± 4.3	11.2 ± 3.9	0.948
Lymphocytes (%)	15.2 (12.5-21.3)	18.0 (15.5-31.2)	18.1 (14.3-23.7)	0.186
Monocytes (%)	6.0 (5.3-8.5)	6.1 (5.1-7.9)	5.9 (4.9-7.4)	0.862
Neutrophil granolocytes (%)	77.2 (69.3-81.7)	66.0 (62.5-73.2)	74.1 (70.0-79.2)	**0.047** [#]
Eosinophil granulocytes (%)	0.8 (0.1-2.1)	0.6 (0.0-1.0)	0.5 (0.2-1.0)	0.727
Basophil granulocytes (%)	0.2 (0.1-0.3)	0.1 (0.0-0.6)	0.2 (0.1-0.5)	0.379
Week-6 *pp*				
N	**15**	**11**	**9**	
Leukocytes / nl	6.3 ± 1.6	6.6 ± 0.5	7.1 ± 1.3	0.307
Lymphocytes (%)	34.9 ± 8.7	30.3 ± 6.0	28.6 ± 5.0	0.103
Monocytes (%)	7.3 ± 2.3	7.0 ± 2.0	6.1 ± 2.3	0.490
Neutrophil granolocytes (%)	55.3 (45.4-64.3)	60.2 (56.4-63.0)	60.9 (54.1-65.8)	0.193
Eosinophil granulocytes (%)	3.0 (1.8-4.2)	1.8 (1.6-2.6)	2.1 (1.5-4.6)	0.226
Basophil granulocytes (%)	0.4 (0.3-0.5)	0.3 (0.2-0.5)	0.4 (0.2-0.8)	0.314

[#] According to pairwise multiple comparison procedures (Dunn's Method): $p > 0.05$ obese vs. obese group

Supplemental table 4: Regression of adipose tissue distribution up to year-1 on maternal plasma metabolic markers at 3rd trimester

		Maternal C-peptide					Maternal insulin					Maternal leptin				
		Unadjusted analysis		Adjusted analysis			Unadjusted analysis		Adjusted analysis			Unadjusted analysis		Adjusted analysis		
	N	β	P-value	β	P-value	Adj. model r^2	β	P-value	β	P-value	Adj. model r^2	β	P-value	β	P-value	Adj. model r^2
Week-1																
SFT	43	0.398	0.007	0.325	0.071	0.195; p=0.026	0.242	0.122	0.108	0.541	0.087; p=0.163	0.295	0.052	-0.113	0.612	0.126; p=0.085
SCA	36	0.135	0.432	0.063	0.719	0.203; p=0.046	0.122	0.477	-0.002	0.990	0.199: p=0.049	**0.332**	**0.048**	0.097	0.684	0.204; p=0.045
PPA	36	**0.539**	**0.001**	**0.533**	**0.001**	0.430; p=0.001	**0.508**	**0.002**	**0.444**	**0.010**	0.345; p=0.004	0.261	0.124	-0.031	0.402	0.202; p=0.047
Week-6																
SFT	40	0.116	0.489	0.256	0.163	0.137; p=0.110	0.318	0.049	0.307	0.087	0.164; p=0.078	0.003	0.986	-0.359	0.146	0.122; p=0.127
SCA	40	0.073	0.660	0.117	0.515	0.146; p=0.098	0.294	0.069	0.293	0.093	0.211; p=0.040	0.182	0.262	0.040	0.868	0.123; p=0.126
PPA	40	0.055	0.739	-0.009	0.960	0.179; p=0.063	0.332	0.039	0.232	0.174	0.227; p=0.031	0.260	0.105	-0.001	0.996	0.209; p=0.038
Month-4																
SFT	39	0.009	0.958	0.054	0.785	0.118; p=0.145	0.197	0.237	0.241	0.208	0.162; p=0.085	-0.039	0.814	-0.254	0.327	0.080; p=0.213
SCA	39	-0.080	0.633	-0.008	0.967	0.050; p=0.295	0.135	0.418	0.241	0.226	0.096; p=0.185	0.031	0.853	-0.023	0.934	-0.046; p=0.624
PPA	39	0.095	0.565	0.267	0.212	-0.046;p=0.622	-0.023	0.887	0.053	0.805	-0.098; p=0.816	0.120	0.460	0.368	0.319	-0.057; p=0.671
Year-1																
SFT	41	-0.047	0.774	-0.220	0.288	-0.026;p=0.548	0.233	0.148	0.157	0.451	-0.044; p=0.621	-0.006	0.969	-0.185	0.482	-0.064; p=0.705
SCA	41	0.152	0.348	0.003	0.989	-0.007;p=0.476	0.305	0.056	0.013	0.961	-0.040; p=0.607	0.213	0.182	0.195	0.334	0.022; p=0.371
PPA	41	0.225	0.162	0.202	0.275	0.177; p=0.061	0.251	0.118	-0.215	0.358	0.159; p=0.074	0.181	0.257	0.120	0.520	0.156; p=0.081

β: standardized regression coefficient; HMW: high molecular weight; PPA: preperitoneal adipose tissue; r^2: coefficient of determination. S_A: HMW-total adiponectin ratio; SCA: subcutaneous adipose tissue; SFT: sum of the 4 skin fold thickness measurements (biceps + triceps + subscapular + suprailiac). Variables for adjusted analysis: infant sex, pregnancy duration, respective breastfeeding status, maternal pre-pregnancy BMI, $AUC_{Glucose}$ (OGTT) and gestational weight gain.

Continued supplemental table 4: Regression of adipose tissue distribution up to year-1 on maternal plasma metabolic markers at 3rd trimester

		Maternal total adiponectin					Maternal HMW adiponectin					Maternal S_A				
		Unadjusted analysis		Adjusted analysis			Unadjusted analysis		Adjusted analysis			Unadjusted analysis		Adjusted analysis		
	N	β	P-value	β	P-value	Adj. model r^2	β	P-value	β	P-value	Adj. model r^2	β	P-value	β	P-value	Adj. model r^2
Week-1																
SFT	43	-0.251	0.100	-0.077	0.638	0.125; p=0.087	-0.278	0.068	-0.077	0.638	0.125; p=0.087	-0.238	0.120	0.031	0.860	0.121; p=0.093
SCA	36	-0.037	0.831	0.047	0.776	0.201; p=0.047	-0.040	0.432	0.047	0.776	0.201: p=0.047	-0.115	0.502	-0.007	0.969	0.199; p=0.049
PPA	36	**-0.391**	**0.018**	-0.299	0.056	0.271; p=0.016	**-0.481**	**0.003**	**-0.338**	**0.038**	0.288; p=0.012	**-0.479**	**0.003**	-0.280	0.115	0.241; p=0.026
Week-6																
SFT	40	0.039	0.810	0.095	0.550	0.070; p=0.232	-0.039	0.812	0.126	0.498	0.075; p=0.220	-0.157	0.340	0.056	0.283	0.064; p=0.248
SCA	40	0.033	0.842	0.146	0.417	0.140; p=0.101	-0.005	0.977	0.146	0.417	0.140; p=0.101	-0.101	0.537	0.105	0.587	0.130; p=0.115
PPA	40	**-0.318**	**0.045**	0.256	0.105	0.272; p=0.013	**-0.325**	**0.041**	-0.244	0.147	0.260; p=0.017	**-0.326**	**0.040**	-0.181	0.323	0.233; p=0.026
Month-4																
SFT	39	0.108	0.514	0.060	0.735	0.055; p=0.277	0.105	0.525	0.131	0.479	0.067; p=0.246	0.054	0.742	0.202	0.295	0.085; p=0.203
SCA	39	0.243	0.137	0.242	0.187	0.012; p=0.409	0.282	0.081	**0.387**	**0.041**	0.088; p=0.196	0.239	0.143	0.475	0.015	0.138; p=0.109
PPA	39	-0.053	0.746	-0.015	0.937	-0.090; p=0.799	0.014	0.930	0.077	0.694	-0.085; p=0.780	0.105	0.518	0.148	0.426	0.123; p=0.718
Year-1																
SFT	41	0.177	0.269	0.196	0.278	-0.042; p=0.615	0.169	0.290	0.226	0.234	-0.034; p=0.583	0.102	0.526	0.208	0.304	-0.045; p=0.631
SCA	41	-0.011	0.946	0.054	0.761	-0.037; p=0.595	-0.026	0.872	0.109	0.562	-0.029; p=0.564	-0.090	0.575	0.119	0.552	-0.029; p=0.561
PPA	41	-0.299	0.057	-0.208	0.195	0.180; p=0.054	-0.224	0.159	-0.105	0.539	0.147; p=0.087	0.084	0.603	-0.137	0.416	0.154; p=0.079

β: standardized regression coefficient; HMW: high molecular weight; PPA: preperitoneal adipose tissue; r^2: coefficient of determination. S_A: HMW-total adiponectin ratio; SCA: subcutaneous adipose tissue; SFT: sum of the 4 skin fold thickness measurements (biceps + triceps + subscapular + suprailiac). Variables for adjusted analysis: infant sex, pregnancy duration, respective breastfeeding status, maternal pre-pregnancy BMI, $AUC_{Glucose}$ (OGTT) and gestational weight gain.

Supplemental table 5. Common and differentially regulated placentas genes of obese women with and without GDM and lean women [#]

Gene symbol	Gene name	Gene ontology (Molecular Function)	OB vs. L	OB GDM vs. L	OB GDM vs. OB
Common regulated genes in obese and obese GDM vs. lean group (n=35)					
ADAMTS6	ADAM metallopeptidase with thrombospondin type 1 motif, 6	Metalloendopeptidase activity, zinc ion binding	1.31	1.32	-
BTBD16	BTB (POZ) domain containing 16	-	1.78	2.33	-
C7orf28B	Chromosome 7 open reading frame 28B	-	-1.59	-1.93	-
CFD	Complement factor D (adipsin)	Serine-type endopeptidase activity	-1.40	-1.48	-
CLCNKA	Chloride channel Ka	Voltage-gated chloride channel activity	1.39	1.55	-
CLDN8	Claudin 8	Identical protein binding, structural molecule activity	1.53	2.02	-
CNN1	calponin 1, basic, smooth muscle	Actin binding, calmodulin binding	-1.48	-1.55	-
ENPP4	Ectonucleotide pyrophosphatase/phosphodiesterase 4	Hydrolase activity	1.38	1.30	-
FER1L5	Fer-1-like 5 (C. elegans)	-	1.34	1.49	-
HIST1H4H	Histone cluster 1, H4h	-	1.62	1.69	-
HMGCS2	3-Hydroxy-3-methylglutaryl-Coenzyme A synthase 2 (mitochondrial)	Hydroxymethylglutaryl-CoA synthase activity	1.67	2.26	-
HPSE	Heparanase	Beta-glucuronidase activity, syndecan binding	1.92	2.18	-
HSPA1A	Heat shock 70kDa protein 1A	-	-1.67	-1.82	-
JUNB	Jun B proto-oncogene	DNA binding, RNA polymerase II regulatory region sequence-specific, transcription coactivator/corepressor activity, protein binding	-1.32	-1.30	-
KRT14	Keratin 14	Protein binding, structural constituent of cytoskeleton	-1.34	-1.36	-
LOC121838	Predicted: misc_RNA	-	1.71	2.03	-
LOC653648	Predicted:similar to neurotrophic tyrosine kinase, receptor, type 2	-	1.39	1.50	-
LOC728431	PREDICTED: hypothetical LOC728431	-	1.46	1.45	-
LVRN	Laeverin	Metalloendopeptidase activity, zinc ion binding	1.41	1.43	-
MIR1974	MicroRNA 1974	-	2.61	2.74	-
MYADM	Myeloid-associated differentiation marker	-	-1.53	-1.47	-
NMNAT2	Nicotinamide nucleotide adenylyltransferase 2	ATP binding, nicotinamide/nicotinate-nucleotide adenylyltransferase activity	1.65	1.31	-
PCDH11X	Protocadherin 11 X-linked	Calcium ion binding	1.37	1.88	-
PHYHIPL	Phytanoyl-CoA 2-hydroxylase interacting protein-like	-	1.34	1.43	-
PKIA	Protein kinase (cAMP-dependent, catalytic) inhibitor alpha	cAMP-dependent protein kinase inhibitor activity, protein kinase A catalytic subunit binding	1.41	1.54	-
PRL	Prolactin	Hormone activity prolactin receptor binding, protein binding	-1.67	-1.67	-
PSG6	Pregnancy specific beta-1-glycoprotein 6	-	1.31	1.37	-
TCL6	T-cell leukemia/lymphoma 6	-	1.64	2.00	-
TLN2	Talin 2	Actin binding, insulin receptor binding, structural constituent of cytoskeleton	1.33	1.36	-

Continued supplemental table 5. Common and differentially regulated placentas genes of obese women with and without GDM and lean women [#]

Gene symbol	Gene name	Gene ontology (Molecular Function)	OB vs. L	OB GDM vs. L	OB GDM vs. OB
TMPRSS2	Transmembrane protease, serine 2	Scavenger receptor activity, serine-type endopeptidase activity, serine-type peptidase activity	1.33	1.56	-
TPRXL	Tetra-peptide repeat homeobox-like	-	1.30	1.37	-
UPLP	Uroplakin-like protein	-	-1.30	-1.35	-
USP27X	Predicted: Ubiquitin specific peptidase 27, X-linked	Cysteine-type peptidase activity ubiquitin thiolesterase activity	1.33	1.35	-
USP46	Ubiquitin specific peptidase 46	Protein binding, ubiquitin thiolesterase activity, ubiquitin-specific protease activity	1.30	1.50	-
ZNF114	Zinc finger protein 114	DNA binding, zinc ion binding	1.43	1.94	-
Common regulated genes in obese GDM vs. normoglycemic obese and lean group (n= 151)					
ABHD12	Abhydrolase domain containing 12	Acylglycerol lipase activity	-	1.43	1.35
AF131784	Clone 25194 mRNA sequence	-	-	1.44	1.34
AFAP1	Actin filament associated protein 1	Actin binding	-	1.46	1.45
AGR3	Anterior gradient homolog 3	Dystroglycan binding, protein binding	-	1.47	1.45
AKIRIN1	Akirin 1	-	-	1.40	1.30
ANGPTL2	Angiopoietin-like 2	Receptor binding	-	-1.35	-1.36
ANO3	Anoctamin 3	NOT intracellular calcium activated chloride channel activity	-	1.95	1.98
ANXA4	Annexin A4	Calcium ion binding, phospholipase inhibitor activity,calcium-dependent phospholipid binding	-	1.55	1.53
ARHGAP4	Rho GTPase activating protein 4	Rho GTPase activator activity, SH3/SH2 adaptor activity	-	-1.30	-1.31
ARHGEF6	Rac/Cdc42 guanine nucleotide exchange factor 6	GTPase activator activity, Rho guanyl-nucleotide exchange factor activity, phospholipid binding	-	-1.31	-1.50
ARL17B	ADP-ribosylation factor-like 17B	GTP binding	-	-2.04	-1.83
ARL17P1	ADP-ribosylation factor-like 17 pseudogene 1	-	-	-2.12	-1.86
ATP2C2	ATPase, Ca++ transporting, type 2C, member 2	ATP binding, calcium-transporting ATPase activity, metal ion binding	-	-1.53	-1.57
BAMBI	HBMP and activin membrane-bound inhibitor homolog	Frizzled binding, type II transforming growth factor beta receptor binding	-	-1.38	-1.37
BMP4	Bone morphogenetic protein 4	BMP receptor binding, chemoattractant/cytokine activity, growth factor activity, heparin binding	-	-1.50	-1.39
BMP5	Bone morphogenetic protein 5	BMP receptor binding, cytokine activity, growth factor activity	-	-1.43	-1.37
C20orf54	Chromosome 20 open reading frame 54	Riboflavin transporter activity	-	1.36	1.38
C6orf52	Predicted:Chromosome 6 open reading frame 52	-	-	-1.32	-1.38
C9orf84	Chromosome 9 open reading frame 84	-	-	1.33	1.33
CBLC	Cas-Br-M (murine) ecotropic retroviral transforming sequence c	SH3 domain binding, calcium ion binding, epidermal growth factor receptor binding, phosphotyrosine binding, signal transducer activity, ubiquitin-protein ligase activity, zinc ion binding	-	1.51	1.35
CCND2	Cyclin D2	protein binding, protein kinase binding	-	-1.35	-1.33

Continued supplemental table 5. Common and differentially regulated placentas genes of obese women with and without GDM and lean women [#]

Gene symbol	Gene name	Gene ontology (Molecular Function)	OB vs. L	OB GDM vs. L	OB GDM vs. OB
CD36	CD36 molecule (thrombospondin receptor)	High-density lipoprotein particle binding, low-density lipoprotein receptor activity, lipoteichoic acid receptor activity, thrombospondin receptor activity, transforming growth factor beta binding	-	-1.47	-1.40
CDH11	Cadherin 11, type 2, OB-cadherin (osteoblast)	Calcium ion binding	-	-1.51	-1.36
CDK10	cyclin-dependent kinase 10	ATP binding, cyclin-dependent protein serine/threonine kinase activity, protein binding	-	-1.39	-1.30
CDO1	Cysteine dioxygenase, type I	Cysteine dioxygenase activity, cysteine dioxygenase activity, ferrous iron binding	-	1.36	1.40
CFB	Complement factor B	Complement binding serine-type endopeptidase activity	-	1.35	1.36
COL16A1	Collagen, type XVI, alpha 1	Integrin binding, receptor binding	-	-1.45	-1.58
COL1A1	Collagen, type I, alpha 1	extracellular matrix structural constituent, identical protein binding, metal ion binding platelet-derived growth factor binding,	-	-1.67	-1.54
COL5A1	Collagen, type V, alpha 1	Extracellular matrix structural constituent, heparin binding , integrin binding, metal ion binding, platelet-derived growth factor binding, proteoglycan binding	-	-1.38	-1.34
COL6A1	Collagen, type VI, alpha 1	Platelet-derived growth factor binding	-	-1.62	-1.45
COL8A2	Collagen, type VIII, alpha 2	Extracellular matrix structural constituent, protein binding, bridging	-	-1.41	-1.44
COMP	Cartilage oligomeric matrix protein	Calcium ion binding, collagen binding, extracellular matrix structural constituent, heparan sulfate proteoglycan binding, heparin binding, protease binding	-	-2.34	-1.58
CRB3	Crumbs homolog 3 (Drosophila)	SH3 domain binding, protein domain specific binding	-	1.39	1.50
CSPG4	Chondroitin sulfate proteoglycan 4	Protein kinase binding, signal transducer activity	-	-1.32	-1.57
CTHRC1	Collagen triple helix repeat containing 1	Wnt-protein binding, frizzled binding	-	-1.41	-1.47
CTSC	Cathepsin C	Chloride ion binding, cysteine-type peptidase, activityserine-type endopeptidase activity, protein self-association	-	-1.48	-1.48
CXCR7	Chemokine (C-X-C motif) receptor 7	C-X-C chemokine binding, C-X-C chemokine receptor activity, coreceptor activity, scavenger receptor activity	-	-1.44	-1.43
CYP4X1	Cytochrome P450, family 4, subfamily X, polypeptide 1	Aromatase activity, heme binding, iron ion binding	-	-1.32	-1.33
CYTL1	Cytokine-like 1	Receptor binding	-	-1.70	-1.65
DCN	Decorin	Collagen binding, extracellular matrix binding, glycosaminoglycan binding, protein N-terminus binding	-	-1.34	-1.36
DEPDC1B	DEP domain containing 1B	GTPase activator activity	-	1.73	1.37
DGKZ	Diacylglycerol kinase, zeta 104kDa	ATP binding, NAD+ kinase activity, diacylglycerol kinase activity, enzyme inhibitor activity, lipid kinase activity, metal ion binding, protein C-terminus binding	-	1.38	1.34

Continued supplemental table 5. Common and differentially regulated placentas genes of obese women with and without GDM and lean women [#]

Gene symbol	Gene name	Gene ontology (Molecular Function)	OB vs. L	OB GDM vs. L	OB GDM vs. OB
DHRS4	Dehydrogenase/reductase (SDR family)	3-keto sterol reductase activity, carbonyl reductase (NADPH) activity, oxidoreductase activity, acting on NAD(P)H, quinone or similar compound as acceptor	-	-1.40	-1.37
DIO3OS	DIO3 opposite strand (non-protein coding)	-	-	-1.43	-1.48
DKK3	Dickkopf homolog 3 (Xenopus laevis)	-	-	-1.41	-1.35
EDARADD	EDAR-associated death domain	-	-	1.37	1.36
ENPP1	Ectonucleotide pyrophosphatase/phosphodiesterase 1	3'-phosphoadenosine 5'-phosphosulfate binding, ATP binding, NADH pyrophosphatase activity, insulin receptor binding, metal ion binding, nucleoside-triphosphate diphosphatase activity, phosphodiesterase I activity polysaccharide binding, protein homo-dimerization activity, scavenger receptor activity	-	-1.37	-1.39
ENPP2	Ectonucleotide pyrophosphatase/phosphodiesterase 2	alkylglycerophosphoethanolamine phosphodiesterase activity, calcium ion binding, hydrolase activity, lysophospholipase activity, nucleotide diphosphatase activity, phosphodiesterase I activity, polysaccharide binding, scavenger receptor activity, transcription factor binding, zinc ion binding	-	-1.38	-1.44
FAM107B	Family with sequence similarity 107, member B	-	-	1.31	1.37
FBLN2	Fibulin 2	Calcium ion binding, extracellular matrix binding, extracellular matrix structural constituent	-	-1.41	-1.45
FGFR3	Fibroblast growth factor receptor 3	Protein kinase activity,adenyl ribonucleotide binding, transmembrane receptor activity, phosphotransferase activity	-	-1.47	-1.68
FLJ10781	Hypothetical protein FLJ10781	-	-	-1.31	-1.34
FLJ12684	Hypothetical protein FLJ12684	-	-	1.34	1.37
FMOD	Fibromodulin	-	-	-1.56	-1.32
GABBR2	Gamma-aminobutyric acid (GABA) B receptor, 2	Contributes to G-protein coupled GABA receptor activity, protein binding	-	1.54	1.67
GAS6	Growth arrest-specific 6	Phosphatidylserine binding, protein tyrosine kinase activator activity, voltage-gated calcium channel activity, cysteine-type endopeptidase inhibitor activity involved in apoptotic process		-1.36	-1.36
GLIS3	GLIS family zinc finger 3	DNA binding, metal ion binding, sequence-specific DNA binding transcription factor activity	-	1.36	1.41
GREM2	Gremlin 2, cysteine knot superfamily, homolog (Xenopus laevis)	Cytokine activity		1.36	1.44
HEY2	Hairy/enhancer-of-split related with YRPW motif 2	RNA polymerase II core promoter sequence-specific DNA binding transcription factor activity, histone deacetylase binding, microsatellite binding, protein binding transcription factor activity, protein dimerization activity	-	-1.39	-1.36
HIST1H2BG	Histone cluster 1, H2bg	-	-	1.64	1.70
HIST1H2BJ	Histone cluster 1, H2bj	DNA binding, protein heterodimerization activity	-	1.37	1.52
HIST1H3D	Histone cluster 1, H3d	-	-	1.38	1.37
HOXC4	Homeobox C4	HMG box domain binding, sequence-specific DNA binding transcription factor activity	-	-1.32	-1.41

Continued supplemental table 5. Common and differentially regulated placentas genes of obese women with and without GDM and lean women [#]

Gene symbol	Gene name	Gene ontology (Molecular Function)	OB vs. L	OB GDM vs. L	OB GDM vs. OB
HOXC6	Homeobox C6	Sequence-specific DNA binding transcription factor activity, transcription corepressor activity	-	-1.39	-1.48
HPCAL1	Hippocalcin-like 1	-	-	1.46	1.34
HSPA12A	Heat shock 70kDa protein 12A	ATP binding	-	-1.40	-1.33
HSPC047	HSPC047 protein	-	-	0.75	-1.37
IGSF3	Immunoglobulin superfamily, member 3	-	-	1.33	1.44
KCNJ8	Potassium inwardly-rectifying channel, subfamily J, member 8	ATP binding, ATP-activated inward rectifier potassium channel activity, sulfonylurea receptor binding	-	-1.41	-1.46
KCNT1	Potassium channel, subfamily T, member 1	calcium-activated potassium channel activity , voltage-gated potassium channel activity	-	-1.36	-1.60
KLHDC8B	Kelch domain containing 8B	-	-	-1.32	-1.45
LAMC3	Laminin, gamma 3	Structural molecule activity	-	-1.54	-1.59
LGR4	Leucine-rich repeat-containing G protein-coupled receptor 4	NOT G-protein coupled receptor activity, protein binding, transmembrane signaling receptor activity I	-	1.37	1.36
LILRB5	Leukocyte immunoglobulin-like receptor, subfamily B (with TM and ITIM domains), member 5	Transmembrane signaling receptor activity	-	-1.37	-1.32
LOC100134144	Predicted:similar to KIAA1783 protein	-	-	-1.39	-1.39
LOC286297	Predicted: hypothetical protein LOC286297	-	-	1.32	1.30
LOC643293	Predicted: hypothetical protein LOC643293	-	-	-1.33	-1.37
LOC644297	Predicted: similar to Apoptosis-related protein 2	-	-	-1.57	-1.70
LOC644885	Predicted hypothetical LOC644885	-	-	1.38	1.42
LOC653492	Predicted: similar to Pregnancy-specific beta-1-glycoprotein 8 precursor (PSBG-8)	-	-	1.82	1.87
LOC727866	Predicted similar to transmembrane protein 29	-	-	1.38	1.32
LOC728103	Predicted: hypothetical LOC728103	-	-	1.38	1.49
LOC728334	Predicted: hypothetical LOC728334	-	-	1.36	1.42
LOC729008	Predicted: similar to Apoptosis-related protein 2 (APR-2)	-	-	-1.45	-1.55
MAFF	V-maf musculoaponeurotic fibrosarcoma oncogene homolog F (avian)	Sequence-specific DNA binding transcription factor activity	-	1.35	1.45
MATN2	Matrilin 2	Calcium ion binding, protein binding	-	-1.40	-1.50
MEG3	Maternally expressed 3 (non-protein coding)	-	-	-1.39	-1.41
MFAP4	Microfibrillar-associated protein 4	-	-	-1.72	-1.57
MGC61598	Predicted: similar to ankyrin-repeat protein Nrarp	-	-	-1.32	-1.35
MGP	Matrix Gla protein (MGP), mRNA.	Calcium ion binding, extracellular matrix structural constituent, structural constituent of bone	-	-1.55	-1.54

Continued supplemental table 5. Common and differentially regulated placentas genes of obese women with and without GDM and lean women [#]

Gene symbol	Gene name	Gene ontology (Molecular Function)	OB vs. L	OB GDM vs. L	OB GDM vs. OB
MGST1	Microsomal glutathione S-transferase 1	Glutathione peroxidase activity, glutathione transferase activity		1.53	1.45
MMP23B	Matrix metallopeptidase 23B (MMP23B), mRNA.	Metalloendopeptidase activity, zinc ion binding	-	-1.34	-1.31
MRI1	Methylthioribose-1-phosphate isomerase homolog (S. cerevisiae)	S-methyl-5-thioribose-1-phosphate isomerase activity IBA identical protein binding	-	-1.40	-1.30
NBPF15	Neuroblastoma breakpoint family, member 15	-	-	1.43	1.35
NDN	Necdin homolog (mouse)	DNA binding IEA gamma-tubulin binding	-	-1.43	-1.40
OLFML2A	Olfactomedin-like 2A	Extracellular matrix binding, protein homodimerization activity	-	-1.31	-1.49
OLFML2B	Olfactomedin-like 2B	Extracellular matrix binding	-	-1.38	-1.30
OR2L13	Olfactory receptor, family 2, subfamily L, member 13	G-protein coupled receptor activity, olfactory receptor activity, protein binding	-	1.39	1.35
OR51E1	Olfactory receptor, family 51, subfamily E, member 1	G-protein coupled receptor activity IEA olfactory receptor activity	-	-1.46	-1.45
OSMR	Oncostatin M receptor	Growth factor binding, contributes to oncostatin-M receptor activity	-	1.40	1.42
P11	26 serine protease	RNA binding, endoribonuclease activity, growth factor activity, manganese ion binding, polysaccharide binding scavenger receptor activity, serine-type peptidase activity	-	1.47	1.31
P2RY13	Purinergic receptor P2Y, G-protein coupled, 13	G-protein coupled purinergic nucleotide receptor activity	-	0.74	-1.31
PAMR1	Peptidase domain containing associated with muscle regeneration 1	Catalytic activity	-	-1.63	-1.47
PARM1	Prostate androgen-regulated mucin-like protein 1	-	-	-1.38	-1.41
PCDH11X	Protocadherin 11 X-linked	Calcium ion binding	-	1.88	1.50
PDPN	Podoplanin	NOT amino acid transmembrane transporter activity, NOT folic acid transporter activity, NOT water transmembrane transporter activity	-	-1.37	-1.34
PIK3CB	Phosphoinositide-3-kinase, catalytic, beta polypeptide	Phosphatidylinositol-4,5-bisphosphate 3-kinase activity, ATP binding, insulin receptor substrate binding	-	1.31	1.40
PITX2	Homeodomain 2	chromatin DNA binding, RNA polymerase II core promoter proximal region sequence-specific DNA binding transcription factor activity involved in positive/negative regulation of transcription, phosphoprotein binding, protein homodimerization activity	-	-1.52	-1.49
PKIB	Protein kinase (cAMP-dependent, catalytic) inhibitor beta	cAMP-dependent protein kinase inhibitor activity	-	1.43	1.36
PLVAP	Plasmalemma vesicle associated protein	protein homodimerization activity	-	-1.40	-1.42
PRKAG2	Protein kinase, AMP-activated, gamma 2 non-catalytic subunit	ATP binding, cAMP-dependent protein kinase inhibitor activity,phosphorylase kinase regulator activity	-	1.61	1.49
PROK1	Prokineticin 1	Growth factor activity	-	-1.46	-1.56

Continued supplemental table 5. Common and differentially regulated placentas genes of obese women with and without GDM and lean women [#]

Gene symbol	Gene name	Gene ontology (Molecular Function)	OB vs. L	OB GDM vs. L	OB GDM vs. OB
PROM1	Prominin 1	Actinin binding, cadherin binding	-	-1.41	-1.48
PSG1	Pregnancy specific beta-1-glycoprotein 1	-	-	1.41	1.34
PSG5	Pregnancy specific beta-1-glycoprotein 5	Protein binding	-	1.85	2.18
PTH1R	Parathyroid hormone 1 receptor	G-protein coupled receptor activity	-	-1.37	-1.51
PTK7	PTK7 protein tyrosine kinase 7	ATP binding, protein binding, transmembrane receptor protein tyrosine kinase activity	-	-1.35	-1.33
RARRES2	Retinoic acid receptor responder (tazarotene induced) 2	Protein binding, receptor binding		-1.54	-1.37
REEP3	Receptor accessory protein 3	-	-	1.48	1.50
RGS11	Regulator of G-protein signaling 11	GTPase activator activity, signal transducer activity	-	-1.33	-1.33
RNU4-2	RNA, U4 small nuclear 2	-	-	-1.53	-1.45
RUNX1T1	Runt-related transcription factor 1; translocated to, 1 (cyclin D-related)	Sequence-specific DNA binding transcription factor activity, protein homodimerization activity, metal ion binding	-	-1.34	-1.49
SERPINI1	Serpin peptidase inhibitor, clade I (neuroserpin), member 1	Serine-type endopeptidase inhibitor activity	-	1.86	1.61
SGCA	Sarcoglycan, alpha (50kDa dystrophin-associated glycoprotein)	Calcium ion binding	-	-1.43	-1.35
SLAMF1	Signaling lymphocytic activation molecule family member 1	Antigen binding, transmembrane signaling receptor activity	-	-1.45	-1.32
SLC22A3	Solute carrier family 22 (extraneuronal monoamine transporter), member 3	Dopamine transmembrane transporter activity, organic cation transmembrane transporter activity, quaternary ammonium group transmembrane transporter activity, toxin transporter activity	-	-1.39	-1.42
SLC2A10	Solute carrier family 2 (facilitated glucose transporter), member 10	Sugar:hydrogen symporter activity	-	-1.31	-1.30
SLC3A2	Activators of dibasic and neutral amino acid transport	Calcium:sodium antiporter activity,catalytic activity, cation binding, neutral amino acid transmembrane transporter activity, protein binding	-	1.37	1.43
SLC6A6	Neurotransmitter transporter, taurine	Neurotransmitter:sodium symporter activity, taurine binding, taurine:sodium symporter activity	-	1.40	1.32
SLC7A5	Amino acid transporter light chain, L system	L-amino acid transmembrane transporter activity, neutral amino acid transmembrane transporter activity	-	1.39	1.31
SLCO4A1	Solute carrier organic anion transporter family, member 4A1	Transporter activity	-	1.76	1.63
SMARCD3	SWI/SNF related, matrix associated, actin dependent regulator of chromatin, subfamily d, member 3	Ligand-dependent nuclear receptor transcription coactivator activity, nuclear hormone receptor binding, transcription coactivator activity	-	-1.34	-1.33
SPAG8	Sperm associated antigen 8	Microtubule binding	-	1.50	1.36
SPARC	Secreted protein, acidic, cysteine-rich (osteonectin)	Calcium ion binding, collagen binding, extracellular matrix binding	-	-1.34	-1.33
SPTLC3	Serine palmitoyltransferase, long chain base subunit 3	Pyridoxal phosphate binding, serine C-palmitoyltransferase activity		1.33	1.42
ST3GAL1	ST3 beta-galactoside alpha-2,3-sialyltransferase 1	Beta-galactoside (CMP) alpha-2,3-sialyltransferase activity	-	1.50	1.43

Continued supplemental table 5. Common and differentially regulated placentas genes of obese women with and without GDM and lean women [#]

Gene symbol	Gene name	Gene ontology (Molecular Function)	OB vs. L	OB GDM vs. L	OB GDM vs. OB
TCF21	Transcription factor 21	E-box binding, RNA polymerase II core promoter proximal region sequence-specific DNA binding transcription factor activity involved in positive/negative regulation of transcription, androgen receptor binding, bHLH transcription factor binding, histone deacetylase binding, protein dimerization activity	-	-1.55	-1.45
TFPI	Tissue factor pathway inhibitor (lipoprotein-associated coagulation inhibitor)	Serine-type endopeptidase inhibitor activity	-	1.54	1.42
TGFBI	Transforming growth factor, beta-induced, 68kDa	Extracellular matrix binding, integrin binding	-	-1.39	-1.38
THBS2	Thrombospondin 2	Calcium ion binding, heparin binding	-	-1.51	-1.39
TIMP4	TIMP metallopeptidase inhibitor 4	Metal ion binding, metalloendopeptidase inhibitor activity	-	-1.50	-1.71
TLR3	Toll-like receptor 3	Double-stranded RNA binding , transmembrane receptor activity	-	1.33	1.39
TMEM119	Transmembrane protein 119	-	-	-1.40	-1.43
TMEM16C	Transmembrane protein 16C	NOT intracellular calcium activated chloride channel activity	-	2.06	2.03
TSPAN33	Tetraspanin 33	-	-	-1.34	-1.31
VIPR2	Vasoactive intestinal peptide receptor 2	G-protein coupled receptor activity, vasoactive intestinal polypeptide receptor activity	-	-1.38	-1.43
WDR72	WD repeat domain 72	-	-	-1.61	-2.40
WNT7A	Wingless-type MMTV integration site family, member 7A	Receptor binding, molecular transducer activity,	-	1.78	1.81
XAGE3	X antigen family, member 3	Protein binding	-	1.36	1.33
XPNPEP2	X-prolyl aminopeptidase (aminopeptidase P) 2, membrane-bound	Aminopeptidase activity, metal ion binding, metallopeptidase activity	-	1.33	1.34
ZNF114	Zinc finger protein 114	DNA binding, metal ion binding	-	1.94	1.36

[#] According to the intersection areas between the three datasets, **see Figure 20**. Analysis was performed in term placentas of lean (n=9), obese (n=10) and obese GDM (n=8) women. L: Lean; OB: Obese.

Supplemental table 6: Gene networks identified by Ingenuity pathway analysis

A) Obese vs. lean group

Top Functions	Score	Focus genes	Genes in Network
Cell Death and Survival, Cellular Development, Cellular Growth and Proliferation	41	20	26s Proteasome,↓**ACTC1**, Actin, Akt, ↑**CARD8,** caspase, ↓**CCZ1/CCZ1B,** CD3**,** ↓**CFD,** Collagen type 1, Cyclin A, ↓**DPP4,** ↓**FLT1,** Focal adhesion kinase, ↓**GAPDH,** ↑**HES5,** ↑**HIST1H4A (includes others),** Histone h3, Histone H4, HSP, Hsp70, ↑**HSPA6, HSPA1A/HSPA1B,** ↓**HSPH1,** ↓**IGDCC3,** ↓**ILK,** Integrin, ↓**KRT14,** ↑**LOC100287163/ZNF717,** ↑**NDRG2,** Notch,↑ **NOTCH1,** ↓**PPP2CB,** ↑**PRAME,** RNA polymerase
Cardiovascular System Development and Function, Organismal Development, Cellular Development	23	17	Alp, Ap1, ↑**BMPER**, Cg, Creb, ↑**DBH**, ↓**DUSP5**, ERK1/2, ↓**ERRFI1**, ↑**FABP4**, Fgf, ↑**FGF12**, FSH, ↑**HAS3**, hemoglobin, ↑**HPSE**, ↓**HS6ST2**, IgG2a, IgG2b, ↓**JUNB**, ↑**LCP1**, ↓**LDLR**, MAP2K1/2, PDGF BB, Pka catalytic subunit, ↑**PKIA**, ↓**PRL**, Proinsulin, ↓**SLC40A1**, Smad1/5/8, ↓**SPINK1**, TCF, Tgf beta, ↓**XDH**
Cellular Assembly and Organization, Post-Translational Modification, Hematological Disease	24	13	↓**ANKRD37,** ↓**ANO1**, ANO2, ANO6, ARIH2, BRD8, DNTTIP2, ↑**ENPP4**, FEM1B, KAT5, ↑**KRT86**, LBR, ↑**LOC285419**, ↓**MARC1,** ↑**MARC2**, MARCH2, ↑**MARCH4**, MECP2, ↓**NCCRP1**, nitrate reductase, NR1D2, PSIP1, PTPRS, SCN2A, ↑**SIL1**, TDG, TELO2, ↓**TLDC1**, TNFRSF10A, ↓**TPBG**, UBC, ULBP1, ↓**UPK3BL**, YEATS4, ZBTB7B

Focus genes (in bold) are genes identified in the list of differentially expressed genes. Analysis was performed in term placentas of lean (n=9), obese (n=10) and obese GDM (n=8) women.

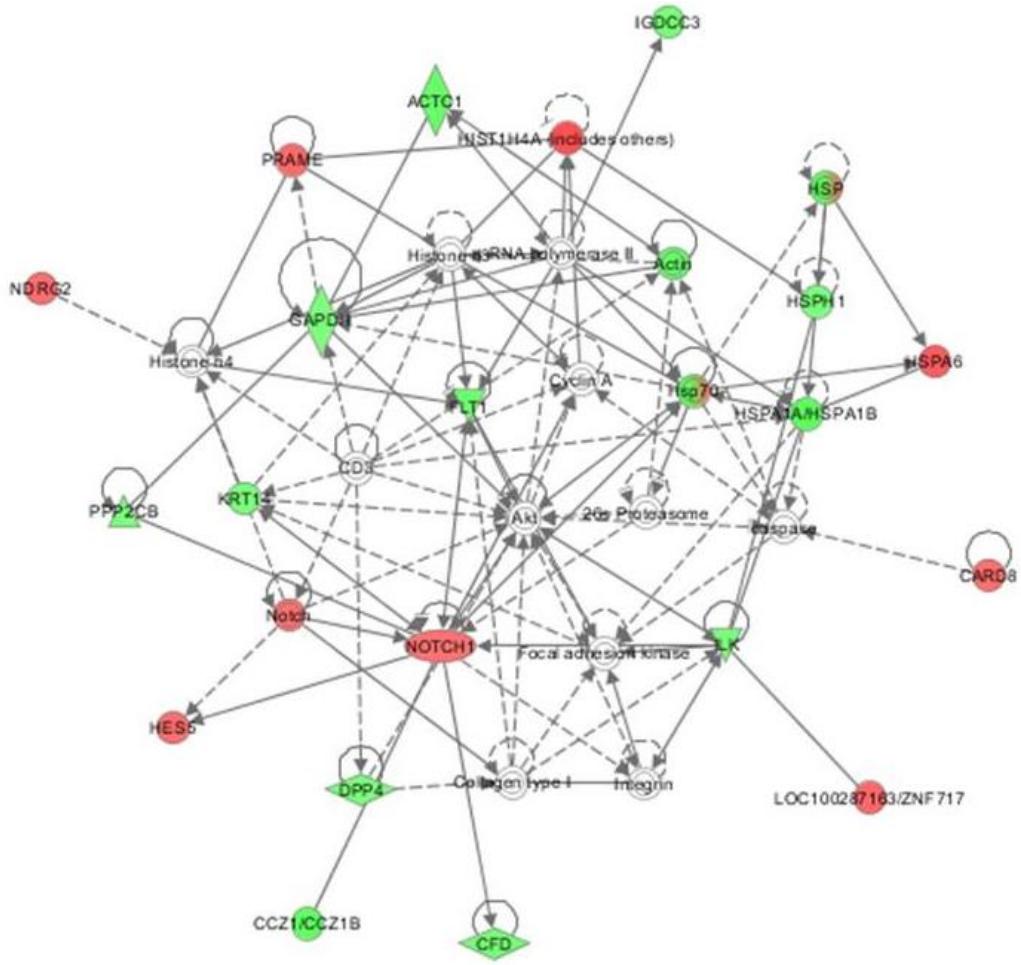

Continued supplemental table 6: Gene networks identified by Ingenuity pathway analysis

B) Obese GDM vs. lean group

Top Functions	Score	Focus genes	Genes in Network
Connective Tissue Disorders	43	26	↓**AMY2A,** amylase, ↓**ANTXR1,** ↓**ARHGAP4,** ↓**CHI3L1,** ↓**COL16A1,** ↓**COL1A1,** ↓**COL3A1,** ↓**COL5A1,** ↓**COL5A2,** ↓**COL6A1,** ↓**COL6A2,** ↓**COL8A2**, collagen, Collagen type VI, Collagen type XVIII, ↓**CSPG4,** ↓**DCN,** ↓**EGFL7**, ERK1/2, ETS, ↓**FOSB,** ↓**GAS6,** ↓**GFRA2,** ↓**mir-126**, NADPH oxidase, Pki, ↑**PKIA,** ↑**PKIB,** ↑**PLAC1,** ↑**RAB27B,** ↑**SGPP1**, Smad2/3, ↓**SPARC,** ↑**TMC5**
Cancer, Connective Tissue Disorders, Organismal Injury and Abnormalities	33	22	↓**ACKR3**, Adapter protein 2, ADCY, ADRB, ↑**AFF1,** ↓**APLNR,** Beta Arrestin, Clathrin, Creb, ↓**ENPP2**, ↑**GABBR2**, GNRH, Gpcr, ↑**GPR126**, Gs-coupled receptor, ↑**GULP1,** ↑**HMGCS2,** ↑**LGR4,** ↑**MC5R,** ↑**MED13,** ↑**MED12L,** mediator, ↑**NBF10 (includes others),** ↑**NCOA3,** ↓**NDN,** ↑**NIN,** P110, ↓**P2RY13,** ↓**PHT1R**, RNA polymerase II, ↓**RSPO2,** ↑**SLCO4A1**, Vegf, ↓**VIPR2,** ↑**ZNF268**
Cellular Growth and Proliferation	29	20	↑**ADAM12**, Akt, ↓**ANGPTL1,** ↓**BMP5,** ↓**CD9**, ↑**CSF2RB**, elastase, ↓**EPHA3**, Fgf, Gm-csf, ↓**IER3,** ↓**INPP5E**, Integrin, IRS, JAK, Laminin, Laminin1, ↓**LEF1**, Mek, MTORC1, Notch, ↓**NOX4,** ↓**NRARP**, ↑**OSMR**, ↓**PARM1**, PI3Kp85, ↑**PIK3CB**, ↓**PROK1**, ↓**PROM1**, Rap1, RSk, ↑**SDC1,** ↑**SLC3A2,** ↑**SLC7A5,** ↓**SLIT2**

Focus genes (in bold) are genes identified in the list of differentially expressed genes. Analysis was performed in term placentas of lean (n=9), obese (n=10) and obese GDM (n=8) women.

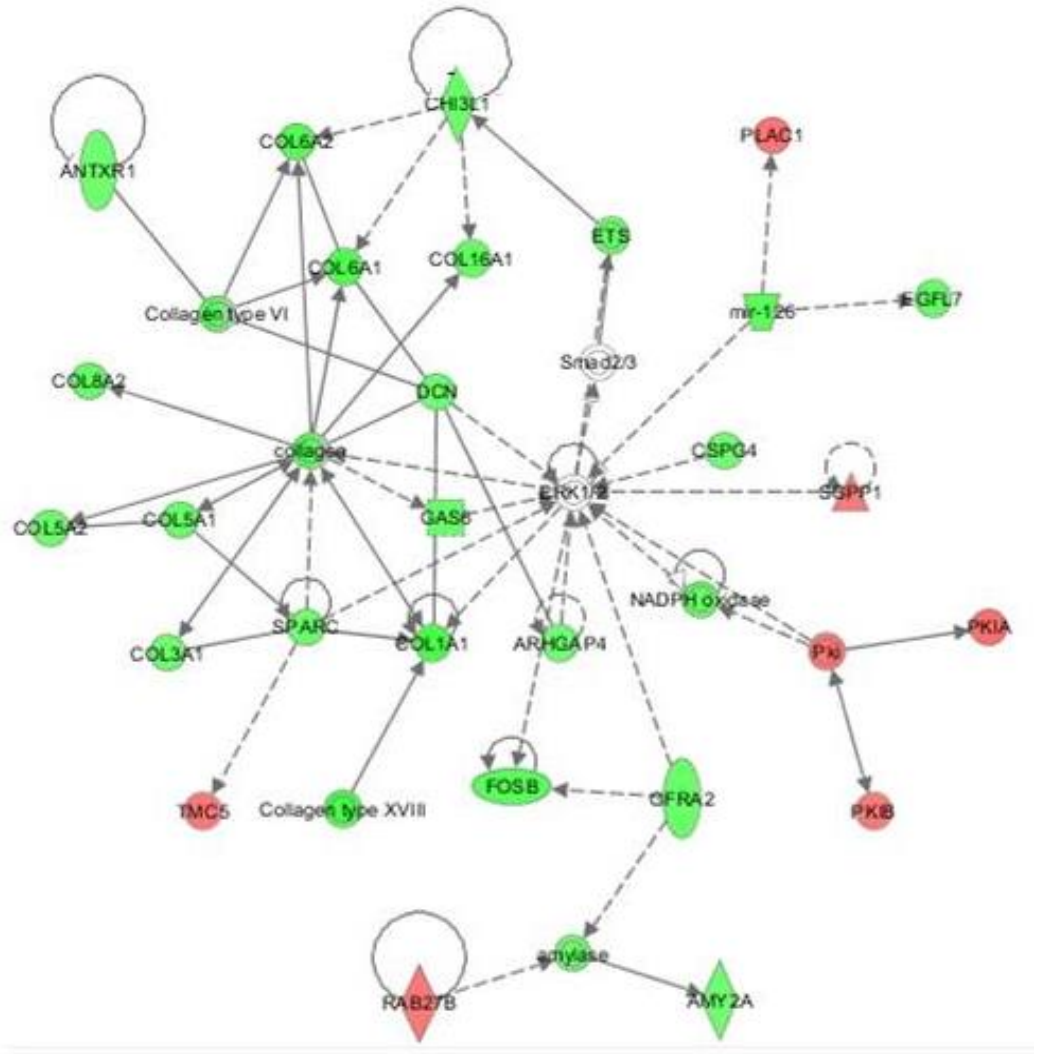

Continued supplemental table 6: Gene networks identified by Ingenuity pathway analysis

C) Obese GDM vs. obese group

Top Functions	Score	Focus genes	Genes in Network
Cardiovascular System Development and Function, Organismal Development, Gene Expression	41	26	Akt, BMP, ↓**BMP4** ↓**BMP5,** ↑**CD46,** ↓**CNTNAP1**, Collagen type VI, ↓**DACH1**, Enolase, ↓**FMOD,** ↓**FOXF1,** ↑**GREM2,** ↓**GUCY1A3,** Hedgehog, ↓**HEY2,** ↓**HEYL,** ↓**HIF3A,** ↓**ID1,** ↓**KLF2,** ↓**LYL1,** ↓**MGP,** Notch, ↓**NOTCH1,** ↓**NRARP,** ↓**PARM1,** ↑**PCDH11X/PCDH11Y,** ↓**PHLDB1,** ↓**PROK1,** ↓**PROM1,** ↑**RNF14,** Secretase gamma, Smad, ↓**SMARCD3,** SMOOTH MUSCLE ACTIN, ↓**TAGLN**
Cellular Development, Hematological System Development and Function, Hematopoiesis	39	25	↑**AES,** ↑**CEBPA,** Cg, ↑**DUSP5,** FSH, ↑**GGH,** ↓**HES5,** ↓**HLX,** ↓**HOXC6**, ↓**IGFBP3**, Importin alpha, JINK1/2, ↓**JUN,** Lh, ↓**MMP23B,** ↑**NBPF10 (includes others),** NMDA Receptor, ↑**PKIB,** PTPase, ↓**PTPDC1,** ↓**PTPRB,** ↓**PTPRD,** ↓**RARB,** ↓**RUNX1,** ↓**RUNX1T1,** secreted MMP, ↑**SERPINI1,** ↑**SLC6A6,** ↑**SMARCA1,** ↓**THBS2,** thymidine kinase, ↓**TIMP4,** ↓**TM4SF1,** ↓**TRO,** VitaminD3-VDR-RXR
Connective Tissue Disorders	35	24	↑**C15orf48,** ↑**CBLC,** ↓**COL11A1,** ↓**COL16A1,** ↓**COL18A1,** ↓**COL1A1,** ↓**COL1A2,** ↓**COL5A1,** ↓**COL6A1,** ↓**COL8A2,** collagen, Collagen type I, Collagen type III, Collagen type XVIII, Collagen(s), ↓**DCN,** ↓**EFEMP2,** ERK, ↓**FAM124B,** ↓**FAP,** ↓**FBLN2,** Fibrin, ↓**GAS6,** Hsp27, ↓**IGFBP7,** ↑**MAFF,** ↓**PLA2G5**, Ppp2c, Raf, Smad2/3Smad4, ↓**SPARC,** ↓**TGFBI,** ↓**TMEM173,** ↓**VWF,** ↑**XPNPEP2**

Focus genes (in bold) are genes identified in the list of differentially expressed genes. Analysis was performed in term placentas of lean (n=9), obese (n=10) and obese GDM (n=8) women.

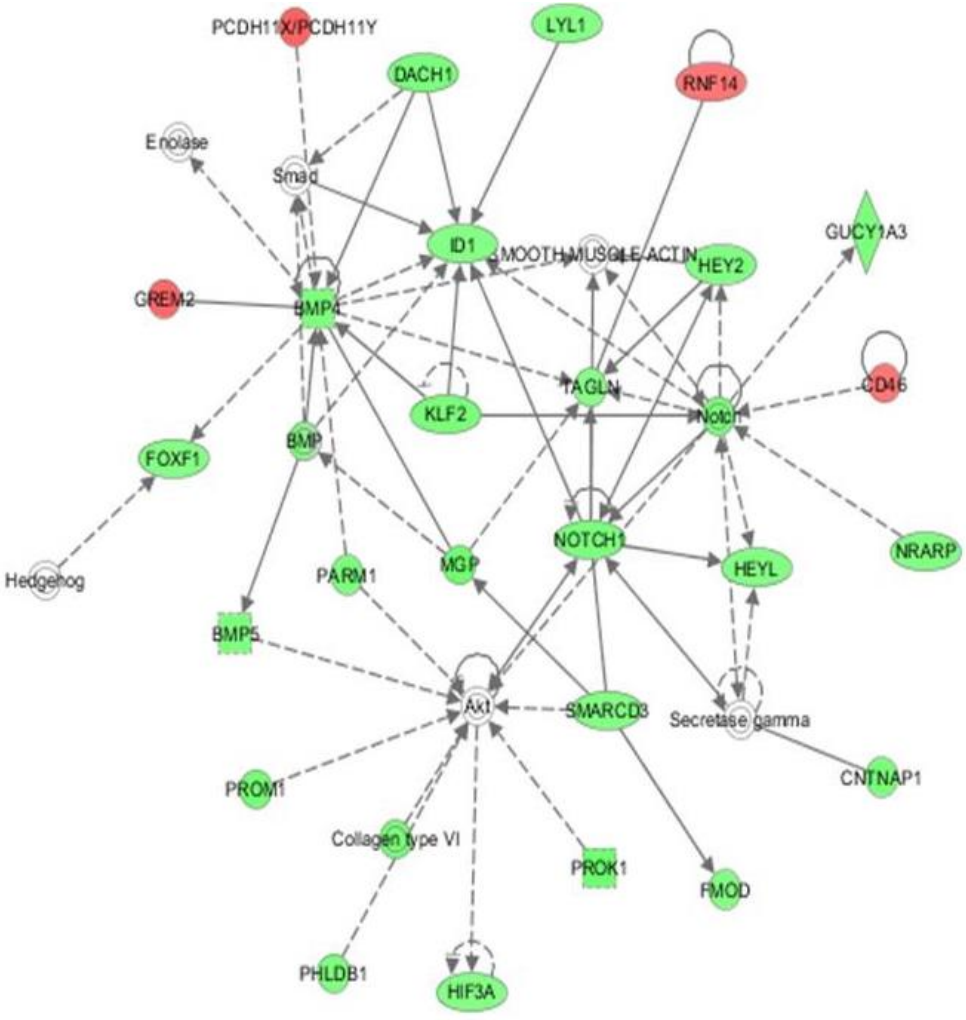

Supplemental table 7: Mean group expression and corresponding regulations of gene loci associated with type 2 diabetes retrieved from the placental microarray analysis

Gene symbol	Gene name	L Mean expression	OB Mean expression	OB GDM Mean expression	FC OB vs L	FC OB GDM vs L	FC OB GDM vs OB
ADAMTS9	ADAM metallopeptidase with thrombospondin type 1 motif, 9	220	196	177	-1.12	-1.24	-1.11
ADCY5	Adenylate cyclase 5	< Background					
ADRA2A	Adrenergic, alpha-2A-, receptor	47	53	46	1.11	-1.03	-1.15
ANK1	Ankyrin 1, erythrocytic	29	27	25	-1.07	-1.14	-1.07
ATP11A	ATPase, class VI, type 11A	37	39	39	1.06	1.06	1.00
BCL11A	B-cell CLL/lymphoma 11A (zinc finger protein)	32	35	34	1.12	1.08	-1.03
C2CD4B	C2 calcium-dependent domain containing 4B	76	81	62	1.07	-1.21	-1.30
CAMK1D	Calcium/calmodulin-dependent protein kinase ID	35	32	34	-1.03	-1.04	-1.01
CDKAL1	CDK5 regulatory subunit associated protein 1-like 1	111	120	103	1.08	-1.07	-1.16
CDKN2A	Cyclin-dependent kinase inhibitor 2A (melanoma, p16, inhibits CDK4)	32	29	30	-1.10	-1.06	1.03
CDKN2B	Cyclin-dependent kinase inhibitor 2B (p15, inhibits CDK4)	68	60	69	-1.13	1.00	1.14
CENTD2	Cyclin N-terminal domain containing 2	< Background					
CHCHD9	Coiled-coil-helix-coiled-coil-helix domain containing 9	860	811	846	-1.06	-1.02	1.04
CRY2	Cryptochrome 2 (photolyase-like)	213	204	189	-1.05	-1.13	-1.07
DGKB	Diacylglycerol kinase, beta 90kDa	< Background					
DUSP9	Dual specificity phosphatase 9	175	141	158	**-1.24***	-1.11	1.12
FADS1	Fatty acid desaturase 1	131	123	117	-1.07	-1.12	-1.05
FN3K	Fructosamine 3 kinase	< Background					
FTO	Fat mass and obesity associated	117	123	126	1.07	1.07	1.00
G6PC2	Glucose-6-phosphatase, catalytic, 2	27	26	24	-1.01	-1.13	-1.11
GCK	Glucokinase (hexokinase 4, maturity onset diabetes of the young 2)	< Background					
GCKR	Glucokinase (hexokinase 4) regulator	< Background					
GIPR	Gastric inhibitory polypeptide receptor	< Background					
GLIS3	GLIS family zinc finger 3	85	83	116	-1.04	**1.36***	**1.41***
HFE	Hemochromatosis	34	36	32	1.05	-1.07	-1.12
HHEX	Hematopoietically expressed homeobox	136	130	112	-1.05	-1.21	-1.16
HK1	Hexokinase 1	1961	1928	1929	-1.02	-1.02	1.00
HMGA2	High mobility group AT-hook 2	32	33	34	1.00	1.04	1.04
HNF1A	HNF1 homeobox A	< Background					
HNF1B	HNF1 homeobox B	< Background					
IGF1	Insulin-like growth factor 1	58	56	63	-1.05	1.07	1.12
IGF2BP2	Insulin-like growth factor 2 binding protein 2	1182	1185	1302	1.00	1.10	1.10
IRS1	Insulin receptor substrate 1	186	151	138	-1.23	**-1.35***	-1.09
JAZF1	JAZF zinc finger 1	186	184	145	-1.01	**-1.28****	**-1.27****

Continued supplemental table 7: Mean group expression and corresponding regulations of gene loci associated with type 2 diabetes retrieved from the placental microarray analysis

Gene symbol	Gene name	L Mean expression	OB Mean expression	OB GDM Mean expression	FC OB vs L	FC OB GDM vs L	FC OB GDM vs OB
KCNJ11	Potassium inwardly-rectifying channel, subfamily J, member 11	< Background					
KCNQ1	Potassium voltage-gated channel, KQT-like subfamily, member 1	< Background					
KLF14	Kruppel-like factor 14	< Background					
MADD	MAP-kinase activating death domain	80	79	79	-1.01	-1.01	1.00
MTNR1B	Melatonin receptor 1B	< Background					
NOTCH2	Notch homolog 2 (Drosophila)	152	166	152	-1.09	1.00	-1.09
PPARG	Peroxisome proliferator-activated receptor gamma	986	995	1020	1.01	1.03	1.02
PPRC1	Peroxisome proliferator-activated receptor gamma, coactivator-related 1	353	332	318	-1.06	-1.11	-1.04
PROX1	Prospero homeobox 1	353	332	318	-1.06	-1.11	-1.04
PRRX1	Paired related homeobox 1	82	69	53	-1.15	-1.54*	-1.34
SLC2A2	Solute carrier family 2 (facilitated glucose transporter), member 2	< Background					
SLC30A8	Solute carrier family 30 (zinc transporter), member 8	< Background					
SPTA1	Spectrin, alpha, erythrocytic 1 (elliptocytosis 2)	59	58	58	-1.02	-1.02	1.00
TCF7L2	Transcription factor 7-like 2 (T-cell specific, HMG-box)	65	64	58	1.01	-1.14	-1.15
THADA	Thyroid adenoma associated	120	116	113	-1.04	-1.07	-1.03
TMPRSS6	Transmembrane protease, serine 6	59	48	49	-1.24	-1.21	1.03
TP53INP1	Tumor protein p53 inducible nuclear protein 1	319	272	336	-1.17*	1.06	1.24*
TSPAN8	Tetraspanin 8	65	63	63	-1.03	-1.02	1.01
VPS13C	Vacuolar protein sorting 13 homolog C (S. cerevisiae)	46	50	52	1.10	1.13	1.03
WFS1	Wolfram syndrome 1 (wolframin)	1089	986	1213	-1.10	1.11	1.23
ZBED3	Zinc finger, BED-type containing 3	30	30	29	-1.01	-1.04	-1.03
ZFAND6	Zinc finger, AN1-type domain 6	348	377	416	1.08	1.20*	1.10

** $p < 0.01$; * $P < 0.05$; significant genes are presented in bold type. Diabetes-associated genes were retrieved from Herder et al. [13]. Analysis was performed in term placentas of lean (n=9), obese (n=10) and obese GDM (n=8) women. L: lean, OB: obese.

Supplemental table 8: Correlation between placental gene expressions and maternal plasma inflammatory parameters IL6 and CRP

Maternal plasma parameters at 3rd trimester				
	N	**r**	**Maternal plasma IL6**	**Maternal plasma CRP**
Maternal plasma CRP	39	r_1	**0.418 *****	-
		r_2	**0.359 ***	-
Placental IL1B expression	39	r_1	-0.119	0.072
		r_2	0.047	0.242
Placental IL6 expression	39	r_1	0.022	0.097
		r_2	-0.022	0.112
Placental IL8 expression	39	r_1	-0.245	0.002
		r_2	-0.142	0.089
Placental CRP expression	39	r_1	-0.184	0.090
		r_2	-0.089	0.286
Placental TNFα expression	39	r_1	0.052	0.307
		r_2	0.032	0.292
Placental MCP-1 expression	39	r_1	0.041	0.171
		r_2	0.054	0.262
Placental CD14 expression	39	r_1	-0.248	-0.079
		r_2	-0.169	0.162
Placental CD68 expression	39	r_1	-0.190	-0113
		r_2	-0.115	0.041

r = correlation coefficient; r_1: unadjusted Spearman correlation coefficient; r_2: partial correlation coefficient adjusted for covariates infant sex, gestational age, maternal pre-pregnancy BMI, gestational weight gain and $AUC_{Glucose}$ (OGTT). *** P < 0.001; * p < 0.05. Significant values are presented in bold type.

Supplemental table 9: Minimum information für publication of RT-qPCR experiments (MIQE) checklist for authors, reviewers and editors [208]

Item to check	Importance [1]	Checklist
Experimental design		
Definition of experimental and control groups	E	Experimental groups: placentas of control group (BMI 18.5-25 kg/m^2), obese group (BMI > 30 kg/m^2) and obese GDM group (BMI > 30 kg/m^2; diet-controlled and insulin treated). Women underwent 75g OGTT: fasting glucose > 5.1 mmol/L (92 mg/dL), 1 h glucose > 10.0 mmol/L (180 mg/dL), 2 h glucose > 8.5 mmol/L (153 mg/dL). GDM is diagnosed if ≥ 1 of the thresholds was met or exceeded [40].
Number within each group	E	Lean: 14, Obese: 13; Obese GDM: 16 (diet-controlled n=7, insulin treated n=9)
Assay carried out by core lab or investigator's lab?	D	Assay carried out by investigator's lab
Acknowledgement of authors' contributions	D	Kirsten Uebel
Sample		
Description	E	Human placenta villous fraction was sampled from each of the four quadrants, with the same distance from placental middle avoiding the sampling of macroscopic abnormalities. 1 cm^3 of maternal basal plate and fetal chorionic plate were dissected from chorionic villous tissue and all 3 fractions corresponding to the quadrants were obtained separately. For nucleic acid extraction the four quadrants per placenta were pooled.
Volume/mass of sample	D	Per placenta 1 cm^3 per quadrant
Microdissection or macrodissection	E	Macrodissection
Processing procedure	E	Placentas were stored at 4°C until dissection. Samples were frozen in liquid nitrogen and stored at -80°C
If frozen - how and how quickly?	E	Frozen between 30 min and 90 min
If fixed - with what, how quickly?	E	No fixation was done
Sample storage conditions and duration (especially for FFPE samples)	E	Samples were stored at -80°C from April 2010 until Februrary.2012 (first to last delivery of the *GesA* study)

Continued supplemental table 9: Minimum information für publication of RT-qPCR experiments (MIQE) checklist for authors, reviewers and editors [208]

Item to check	Importance [1]	Checklist
Nucleic acid extraction		
Procedure and/or instrumentation	E	Total RNA was extracted with a combined approach of TRI Reagent® RNA Isolation Reagent and midi RNeasy Kit. The placental pieces from the four quadrants were grounded and homogenized in 10µl TRI Reagent® RNA Isolation Reagent per 1 mg placental tissue by a rotor-strator homogenizer. Purified total RNA was eluted in RNAse-free H_2O supplied by the midi RNeasy kit.
Name of kit and details of any modifications	E	TRI Reagent® RNA Isolation Reagent (Sigma-Aldrich, Taufkirchen, Germany) and midi RNeasy Kit (Qiagen, Hilden, Germany) # 75144. The instructions of the TRI Reagent® RNA Isolation Reagent manual were complied until the separation of watery and organic phases. The midi RNeasy Kit was applied according to the manufacturer's instructions.
Source of additional reagents	D	Chloroform (Carl Roth GmbH & Co. KG, Karlsruhe, Germany), 96 % Ethanol (J.T. Baker, Mallinckrodt, Deventer, Netherlands), RNAse ZAP (Sigma-Aldrich Chemie GmbH, Taufkirchen, Germany)
Details of DNase or RNAse treatment	E	DNase I treatment was used according to the manufacturer's instructions (RNase-Free DNase Set, Qiagen, Hilden, Germany) # 79254.
Contamination assessment (DNA or RNA)	E	Agarose gel electrophoresis was applied for all samples to exclude DNA contamination. Additionally, reverse transcription controls with no RT enzyme (-RTs) were used to assess DNA contamination for each primer in a pool containing all total RNA samples.
Nucleic acid quantification	E	Total RNA concentration was determined by measuring absorbance at 260 nm UV light
Instrument and method	E	Total RNA concentration was measured by NanodropTM 1000 Spectrophotomerter (Peqlab biotechnology GmbH, Erlangen, Germany)
Purity (A260/A280)	D	All total RNA samples showed a 260/280 ratio of around 2.0.
Yield	D	Yield of total RNA samples were in the range of 969 - 1929 ng/µl
RNA integrity method/instrument	E	Agilent 2100 Bioanalyzer (Agilent Technologies GmbH, Böblingen, Germany)
RIN/RQI or Cq of 3' and 5' transcripts	E	RIN factor of all samples was above 6.5
Electrophoresis traces	D	Electropherograms of the Agilent 2100 Bioanalyzer were controlled
Inhibition testing (Cq dilutions, spike or other)	E	No inhibition testing was performed

Continued supplemental table 9: Minimum information für publication of RT-qPCR experiments (MIQE) checklist for authors, reviewers and editors [208]

Item to check	Importance [1]	Checklist
Reverse Transcription		
Complete reaction conditions	E	One-step RT-qPCR was performed
Amount of RNA and reaction volume	E	10 ng RNA in 20 µl reaction volume
Priming oligonucleotide (if using GSP) and concentration	E	Specific primers were used in one-step RT-qPCR. Self-designed primer paires (10 pmol/µl) were used with an end concentration of 0,5 µM.
Reverse transcriptase and concentration	E	Omniscript and Sensiscript Reverse Transcriptases from QuantiTect SYBR Green RT-PCR Kit; 0.2 µl in 20µl reaction volume
Temperature and time	E	50 °C for 30 min, 95 °C for 15 min
Manufacturer of reagents and catalogue numbers	D	QuantiTect SYBR Green RT-PCR Kit (Qiagen, Hilden, Germany), # 204245
Cqs with and without RT	D	All used primer pairs showed either no amplification or differences between total RNA pool and the minus RT pool > 7 ΔCq
Storage conditions of cDNA	D	There was no storage of cDNA because of the application of the one-step RT-qPCR.
qPCR target information		
If multiplex, efficiency and LOD of each assay.	E	A multiplex approach was not applied
Gene symbol	E	Provided in **chapter 8.1**
Sequence accession number	E	Provided in **chapter 8.1**
Location of amplicon	D	Provided in **chapter 8.1**
Amplicon length	E	Provided in **chapter 8.1**
In silico specificity screen (BLAST, etc)	E	All primers were blasted with Oligo Calc: Oligonucleotide Properties Calculator on http://www.basic.northwestern.edu/biotools/oligocalc.html and in silico-PCR was performed with http://genome.ucsc.edu/cgi-bin/hgPcr
Pseudogenes, retropseudogenes or other homologs?	D	-
Sequence alignment	D	-
Secondary structure analysis of amplicon	D	Only secondary structure of self-designed primer-pairs was controlled with Oligo Calc: Oligonucleotide Properties Calculator on http://www.basic.northwestern.edu/biotools/oligocalc.html
Location of each primer by exon or intron (if applicable)	E	Provided in **chapter 8.1**
What splice variants are targeted?	E	As many splice variants as possible were targeted by one primer-pair

Continued supplemental table 9: Minimum information für publication of RT-qPCR experiments (MIQE) checklist for authors, reviewers and editors [208]

Item to check	Importance [1]	Checklist
qPCR oligonucleotides		
Primer sequences	E	Provided in **chapter 8.1**
RTPrimerDB Identification Number	D	Was not used
Probe sequences	D	No probes were used
Location and identity of any modifications	E	No modificantions were applied
Manufacturer of oligonucleotides	D	Self-designed primer-pairs were purchased from metabion GmbH (Martinsried, Germany)
Purification method	D	Self-designed primer-pairs: standard grade, deprotected and desalted
qPCR protocol		
Complete reaction conditions	E	One-step RT-qPCR was carried out on a "Mastercycler ep Realplex" using QuantiTect SYBR Green RT-PCR Kit (final reaction volume: 20 µl). Reaction mix consisted of 10 µl 2x Quantitect SYBR Green RT-PCR Master Mix, 6,8 µl rnase-free H2O, 1 µl Primer-mix 10 pmol/µl per primer, 0.2 µl QuantiTect RT Mix and 1 µl of 10 ng/µl template RNA. The RT-qPCR was initiated with 50 °C for 30 min and 95 °C for 15 min. 40 Cycles with 95 °C for 15 sec, 60 °C for 30 sec and 72 °C for 30 sec were followed by 95 °C for 15 sec as well as a melting curve from 60 to 95 °C with ramp duration of 20 min. The programm ended with 95 °C for 15 sec. All reactions were done in duplicate.
Reaction volume and amount of cDNA/ DNA/ RNA	E	Reaction volume: 20 µl; Amount of total RNA: 10 ng/µl
Primer, (probe), Mg++ and dNTP concentrations	E	Concentration of each primer: 200pmol; Mg^{2+}: 2.5 mM as provided in 2x QuantiTect SYBR Green RT-PCR Master Mix; dNTP: unknown, provided in 2x QuantiTect SYBR Green RT-PCR Master Mix
Polymerase identity and concentration	E	HotStarTaq DNA Polymerase included in 2x QuantiTect SYBR Green RT-PCR Master Mix, concentration unknown
Buffer/kit identity and manufacturer	E	QuantiTect SYBR Green RT-PCR Kit (Qiagen, Hilden, Germany), # 204245
Exact chemical constitution of the buffer	D	QuantiTect SYBR Green RT-PCR Buffer contains Tris·Cl, KCl, $(NH4)_2SO_4$, 5 mM $MgCl_2$, pH 8.7 (20°C) included in 2x QuantiTect SYBR Green RT-PCR Master Mix
Additives (SYBR Green I, DMSO, etc.)	E	SYBR Green I and ROX as included in 2x QuantiTect SYBR Green RT-PCR Master Mix; no other additives listed
Manufacturer of plates/tubes and catalog number	D	Eppendorf twin.tec real-time PCR plate 96well, with white wells (# 0030 132.530, Eppendorf, Hamburg, Germany), Eppendorf Heat Sealing Film (# 0030 127.838, Eppendorf, Hamburg, Germany)
Complete thermocycling parameters	E	1x 50 °C for 30 min, 1x 95 °C for 15 min, 40x : 95 °C 15sec. / 60 °C for 30 sec. / 72 °C for 30 sec, 95 °C 15 sec., Melting curve: 60 -95 °C in 20 min, 95 °C 15 min.
Reaction setup (manual/robotic)	D	Manual
Manufacturer of qPCR instrument	E	Mastercycler ep Realplex (Eppendorf, Hamburg, Germany)

Continued supplemental table 9: Minimum information für publication of RT-qPCR experiments (MIQE) checklist for authors, reviewers and editors [208]

Item to check	Importance [1]	Checklist
qPCR validation		
Evidence of optimisation (from gradients)	D	-
Specificity (gel, sequence, melt, or digest)	E	Melting curve for the incidence of only one specific peak was controlled. Additionally, agarose gel electrophoresis (2 %) with ethidiumbromide for one specific peak band at the expected size of the calculated amplicon length was performed. No template controls (NTC) were applied in each run to detect primer dimerisation and unspecific amplifications.
For SYBR Green I, Cq of the NTC	E	In the majority of cases, no Cqs values were detectable in the NTCs. In the other cases, the Cq of the NTC was more than 5 Cqs higher than the median Cq of the placental RNAs. Cq values of NTCs are available upon request
Standard curves with slope and y-intercept	E	No use of standard curves
PCR efficiency calculated from slope	E	PCR efficiencies were calculated with LinReg PCR [209]
Confidence interval for PCR efficiency or standard error	D	PCR efficiency (mean of all qPCR experiments): 84.2 ± 9.2 %
r2 of standard curve	E	Standard curves were not applied
Linear dynamic range	E	Standard curves were not applied
Cq variation at lower limit	E	-
Confidence intervals throughout range	D	-
Evidence for limit of detection	E	-
If multiplex, efficiency and LOD of each assay.	E	-

Continued supplemental table 9: Minimum information für publication of RT-qPCR experiments (MIQE) checklist for authors, reviewers and editors [208]

Item to check	Importance [1]	Checklist
Data analysis		
qPCR analysis program (source, version)	E	RT-qPCR analysis program was not applied.
Cq method determination	E	Threshold was determined by CalqPlex retrieved by the realplex 2.0 software
Outlier identification and disposition	E	Biological outliers were included in the analysis
Results of NTCs	E	In the majority of cases, no Cqs in the NTCs were detected, whereas the Cq of the NTC was usually more than 5 Cqs higher than the median Cq of the placental RNAs. A difference < 5 Cqs between NTCs and median template RNAs could be attributed to artefacts or primer dimerisation. Cq values of NTCs are available upon request
Justification of number and choice of reference genes	E	ACTB and H2AFZ were tested with BestKeeper [210] and for differences in mean Cq value between the analysis groups. The genes were suitable as reference genes
Description of normalisation method	E	The geometric mean of ACTB and H2AFZ was used for normalization.
Number and concordance of biological replicates	D	13 -16 biological replicates were analysed.
Number and stage (RT or qPCR) of technical replicates	E	Technical replicates: RT and qPCR duplicates
Repeatability (intra-assay variation)	E	Not determined
Reproducibility (inter-assay variation, % CV)	D	Not determined
Power analysis	D	Not determined
Statistical methods for result significance	E	Normal distribution of ΔCq values: One-Way ANOVA with Sidak post hoc test; failed normal distribution or equal variance test: Kruskal-Wallis test with Dunn`s post hoc test
Software (source, version)	E	IBM SPSS statistics software;version 20.0, IBM Deutschland GmbH, Ehningen, Germany
Cq or raw data submission using RDML	D	Cq values are available upon request

[1] All essential information (E) must be submitted with the manuscript. Desirable information (D) should be submitted if available.

10 List of Figures

11 List of tables

12 List of supplemental figures and tables

13 Acknowledgement

First, I am very grateful to **Prof. Dr. J. J. Hauner** for giving me the opportunity to work in this field of research, his trust in me and his valuable support during this thesis.

I would like to show my greatest appreciation to my supervisor **Dr. Bernhard L. Bader** for his profound knowledge and his tireless commitment for sciences. I am very grateful for his invaluable feedback and the constructive discussion that particularly contributed to the success of this thesis.

I want to thank **Prof. Dr. Martin Klingenspor** for evaluating this thesis and **Prof. Dr. Dirk Haller** for taking the dissertation committee chair.

I would particularly like to thank **Prof. Dr. Susanne Ulbrich** and **Prof. Dr. Martin Klingenspor** for mentoring and coordinating the PhD-Graduate School “Nutritional adaptation and epigenetic mechanisms”. I owe a very important debt to my colleagues of the PhD Graduate School **Jana Hemmerling, David Lasar** and **Veronika Pistek** for the productive discussions as well as their incessant motivation and support.

Dr. Eva Sedlmeier made enormous contribution to the success of this thesis. I owe my deepest gratitude for her untiring encouragement in my project and her great enthusiasm for placental analysis. She is one of the most helpful persons I could imagine and I still appreciated her as supportive adviser and friend beyond the end of her work at our department.

I am sincerely grateful to **Dr. Tobias Ludwig**, who accompanied my work from the very beginning and even after leaving the department and always affirmed me to stay on the ball. I appreciated his amiable and helpful attitude and I could benefit a lot from his structured work approach. It would have been a lonely lab without him.

My heartfelt appreciation goes to **Dr. Daniela Much** and **Dr. Stefanie Brunner** for their elaborate introduction and invaluable assistance in the daily work of the clinical study, their open ear for all my questions and their friendship through all these years.

I further had the support and encouragement of **Dr. Christoph Dahlhoff, Katharina Heller,** and all colleagues from the Chair of Nutritional Medicine, particularly **Dr. Kathrin Rauh,**

Dr. Julia Stoll, Christina Brei and **Stefanie Worsch** and I would like to offer my special thanks for sharing their expertise and providing inspiring discussions.

I am particularly grateful for the lab and study assistance given by **Manuela Hubersberger**, **Elisabeth Hofmair** and **Sylvia Tholl**.

I owe a great debt of gratitude to **Verena Schulte**, physician, and **Dr. Daniela Much** for performing and teaching me the ultrasound imaging as well as the analyses of corresponding datasets. A special mention goes to **Karina Pusch** for performing the inter-observer analysis of the ultrasonographic data. In this context, I also thank **Prof. Dr. E. J. Rummeny** and **Dr. Jan Bauer** (Institute of Radiology, Klinkum Rechts der Isar) for giving me and my colleagues free access to the ultrasonographic system. Furthermore, I thank **Prof. Dr. Karl-Theo M Schneider** (Abteilung für Geburtshilfe und Perinatalmedizin der Frauenklinik, Klinkum rechts der Isar) and his team for their involvement in the trial.

I am deeply grateful to **PD Dr. Kurt Gedrich** (Biochemistry Unit, ZIEL) and **Dr. Tibor Schuster** (Institute for Medical Statistics and Epidemiology, Klinkum Rechts der Isar) for their substantial statistical advice.

I address my special thanks to **Dr. Martin Irmler** (Institute of Experimental Genetics, Helmholtz Zentrum München) and his team for offering the Illumina platform, performing the DNA microarray analysis and supporting the biostatistical assessment.

I want to thank **all the families and their infants** for participating in the *GesA*-study.

Finally, from my heart I thank my parents, **Margitte and Reinhard Uebel**, for any kind of support and trust I could think of. I am dedicating this thesis to them.

14 Funding

This project was financed by the *Deutsche Diabetes-Stiftung*.

There was no intervention from any sponsor with any of the research aspects of the study including study design, intervention, data collection, data analysis and interpretation as well as writing of manuscripts.

15 **Publications**

Kirsten Uebel, Karina Pusch, Kurt Gedrich, Karl-Theo Schneider, Hans Hauner and Bernhard L Bader. **Effect of maternal obesity with and without gestational diabetes on offspring subcutaneous and preperitoneal adipose tissue development from birth up to year-1.** BMC Pregnancy Childbirth. 2014 Apr 11;14:138.

Christoph Dahlhoff, Stefanie Worsch, Manuela Sailer, Björn A. Hummel, Jarlei Fiamoncini, Kirsten Uebel, Rima Obeid, Christian Scherling, Jürgen Geisel, Bernhard L. Bader, Hannelore Daniel. **Methyl-donor supplementation in obese mice prevents the progression of NAFLD, activates AMPK and decreases acyl-carnitine levels.**
Molecular metabolism. 2014 May 3; 565-580